

# **Biogeochemistry of Nitrogen Isotopes in Northern Indian Ocean**

**Thesis submitted to**

**The Maharaja Sayajirao University of Baroda,  
Vadodara, India**

**For the degree of**

**Doctor of Philosophy in Geology**

**By**

**Sanjeev Kumar**

**November, 2004**



**Planetary and Geosciences Division  
Physical Research Laboratory,  
Navrangpura, Ahmedabad-380 009, India**

# Certificate

I hereby declare that the work presented in this thesis is original and has not formed the basis for the award of any degree or diploma by any university or institution.

**Sanjeev Kumar (Author)**  
Planetary and Geosciences Division  
Physical Research Laboratory  
Navrangpura, Ahmedabad-380 009  
India

Certified by:

**Prof. R.Ramesh (Guide)**  
Planetary and Geosciences Division  
Physical Research Laboratory  
Navrangpura, Ahmedabad-380 009  
India

**Prof. P.P.Patel (Co-guide)**  
Department of Geology  
The Maharaja Sayajirao University of Baroda  
Vadodara -390 002  
India

**To  
My Mother**

# Abstract

The present work focuses on the biogeochemistry of nitrogen and its isotopes in the Northern Indian Ocean (the northeastern Arabian Sea and the Bay of Bengal)\*. Availability of nitrogen in the euphotic zone is an important modulator of the oceanic primary productivity and export production and, therefore, of carbon dynamics. Interrelated physical processes and biogeochemical transformation processes contribute to nitrogen availability and the fertility of the upper ocean. Our knowledge remains rudimentary in the northeastern Arabian Sea and in particular, the Bay of Bengal, with respect to the quantitative relationships and feedbacks between C and N cycles. The present work aims to understand the biogeochemical aspect of nitrogen and its isotopes in the northeastern Arabian Sea and the Bay of Bengal by

- (i) Estimating the natural isotopic variability of nitrogen in surface suspended matter.
- (ii) Estimating the new and regenerated productions.

The northeastern Arabian Sea was studied during the Indian JGOFS but new production measurements were not made. *This is a first attempt to quantify the new and regenerated productions in both the basins\**. The Bay of Bengal has been studied during pre (April-May 2003) and post (September-October 2002) monsoon seasons, whereas the northeastern Arabian Sea has been studied during the middle and waning phases of winter monsoon (January and Late February-Early March).

The results from the Bay of Bengal reveal consistent high new production during both seasons; however, the productivity is higher during premonsoon than postmonsoon. New production during April-May 2003 (overall average~ 5.45 with shelf region average of 6.94 and offshore average of 3.58 mmolN m<sup>-2</sup>d<sup>-1</sup>) and September-October 2002 (overall average~ 2.61 with shelf stations averaging around 2.26 and offshore region around 3.06 mmolN m<sup>-2</sup> d<sup>-1</sup>) in the Bay of Bengal are indeed comparable to the high new production off India, 5.2±2.3 mmolN m<sup>-2</sup> d<sup>-1</sup> reported for the Arabian Sea. This observed high new production in the moderately productive Bay of Bengal could be one of the reasons for the observed high organic carbon fluxes in the sediment traps at depth; these fluxes in the Bay are comparable to those of the highly productive Arabian Sea. New production is known to be coupled with export fluxes on longer time scales, i.e., of sediment traps. The observed high new production

also verifies the earlier conjecture put forward to explain the observed low pCO<sub>2</sub> in the surface Bay.

$\delta^{15}\text{N}$  measurements in surface suspended matter of shelf as well as northern offshore Bay of Bengal show signatures of mixing between continental inputs and marine sources. Dilution by the detrital organic material brought in by rivers leads to a consistently lower  $\delta^{15}\text{N}$ . The depth profiles of  $\delta^{15}\text{N}$  show an increase by a maximum of around 4‰ between the top 60m and 300m indicating the role of higher sinking rates of particles ballasted by aggregates of organic and mineral matter in the Bay.

New production study performed in the Arabian Sea shows an almost five fold rise in the average new production from January ( $\sim 2.3 \text{ mmol N m}^{-2}\text{d}^{-1}$ ) to late February-early March ( $\sim 12.7 \text{ mmol N m}^{-2}\text{d}^{-1}$ ). The observed increase may be due to lateral advection of nitrate from a nearby region or due to nitrate entrained during January whose residence time was  $\sim 50$  days. This nitrate might have sustained the bloom during February-March, once the light conditions became optimum due to waning winter cooling.

The f- ratio during January, in general, shows an increasing trend from the south (off Goa) to the north (off Gujarat), clearly depicting the systematic effect of intensification of winter cooling. Northeast trade winds prevalent in the region during this season bring the cool, dry air and cause an increase in the evaporation and heat loss from the surface, and cooling and consequent increase in the density leading to convective mixing. This results in the deepening of the mixed layer and consequent transport of nutrients from the base of the mixed layer and upper thermocline to the surface, to increase the new production.

The nitrogen isotopic composition of the surface suspended matter reveals an overall increase by  $\sim 5\%$  in  $\delta^{15}\text{N}$  in the region from January to March. This increase is possible due to an overall increase in the nitrogen isotopic composition of the source ( $\delta^{15}\text{N}$ ) nutrients or due to a change in the fractionation behaviour of the phytoplankton. The analysis of nutrient regime suggests that if the deeper nitrate is the source during both the months, the observed increase may be indicative of an intensified denitrification leading to an isotopic enrichment of the source nitrate. And if the nitrate entrained during January is the source, the continuous uptake by the phytoplankton might have led to an isotopic enrichment observed during March.

The observed new production and f-ratio results can be used to prepare new production maps of the region using satellite data for better spatial and temporal coverage.

Thus this thesis provides a new and comprehensive data set on new and total productions, natural variability of  $\delta^{15}\text{N}$  in suspended matter for different seasons from the northern Indian Ocean, and helps in gaining insight into their nitrogen and carbon cycles.

## Acknowledgements

"Gratitude is the heart's memory". At this moment when I am winding up my Ph.D. thesis I wish to express a few words of gratitude for these people who gave their unflinching support with dedicated spirit and have been part of my life as teachers, friends and colleagues.

First and foremost I owe a deep sense of gratitude to my thesis supervisor Prof. R.Ramesh for his guidance, enduring encouragement and tolerance he has shown to me all throughout. I have been greatly benefited from his vast scientific knowledge and positive attitude. His ardent encouragement for achieving something in life has forced me to change my otherwise downbeat approach. On the personal side, he did not hesitate to invite his students to become an extended part of his life. I also sincerely thank Prof. P.P. Patel (Dept. of Geology, M.S. University of Baroda) for his interest in the work.

I am very much indebted to Prof. S. Krishnaswami, Prof. S.K. Bhattacharya, Prof. M.M. Sarin, Prof. S.V.S. Murty, Dr. T.R. Venkatesan, Dr. Kanchan Pande, Dr. P.N. Shukla of PRL and Dr. L.S. Chamyal of M.S. University of Baroda for encouragement during various stages, which has helped me to improve this work.

I also thank Dr. B.H. Subbaraya and Dr. R.R. Navalgund for putting me in touch with Space Applications Centre, Ahmedabad (SAC) scientists and for continued funding to the project under ISRO-GBP.

I cannot forget to thank my National Institute of Oceanography, Goa (NIO) colleagues for their help during this work. I am thankful to Dr. S. Prasanna Kumar and Late Dr. M. Madhuratap for giving me an opportunity to participate in the BOBPS cruises. Thanks are due to Dr. S. Sardesai, Dr. N. Ramaiah and Dr. N.B. Bhosle for nitrate and Chl *a* data during BOBPS cruises. I also thank Dr. Prabhu Matondakar and Dr. S.W.A. Naqvi of NIO for Chl *a* and nutrient data during Arabian Sea cruises. I thank my friends Jane, Loreta, Nisha, Xavita, Nuncio, Sapna, Asha, Anil and Jyoti Babu from NIO for making the BOBPS cruises memorable.

I am grateful to Prof. M. UdayaKumar, Dr. M.S. Sheshshayee (Shesha) and Dr. Bindu Madhava for making my analysis trips to Bangalore fruitful. I would always remember their company to "Green Park". I am thankful to Ram Mhatre of Thermo Electron and Bhushana for his help in various ways during my stay at Bangalore.

My sincere thanks to Dr. Andy Rees (Plymouth Marine Laboratory, U.K.), Dr. Paul Harrison (Hong Kong university of Science and Technology, Hong Kong) and Dr. N.Waser (University of British Columbia, Canada) for their patience to answer my queries regarding the <sup>15</sup>N technique during the initial stages of this work. I also thank Dr. M.V.M. Wafar of NIO for making me understand a few intricacies of the technique.

I wish to thank Dr. S. Nayak, Mr. R.M.Dwivedi, Ms. Mini Raman and Mr. Prakash Chauhan of SAC for arranging Arabian Sea cruises and help during remote sensing data analysis presented in the thesis. I also thank my friends Yashwant, Sushil,

Indrani, Arvind, Desmukh and Mukesh for their help and cups of tea whenever I went to SAC.

I thank Dr. M. Sudhakar and Mr. Subrahmanyam of NCAOR, Goa for helping me during ORV Sagar Kanya cruises. I also wish to thank the captain and crew of ORV Sagar Kanya (SK-182, SK-186 and SK-191) and FORV Sagar Sampada (SS-212) for their help during this work.

If I could complete four cruises on short notices it was because of help from N. B. Vaghela (radiocarbon lab), Bhavsar Bhai (chemistry lab), V.R. Shah (purchase) and Ramesh Bhavsar (stores). I thank Mrs. Ghiya, Mrs. Nishta A. Kumar, Mrs. Uma and Mr. Keyur of PRL Library for their support. I also thank the staff members of the computer centre.

Life would have been monotonous without my colleagues at PRL. First of all I would like to thank the "veterans" for scientific and non-scientific discussions during tea and lunch breaks. My sincere thanks to Jyoti, Ravi, Sunil, Dipu, Rama, A.D. Shukla, M.G. Yadava, Padiyajee, R.A. Jani and K. Rao for encouragement and support.

The road to this work has been long and winding, so I would also like to thank some people from early days. My thanks to PRL seniors Nandu, Kunnu, Vinay, Rajesh Rajneesh, Jitti, Soumen Da, Subrata and Koushik, who are in different parts of the world today, for creating lively atmosphere at PRL and hostel as long as they were here.

I am bereft of words when it comes to my batch mates. It would be impossible to forget them as each one is blessed with peculiar virtues: Santosh (provides 24 hours non-stop entertainment for free!), Neeraj (is 'very interactive' person), Sanyal (gets irritated and laughs aloud in no time), Manoj (always wore his heart on sleeves until he got married of course!), Sajan (always full of energy except in class rooms: rest time!), Pandey (an expert in interpreting the rules according to his own conveniences) and Harish (*motabhai!*). I thoroughly enjoyed their company and thank them from my heart. I especially thank Anirban who was always there for me whenever it mattered the most. I treasure his friendship. I also want to thank Pathak and Manish with whom I have shared innumerable cups of tea at *Kaka's dukan*. I thank my friends Lokesh, Sudhir, Jayendra, Sudeshna, Satraj, Tarak, Vinay, Morthekai, Jayesh, Nagar, Ganguly, Vikas, Satya and many others for making me feel at home.

Last but not least I thank my father and my brother Rajeev for their invaluable support all throughout without which it would have been difficult for me. I especially thank my mother who has always supported my dreams and aspirations. I thank her for all she is and all she has done for me.

# Contents

---

---

	List of tables	(v)
	List of figures	(vii)
<b>Chapter 1</b>	<b>Introduction</b>	<b>1-23</b>
1.1	Isotopic Fractionation of Nitrogen.....	3
1.2	Natural distribution of $^{15}\text{N}/^{14}\text{N}$ .....	5
1.3	Biogeochemical transformation of nitrogen in the marine environment.....	5
1.3.1	Nitrogen Fixation .....	6
1.3.2	Assimilation.....	7
1.3.3	Nitrification.....	8
1.3.4	Denitrification.....	8
1.3.5	Mineralisation.....	9
1.4	Global distribution of Nitrogen.....	9
1.5	Role of nitrogen and its isotopes in understanding the ocean biogeochemistry.....	9
1.5.1	Primary production and biological pump: Role in carbon cycle....	11
1.5.2	Concept of New and Regenerated production.....	13
1.5.3	Estimation of New, Regenerated and Export production.....	15
1.5.4	Basis for using nitrogen for new and regenerated production.....	16
1.5.5	$\delta^{15}\text{N}$ in suspended particulate matter.....	16
1.6	Earlier productivity related works in the world ocean and the study Area.....	17
1.7	Scope of the present work.....	19
1.8	Outline of the thesis.....	20
1.9	Scientific questions addressed.....	21
<b>Chapter 2</b>	<b>Materials and methods</b>	<b>23-53</b>
2.1	Introduction.....	25
2.2	New and Regenerated production estimation.....	26
2.3	Sampling.....	27
2.3.1	Bay of Bengal.....	27
2.3.2	Northeastern Arabian Sea.....	31
2.4	Nutrients.....	35
2.5	Tracer addition.....	36
2.6	Incubation.....	36
2.7	Filtration.....	37
2.8	Isotopic Analysis and Instrumentation.....	38
2.8.1	Principle of Analysis.....	38
2.8.2	Instrumentation.....	39

2.9	Standards Used and precision.....	43
2.10	<sup>15</sup> N atom% Measurement .....	43
2.10.1	<sup>15</sup> N atom% for blank samples.....	43
2.10.2	Error in <sup>15</sup> N atom% estimation.....	44
2.10.3	Linearity for <sup>15</sup> N atom%.....	44
2.11	Estimation of Particulate Nitrogen Content .....	45
2.11.1	Error in the Particulate Nitrogen Content estimates.....	47
2.12	Estimation of uptake rate.....	49
2.12.1	Concept of the general equation for uptake.....	49
2.12.2	Equation used for the calculation of uptake rate during the present study and involved uncertainties.....	50
2.13	Quality Control.....	52
2.14	Physical and chemical parameters.....	52
 <b>Chapter 3 The Northeastern Arabian Sea</b>		<b>54-107</b>
3.1	Introduction.....	55
3.2	<sup>14</sup> C based Productivity in the Arabian Sea.....	58
3.3	<sup>15</sup> N based productivity in the Northwestern and the Central Arabian Sea.....	62
3.4	Chlorophyll a, nutrients and physical parameters during January 2003 in the Northeastern Arabian Sea.....	63
3.4.1	Chlorophyll a.....	63
3.4.2	Nutrients.....	64
3.4.3	Hydrographic and meteorological conditions.....	66
3.5	<sup>15</sup> N based productivity study during January 2003.....	69
3.5.1	Total Production.....	69
3.5.2	New Production.....	71
3.5.3	Regenerated production.....	73
3.5.4	Rationale for preference of ammonium over nitrate.....	74
3.5.5	Vertical profile of Nitrate and Ammonium Uptake .....	76
3.5.6	f-ratio during January 2003.....	78
3.5.7	Effect of winter cooling on the f-ratio.....	80
3.5.8	Low f-ratio despite presence of nutrients in the water column.....	81
3.6	Chlorophyll a, nitrate and physical parameters during late February- early March 2003 in the Northeastern Arabian Sea.....	82
3.6.1	Chlorophyll a.....	82
3.6.2	Nitrate.....	84
3.6.3	Hydrographic and meteorological conditions.....	85
3.7	<sup>15</sup> N based productivity study during late February-early March 2003.....	88
3.7.1	Total Production.....	88
3.7.2	Regenerated Production.....	89
3.7.3	New production.....	90
3.7.4	Vertical profiles of nitrate uptake.....	92
3.7.5	f-ratio.....	93
3.7.6	Source of nutrients for the sustenance of the bloom.....	94

3.8	Natural Isotopic Composition of Surface Suspended Matter.....	96
3.8.1	January.....	98
3.8.2	Late February- Early March.....	98
3.8.3	Possible reasons for increased $\delta^{15}\text{N}$ .....	100
3.9	Conclusions.....	107

## **Chapter 4 The Bay of Bengal 108-172**

4.1	Introduction.....	109
4.2	Effect of tracer concentration and incubation time on the uptake rate of nutrients.....	110
4.2.1	Material and Methods.....	112
4.2.2	Physical conditions and nutrients at the experimental stations.....	113
4.2.3	Results and Discussion.....	115
4.3	Earlier measurements of $^{14}\text{C}$ based Productivity and Chl <i>a</i> in the Bay of Bengal.....	123
4.4	Chlorophyll <i>a</i> , nitrate and physical parameters during the postmonsoon (September-October) 2002.....	124
4.4.1	Chlorophyll <i>a</i> .....	124
4.4.2	Nitrate.....	125
4.4.3	Hydrographic and meteorological conditions.....	126
4.5	$^{15}\text{N}$ based productivity study during postmonsoon 2002.....	128
4.5.1	Total Production.....	128
4.5.2	New Production.....	129
4.5.3	Regenerated Production.....	131
4.5.4	f-ratio.....	132
4.6	Chlorophyll <i>a</i> , nitrate and physical parameters during premonsoon (April-May 2003) .....	133
4.6.1	Chlorophyll <i>a</i> .....	133
4.6.2	Nitrate.....	134
4.6.3	Hydrographic and meteorological Conditions.....	135
4.7	$^{15}\text{N}$ based productivity study during premonsoon 2003.....	137
4.7.1	Total Production.....	137
4.7.2	New Production.....	138
4.7.3	Regenerated Production.....	140
4.7.4	f-ratio.....	142
4.8	Implications of the new production measurements in the Bay of Bengal .....	143
4.9	Relationship between new and total production: possible implication.....	147
4.10	Possible nutrient sources to the Bay of Bengal.....	150
4.11	Natural Nitrogen Isotopic Composition of Suspended Matter.....	154
4.11.1	Surface suspended matter.....	154
4.11.2	Depth profiles of $\delta^{15}\text{N}$ of suspended matter.....	160
4.12	Primary productivity estimation using IRS P4 OCM.....	163
4.12.1	OCM data processing for Oceanic constituents.....	164
4.12.2	Estimation of Primary production.....	166
4.12.3	Discussion.....	168
4.13	Conclusion.....	172

<b>Chapter 5</b>	<b>Summary and scope for future work</b>	<b>173-181</b>
5.1	Important findings of this study.....	174
5.5.1	New productivity study in the Bay of Bengal.....	174
5.5.2	Results from uptake experiment.....	176
5.5.3	Natural isotopic composition of nitrogen in suspended matter of the Bay of Bengal.....	176
5.5.4	Total productivity comparison with IRSP4 data.....	177
5.5.5	New and regenerated production in the Northeastern Arabian Sea.....	177
5.5.6	Natural isotopic composition of nitrogen in the suspended matter of the Arabian Sea.....	178
5.2	Scope for future work.....	179
<b>References</b>	.....	<b>182-202</b>

# List of Tables

Table	Page
1.1	Common species of marine nitrogen..... 2
1.2	Global distribution of nitrogen (Tg N yr <sup>-1</sup> )..... 10
1.3	New or export production in different regions..... 17
2.1	Details of the cruises undertaken for the present study..... 25
2.2	Sampling locations along with dates of sampling during both pre and postmonsoon in the Bay of Bengal..... 28
2.3	Details of the sample depths during premonsoon season in the Bay of Bengal..... 31
2.4	List of stations with locations and dates of sampling during January 2003..... 33
2.5	Sampling depths during January 2003 in the Arabian Sea..... 33
2.6	List of stations along with locations and sampling dates during late February-early March..... 34
2.7	Sampling depths during Feb-March 2003 in the Arabian Sea..... 34
2.8	The calculated urea and ammonium concentrations using mesozooplankton displacement volume..... 35
2.9	Values and precision obtained during present study for standard materials used..... 43
2.10	The average value of <sup>15</sup> N atom% in the blank samples during the present study..... 44
2.11	The percentage error in <sup>15</sup> N atom% estimation during present study.... 44
2.12	A typical example for the method used for the calibration for the estimation of total nitrogen ..... 46
2.13	Calibration equations used for the estimation of total nitrogen content during the present study..... 48

<b>Table</b>	<b>Page</b>
<b>2.14</b> Percentage error in particulate nitrogen content in the Arabian Sea and the Bay of Bengal.....	49
<b>3.1</b> <sup>14</sup> C based average total productivity values reported for different seasons and locations in the Arabian Sea.....	61
<b>3.2</b> <sup>15</sup> N based productivity and f-ratio estimates during January 2003 in the Arabian Sea.....	79
<b>3.3</b> <sup>15</sup> N based productivity and f-ratio estimates during late February - early March 2003 in the Arabian Sea.....	94
<b>3.4</b> PON content and nitrogen isotopic composition in surface suspended matter during January and late February-early March.....	99
<b>4.1</b> Physical parameters at the experimental stations.....	114
<b>4.2</b> Comparison of specific uptake and uptake rates at two different stations for 4 h incubation at 0.01µM concentration.....	120
<b>4.3</b> Time-averaged fluxes of organic carbon (gC.m <sup>-2</sup> yr <sup>-1</sup> ) in sediment traps, 1000 m above sea floor.....	144
<b>4.4</b> The nitrate, ammonium and urea uptake rates in the Bay of Bengal during pre and postmonsoon.....	148
<b>4.5</b> PON content and δ <sup>15</sup> N of surface suspended matter observed during pre and post monsoon in the Bay of Bengal.....	155
<b>4.6</b> δ <sup>15</sup> N of particulate organic nitrogen in surface suspended matter from different oceanic regions of the world.....	160
<b>4.7</b> The technical specifications of IRS P4 OCM.....	164

# List of Figures

---

---

<b>Figures</b>		<b>Page</b>
<b>1.1</b>	Evolution of isotopic composition of substrate ( $\text{NO}_3^-$ ) and product ( $\text{N}_2$ ) for different fractionation factors as denitrification progresses....	4
<b>1.2</b>	Summary of $\delta^{15}\text{N}$ in biogenic nitrogen containing substances in the marine environment.....	5
<b>1.3</b>	Important biogeochemical transformations involving nitrogen and their relationships.....	6
<b>1.4</b>	Summary of US JGOFS primary productivity observations as compiled by Falkowski et al. (2003).....	12
<b>1.5</b>	Simplified nitrogen cycle in euphotic zone modified after Dugdale and Goering (1967).....	14
<b>1.6</b>	Export ratios calculated as a function of temperature and net photosynthesis rate (Laws et al. 2000).....	14
<b>1.7</b>	Export flux of particulate organic carbon ( $^{234}\text{Th}$ method) vs primary productivity (Buessler 1998) (source: Treguer et al. 2003).....	15
<b>2.1</b>	Locations showing all the CTD stations as well as new and regenerated production stations (PP).....	28
<b>2.2</b>	Sampling of seawater onboard ORV Sagar Kanya. ....	29
<b>2.3</b>	Sample Locations in the NE Arabian Sea.....	32
<b>2.4</b>	Filtration unit used during the present study.....	37
<b>2.5</b>	Schematic diagram showing the elemental analyzer set up.....	40
<b>2.6</b>	A typical chromatogram (for ammonium sulphate ~ 0.053mg) obtained during the present study.....	42
<b>2.7</b>	The linearity of $^{15}\text{N}$ atom% for (a) atropine and (b) ammonium sulphate over widely varying sample amounts.....	45
<b>2.8</b>	A typical example of calibration curves using different materials (atropine, ammonium sulphate and potassium nitrate).....	47

<b>Figures</b>	<b>Page</b>
3.1 A schematic representation of identified current branches during Northeast (top) and southwest (bottom) monsoon.....	56
3.2 Findlater jet along with region assumed to have positive and negative wind stress curl (Brock et al 1991).....	57
3.3 Euphotic zone integrated concentration (left panel) and vertical profile (right panel) of Chlorophyll <i>a</i> .....	64
3.4 The euphotic zone integrated (left panel) and vertical profile (right panel) of ambient nitrate at different stations during January 2003....	64
3.5 The euphotic zone integrated (left panel) and vertical profile (right panel) of ambient ammonium at different stations.....	65
3.6 The long-term average Sea surface Temperature (SST) of the Arabian Sea during January.....	66
3.7 Air temperature at different stations at the time of sampling (right panel) during January 2003.....	67
3.8 The monthly average of wind speed and direction over Arabian Sea (left panel, Source: Quikscat).....	67
3.9 Air pressure at the time of sampling during January 2003.....	68
3.10 Temperature profiles at different stations obtained with Satlantic Radiometer during January 2003.....	68
3.11 Salinity variation from south to north at sampling time during January 2003.....	68
3.12 <sup>15</sup> N based total productivity (estimated as sum of nitrate, ammonium and urea uptakes) observed during present study.....	69
3.13 New production observed at different locations during January 2003.....	71
3.14 Relationship between new and total production (excluding PP2) observed during January 2003 in the Arabian Sea.....	72
3.15 New (nitrate uptake) and Regenerated (ammonium + urea uptake) production observed in the Arabian Sea during present study.....	74
3.16 Vertical profile of nitrate uptake rates at discrete depths at different locations.....	76
3.17 Vertical profile of ammonium uptake rates at different depths at various locations.....	77

<b>Figures</b>	<b>Page</b>
<b>3.18</b> f-ratio observed (with and without urea) during January 2003.....	79
<b>3.19</b> The observed negative relationship between f-ratio and euphotic zone integrated nitrate (left panel).....	81
<b>3.20</b> Euphotic zone integrated (left panel) and vertical profiles (right panel) of Chlorophyll <i>a</i> at productivity stations.....	83
<b>3.21</b> The euphotic zone integrated (left panel) and vertical profiles (right panel) of ambient nitrate at different stations.....	84
<b>3.22</b> The long-term average Sea Surface Temperature (SST) of the northeastern Arabian Sea for the study period (1-10 March).....	85
<b>3.23</b> Air temperature measured over the northeastern Arabian Sea during sampling.....	86
<b>3.24</b> Wind speed over the Arabian Sea during Late February-early March..	86
<b>3.25</b> Air Pressure during sampling time in the Arabian Sea.....	86
<b>3.26</b> Temperature profile at different stations obtained with Satlantic Radiometer during Late February-Early March 2003.....	87
<b>3.27</b> <sup>15</sup> N based total productivity during late February-early March 2003...	89
<b>3.28</b> Components of regenerated production (ammonium and urea uptake).....	89
<b>3.29</b> New production observed at different locations during late February-early March in the northeastern Arabian Sea.....	90
<b>3.30</b> Observed relationship between new and total production in the Arabian Sea during late February and early March 2003.....	91
<b>3.31</b> Relationship between new production and euphotic zone integrated nitrate observed in the Arabian Sea.....	91
<b>3.32</b> Vertical profiles of nitrate uptake rates at various locations in the northeastern Arabian Sea during late February-early March.....	93
<b>3.33</b> f-ratios observed (with and without urea) in the northeastern Arabian Sea during the present study.....	94
<b>3.34</b> Relationship between the temperature based mixed layer depth and the residence time of nitrate in the water column.....	95

<b>Figures</b>	<b>Page</b>
<b>3.35</b> Relationship between $\delta^{15}\text{N}$ and PON during both cruises.....	99
<b>3.36</b> Relationship between $\delta^{15}\text{N}$ and $\text{NO}_3$ concentration during both cruises.....	100
<b>3.37</b> Geographical limits of the Arabian Sea denitrification zone delineated by Naqvi (1991).....	102
<b>3.38</b> Isotopic composition of nitrate and nitrogen gas with depth.....	103
<b>3.39</b> Relationship between fraction of remaining nitrate (f) and its isotopic composition for different fractionation factors.....	107
<b>4.1</b> Mean monthly water discharge of Ganges (averaged over 1985-1992) and Brahmaputra (averaged over 1969-1975).....	110
<b>4.2</b> The result of experiment 1 showing variation in specific uptake rate (top panel), uptake rate (middle panel) and f-ratio (bottom panel).....	115
<b>4.3</b> The result of experiment 2 showing variation in the specific uptake rate (top), uptake rate (middle) and f-ratio (bottom) .....	118
<b>4.4</b> Comparison of uptake results obtained from in-situ and simulated in-situ experiments.....	121
<b>4.5</b> The specific uptake rate at PP2 (left) and PP7 (right) for the incubation at different intervals during a day.....	122
<b>4.6</b> Euphotic zone integrated (left) and vertical profiles of Chl <i>a</i> at different productivity stations (right) in the Bay of Bengal.....	125
<b>4.7</b> Figures showing euphotic zone integrated (left) and vertical profiles of nitrate at different productivity stations.....	126
<b>4.8</b> The spatial distribution of salinity (top left), SST (top right), MLD (bottom left) and typical wind speed.....	127
<b>4.9</b> The euphotic zone integrated total column productivity (left) and relationship with $^{14}\text{C}$ based productivity (right), during postmonsoon.	128
<b>4.10</b> The euphotic zone column integrated nitrate uptake (left panel) and depth profile of nitrate uptake at different stations (right panel).....	130
<b>4.11</b> Euphotic zone integrated column uptake of ammonium (top left) and urea (top right).....	131

<b>Figures</b>	<b>Page</b>
<b>4.12</b> The upper bound of f-ratio (left) and relationship between f-ratio and total production during post monsoon in the Bay of Bengal.....	132
<b>4.13</b> Euphotic zone integrated (left) and vertical profiles of Chl <i>a</i> at different productivity stations during premonsoon .....	133
<b>4.14</b> Euphotic zone integrated (left) and vertical profiles of nitrate at different productivity stations .....	135
<b>4.15</b> Comparison of Salinity (top left), MLD (top right) and SST (bottom) during pre and postmonsoon in the Bay of Bengal.....	136
<b>4.16</b> The euphotic zone integrated total column productivity (left) and relationship with <sup>14</sup> C based productivity.....	138
<b>4.17</b> The euphotic zone column integrated nitrate uptake (left panel) and depth profiles of nitrate uptake at different stations.....	139
<b>4.18</b> Euphotic zone integrated column uptake of ammonium (top left) and urea (top right) during premonsoon. ....	141
<b>4.19</b> The upper bound of f-ratio (left) and relationship between f-ratio and total production during pre monsoon in the Bay of Bengal.....	142
<b>4.20</b> Relationship between total and new production. Top panel represents the Arabian Sea data from Watts and Owens (1999).....	149
<b>4.21</b> The relationship between $\delta^{15}\text{N}$ and PON during post (filled circles and squares represent offshore and shelf stations) and premonsoon.	155
<b>4.22</b> The relationship between salinity and $\delta^{15}\text{N}$ for post (filled circles and squares represent offshore and shelf stations) and premonsoon.	157
<b>4.23</b> The depth profiles of $\delta^{15}\text{N}$ and PON during premonsoon in Bay of Bengal at different stations. The filled and unfilled circles indicate $\delta^{15}\text{N}$ and PON respectively.	161
<b>4.24</b> The Log-Log plot of euphotic zone integrated insitu primary productivity estimated by <sup>15</sup> N technique and corresponding climatological mixed layer integrated OCM values. ....	169
 Plates showing OCM data based productivity maps for the Bay of Bengal	 170-171

# **Chapter 1**

## **Introduction**

---

---

Although Nitrogen (N) is one of the highly depleted elements on solid earth, it plays a tremendously important role in the environment, which encompasses regulating the oxygen in the atmosphere (Holland 1970) to carbonate compensation depth in the deep ocean (Ben-Yaakov et al. 1974). The cycling of nitrogen in our ecosystem is also one of the most important environmental issues. The primary production of food by photosynthesis is directly related to the nitrogen cycle and the productivity of many ecosystems is known to be controlled by nitrogen availability (Vitousek et al. 2002). Approximately 78% of the atmosphere is diatomic nitrogen (N<sub>2</sub>) but nitrogen in this form is normally unavailable for consumption by organisms due to the strong triple bond between two nitrogen atoms (N≡N). The limitation of the availability of nitrogen in reactive or biologically active forms (NO<sub>3</sub><sup>-</sup>, NH<sub>4</sub><sup>+</sup>, NH<sub>3</sub>, HNO<sub>3</sub> etc.) to grow more food due to demand from the growing human population has led to a very significant alteration of the nitrogen cycle in air, land and water at local, regional, and global scales (Galloway et al. 2004).

Nitrogen was formally named the 7<sup>th</sup> element of the periodic table (atomic number: 7) by Jean Antoine Claude Chaptal (1756-1832). Nitrogen has an atomic weight of 14.0067 and mass number 14. The whole earth abundance of N is only 0.03%, out of which 97.76% is stored in rocks, 2.01% in the atmosphere and the remaining in hydrosphere and biosphere (Hubner 1986). Nitrogen has five valence electrons and can take on oxidation states between +5 (NO<sub>3</sub><sup>-</sup>) and -3 (NH<sub>4</sub><sup>+</sup>). Most of the nitrogen compounds are soluble in water or are gaseous and do not form minerals except under special conditions. Most abundant minerals are NaNO<sub>3</sub> (sodaniter) and α-KNO<sub>3</sub> (niter) that occur in non-marine evaporate deposits in the arid regions of the earth. The most common species of marine nitrogen are listed in Table 1.1.

**Table 1.1** Common species of marine nitrogen.

<b>Species</b>	<b>Molecular Formula</b>	<b>Oxidation Number of Nitrogen</b>
Nitrate ion	NO <sub>3</sub> <sup>-</sup>	+V
Nitrite ion	NO <sub>2</sub> <sup>-</sup>	+III
Nitrous Oxide gas	N <sub>2</sub> O	+I
Nitric Oxide gas	NO	+II
Nitrogen gas	N <sub>2</sub>	0
Ammonia gas	NH <sub>3</sub>	-III
Ammonium ion	NH <sub>4</sub> <sup>+</sup>	-III
Organic amine	RNH <sub>2</sub>	-III

Nitrogen has two stable isotopes:  $^{14}\text{N}$  and  $^{15}\text{N}$  whose abundances in nature are 99.634 and 0.366% respectively. Nitrogen isotopic composition is generally reported in permil (‰) using the standard definition of  $\delta$  (delta):

$$\delta^{15}\text{N} (\text{‰}) = \left[ \left\{ \frac{(^{15}\text{N}/^{14}\text{N})_{\text{sample}}}{(^{15}\text{N}/^{14}\text{N})_{\text{standard}}} \right\} - 1 \right] * 1000$$

The standard for nitrogen is  $\text{N}_2$  in atmospheric air whose average abundance of  $^{15}\text{N}$  is constant with  $^{15}\text{N}/^{14}\text{N} = 1/272$  (Junk and Svec 1958).

## 1.1 Isotopic Fractionation of Nitrogen

Isotopic fractionation of light elements like N is a characteristic phenomenon in chemical, physical and biological processes that can be either reversible equilibrium or irreversible unidirectional kinetic reactions. Equilibrium controlled isotopic fractionation can be predicted theoretically (Urey 1947), whereas kinetically controlled fractionation (most biochemical processes) is determined empirically. The isotope effect of N is expressed in terms of fractionation factor ( $\alpha$ ). The fractionation factor for equilibrium exchange reaction  $\text{A} \leftrightarrow \text{B}$  is defined as:  $\alpha_{\text{B/A}} = (^{15}\text{N}/^{14}\text{N})_{\text{B}} / (^{15}\text{N}/^{14}\text{N})_{\text{A}}$ . Nitrogen is cycled in the marine environment in a complex manner mainly through metabolic nitrogen transformations that involves irreversible kinetic fractionation. The kinetic fractionation factors in such cases are highly variable depending on the kinetic mode of individual metabolic reactions, concentration of products and reactants, environmental conditions, and species of the organism. In general, the lighter isotope reacts faster resulting in a product isotopically lighter than the reactant, in contrast to reversible equilibrium reactions where products can be heavier or lighter than the original reactant. Kinetic fractionation factors can be defined as:

$$\alpha = (^{15}\text{N}/^{14}\text{N})_{\text{product}} / (^{15}\text{N}/^{14}\text{N})_{\text{reactant}}$$

Isotopic enrichment factor ( $\epsilon$ ) is defined as:  $\epsilon = (\alpha - 1) * 1000 \text{ ‰}$

The Rayleigh equation is used to describe the evolution of isotopic composition of the reactant (substrate) during both kinetic and equilibrium processes. The commonly used formulation for Rayleigh equation for a system with constant fractionation factor is given as:

$$R = R_0 f^{(\alpha-1)}$$

Where,  $R = ^{15}\text{N}/^{14}\text{N}$  of the substrate at any time,

$R_0 =$  initial  $^{15}\text{N}/^{14}\text{N}$  of the substrate,

$f$  = fraction of the remaining substrate, and

$\alpha$  = the fractionation factor between the product and the substrate.

In terms of isotopic composition the same can be expressed as:

$$\delta = \delta_0 + (\alpha - 1) * 1000 * \ln f = \delta_0 + \epsilon * \ln f$$

Where,  $\delta$  and  $\delta_0$  are the isotopic compositions of the substrate at any later time and the initial isotopic composition of the substrate.

In metabolic reactions, organisms prefer lighter ( $^{14}\text{N}$ ) over the heavier isotope ( $^{15}\text{N}$ ) resulting in an isotopically lighter product than the remaining substrate. For example, during the process of denitrification the microbes convert nitrate into final product  $\text{N}_2$  ( $\text{NO}_3^- \rightarrow \text{N}_2$ ) whose  $\delta^{15}\text{N}$  is always lighter than that of the residual  $\text{NO}_3^-$ . However, the isotopic composition of product is highly dependent on the value of the isotopic fractionation factor and fraction of reservoir left. Figure 1.1 shows a typical example of denitrification for different fractionation factors where  $\text{N}_2$  is the cumulative product  $\delta^{15}\text{N} = [-f/(1-f)] * (\delta_0 + \epsilon * \ln f)$  and  $\text{NO}_3^-$  is the residual substrate ( $\delta^{15}\text{NO}_3^-_{\text{initial}} = 0\text{‰}$ ).

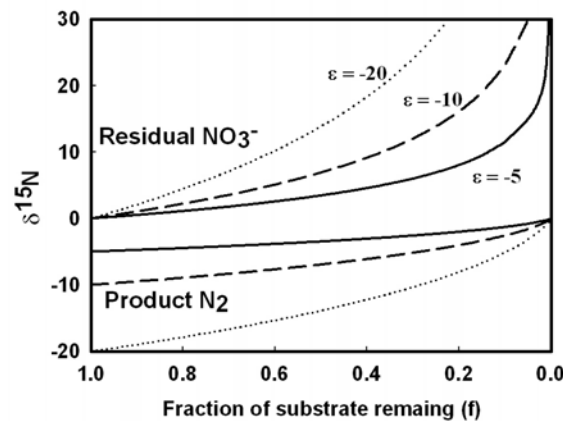


**Figure 1.1** Evolution of isotopic composition of substrate ( $\text{NO}_3^-$ ) and product ( $\text{N}_2$ ) for different fractionation factors as denitrification progresses.

The biological processes like nitrification ( $\text{organic-N} \rightarrow \text{NH}_4^+ \rightarrow \text{NO}_2^- \rightarrow \text{NO}_3^-$ ) or denitrification ( $\text{NO}_3^- \rightarrow \text{NO}_2^- \rightarrow \text{N}_2$ ) consists of number of steps with each step having a potential for isotopic fractionation. The overall isotopic fractionation for such reactions is highly dependent on environmental conditions, the number and types of intermediate steps, sizes of reservoirs of various compounds involved in the reactions and species of the organisms etc., making the estimation of isotopic fractionation in natural systems

very complex. Generally most of the isotopic fractionation is caused by the slowest step called "rate determining step" which is commonly associated with a large pool of substrate, with a small amount of material used (Kendall 1998).

## 1.2 Natural distribution of $^{15}\text{N}/^{14}\text{N}$

The overall range of reported  $\delta^{15}\text{N}$  values in natural systems covers 100‰, from about -50‰ to +50‰; however, most values fall within the much narrower spread from -10‰ to +20‰ (Heaton 1986; Owens 1987; Peterson and Fry 1987). The nitrogen isotopic variation in biological material was reported by Schoenheimer and Rittenberg (1939) for the first time whereas Miyake and Wada (1967) were first to report the  $^{15}\text{N}/^{14}\text{N}$  ratios of nitrogenous compounds occurring in marine environment. In general, marine organic material has higher  $^{15}\text{N}/^{14}\text{N}$  ratio than the terrestrial organic material mainly due to the different isotopic compositions of source materials. The major source of nutrient nitrogen for land plants is molecular nitrogen ( $\delta^{15}\text{N} = 0‰$ ) in the atmosphere (Sweeney et al. 1978) which is depleted with respect to nutrient sources available for marine phytoplankton ( $\delta^{15}\text{N}$  of nitrate  $\sim 3\text{-}7‰$  and  $\delta^{15}\text{N}$  of ammonium  $\sim$

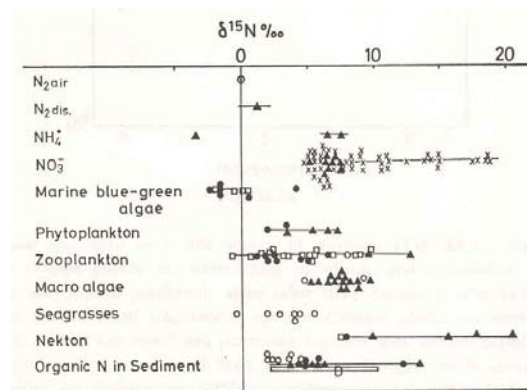


**Figure 1.2** Summary of  $\delta^{15}\text{N}$  in biogenic nitrogen containing substances in the marine environment (Miyake and Wada 1967; Cline and Kaplan 1975; Wada and Hattori 1976; Wada 1980).

6-8‰; Miyake and Wada 1967). On an average,  $\delta^{15}\text{N}$  of marine biogenic nitrogen relative to the atmospheric nitrogen is +7‰ (Wada 1980) and it increases along the food chain with each trophic step (DeNiro and Epstein 1981).  $^{15}\text{N}$  abundance in pelagic plankton is strongly related with the form and isotopic composition of inorganic nitrogen used for their growth (Wada and Hattori 1976). Figure 1.2 presents the summary of biogenic nitrogen bearing substances (Wada 1980) in the marine environment.

### 1.3 Biogeochemical transformation of nitrogen in the marine environment

Nitrogen is redistributed and recombined continuously by biochemical, physical and geological processes. The most important biochemical reactions and their interrelationship is shown in Figure 1.3:

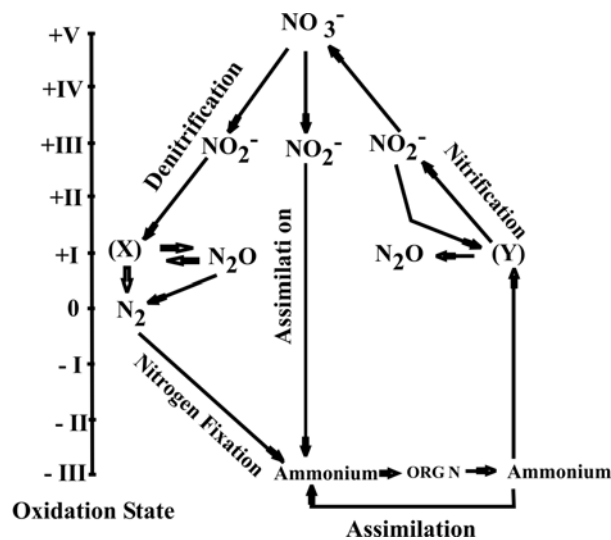
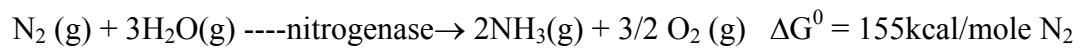


**Figure 1.3** Important biogeochemical transformations involving nitrogen and their relationships.

#### 1.3.1 Nitrogen Fixation

Nitrogen fixation is a process where unreactive atmospheric N<sub>2</sub> is converted into different forms of reactive nitrogen (NO<sub>x</sub>, NH<sub>y</sub>, and organic N) by a variety of algae and bacteria, both symbiotic and free living. The N<sub>2</sub> fixation in the oceanic environment takes place mainly by nonheterocystous cyanobacteria *Trichodesmium* and is understood to be a process of great importance in the oceanic nitrogen cycle and the biological sequestration of carbon (Capone 2001; Capone et al. 1997). Fixation of atmospheric N<sub>2</sub> by blue-green algae and other bacteria by the enzyme nitrogenase commonly produces organic material with δ<sup>15</sup>N comparable to or slightly lower than 0‰ (e.g., ~ 0.6‰; Emerson et al. 1991). Fogel and Cifuentes (1993) have shown fractionations (ε) ranging from -3 to +1‰ in concurrence with -2 to 0‰ reported by Minagawa and Wada (1986). Due to these lower values of δ<sup>15</sup>N of organic materials compared to those produced by other mechanisms, low δ<sup>15</sup>N in organic matter is often cited as evidence for N<sub>2</sub> fixation. The most simplified equation describing the nitrogen fixation reaction is (Sweeney et al. 1978):



There are two major limitations to biological nitrogen fixation:

- (I) The requirement for high amount of input energy to overcome the high activation energy of  $\text{N}\equiv\text{N}$ . Therefore organisms with highly developed catalytic system alone are able to fix nitrogen.
- (II) Nitrogen fixation is a reductive process and is highly sensitive to the presence of oxygen.

### **1.3.2 Assimilation**

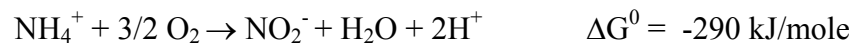
Assimilation refers to incorporation or uptake of N-bearing compounds like nitrate, ammonium and nitrite by organisms. Under normal oceanic conditions, nitrate is the most stable and therefore, the most common form of combined nitrogen (Delwiche 1981); however, ammonium may become significant where rate of degradation is greater than assimilation or nitrification. For those organisms that can directly utilise ammonium (termed as ammonium assimilation), this can be a significant nitrogen source. Direct ammonium assimilation results in a significant energy saving to provide the organisms a competitive advantage. During the assimilation process, oxidized forms of nitrogen are first reduced to ammonium by nitrate or nitrite reductases to be eventually assimilated into organic matter. The assimilation of N-bearing compounds by marine organisms is associated with isotopic fractionation where organisms prefer  $^{14}\text{N}$  to  $^{15}\text{N}$  forming one of the most important isotopic fractionation processes in the biogeochemical cycle of N in the ocean. However, the mechanism that controls this fractionation is poorly understood (e.g., Handley and Raven 1992). The fractionation for nitrate and ammonium assimilation by marine microorganisms measured in laboratory and field experiments show a wide variation (-27 to 0‰; Wada and Hattori 1978; Montoya and McCarthy 1995; Fogel and Cifuentes 1993; Waser et al. 1998). Assimilations by microorganisms in soils show a range of -1.6 to +1‰ (Hubner 1986) whereas by vascular plants show a range of -2.2 to +0.5‰ relative to soil organic matter (Mariotti et. al. 1980). The much larger range of fractionations observed in aquatic vs. soil environments reflects the interplay of several kinetic and equilibrium isotope effects as a function of environmental conditions.

### 1.3.3 Nitrification

Nitrification is a multi-step oxidation process mediated by several different autotrophic organisms for deriving metabolic energy (Delwiche 1981). Nitrate is the end product of nitrification with various nitrogen oxides ( $\text{NO}_2^-$ ,  $\text{NO}$ ,  $\text{N}_2\text{O}$ ) as intermediate products along with hydroxylamine ( $\text{NH}_2\text{OH}$ ) and other less stable compounds (Jaffe 2000). Because of intermediates like  $\text{N}_2\text{O}$ , a green house gas, nitrification has a significant role in the earth's radiation balance. Nitrification can be expressed in two energy yielding steps:

First, oxidation of ammonium to nitrite principally done by bacteria of genus

*Nitrosomonas*



Second, oxidation of nitrite to nitrate by *Nitrobacter*



Heterotrophic bacteria utilising organic compounds can also perform nitrification but this is much less significant than autotrophs (Bremner and Blackmer 1981). The overall isotopic fractionation involved during nitrification depends upon the rate determining step, i.e., slow oxidation of ammonium by *Nitrosomonas* rather than the oxidation of nitrite to nitrate, which is a rapid process. Miyake and Wada (1971) have reported an enrichment of remaining ammonium pool in the range of 0 to 21‰ in the marine environment whereas 12-29‰ has been reported for soils (Shearer and Kohl 1986) during nitrification.

### 1.3.4 Denitrification

Denitrification is a multi-step process where nitrate is reduced to  $\text{N}_2$  due to chemical or biologically mediated reduction with various nitrogen oxides (e.g.  $\text{N}_2\text{O}$ ,  $\text{NO}$ ) as intermediate products. Depending on the redox condition the organisms use different oxidized entities as electron acceptor during the degradation of organic matter in the general order:  $\text{O}_2$ ,  $\text{NO}_3^-$ ,  $\text{SO}_4^{2-}$ . When the conditions become anoxic ( $< 4\mu\text{M}$  in ocean water column; Devol 1978) the facultative bacteria (approximately 17 genera of anaerobic bacteria can utilise  $\text{NO}_3^-$ ) switch over to nitrate ions, which are the next most abundant source of free energy available for the oxidation of organic matter. Denitrification is of vital geochemical significance as  $\text{N}_2$  refluxed (80-100% of the

nitrogen release; Delwiche 1981) to the atmosphere makes it the only process where the major end product is removed from the biological nitrogen cycle. Under certain environmental conditions (low pH and higher O<sub>2</sub>) N<sub>2</sub>O can become a major product but the overall rate of denitrification decreases under such conditions. Denitrification also balances the natural fixation of nitrogen but the increasing industrial nitrogen fixation has the potential to change this balance (Delwiche 1970). Denitrification causes the  $\delta^{15}\text{N}$  of the residual nitrate to increase exponentially as nitrate concentration decreases. Different enrichment levels of residual nitrate have been reported: 0 to 21‰ (Miyake and Wada 1971); 14-23‰ (Blackmer and Bremner 1977). The highest enrichment of 40‰ has been reported for the oxygen depleted layer of eastern tropical North Pacific by Cline and Kaplan (1975).

### **1.3.5 Mineralisation**

Mineralisation is the decomposition of organic matter to inorganic matter. During mineralisation organic nitrogen is degraded to simple nitrogen compounds with ammonium as the final product. The excretion of waste nitrogen as urea or uric acid (sometimes ammonium) by marine organisms also comes under mineralisation. However, the major process of mineralisation is the degradation of organic matter by heterotrophic bacteria that includes dissolution of soluble substances, autolysis, deamination, ammonification, coagulation of dissolved substances and bacterial growth (Wada 1980). Mineralisation usually causes a small fractionation ( $\pm 2\text{‰}$ ).

## **1.4 Global distribution of Nitrogen**

The global distribution of various forms of nitrogen and its fluxes are listed in Table 1.2 as compiled by Galloway et al. (2004) from different sources. This Table presents the present, past and predicted future estimates of nitrogen in different reservoirs of the earth.

## **1.5 Role of nitrogen and its isotopes in understanding the ocean biogeochemistry**

Nitrogen availability in the marine euphotic zone is a significant modulator of the oceanic primary productivity and export production and, therefore, of C dynamics in diverse and expansive areas of the world's ocean. Intertwined sets of physical

processes and biological reactions of N contribute to N availability and the relative fertility of the upper ocean. However, the key processes of the N cycle and their

**Table 1.2** Global distribution of nitrogen ( $\text{Tg N yr}^{-1}$ ) compiled by Galloway et al. (2004).

	1860	Early 1990s	2050
<b>Nr Creation</b>			
Natural	246	233	224
Anthropogenic	15	156	267
<b>Total</b>	<b>262</b>	<b>389</b>	<b>492</b>
<b>Atmospheric Emission</b>			
<b>NO<sub>x</sub></b>			
Fossil Fuel Combustion	0.3	24.5	52.2
Lightning	5.4	5.4	5.4
Other emissions	7.4	16.1	23.9
<b>NH<sub>3</sub></b>			
Terrestrial	14.9	52.6	113
Marine	5.6	5.6	5.6
<b>N<sub>2</sub>O</b>			
Terrestrial	8.1	10.9	13.1+?
Marine	3.9	4.3	5.1
<b>Total (NO<sub>x</sub> and NH<sub>3</sub>)</b>	<b>13.1</b>	<b>46</b>	<b>82</b>
<b>Atmospheric deposition</b>			
<b>NO<sub>y</sub></b>			
Terrestrial	6.6	24.8	42.2
Marine	6.2	21	36.3
Subtotal	12.8	45.8	78.5
<b>NH<sub>x</sub></b>			
Terrestrial	10.8	38.7	83
Marine	8	18	33.1
Subtotal	18.8	56.7	116.1
<b>Total</b>	<b>31.6</b>	<b>103</b>	<b>195</b>
<b>Riverine Fluxes</b>			
Nr input into rivers	69.8	118.1	149.8
Nr export to inland systems	7.9	11.3	11.7
Nr export to coastal areas	27	47.8	63.2
<b>Denitrification</b>			
<b>Continental</b>			
Terrestrial		67	95
Riverine		47.8	63.2
<b>Subtotal</b>	<b>98</b>	<b>115</b>	<b>158</b>
<b>Estuary and Shelf</b>			
Riverine nitrate	27	47.8	63.2
Open Ocean nitrate	145	145	145
<b>Subtotal</b>	<b>172</b>	<b>193</b>	<b>208</b>

Nr refers to all biologically active, photochemically reactive and radiatively active nitrogen compounds ( $\text{NH}_3$ ,  $\text{NH}_4^+$ ,  $\text{NO}_x$ ,  $\text{HNO}_3$ ,  $\text{N}_2\text{O}$ ,  $\text{NO}_3^-$ , urea, amines and proteins).

relationships relating to upper ocean carbon dynamics vary among ocean environments. Our knowledge of the N cycle in the northeastern Arabian Sea and in particular, the Bay of Bengal remains rudimentary with respect to the quantitative relationships, controls and feedbacks. The present work aims to understand the biogeochemical aspect of nitrogen and its isotope in the northeastern Arabian Sea and the Bay of Bengal by estimating the natural isotopic variability in the surface suspended matter along with new and regenerated production using nitrogen isotope. The results obtained would help in understanding the nutrient utilization behavior and carbon fixation potential of the two basins. The following subsections discuss a few biogeochemical aspects relevant to the present work.

### **1.5.1 Primary production and biological pump: Role in carbon cycle**

Carbon dioxide is a green house gas and has an important influence on the radiative budget of atmosphere (Hansen et al. 1981). The concentration of carbon dioxide in atmosphere is constantly increasing due to anthropogenic emissions by about  $1\text{ppm yr}^{-1}$  (Keeling and Bacastow 1977) and is presently around more than 30% higher than before the industrial revolution (Keeling and Whorf 2000). Increasing concentration of  $\text{CO}_2$  in atmosphere is known to increase the earth's temperature by trapping the long wavelength radiation emitted by earth. Houghton et al. (2001) have suggested the rise in earth's temperature by  $0.6\pm 0.2^\circ\text{C}$ . The estimates of carbon sources and sinks for 1980s (Houghton et al. 2001) suggest that the rate of growth of  $\text{CO}_2$  in atmosphere ( $3.3\pm 0.1\text{ Pg C Yr}^{-1}$ ) is less than the rate at which it is being injected ( $5.4\pm 0.3\text{ Pg C Yr}^{-1}$ ). This difference is being taken up by ocean and terrestrial biosphere. The ocean takes up  $\text{CO}_2$  either chemically (solubility of  $\text{CO}_2$  and chemical buffering capacity of seawater) or biologically; the latter by the process of photosynthesis mainly by unicellular microscopic organisms known as phytoplankton. During photosynthesis phytoplankton take dissolved  $\text{CO}_2$  (or  $\text{HCO}_3^-$  depending on species) from the surface layer of ocean, and in presence of sunlight and water, make their bodies, essentially converting the inorganic carbon present in the surface ocean into organic carbon:



The rate at which the inorganic carbon is converted into organic carbon is known as primary productivity (PP) or total productivity and is expressed in terms of  $\text{mgC m}^{-2}\text{d}^{-1}$  or  $\text{mgC m}^{-2}\text{yr}^{-1}$ . The summary of US JGOFS primary productivity observations in

different parts of world ocean is shown in the Figure 1.4. Model estimates of global Net Primary Productivity (NPP) range from 45-57 Pg C yr<sup>-1</sup>, which is almost one half of the total NPP on the earth (Field et al., 1998). Model estimates by Maier-Reimer et al. (1996) suggest that the stopping of photosynthesis by phytoplankton would cause a

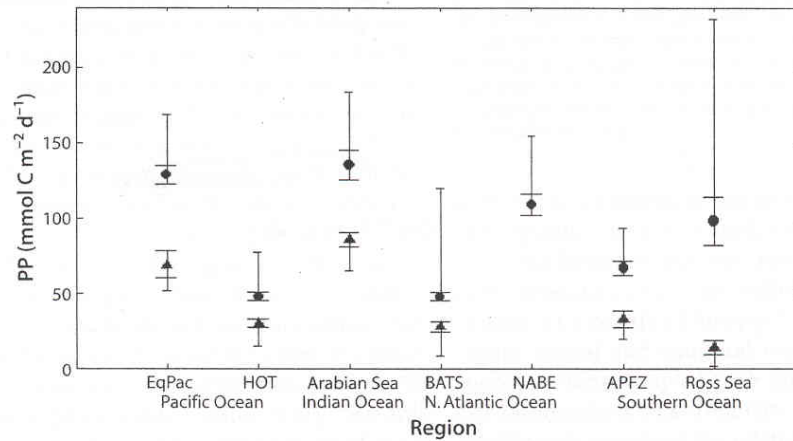
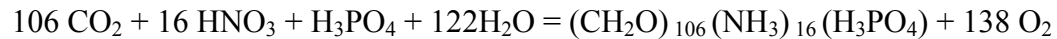


**Figure 1.4** Summary of US JGOFS primary productivity observations as compiled by Falkowski et al. (2003). Data sources are: EqPac (Barber et al. 1996), HOT (Karl et al. 1996); Arabian Sea (Barber et al. 2001), BATS (Steinberg et al. 2000), NABE, APFZ, and Ross Sea (Smith et al. 2000).

doubling of the atmospheric CO<sub>2</sub>. After completing their life cycle, organic matter produced in the surface layer of ocean sinks to the deeper layers and the sinking flux of organic matter (particle sinking, advection and diffusion of dissolved organic matter, and vertical migration of zooplankton) is said to be “exported”. The fraction of PP exported to the ocean interior is called “Export Production” (Berger et al. 1987). Once the organic matter crosses the main ocean thermocline (ventilation depth) they cannot ascend to the euphotic zone and suffer intense biodegradation and recycling in ocean interior to release nutrients and dissolved CO<sub>2</sub>. The upward transport of these released materials is very slow and they will not return to the surface water in centuries to millennium time scales, causing an enrichment of the ocean interior with inorganic carbon significantly higher than that predicted from equilibrium with the atmosphere. This process of organic matter sinking and regeneration of dissolved inorganic carbon effectively removes CO<sub>2</sub> from atmosphere by 400ppm (Watson and Orr 2003) and is known as the “Biological Pump”.

Phytoplankton need nutrients like nitrogen (N) and phosphorus (P) along with light and CO<sub>2</sub> for photosynthesis. The growth of phytoplankton is hampered if any of

these factors are "limiting". The traditional stoichiometric formula for the composition of marine phytoplankton organic matter:



suggests that the phytoplankton take up C: N: P in a fixed ratio of 106:16:1 known as the Redfield ratio (Redfield 1934), which is remarkably close to their ratio in the seawater. The productivity in the ocean is often limited by the supply of nutrients particularly N and P. There is considerable dispute as to which of these nutrients is limiting. Biologists favour N (Walsh 1981; Perry and Eppley 1981) whereas Geochemists (Broecker 1982) favour P as the limiting nutrient. However, nitrogen seems to be the limiting nutrient for life in the ocean today, whereas phosphorus may play a critical role on time scales of  $10^5$  years and longer (McElroy 1983).

### 1.5.2 Concept of New and Regenerated production

The concept of new and regenerated production was first proposed by Dugdale and Goering (1967) depending on the source of nitrogenous nutrients available in the euphotic zone for the phytoplankton to take up.

- (I) **New Production:** Part of primary production resulting from exogenous nitrogen inputs in the euphotic zone like newly incorporated  $\text{NO}_3^-$  or  $\text{N}_2$  from deeper waters and atmospheric or riverine input of nitrate and ammonium.
- (II) **Regenerated production:** Part of primary production that sustains on recycled nitrogen in the form of  $\text{NH}_4^+$ , urea, amino acids and dissolved organic nitrogen (DON) derived from excretory activities of animals and metabolism of heterotrophic organisms. There can be a contribution to the regenerated production from nitrate, due to bacterial nitrification within the photic zone (Dore and Karl 1996).

A simplified cycle of nitrogen proposed by Dugdale and Goering (1967) is shown in Figure 1.5. Under a quasi-steady state condition or an ideal closed system, ammonium can circulate indefinitely if there is no loss from phytoplankton population. However, ocean primary production system is real and there are losses through sinking and mixing and by predation by zooplankton. The sum of losses in form of export production is balanced by nitrate uptake or by nitrogen fixation or by any other possible sources of non-regenerated nitrogen i.e., export production is equal to new production

under a steady state condition (Eppley and Peterson 1979). However, on longer time scales new production is known to be coupled to export production even under non steady state (Eppley et al. 1983) and is referred interchangeably as new production (Sarmiento and Siegenthaler 1992). The ratio of new to total production is called the f-ratio (Eppley and Peterson 1979):

$$\text{New production} / \text{Total Production} = \text{f-ratio.}$$

The f-ratio represents the probability that a nitrogen atom is assimilated by phytoplankton due to new production and (1-f) is the probability of assimilation by regenerated production. The number of times a nutrient is recycled in euphotic zone before sinking in particulate form is given by (1-f)/f.

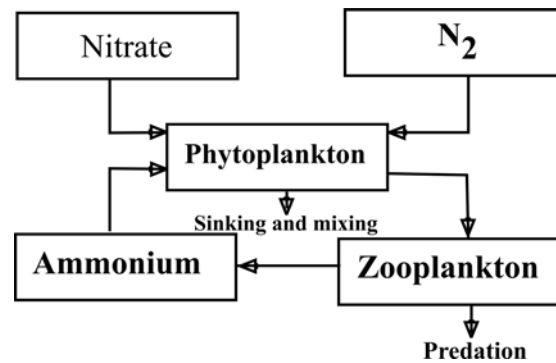


**Figure 1.5** Simplified nitrogen cycle in euphotic zone modified after Dugdale and Goering (1967).

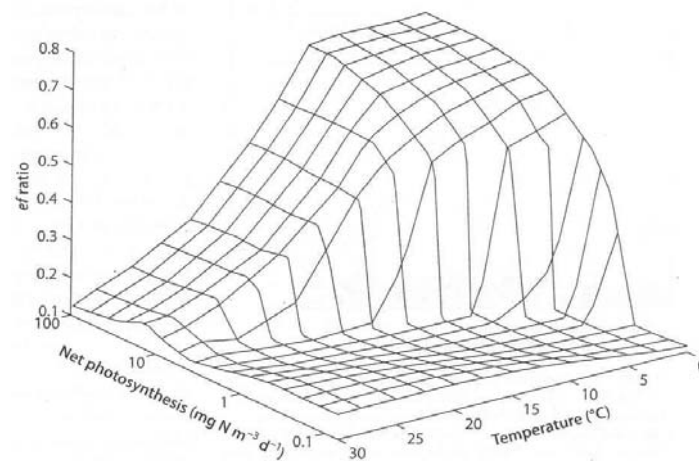


**Figure 1.6** Export ratios calculated as a function of temperature and net photosynthesis rate (Laws et al. 2000).

In the open ocean approximately 90% of NPP is supported by regenerated nutrients produced by small grazers and heterotrophic bacteria (Harrison 1980) and bacterial

productivity may average 20% of the NPP (Cole et al. 1988; Ducklow 1999). In general, a hyperbolic relationship exists between primary production and f-ratio (Eppley and Peterson 1979). The ratio of export to primary production is referred as e-ratio (Murray et al. 1989) and is found to be a function of primary production per unit volume and temperature (Figure 1.6; Laws et al. 2000)

### 1.5.3 Estimation of New, Regenerated and Export production

The  $^{15}\text{N}$  labelled nitrate and ammonium is used as a tracer for estimating new and regenerated production (JGOFS report 1996). New production has also been reported to be estimated from the rate of change of nitrate concentration (Allen et al. 1996). The methods and techniques used for new and regenerated production estimation during present study have been discussed in detail in the next chapter. Nitrogen fixation in some part of oceans (Karl et al. 1997; Zehr et al. 2001) and nitrification between 1 and 0.1% light level (Dore and Karl 1996) is known to contribute significantly to new production whereas release of  $\text{DO}^{15}\text{N}$  from cells during incubation results in its underestimation (Bronk et al. 1994). Export flux is generally studied by sediment traps moored in the deep ocean (Honjo et al. 1992) but microbial activity at shallower depths and behaviour of traps in moving fluids pose limitations to the method. However, export production is estimated using  $^{234}\text{Th}$  method where export flux of Th is converted to carbon knowing the ratio of carbon to  $^{234}\text{Th}$  (Buesseler et al. 1992). Most estimates of export production provide only the flux of sinking organic matter and do not include advection of dissolved organic matter (DOM) and migration of zooplankton. Therefore, the estimates of new production using only  $^{15}\text{NO}_3$  and export production for only

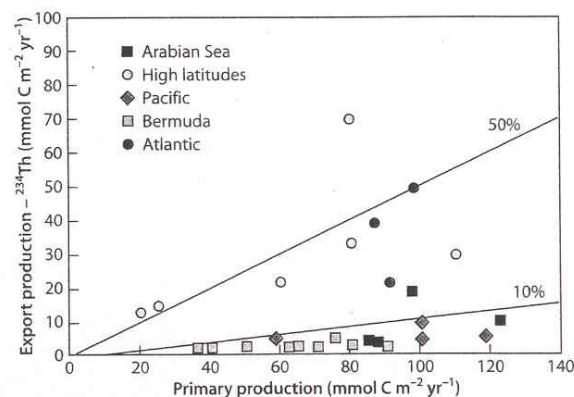


**Figure 1.7** Export flux of particulate organic carbon ( $^{234}\text{Th}$  method) vs primary productivity (Buesseler 1998) (source: Treguer et al. 2003).

particulate matter provide lower estimates of new and export productions. The relationship observed between primary production and export flux derived from  $^{234}\text{Th}$  shows that the export flux is more than 50% of the annual primary productivity in high latitudes and usually less than 10% in oligotrophic gyres (Figure 1.7).

#### **1.5.4 Basis for using nitrogen for new and regenerated production**

New and regenerated production can be estimated from any major elements contained in phytoplankton but nitrogen is used for the following advantageous reasons (Dugdale and Goering 1967):

- (i) It is a major structural component of cells and reasonably constant in its ratio to C and P.
- (ii) It shows less scatter than C and P as these two are not only structural components but also continuously turned over in energetic processes of organisms.
- (iii) Various forms of inorganic nitrogen allow to distinguish allochthonous and autochthonous inputs.

#### **1.5.5 $\delta^{15}\text{N}$ in suspended particulate matter**

Abundance of  $^{15}\text{N}$  in marine organic and inorganic pools is known to vary significantly over range of spatial and temporal scales (Saino and Hattori 1980; Owens 1987; Altabet 1996; Rau et al. 1998). These variations are basically caused by mass dependent fractionations associated with various biogeochemical transformations. These  $^{15}\text{N}$  signals have the potential to provide the information on the mechanisms and rates of these transformations and largely reflect the isotopically selective processing of nitrogen by biota (Rau et al. 1998). Isotopic fractionation associated with particulate nitrogen formation governs the isotopic signature in the particulate nitrogen and therefore  $\delta^{15}\text{N}$  of suspended particulate matter ( $\delta^{15}\text{N}_{\text{sus}}$ ) records the nitrogen availability in the euphotic zone (Wada and Hattori 1991). The isotopic fractionation imparted during the biological incorporation of nitrogen substrates into particulate matter varies with substrate concentration as well as with algal species, physiology and growth rate (Wada and Hattori 1978; Wada 1980; Montoya and McCarthy 1995; Waser et al. 1998). Observed significant correlation between  $\delta^{15}\text{N}_{\text{sus}}$  and nitrate concentration and variation in  $\delta^{15}\text{N}_{\text{sus}}$  have been explained by Rayleigh fractionation kinetics for

closed system (Altabet 1996) implying the usability of  $\delta^{15}\text{N}_{\text{sus}}$  as index of nutrient availability and utilization. Consequently,  $\delta^{15}\text{N}$  in sediments have been used to reconstruct paleonutrient conditions and biological productivity (Calvert et al. 1992; Francois et al. 1992; Altabet and Francois 1994; Farrell et al. 1995).

## 1.6 Earlier productivity related work in the world ocean and the study Area

The quest for understanding the biogeochemical fluxes have evolved into various interdisciplinary programmes since mid-80's. The VERTEX (Vertical Exchange Processes) in the North Pacific was the first large-scale programme to focus on the coupling of new and export productions. Other programmes with focus on new production were 1888 WECOMA cruise in equatorial pacific (Barber 1992), JGOFS equatorial pacific (EQPAC, Barber et al. 1994), Research on Antarctic Coastal Ecosystem Rates (RACER; Huntley et al. 1991), Subarctic Pacific Ecosystem research (SUPER) in the north Pacific (Miller et al. 1991; Miller 1993), 1988 Black Sea Expedition (Murray 1991), the JGOFS North Atlantic Bloom Experiment (NABE, Ducklow and Harris 1993), and the JGOFS time series experiments at Bermuda and Hawaii (Lohrenz et al. 1992; Malone et al. 1993; Roman et al. 1993). The new or export production data obtained from different areas using different methods in world ocean are listed in Table 1.3.

**Table 1.3** New or export production in different regions (compiled by Falkowski et al. 2003).

Areas	New or Export Production $\text{mg N m}^{-2} \text{d}^{-1}$	References
BATS	7.8	Michaels et al. (1994)
HOT	12.2	Emerson et al. (1997)
NABE	98	Bender et al. (1992)
		McGillicuddy et al. (1995)
EqPac-normal	32.1	McCarthy et al. (1996)
EqPac-El Nino	12.3	McCarthy et al. (1996)
Arabian Sea	29.2	McCarthy et al. (1999)
Ross Sea	165	Asper and Smith (1999)
Subarctic Pacific	40.3	Sambrotto and Lorenzen (1987)
		Emerson et al. (1993)
Station P		Wong et al. (1998)
Peru-normal	339	Wilkerson et al. (1987)
Peru-El Nino	256	Wilkerson et al. (1987)
Greenland Polynya	35.6	Smith (1995)

On the basis of new production global ocean can be divided into three regions (Ducklow 1995): (i) regions where nitrate is renewed each winter and depleted in spring (ii) regions where high level of nitrate persists throughout the year (iii) regions where nitrate is permanently depleted in the euphotic zone. The supply of nitrate due to mixing during winter is known to increase new production or causes phytoplankton blooms in the different oceanic regions of the world, such as coastal and shelf regions (Townsend et al. 1992; Hansell et al. 1993); Southern Ocean (Holm-Hansen and Mitchell 1991; Sullivan et al. 1993) and North Atlantic (Sambrotto et al. 1993). In such cases, production and consumption processes get uncoupled (Karl et al. 1991; Banse 1992) leading to episodic export of biomass (Honjo and Manganini 1993). There are regions like subarctic north Pacific and central equatorial Pacific where surface nitrate is high but biomass level is low and these are known as "high-nutrient, low-chlorophyll" or HNLC regions (Cullen 1991). In general new production has been reported to be low in HNLC (Dugdale et al. 1992). High grazing rate (Frost and Franzen 1992) or ammonium excretion from grazers are speculated to inhibit nitrate uptake (Wheeler and Kokkinakis 1990). In the oligotrophic gyres, the surface ocean is almost devoid of nitrate, but is known to maintain a significant new production even in the absence of new nitrate from deeper layers. The other sources suggested for such significant new production are nitrate enriched buoyant mats of diatoms (Villareal et al. 1993) or atmospheric inputs of nitrogen species. However, the latter causes only 1-2% of global new production. Sometimes the atmospheric inputs of nutrients can drive local blooms (Michaels et al. 1993) or can stimulate new production in nutrient poor waters (DiTullio and Laws 1991).

The western Arabian Sea has been studied thoroughly for its physical, chemical and biological characteristics during the JGOFS (Smith 2001). The northeastern Arabian Sea, a part of the present study area, was also studied for its physical, chemical and biological aspects. However, new production in this region was not measured. The present work is **the first attempt** to estimate the new production in the region. Another part of the study area, i.e., the Bay of Bengal, remains almost an unexplored basin regarding its biogeochemical aspect. The present work estimates the new production in the Bay of Bengal for **the first time** and correlates it with the organic carbon fluxes observed by the sediment trap data (Ittekkot et al. 1991; Unger et al. 2003).

New and regenerated production in the northwestern Arabian Sea was estimated thoroughly during JGOFS by three different groups: McCarthy et al. (1999);

Watts and Owens (1999) and Sambrotto (2001). McCarthy et al. (1999) focussed on nitrogen dynamics during the northeast (NE) monsoon to ascertain the relative importance of different nitrogenous nutrients and regeneration process. They found evidence for a widespread suppressing effect of  $\text{NH}_4^+$  on the  $\text{NO}_3^-$  uptake and a high affinity for low concentrations of  $\text{NH}_4^+$ , leading to low f-ratios of 0.15 and 0.13 during the early and late NE monsoon. The regeneration rate of  $\text{NH}_4^+$  was found comparable to its uptake rate maintaining a constant mixed layer concentration. Watts and Owens (1999) measured nitrate, ammonium and urea assimilation rates during intermonsoon and found the integrated total nitrogen assimilation rates varying between 1.1 and  $23.6 \text{ mmol N m}^{-2} \text{ d}^{-1}$ . Ammonium was found to be the preferred substrate at most of the stations, also reflected in the low f-ratios ( $\leq 0.52$ ). Sambrotto (2001) measured planktonic nitrogen productivity and regeneration during the spring intermonsoon and the southwest monsoon in the northern Arabian Sea and found the new production and f-ratio varying from 0.1 to  $13 \text{ mmol N m}^{-2} \text{ d}^{-1}$  and 0.03 to 0.4 respectively. The inclusion of urea uptake rate in the total production lowered the f-ratio by 29%. Although the above mentioned three studies were carried out in different seasons, regenerated production was found to be consistently more important than new production in the Arabian Sea, leading to a lower f-ratio.

### **1.7 Scope of the present work**

The present work investigates the biogeochemical aspects of nitrogen and its isotopes in the northeastern Arabian Sea and the Bay of Bengal by estimating the variations in natural nitrogen isotopic composition of suspended matter and new and regenerated production during different seasons. To achieve this goal the following studies were carried out:

- 1.** Measurement of the natural isotopic composition and concentration of nitrogen in surface suspended particulate matter of the northeastern Arabian Sea during January and late February-early March 2003. The aim of this study was to assess the possible change in nutrient source and its effect on nitrogen isotopic composition of suspended matter during the middle and waning phases of winter cooling.
- 2.** Measurement of the natural isotopic composition and concentration of nitrogen in surface suspended particulate matter in the Bay of Bengal during pre and

postmonsoon seasons. This would help in understanding the nitrogen isotope biogeochemistry of suspended matter and assessment of possible nutrient sources for the phytoplankton in the region, particularly the effect of freshwater discharge.

**3.** Obtaining the vertical profile of nitrogen isotopic composition and concentration of suspended matter in the Bay of Bengal. This would help in understanding the process of degradation or degeneration of suspended matter at depth.

**4.** New production estimation in the northeastern Arabian Sea during January and late February-early March 2003. This would help to understand the effects of winter cooling on new production and change in new production from one month to another.

**5.** The estimation of new and total production in the Bay of Bengal during pre and postmonsoon seasons. The result would help in understanding the possible role of moderately productive oceanic regimes in the global carbon cycle.

**6.** The estimation of primary productivity for the Bay of Bengal using indigenous satellite data (IRS P4 OCM - Ocean Colour Monitor) in order to have a wide spatial and temporal coverage of the region. The results obtained have been compared with *insitu* data.

**7.** Experiments were performed to assess the variation in the uptake rates of different nitrogenous nutrients due to variations in time and concentrations of substrates. This would help in fixing the right incubation period and substrate addition for future new production experiments for optimum results.

## **1.8 Outline of the thesis**

This thesis has been divided into five chapters. Their contents are as follows:

**Chapter 1** describes in general nitrogen isotopes and their fractionation behaviour during different biogeochemical transformations. It also deals with the natural variability of nitrogen isotopic composition along with the concepts of new and

regenerated productions and a brief review of relevant literature on the world ocean and the study area.

**Chapter 2** deals with the sampling details during the cruises and experimental methods followed during present study.

**Chapter 3** discusses the results obtained during present study for the Arabian Sea, including the natural variability of nitrogen isotopes and new and regenerated production estimates during January and late February-early March. It also discusses the effect of winter cooling on new production and the reason for bloom during early March.

**Chapter 4** deals with the results of present study for the Bay of Bengal that include the results of the uptake experiments, new and conservative estimates of regenerated production during post and premonsoon seasons and also the surface and vertical variation in the nitrogen isotopic composition of suspended matter. It also investigates the reasons for comparable organic carbon fluxes in sediment traps in the Arabian Sea and the Bay of Bengal and possible nutrient sources for the sustenance of the observed new production.

**Chapter 5** summarises the results obtained during present study, highlighting the important findings. It also presents the scope for future research that may lead to a better understanding of nitrogen and carbon cycles of this region.

### **1.9 Scientific questions addressed:**

The present study has attempted to answer the following scientific questions:

Arabian Sea:

- What is the isotopic composition and concentration of particulate organic nitrogen (PON) during the middle and the waning phases of the northeast (NE) monsoon?
- What is the effect of winter cooling on the isotopic composition and the concentration of PON?

- Does the change in the isotopic composition and the concentration of PON a reflection of a changed nutrient regime?
- Has the change in nutrient regime to do with denitrification or is it a simple surficial phenomenon?
- What are the new and total production values during the NE monsoon?
- Does winter cooling influence the new production and the f-ratio?
- What is the change in new production from peak winter cooling to its waning phase?
- What are the possible sources of nutrients that sustain the bloom during the late NE monsoon?
- Why is there limited new production despite the availability of nitrate during winter cooling?

#### Bay of Bengal:

- What are the new and total production values during pre and post monsoon?
- What is the role of Bay of Bengal in the global carbon cycle?
- Do the moderately productive basins have really a limited role to play in carbon and nitrogen cycles?
- Is higher new production responsible for low surface  $p\text{CO}_2$  as previously hypothesised?
- High new production: a possible reason for oxygen minimum zone (OMZ)?
- What are the possible nutrient sources?
- What are the isotopic composition and PON concentration during different seasons?
- Does terrestrial influence significantly modify the isotopic composition of suspended matter?
- How does the isotopic composition of suspended matter change with depth?
- Does the rapid sinking of organic matter influence the isotopic composition at depth?
- Does IRSP4 OCM data provide reliable estimates of total productivity?

## General

- What is the reason for comparable organic carbon fluxes in sediment traps in the Arabian Sea and Bay of Bengal?
- What is the effect of incubation time and concentration on the uptake rate?

# **Chapter 2**

## **Materials and Methods**

---

---

## 2.1 Introduction

The main aim of this thesis, as mentioned in the earlier chapter, is to estimate new and regenerated productions along with natural nitrogen isotopic variability in suspended matter of the northern Indian Ocean and evaluate its carbon fixing capability. To carry out the present study, four cruises were undertaken, two each in the Bay of Bengal and the Arabian Sea. The cruise number, seasons, duration, and the ships on which the studies were carried out are listed in Table 2.1.

**Table 2.1** Details of the cruises undertaken for the present study.

### Bay of Bengal

Cruise No.	Season	Cruise duration	Ship
SK-182	Postmonsoon	17 <sup>th</sup> Sep-11 <sup>th</sup> Oct 2002	ORV Sagar Kanya
SK-191	Premonsoon	16 <sup>th</sup> Apr-6 <sup>th</sup> May 2003	ORV Sagar Kanya

### Arabian Sea

Cruise No.	Season	Cruise duration	Ship
SK-186	NE monsoon	4 <sup>th</sup> Jan-17 <sup>th</sup> Jan 2003	ORV Sagar Kanya
SS-212	Late NE monsoon	28 <sup>th</sup> Feb-5 <sup>th</sup> Mar 2003	FORV Sagar Sampada

The cruises on which present study was carried out in the Bay of Bengal and in the Arabian Sea had different purposes. The Bay of Bengal study was carried out on cruises intended for a programme known as BOBPS (Bay of Bengal Process Studies), aimed at thoroughly studying the Bay's physical, chemical and biological parameters. BOBPS is a Department of Ocean Development programme mainly carried out by scientists from National Institute of Oceanography (NIO), Goa, India. Present study is a part of BOBPS; it was performed in collaboration with NIO scientists where they mainly contributed nitrate and Chl *a* data required for the present study.

The Arabian Sea cruises were undertaken in collaboration with Space Applications Centre (SAC), Ahmedabad, India. These were basically the biological parameter retrieval and validation cruises for Ocean Colour Monitor (OCM), an ocean colour sensor on Indian Remote Sensing Satellite IRS P4 launched in May 1999. Since the objective, group and logistics were different during different cruises of the present study, different sampling procedure and timings were followed. The information

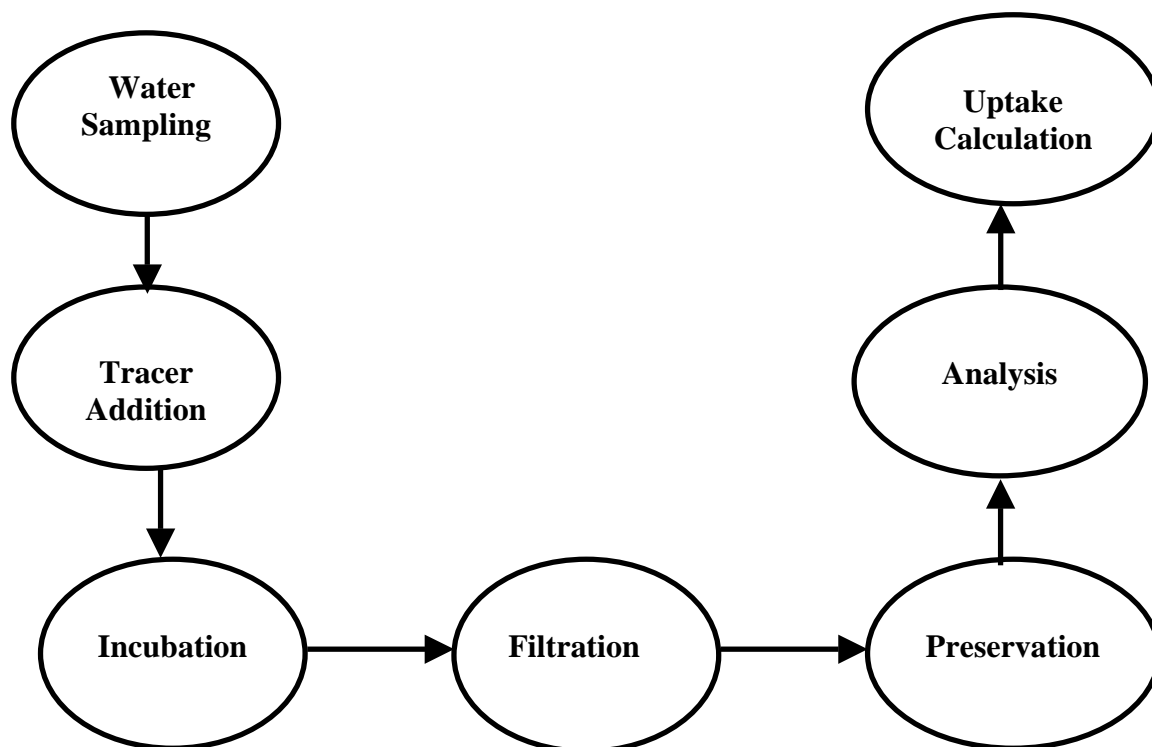
regarding the stations, sampling procedure, nutrient estimation and other physical properties are described in different subsections to follow.

## 2.2 New and Regenerated production estimation

For new and regenerated production estimation the Joint Global Ocean Flux Study (JGOFS) Protocol was followed. The principle and requirements for the measurements are as follows:

**Principle:** During the present study the nitrate uptake would be considered as new production whereas sum of ammonium and urea uptakes would be regenerated production. The measurement of nitrate uptake is based on the incorporation of 'trace' addition of  $^{15}\text{N}$ -labelled nitrate by the phytoplankton during incubation experiments. Similarly the estimation of regenerated production is based on  $^{15}\text{N}$ -labelled ammonium and urea incorporation.

The steps involved in the estimation of new and regenerated production are shown in the flow chart below:



**Requirements:** The determination of the uptake experiments requires the knowledge of following parameters:

- A. The initial substrate concentration ( $\text{NO}_3^-$ ,  $\text{NH}_4^+$  or Urea).
- B. Final concentration of particulate nitrogen.
- C. The final  $^{15}\text{N}$  enrichment of particulate matter.
- D. The enrichment level of dissolved fraction after tracer addition.

### **Preparation of tracer solution**

The  $^{15}\text{N}$ -labelled (99 at% enriched) nitrate ( $\text{NaNO}_3$ ), ammonium ( $\text{NH}_4\text{Cl}$ ) and urea ( $\text{NH}_2\text{-CO-NH}_2$ ) salts in dry chemical form were procured from Sigma-Aldrich (USA). The stock solutions were prepared to contain 0.5mmol of  $\text{NaNO}_3$ ,  $\text{NH}_4\text{Cl}$ , or urea in 250ml of solution (0.5 mmol/250ml). For that 43mg of  $\text{NaNO}_3$  (molecular weight ~85.98 g), 27.24 mg of  $\text{NH}_4\text{Cl}$  (molecular weight ~54.48 g), and 31 mg of urea (molecular weight~62.04 g) were added in three different volumetric flasks containing 250ml of doubled distilled water and mixed thoroughly to make a homogeneous solution and was later transferred to 250ml NALGENE bottles for further use. The working solutions were prepared from the stock solution in two different concentration levels: the first containing 0.01 $\mu\text{mol}$   $\text{NO}_3^-$  ( $\text{NH}_4$  or urea) per ml and other containing 0.1  $\mu\text{mol}$   $\text{NO}_3^-$  per ml of solution. To prepare the former, 5ml of the stock solution (contained 0.01mmol of  $\text{NO}_3^-$ ,  $\text{NH}_4^+$  or urea) was added to 995ml of double distilled water. This solution contained 0.01mmol  $\text{NO}_3^-$ ,  $\text{NH}_4^+$  or urea per 1000ml i.e., 0.01 $\mu\text{mol}$  per ml of solution. The latter solution was prepared by adding 12.5ml of stock solution to 237.5ml of distilled water, which lead to the concentration of 0.1  $\mu\text{mol}$  per ml of solution. The weighing of the salts was done using Thomas Scientific weighing paper on Sartorius microbalance (model no: MC-5; Germany).

## **2.3 Sampling**

### **2.3.1 Bay of Bengal**

The locations where the seawater samples were collected in the Bay of Bengal during post and premonsoon are shown in the Figure 2.1. Nine stations, during both seasons, were sampled for new and regenerated production studies referred henceforth as PP1 to PP9. However, surface water samples were collected at 24 locations for natural isotopic variability studies in the suspended matter. The details of sampling locations along with the dates of sampling are listed in Table 2.2.

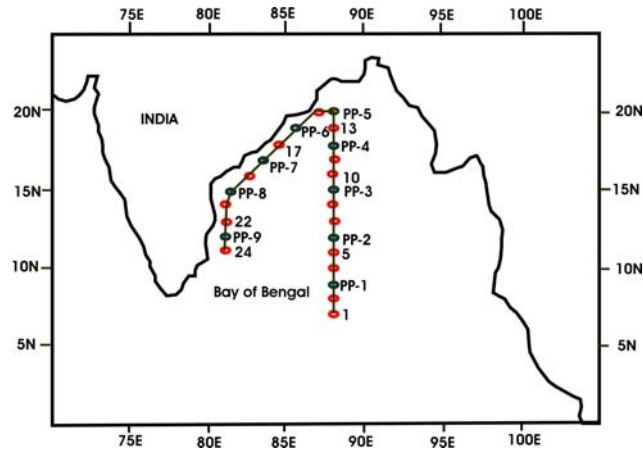


**Figure 2.1** Locations showing all the CTD stations as well as new and regenerated production stations (PP) during post (SK-182) and premonsoon (SK-191) in the Bay of Bengal.

**Table 2.2** Sampling locations along with dates of sampling during both pre and postmonsoon in the Bay of Bengal.

Stns.	New Production Stations	Latitude (°N)	Longitude (°E)	Premonsoon Sampling Date (D/ M /Y)	Postmonsoon Sampling Date (D/ M /Y)
1		7	88	16/04/2003	17/09/2002
2		8	88	17/04/2003	18/09/2002
3	PP1	9	88	18/04/2003	18/09/2002
4		10	88	19/04/2003	20/09/2002
5		11	88	19/04/2003	20/09/2002
6	PP2	12	88	20/04/2003	21/09/2002
7		13	88	21/04/2003	22/09/2002
8		14	88	21/04/2003	22/09/2002
9	PP3	15	88	22/04/2003	23/09/2002
10		16	88	23/04/2003	24/09/2004
11		17	88	23/04/2003	24/09/2002
12	PP4	18	88	24/04/2003	26/09/2004
13		19	88	25/04/2003	26/09/2004
14	PP5	20	88	26/04/2003	29/09/2004
15		20	87	27/04/2003	30/09/2002
16	PP6	19	86	28/04/2003	1/10/2002
17		18	84.5	29/04/2003	2/10/2002
18	PP7	17	83.5	1/05/2003	3/10/2002
19		16	82.5	2/05/2003	5/10/2002
20	PP8	15	81.5	3/05/2003	6/10/2002
21		14	81	4/05/2003	8/10/2002
22		13	81	4/05/2003	9/10/2002
23	PP9	12	81	6/05/2003	10/10/2002
24		11	81	—	11/10/2002

### **Postmonsoon (SK-182)**

Water samples were collected before dawn (around 4:30 hours) by a rosette sampler fitted with 30L Go Flo bottles (General Oceanics, Miami, Florida, USA). A Sea-Bird Electronics CTD was used with the rosette to obtain the conductivity-temperature-depth profile. The temperature sensor of the CTD was calibrated before the cruise. The software package SEASOFT was used for processing the raw CTD data. Water samples were collected when the rosette was hauled up, by tripping the bottles prefixed for the desired depths. The rosette was allowed around one minute stabilisation before the bottles were closed to ensure that the samples from desired depths were collected (Figure 2.2).



**Figure 2.2** Sampling of seawater onboard ORV Sagar Kanya. Left: Rosette attached with 30L Go-Flo bottles and underwater CTD unit being hauled up after temperature-salinity profiling and seawater sampling. Right: deck unit onboard for real time data acquisition and monitoring the sampling operation.

A day prior to the sampling or on the previous station, euphotic depth was estimated using a Secchi disk (also verified on the sampling location later in the day). Euphotic depth was determined as  $\sim 2.8 \times$  Secchi depth, where Secchi depth was determined by appearance or disappearance of Secchi disk in water column. Interestingly, on an average the euphotic zone during postmonsoon was found to be around 60m. However, at PP-6 the euphotic depth was just 40m. Water samples were collected from four different depths to cover the entire euphotic zone; 0, 20, 40 and 60m at all stations except PP6 where depths were altered to 0, 15, 25 and 40m. Once the water samples from different depths reached the deck, the samples were collected in prewashed two and one litre Polycarbonate NALGENE bottles (New York, USA) in duplicate pairs for each tracer (nitrate, ammonium and urea) and each depth. Two litre bottles were used for nitrate and ammonium experiments while one litre bottles were used for the urea

experiment. The bottles were rinsed thoroughly with the seawater of the particular depth before collecting the samples. Beforehand, the bottles were named in such a manner that they represented the station no, depth of sample collection, tracer information (whether for nitrate, ammonium or urea) as well as for primary and duplicate samples (e.g., 11NP representing first station, first depth i.e., surface for Nitrate Primary sample). Subsequently the bottles were lined up in a big plastic crate to avoid confusion. The water sample was collected directly from the Go-Flo bottles without taking the water into carboys to avoid possible contamination. Apart from taking the water samples for nitrate, ammonium and urea experiments, water samples from any chosen depth was collected in three one litre bottles for blank determination. After the collection of the samples was over, they were covered with a thick black cloth from all the sides to prevent light shock to the phytoplankton. This sample collection procedure was over by 5 A.M (IST), before any trace of daylight appeared.

#### **Premonsoon (SK-191)**

The method of sample collection during premonsoon was different from that of postmonsoon. Whereas the sample depth during the postmonsoon was fixed; the sample during the premonsoon was collected based on light levels. Samples were collected from six different light levels of 100, 80, 64, 20, 5, 1 % of surface irradiance to cover the entire euphotic zone. The depths at which the samples had to be taken for the above mentioned light levels were estimated using the formula:

$$Z = (2.8*d / 4.6) \ln (100/x)$$

Where, Z = Sample depth (m)

d = Secchi depth (m)

x = % of light level

All other procedures were same as mentioned for premonsoon sample collection. However, the sample depths varied from one station to another depending on the light penetration at a particular station. The Table 2.3 lists the sample depths during premonsoon season (SK-191). Six litres of water samples were also collected at all new production stations (PP stations) at 0, 30, 60, 100, 300 and 500m depths for studying the vertical variability of natural <sup>15</sup>N in suspended matter in the Bay of Bengal.

**Table 2.3** Details of sample depths during the premonsoon season in the Bay of Bengal.

%Light Used	Sample Depths (m)								
	PP1	PP2	PP3	PP4	PP5	PP6	PP7	PP8	PP9
100	0	0	0	0	0	0	0	0	0
80	3	3	5	5	3	5	5	5	5
64	6	7	10	10	6	10	10	10	10
20	20	25	35	35	20	20	35	35	35
5	40	50	60	60	40	40	60	60	60
1	60	70	100	100	60	60	100	100	100

### 2.3.2 Northeastern Arabian Sea

As mentioned in the earlier chapter, the main aim in the northeastern Arabian Sea was to study the changes in new and regenerated production and  $\delta^{15}\text{N}$  of surface suspended matter during and late northeast monsoon. For this purpose two cruises were undertaken in the year 2003. The first was onboard ORV Sagar Kanya during January and the second one was onboard FORV Sagar Sampada during late February-early March. The cruise tracks were not exactly the same; however, they were concentrated mostly in the same region i.e., off Gujarat. The locations of study are shown in the Figure 2.3. New and regenerated production studies were carried out at seven stations during January and six stations during late February-early March. However, the surface water samples at thirteen stations (except stn.1) during January and five stations (except Stn.1) during late February-early March were collected to assess the natural  $^{15}\text{N}$  isotopic variability in the suspended matter.

#### January

The list of all the stations where the water samples were collected along with new production stations, their exact locations and dates of sampling are shown in Table 2.4. The samples were collected at six different depths at each station to cover the entire euphotic zone (Table 2.5). To know the euphotic depth and the percentage of light at the depth of sampling, a Satlantic radiometer was operated at each station. Apart from the light regime the radiometer also provided the information regarding the water column temperature and chlorophyll concentration. Since the aim of the cruise in the Arabian Sea was not concentrated only on new production and primary productivity measurements, it was not always possible to sample before dawn as in the case of Bay

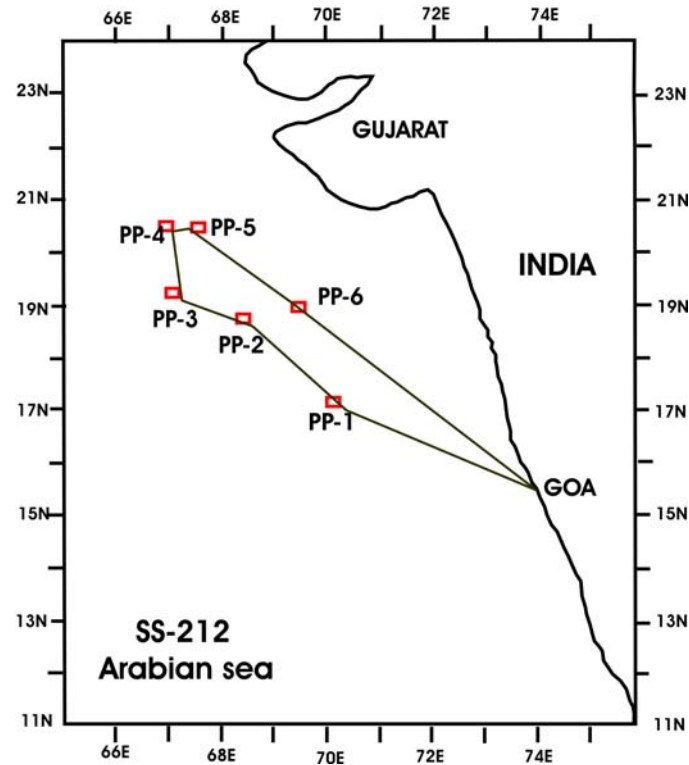
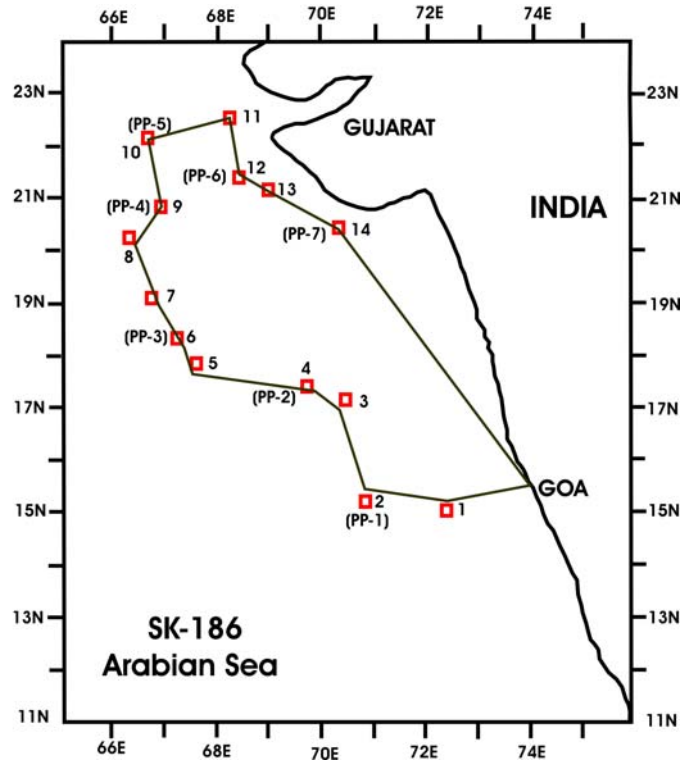


**Figure 2.3** Sample locations in the NE Arabian Sea [January, SK-186 (top) and February-March, SS-212 (bottom)]. During January water samples were collected at 13 stations (except stn.1) for studying natural isotopic variability and new production experiments were performed at PP stations only. During February-March the water samples were collected at 5 stn (except stn.1) for natural variability whereas new production measurements were performed at all the stations shown.

**Table 2.4** List of stations with locations and dates of sampling during January 2003.

Station	New Production Station	Latitude (N)	Longitude (E)	Date (D/ M/ Y)
1		15° 07' 10"	72° 26' 07"	04/01/2003
2	PP1	15° 14' 03"	70° 46' 01"	05/01/2003
3		17° 13' 49"	70° 32' 48"	06/01/2003
4	PP2	17° 29' 32"	69° 44' 26"	07/01/2003
5		17° 53' 35"	67° 41' 49"	08/01/2003
6	PP3	18° 16' 44"	67° 12' 38"	09/01/2003
7		19° 11' 08"	66° 44' 08"	10/01/2003
8		20° 19' 18"	66° 12' 38"	11/01/2003
9	PP4	20° 57' 40"	66° 54' 25"	12/01/2003
10	PP5	22° 12' 10"	66° 41' 41"	13/01/2003
11		22° 31' 18"	68° 14' 17"	14/01/2003
12	PP6	21° 22' 26"	68° 11' 51"	15/01/2003
13		21° 12' 24"	69° 0' 17"	16/01/2003
14	PP7	20° 26' 15"	70° 23' 35"	17/01/2003

**Table2.5** Sampling depths during January 2003 in the Arabian Sea.

Sample Depths (m)						
PP1	PP2	PP3	PP4	PP5	PP6	PP7
0	0	0	0	0	0	0
20	10	20	15	15	10	5
40	30	30	25	30	20	10
50	50	40	40	40	30	15
60	58	60	50	55	45	20
70	65	70	65	65	60	25

of Bengal. Since the expected biomass in the Arabian Sea was higher than that of the Bay, sample was collected in two litre NALGENE bottles for nitrate and one litre NALGENE bottles for ammonium and urea experiments. The method of the sample collection was the same as that followed in the Bay. However, the Go-Flo bottles attached to rosette for the sampling were only of 10 Litre capacity compared to 30 Litre used in the Bay. Hence, sometimes more than one cast was required for the sampling. As in the Bay, special care was taken to prevent the planktons from the light shock; a thick black cloth was used to cover the samples immediately after the collection. The samples for the blanks were also collected at each station at a chosen depth in three one litre bottles, one each for nitrate, ammonium and urea.

## February-March

The exact sampling locations along with the date of sampling are listed in Table 2.6. The sampling during February-March was different from that of January in the Arabian Sea in a way that it was collected based on light levels as listed in Table 2.7, all other details remains the same.

**Table 2.6** List of stations along with locations and sampling dates during late February-early March.

Station	New Production Stations	Latitude (N)	Longitude (E)	Date (D/ M/ Y)
1	PP1	17° 19.02'	70° 11.82'	28/02/2003
2	PP2	18° 48.33'	68° 28.53'	01/03/2003
3	PP3	19° 5.03'	66° 51.82	02/03/2003
4	PP4	20° 44.42'	66° 58.82	03/03/2003
5	PP5	20° 28.88'	67° 30.24'	04/03/2003
6	PP6	18° 57.71'	69° 21.17'	05/03/2003

**Table 2.7** Sampling depths during Feb-March 2003 in the Arabian Sea.

% Light Used	Sampling depths (m)					
	PP1	PP2	PP3	PP4	PP5	PP6
100	0	0	0	—	—	0
80	5	20	—	—	—	—
64	12	25	4	2	2	5.5
20	40	40	17	13	16	19
5	60	60	30	27	27	36
1	85	85	42	42	42	58

This was a typical bloom period in the Arabian Sea and the attenuation of light in the water column was very fast with depth, particularly at stations PP3, PP4 and PP5. It was very difficult to differentiate between the corresponding depths for 100 and 80% light levels given the limitation that the length of Go-Flo bottles itself were around 1m. Because of this limitation the sampling at the above mentioned three stations were done only for four light levels as listed in the Table 2.7. Two litre bottles for nitrate and one litre bottles for ammonium and urea were used.

Sampling of surface water for natural isotopic studies during all the cruises were performed using clean plastic buckets.

## 2.4 Nutrients

The nutrients of interest during the present study were the nitrate, ammonium and urea. In the Bay of Bengal, the nitrate measurements were carried out onboard by Dr. S. Sardesai and her colleagues of National Institute of Oceanography (NIO), Goa, by using column reduction technique (Strickland and Parson 1972). Ammonium and urea measurements could not be performed due to logistic problems. However, indirect estimation of ammonium and urea concentration for a few locations was done for the premonsoon period using the displacement volume of mesozooplankton measured during the cruise. The regeneration of ammonium and urea by zooplankton is well known (Mullin et al. 1975; Jawed 1973). Mesozooplankton biomass in this season in BOB ranged from 0.1 to 1.1 ml.m<sup>-3</sup>. From the displacement volume the dry weight was calculated using the relationship given by Wiebe et al. (1975):

$$\text{Log (Displacement volume)} = -1.842 + 0.865 * \text{Log (dry Weight)}$$

Using average ammonium and urea excretion rates of 0.59 and 0.32 mg at-N (g dry wt)<sup>-1</sup> d<sup>-1</sup>, the release rates of ammonium and urea were calculated for 12 hour residence time of zooplankton in mixed layer (Wafar et al. 1986). Table 2.8 lists the displacement volume of mesozooplankton biomass in the Bay of Bengal during the premonsoon period along with the location, depth, calculated dry weight and ammonium and urea regeneration.

**Table 2.8** The calculated urea and ammonium concentrations using mesozooplankton displacement volume.

Latitude (°N)	Longitude (°E)	Displacement Volume (ml/ 100m <sup>3</sup> )	Depth (m)	Dry Weight (g m <sup>-3</sup> )	Ammonium (µM)	Urea (µM)
9	88	110	0-40	0.14	0.042	0.011
11	88	25	0-60	0.027	0.008	0.002
15	88	10	0-40	0.009	0.003	0.0005
15	81	40	0-20	0.046	0.014	0.004
17	84	110	0-20	0.148	0.043	0.011
19	85	110	0-30	0.148	0.043	0.011

In the Arabian Sea, the nutrient measurements were not done onboard, however, samples were preserved (in deep freeze) to carry out the measurements (nitrate+ammonium) at Dr. S.W.A. Naqvi's lab in NIO, Goa at the end of the cruise using autoanalyzer. The detection limit for nitrate was 0.1µM, in both the methods.

## **2.5 Tracer addition**

Once the samples were collected they were arranged in the dark room. The tracers were added just before the beginning of incubation. During the Bay of Bengal cruises, since the nitrate measurements were available onboard, an attempt was made to add less than 10% of ambient nitrate. In some cases, if the ambient nitrate of the same station was not available due to time constraints, nitrate concentration of the nearest (previous) station was used as the ambient value for tracer addition. Once the nitrate of the same station was estimated, it was used for calculating the actual percentage of tracer added and for the final uptake calculations. Since ammonium and urea could not be estimated, constant amounts of ammonium ( $0.01\mu\text{M}$ ) and urea ( $0.03\mu\text{M}$ ) were added.

For the Arabian Sea, since the nutrient measurements could not be carried out onboard, a pre-fixed amount of nitrate, ammonium and urea concentrations were added. Since the nitrate concentration in the region is well studied for the northeast monsoon, an attempt was made to add less than 10% of typical ambient values. However, when the actual nitrate measurements were performed after the cruise, it was found that the addition was sometimes around 50% of the ambient value. Constant amounts of ammonium ( $0.1\mu\text{M}$ ) and urea ( $0.1\mu\text{M}$ ) were added in the Arabian Sea following Watts and Owens (1999).

Tracer additions were done using well calibrated micro pipettes. The pipette tips were changed after each addition to avoid cross contamination. After the tracer addition the lid of the bottles were closed tightly to avoid any leakage during incubation.

## **2.6 Incubation**

Incubation during the present study was done for four hours from 1000 to 1400 Hrs. (IST) symmetrical to local noon in deck boxes. The appropriate neutral density filters were put on to the bottles to simulate light conditions inside the bottles, to be the same as the depths from which the samples were drawn. The filters were specially prepared for the purpose and were well-calibrated using lux meter (at Dr. M.V.M. Wafar's lab at NIO, Goa) in dry and wet conditions. Flowing seawater from 5m depth was continuously maintained in the deck boxes to regulate the temperature. However, the flowing water from 5m depth may be inappropriate for deeper samples where the

subsurface Chl *a* maxima are situated within or below the thermocline. Exactly at 1400 Hrs., the samples were taken out from the deck boxes for filtration and kept in dark till the filtration was over.

## 2.7 Filtration

After the incubation, the samples were filtered onto Whatman GF/F glass fiber filters (47mm diameter and 0.7 $\mu$ m pore size). These filters were precombusted at 400°C for 4hrs after carefully wrapping them in Al-foil in sets of six. The filtration was done under low pressure (<70mm Hg) on a manifold unit procured from Millipore (Figure 2.4). Separate glass cups were used for nitrate, ammonium and urea samples to avoid cross contamination. A separate cup was dedicated for the filtration of natural samples. Once the filtration of the sample was over it was rinsed with filtered seawater to remove residual  $^{15}\text{NO}_3^-$  from filter interstices. Care was taken not to evacuate the filters to dryness. Once the filtration is over the filter papers were taken out carefully with forceps (separate for nitrate, ammonium and urea) to place into the 47mm diameter petrislides procured from Millipore. Filters were then immediately dried (50°C) for isotopic analysis in the shore laboratory.



**Figure 2.4** Filtration unit used during the present study.

As mentioned in the earlier sections, samples for blank estimation were collected at all the stations during different cruises. The idea here was to estimate the zero time enrichment. For that the same concentration of tracer was added to the blank samples as was added to the new and regenerated production samples. Immediately after the addition of tracer, the sample was filtered and dried for isotopic analysis.

## **2.8 Isotopic Analysis and Instrumentation**

The important requirements for the uptake rate estimation were the total nitrogen content and the atom%  $^{15}\text{N}$  in the post incubation samples. During the present study, broadly, the method of Owens and Rees (1989) for "Determination of Nitrogen-15 at sub-microgram levels of Nitrogen using automated continuous-flow Isotope ratio mass Spectrometry" was followed. The small amount of samples available ( $< 1\mu\text{M}$ ) for analysis poses a severe problem for mass spectrometric analysis in marine applications. Emission spectrometry is another method of analysis in which small amounts of sample ( $< 1\mu\text{M}$ ) can easily be detected but the precision of measurement (typically  $< 0.05\text{at } \%$ ) is too low for marine applications. However, the improvement of electronics, vacuum system and ion optics has enabled to analyse the small amount of samples (comparable to emission spectrometry) with high precision using a mass spectrometer. The continuous on-line analysis by automated isotope ratio mass spectrometers interfaced with elemental analyser provide one such option. Although this single inlet continuous on-line method of analysis is not as precise as dual-inlet analysis, this technique is sufficiently precise ( $\pm 0.005 \text{ at}\%$ ) for the present kind of study (Owens and Rees 1989). The modern design of nitrogen analyser with helium carrier and oxygen pulse was used during the present study, which has the following advantages:

- (1) Oxidation conditions can be optimised by varying oxygen pulse; products can then be checked by mass spectrometer.
- (2) Samples are accompanied by helium, there are no problems due to leakage.
- (3) The range of sample size may be large.
- (4) Memory effects are reduced as the analyser is continuously swept with helium.
- (5) Helium does not interfere with nitrogen isotope analysis.

### **2.8.1 Principle of Analysis**

The samples are combusted in a chamber containing oxidising catalysts at high temperature. Due to the oxidation of all major elements like C, H and N present in the sample, oxides like  $\text{CO}_2$ ,  $\text{H}_2\text{O}$  and  $\text{N}_2\text{O}$  are formed. After the complete combustion of the samples, the gases formed are passed through a reduction chamber, where oxides of nitrogen get converted to  $\text{N}_2$ . The gas mixture is passed through dry absorbants and a gas chromatography column and the purified  $\text{N}_2$  is admitted to an isotope ratio mass

spectrometer tuned for masses 28, 29 and 30. Integration of ion beams of the standards and samples enable both the total nitrogen and  $^{15}\text{N}:^{14}\text{N}$  ratio to be determined.

## **2.8. 2 Instrumentation**

During present study, Elemental Analyser (Flash EA 1112 Series, CE Instruments, Italy) interfaced with Finnigan Delta<sup>Plus</sup> Continuous-Flow Mass Spectrometer (Thermo Quest Finnigan, Bremen, Germany) via ConFloIII was used for analysis. The description of the instruments as well as procedure followed is given below.

### **(A) Elemental Analyser**

A Carlo Erba (CE) elemental analyser was used throughout this study. The mode of operation is based on Dumas principle with high temperature "Flash" combustion. The carrier gas used was 5 grade (99.999%) helium (procured from Praxair-Bangalore) at 80ml/min. 5 grade (99.999%) oxygen (procured from Hydragas-Bombay) was used for combustion. The elemental analyser consists of two reactors: the first one acts as an oxidation or combustion chamber for the samples and the second, as a reduction chamber. Before the start of the experiment the reactors are prepared with the necessary chemicals in 47cm long quartz tube with outer diameter of 18mm and inner diameter of 14mm. The first reactor contains the oxidizing catalysts: silvered cobaltous oxide and chromium oxide separated by quartz wool. The reduction chamber contains reduced copper with quartz wool on the top and bottom. The exact size of the filling materials in the reactors is shown in Figure 2.5. The chemicals were procured from Courtaage Analyses Services (France).

There is a turret on top of the oxidation chamber where samples are loaded, a maximum of 50 at a time. The positions of the samples are numbered from 0 to 49. The sample that has to be analyzed falls in an intermediate zone (well) and is purged with He. After the purging is over, the sample is allowed to fall in the oxidation chamber followed by a pulse of pure oxygen (1 second pulse @  $175\text{ml min}^{-1}$ ). The temperature of the oxidation chamber is normally maintained at  $1060^\circ\text{C}$ . The sample drop and the simultaneous supply of oxygen pulse lead to an increase in the temperature of the chamber to the order of  $1800^\circ\text{C}$ . This rise in temperature leads to 'flash' combustion of the sample resulting into the production of  $\text{CO}_2$ ,  $\text{H}_2\text{O}$  and oxides of nitrogen. The flash combustion can be seen through the hole provided for the purpose as a change in colour

during combustion. Since helium is always flowing as a carrier gas, it carries all the oxides produced due to the combustion of the samples

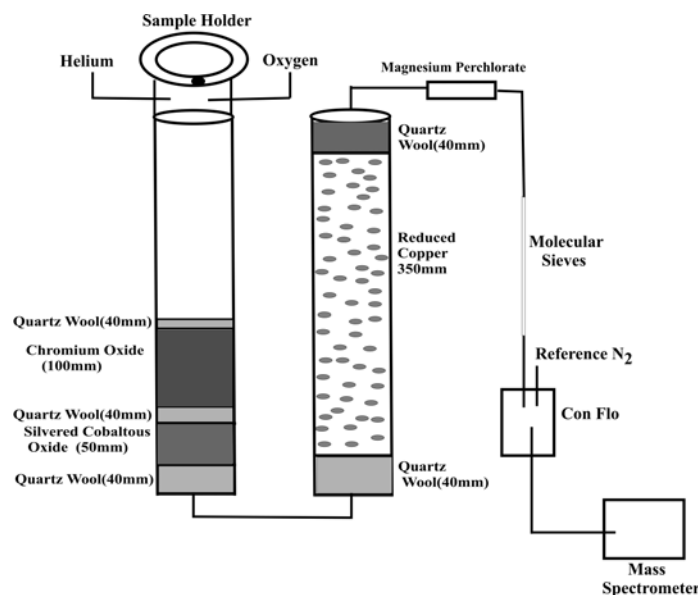


**Figure 2.5** Schematic diagram showing the elemental analyzer set up.

along with it to the reduction chamber containing reduced copper at 680°C. In the reduction chamber, the oxides of nitrogen get reduced to N<sub>2</sub>. After the reduction chamber these gases are passed through magnesium perchlorate (anhydrous) to absorb any water vapor (moisture) that may be present. Subsequently, the gases are passed through a gas chromatographic column (molecular sieve). In the chromatographic column, a mixture of different gases (CO<sub>2</sub>, N<sub>2</sub> etc.) gets separated due to differences in their partitioning behavior between the mobile gas phase and the stationary phase in the column. The components of the sample move at velocities that are influenced by the degree of interaction of each constituent with the stationary nonvolatile phase. The substances having the greater interaction with the stationary phase are retarded to a greater extent and consequently separate from those with smaller interaction leading to their release at different times from the chromatographic column. The retention time for N<sub>2</sub> is less than that of CO<sub>2</sub>. Hence, N<sub>2</sub> comes faster than the CO<sub>2</sub> out of chromatographic column (whose temperature is maintained at 60°C). After the different components elute from the column they pass through Con Flo from where they are allowed into the mass spectrometer for isotopic analysis.

### **Sample Preparation for elemental analyzer**

As mentioned earlier, the samples were filtered on 47mm diameter Whatman GF/F filter paper. An attempt was made to accommodate the whole filter paper in the

carousel of the elemental analyzer by pressing them into a smallest size possible but it was not feasible to accommodate as such. After that the filter papers were cut into two equal halves to make two small pellets. Although it was somehow fitting into the carousel, there was problem in its free fall into the well and subsequently into the oxidation chamber. Because of this the samples were getting stuck into the well (and not falling in the oxidation chamber) falling one over the other and hence the identity of the samples were lost. To avoid these problems and smooth analysis, samples were cut into four equal halves and the small pellets were prepared in thoroughly cleaned silver foils. The silver foils were checked for blank after cleaning. While preparing the samples extra care was taken to not to touch the samples and cleaned silver foils with hand. Two curved forceps were used for the wrapping the samples in silver foil. The smallest possible silver foil (1cm x 1cm) was used to wrap the samples.

### **(B) Con-Flo**

Con-Flo is an interface between elemental analyzer and mass spectrometer. Broadly, it contains three capillaries in a small tubular glass structure: two incoming capillaries bring reference gas and the sample gas to the tubular structure, whereas the third capillary transfers the reference or sample gases from tubular structure to the mass spectrometer.

### **(C) Mass Spectrometer**

The mass spectrometer used for the present study was Finnigan's Delta<sup>plus</sup> Isotope ratio Mass Spectrometer. The Delta<sup>plus</sup> is a single inlet ("online" coupling of gas chromatographs and Elemental Analyzer through Con Flo III) instrument with electron impact ionization source. The energy of ionization electron is 80 eV. The vacuum was maintained by turbomolecular pump at a rate of  $240 \text{ l s}^{-1}$  (type: TMH 260, manufacturer: Balzers) with fore vacuum provided by rotary pump rated at  $1.5 \text{ m}^3\text{s}^{-1}$  (E2M1.5, manufacturer: Edwards). Ions produced are accelerated at 3kV. The ion beam produced exits the ion source into magnetic field through a slit of fixed width (0.3mm) and enters the magnetic field boundary at an angle of  $26.5^\circ$  and exits at the same angle resulting in a radius of 9cm for this system. The maximum strength of the magnetic field was 0.75 Tesla. The resolution of the mass spectrometer ( $m/\Delta m$ ) was 95. The

collector system of the mass spectrometer was MEMCO (Multi-Element-MultiCollector) system with three Faraday collector cups connected to amplifiers.

During the present study two types of samples were analysed:

(A) Natural samples.

(B) Enriched samples (i.e., new and regenerated production samples).

The main interest of the analysis was to find:

(A) The total Nitrogen content in the natural and enriched samples

(B) Nitrogen isotopic composition ( $\delta^{15}\text{N}$ ) in the natural samples and atom%  $^{15}\text{N}$  in the enriched samples.

The operation of the whole system (Elemental analyser + mass spectrometer) was fully computerized and was controlled by Finnigan MAT software ISODAT. A method instructing the timing of different events (i.e., on and off time of reference gas, on and off time of elemental analyser and He dilution) was followed for the analysis. Also the information to find the peak such as start and end slope, peak mean height, peak mean width etc were fed. Acquisition time for a sample was 450 seconds and the nitrogen peak used to appear at around 155 sec after the start of the analysis. A typical chromatogram obtained during analysis is shown in Figure 2.6. The parameters of interest during present study for which ISODAT was customized were: amplitude of 28, 29 and 30 mass peaks, ratio of 29/28 and 30/28, individual and total areas under the peaks of masses 28,29 and 30, atom%  $^{15}\text{N}$  and  $\delta^{15}\text{N}$  w.r.t. air.

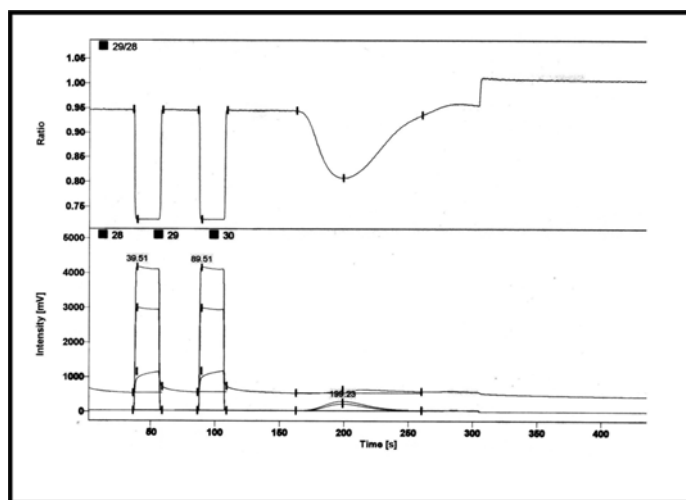


**Figure 2.6** A typical chromatogram (for ammonium sulphate  $\sim 0.053\text{mg}$ ) obtained during the present study.

## 2.9 Standards Used and precision

The isotopic composition of nitrogen ( $\delta^{15}\text{N}$ ) is expressed with respect to air ( $\delta^{15}\text{N} = 0$  ‰). However, it is common practice to use laboratory standards whose isotopic composition is known w.r.t. air. Throughout the present study three standards of known isotopic compositions (procured from IAEA) were used. The laboratory standards with their quoted isotopic compositions and values and precision obtained during the present study are as listed in Table 2.9.

**Table 2.9** Values and precision obtained during the present study for standard materials used.

Standards Used	Isotopic composition (quoted by IAEA) (%o w.r.t. Air)	Values obtained during present study (%o w.r.t. Air)
(NH <sub>4</sub> ) <sub>2</sub> SO <sub>4</sub> [IAEA-N-2]	20.3	20.3±0.3* (n= 15)
KNO <sub>3</sub> [IAEA-NO-3]	4.7	4.9±0.3* (n=13)
KNO <sub>3</sub> [USGS 32]	180	177±2.3* (n=12)

\* standard deviation

## 2.10 <sup>15</sup>N atom% Measurement

The ISODAT software calculates the <sup>15</sup>N atom% for each sample. The <sup>15</sup>N atom% can be calculated if the ratio of <sup>28</sup>N/<sup>29</sup>N is known, as in the case of mass spectrometer, according to following relationship:

$$^{15}\text{N atom\%} = 1 / (2R+1) * 100, \text{ where } R = ^{28}\text{N}/^{29}\text{N}$$

As stated earlier, <sup>15</sup>N atom% was one of the important parameters to be estimated for the samples processed to measure new and regenerated production.

### 2.10.1 <sup>15</sup>N atom% for blank samples

The <sup>15</sup>N atom% in the blank samples (samples which were immediately filtered after addition of tracers) was also estimated. The average values of the blank samples for nitrate, ammonium and urea uptake experiments are listed in Table 2.10. These are the average values of respective blanks for all the stations where the samples for blank were collected. The blank at% values may be taken as zero time enrichment i, e., it

**Table 2.10** The average value of  $^{15}\text{N}$  atom% in the blank samples during the present study (natural level: 0.3678197).

	Nitrate	Ammonium	Urea
<b>Arabian Sea</b>			
SK-186	0.3680±0.0009	0.399±0.040	0.387±0.007
SS-212	0.3718±0.0005	0.3932±0.0008	0.406
<b>Bay of Bengal</b>			
SK-182	0.368±0.001	0.397±0.011	0.411±0.036
SK-191	0.373±0.015	0.384±0.011	0.403±0.014

might provide the measure of the affinity for a particular nutrient by the phytoplankton; in other words, it may provide the measure of the capability of the phytoplankton to take up a particular nutrient in a very short time (time of filtration). For example, the at%  $^{15}\text{N}$  for urea is maximum in the Bay of Bengal and during SS-212 (Feb-March) in the Arabian Sea whereas it is highest for ammonium during SK-186 (January) in the Arabian Sea probably indicating the immediate preference for these nutrients.

### 2.10.2 Error in $^{15}\text{N}$ atom% estimation

The percentage error in  $^{15}\text{N}$  atom% estimation observed during present study is listed in Table 2.11. The maximum error observed was in the case of ammonium uptake experiment and was found to be 2.8 and 3.5% in the Arabian Sea and the Bay of Bengal respectively. In all other cases it was less than 2% and well within the limits observed elsewhere.

**Table 2.11** The percentage error in  $^{15}\text{N}$  atom% estimation during the present study.

	Nitrate	Ammonium	Urea
Arabian Sea	1.76	2.8	1.4
<b>Bay of Bengal</b>			
SK-182	0.20	3.50	0.91
SK-191	0.26	1.82	1.43

### 2.10.3 Linearity for $^{15}\text{N}$ atom%

Since the expected concentration of total nitrogen in marine samples is very less (typically  $\sim 1\mu\text{M}$  or less), it is very important to check for the linearity (Figure 2.7) of

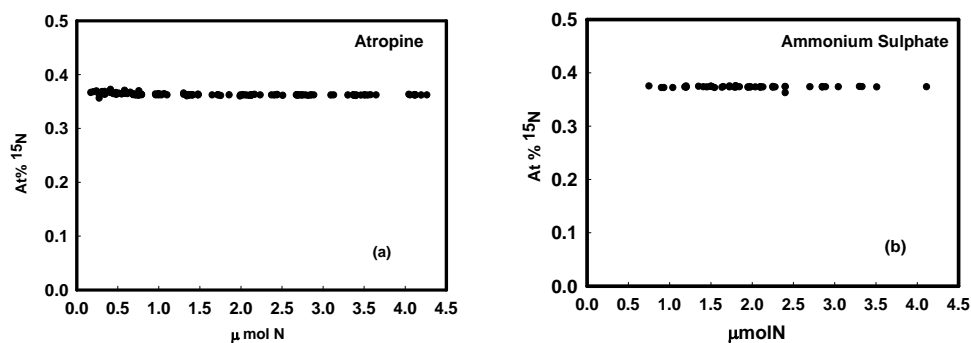


**Figure 2.7** The linearity of <sup>15</sup>N atom% for (a) atropine and (b) ammonium sulphate over widely varying sample amounts.

the desired parameter (atom% <sup>15</sup>N during present study) over the expected sample range. During the present study this exercise was performed using the most commonly used standard material [(NH<sub>4</sub>)<sub>2</sub>SO<sub>4</sub>] and material used for calibration purpose (Atropine) for total nitrogen content. The linearity of the atom% was found up to very small sample amounts (0.2 μM). The precision for [(NH<sub>4</sub>)<sub>2</sub>SO<sub>4</sub>] and atropine during analysis was around 0.001 and 0.009 atom% respectively.

## 2.11 Estimation of Particulate Nitrogen Content

Material which was used mostly for the calibration purpose for estimating the total nitrogen content of the samples was atropine. However, sometimes ammonium sulphate and potassium nitrate were also used to recheck the differences, if any. Atropine is an organic material, which contains only 4.8% nitrogen. This small presence of nitrogen allows the larger quantity to be taken up than potassium nitrate or ammonium sulphate for the same concentration of nitrogen and hence reducing the error in weighing the smaller amounts. Potassium nitrate and ammonium sulphate contain 13.8 and 21.2% nitrogen respectively.

For the calibration for total nitrogen, a range of atropine and ammonium sulphate were weighed (e.g. ranging from 0.10 to 0.80 mg) and corresponding nitrogen contents were calculated by multiplying the percentage of nitrogen in them. For each sample the total area (sum of the areas under the 28, 29 and 30 mass peaks) obtained during analysis was plotted against the nitrogen content and a regression equation was derived to calculate the unknown nitrogen content of samples.

The calibration was performed on day to day basis to take into account any possible sensitivity change. A normal practice during the analysis was to prepare a

standard calibration curve using 10-15 atropine or ammonium sulphate samples after each time reactor of the elemental analyzer was changed (normally reactors were refilled after analyzing 200-250 samples). In addition, each lot of samples (consisting 50 samples) contained at least eight standards, which were used to prepare the calibration curve if any sensitivity change was observed. A typical example of calculation used for the calibration is shown in the Table 2.12 and subsequently its plot

**Table 2.12** A typical example for the method used for the calibration for the estimation of total nitrogen. Number of samples presented are smaller than typically used for calibration.

Samples	Weight (mg)	mg N	Total Area (V*sec)
ATROPINE	0.1	0.0048	2.99
ATROPINE	0.28	0.0134	8.83
ATROPINE	0.39	0.0187	12.35
ATROPINE	0.51	0.0245	16.38
ATROPINE	0.61	0.0293	19.75
ATROPINE	0.73	0.0351	25.24
KNO <sub>3</sub>	0.12	0.0165	10.24
KNO <sub>3</sub>	0.23	0.0317	24.04
KNO <sub>3</sub>	0.38	0.0524	39.44
KNO <sub>3</sub>	0.64	0.0883	66.60
KNO <sub>3</sub>	0.78	0.1076	81.74
(NH <sub>4</sub> ) <sub>2</sub> SO <sub>4</sub>	0.1	0.0212	14.05
(NH <sub>4</sub> ) <sub>2</sub> SO <sub>4</sub>	0.22	0.0466	33.38
(NH <sub>4</sub> ) <sub>2</sub> SO <sub>4</sub>	0.38	0.0805	61.31
(NH <sub>4</sub> ) <sub>2</sub> SO <sub>4</sub>	0.57	0.1208	75.23
(NH <sub>4</sub> ) <sub>2</sub> SO <sub>4</sub>	0.78	0.1653	122.93

and equations in Figure 2.8. The equations derived were normally between milligram of nitrogen (mgN) and total Area obtained. The calibration curves for atropine ( $\text{mgN} = 0.0014 * \text{Area} + 0.0013$ ;  $r^2 = 0.99$ ), ammonium sulphate ( $\text{mgN} = 0.0013 * \text{Area} + 0.0021$ ;  $r^2 = 0.99$ ) and potassium nitrate ( $\text{mgN} = 0.0014 * \text{Area} + 0.0034$ ;  $r^2 = 0.97$ ) suggest almost similar slopes with different intercepts. However the intercept for atropine (0.0013) and ammonium sulphate (0.0021) are closer compared to that of potassium nitrate (0.0034). All the three (atropine, ammonium sulphate and potassium nitrate) put together yielded a calibration equation ( $\text{mgN} = 0.0014 * \text{Area} + 0.0016$ ;  $r^2 = 0.98$ ) very similar to that of

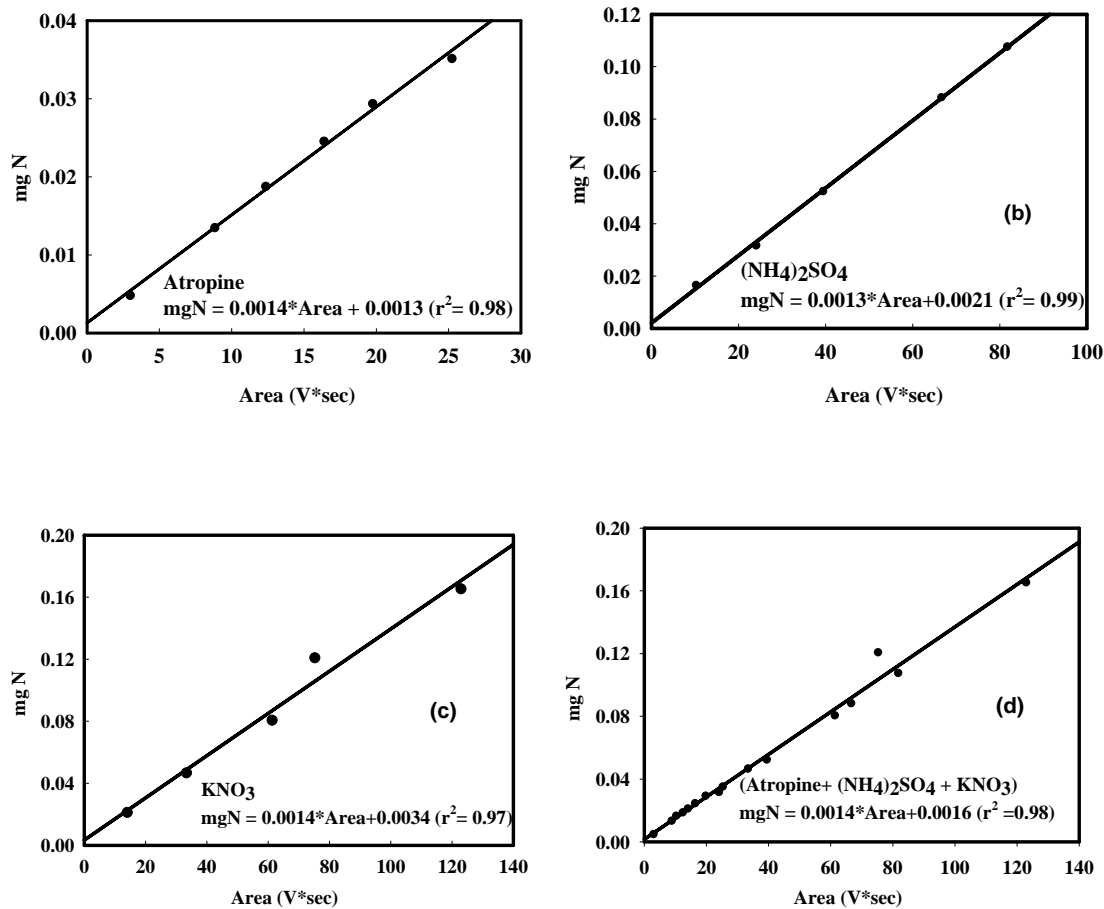


**Figure 2.8** A typical example of calibration curves using different materials (atropine, ammonium sulphate and potassium nitrate).

atropine. This trend was reflected in almost all calibrations used for present study. In general, for the estimation of nitrogen content from unknown samples the calibration equations obtained by atropine was used. Table 2.13 lists the calibration equations actually followed for the estimation of total nitrogen content during present study.

Since the filter papers were cut into four equal halves, the nitrogen content obtained represented one fourth of the water filtered. Therefore, the nitrogen contents obtained were multiplied by the required number to get the molar concentration and were subsequently converted into  $\mu\text{M N}$  ( $\mu\text{g-at N L}^{-1}$ ) using formula:  $\mu\text{M N} = (\text{mg N} * 1000) / 14$ .

### 2.11.1 Error in the Particulate Nitrogen Content estimates

Table 2.14 lists the maximum % error observed during the particulate nitrogen content estimation in the Bay of Bengal and the Arabian Sea. The maximum error of 15% was

observed during the particulate nitrogen estimation for urea samples in the Bay of Bengal, which may be due to small amounts of sample or natural heterogeneities.

**Table 2.13** Calibration equations used for the estimation of total nitrogen content during the present study.

<b>Cruise No.</b>	<b>Samples</b>	<b>Calibration Equations used</b>	<b>r<sup>2</sup></b>
Arabian Sea SK-186	Natural	mg N = 0.00286*Area-0.00005	0.96
	Nitrate	mg N = 0.00133*Area+ 0.00355 (up to 5th station samples)	0.99
		mg N = 0.0014*Area+ 0.0013 (5th to 7th station samples)	0.98
	Ammonium	mg N = 0.0013*Area-0.0008	0.99
	Urea	mg N = 0.0014*Area-0.0014 (upto 4th station) mg N = 0.0023*Area-0.0025 (5th to 7th station)	0.99 0.87
Arabian Sea SS-212	Natural	mg N = 0.00286*Area-0.00005	0.96
	Nitrate	mg N = 0.00138*Area+ 0.00129	0.99
	Ammonium urea	mg N = 0.0013*Area-0.0008 mg N = 0.0014*Area-0.0014	0.99 0.99
Bay of Bengal SK-182	Natural	mg N = 0.0014*Area-0.0006	
	Nitrate	mg N = 0.0014*Area-0.0006 (primary samples) mg N = 0.0009*Area-0.0008 (Duplicate samples)	0.97
		ammonium	mg N = 0.0014*Area-0.0006 (primary samples) mg N = 0.0009*Area-0.0008 (Duplicate samples)
	Urea	mg N = 0.0009*Area-0.0008	0.97
Bay of Bengal SK-191	Natural	mg N = 0.00286*Area-0.00005	0.96
	Nitrate	mg N = 0.000875*Area-0.000329	0.99
		Ammonium	mg N = 0.000875*Area-0.000329 (primary sample upto 3rd station) mg N = 0.0014*Area-0.0012 (Duplicate samples up to 3rd and both primary and duplicate from 4th station onwards)
	Urea	mg N = 0.0015*Area-0.0002	0.87

**Table 2.14** Percentage error in particulate nitrogen content in the Arabian Sea and the Bay of Bengal.

Sample	Arabian Sea	Bay of Bengal
Nitrate	0.5	4.4
Ammonium	3.6	11
Urea	3.1	15

## 2.12 Estimation of uptake rate

Since the advent of the  $^{15}\text{N}$  labeled nitrogen incorporation method for the estimation of uptake rate, several different equations are in use (Neess et al. 1962; Dugdale and Goering 1967; Eppley et al. 1977). All these equations rest on several assumptions, which become invalid under certain conditions.

### 2.12.1 Concept of the general equation for uptake

The concept of uptake equation is based on the isotopic mass balance at the end of incubation experiment (Collos, 1987). The number of  $^{15}\text{N}$  atoms in final particulate nitrogen is equal to the sum of number of  $^{15}\text{N}$  in the initial particulate nitrogen and number of  $^{15}\text{N}$  atoms in the nitrogen taken up.

$$C_p N_f = C_0 N_0 + C_d \Delta N \quad \text{-----} \{1\}$$

Where,  $C_p$  = Atom%  $^{15}\text{N}$  in particulate phase after incubation ( $t = t$ )

$C_0$  = Atom%  $^{15}\text{N}$  in particulate phase at the start of experiment ( $t = 0$ )

$C_d$  = Atom%  $^{15}\text{N}$  in dissolved phase at the start of experiment ( $t = 0$ )

$N_f$  = Particulate nitrogen at end of incubation

$N_0$  = Particulate nitrogen at the start of experiment ( $t = 0$ )

$\Delta N$  = Nitrogen taken up during incubation.

Since,  $N_f = N_0 + \Delta N$

$$N_0 = N_f - \Delta N \quad \text{-----} \{2\}$$

Putting eqn. (2) in eqn. (1)

$$C_p N_f = C_0 (N_f - \Delta N) + C_d \Delta N$$

$$N_f (C_p - C_0) = \Delta N (C_d - C_0)$$

$$\Delta N = N_f (C_p - C_0) / (C_d - C_0)$$

Nitrogen uptake rate

$$\rho_N = \Delta N / \Delta t = N_f (C_p - C_0) / \Delta t (C_d - C_0), \text{ where } \Delta t \text{ is the incubation time.}$$

Following assumptions are made for simplicity:

1. Single nitrogen source for phytoplankton.
2. No excretion of nitrogen by phytoplankton during incubation.
3. Isotopic discrimination is negligible.
4.  $^{15}\text{N}$  atom% in the dissolved phase remains constant.

Collos (1987) argued that the uptake rate estimated using this concept will be closer to the real uptake rate, as bias introduced due to the contribution of unlabeled compound is exactly compensated by biased introduced by final particulate nitrogen and hence uptake rate will be unaffected.

### **2.12.2 Equation used for the calculation of uptake rate during the present study and involved uncertainties**

During present study the equation of Dugdale and Wilkerson (1986) was used for the calculation of uptake rates, where uptake rate was calculated by multiplying the particulate nitrogen content with specific uptake rate (nitrogen taken up per unit particulate nitrogen) at the end of incubation.

$$\text{Specific uptake rate } V = [^{15}\text{N}_{\text{xs}} / (^{15}\text{N}_{\text{enr}} * t)] \text{ and}$$

$$\text{Uptake Rate } (\mu\text{mol N m}^{-2} \text{ d}^{-1}) \rho = V * \text{PON} (t)$$

Where,  $^{15}\text{N}_{\text{xs}}$  = excess  $^{15}\text{N}$  in the post incubation particulate samples  
= measured  $^{15}\text{N}$  atom% -  $^{15}\text{N}$  natural abundance (0.36781 atom %)

PON (t) = Particulate Organic Nitrogen content of sample after incubation  
( $\mu\text{mol N L}^{-1}$ )

t = incubation time in hours.

$^{15}\text{N}_{\text{enr}}$  =  $^{15}\text{N}$  enrichment in the dissolved fraction

$$= [(I_o * S + I_{\text{tr}} * S_t) / (S + S_{\text{tr}}) - ^{15}\text{N natural}]$$

Where,  $I_o$  and  $I_{\text{tr}}$  are the natural  $^{15}\text{N}$  atom% and  $^{15}\text{N}$  atom% of the added tracer, respectively. S and  $S_{\text{tr}}$  are the ambient nutrient concentration and concentration of tracer added, respectively.

This formula was chosen for the calculation because it allows the isotope ratio and particulate nitrogen to be measured on the same sample during mass spectrometry, as in the present study, and therefore provides the most accurate estimate of uptake rate. It also cancels out the effect of detrital nitrogen and does not allow it to underestimate the uptake rate because of its presence:

$$\rho_{\text{cells}} = V_{\text{cell}} * \text{PON}_{\text{cell}} = (V_{\text{meas.}} * \text{PON}_{\text{total}} * \text{PON}_{\text{cells}}) / (\text{PON}_{\text{cells}}) = V_{\text{meas.}} * \text{PON}_{\text{total}}$$

For nitrate and urea, daily uptake rate was calculated assuming a day length of 12 hours and negligible uptake during night time. For ammonium hourly rate was multiplied by 18 to get daily uptake rate (Dugdale and Wilkerson 1986). Ammonium uptakes reported here have not been corrected for isotope dilution (Glibert et al. 1982a). The uptake rates determined in terms of nitrogen can be converted in carbon units by using Redfield ratio (C: N= 106:16).

Apart from analytical uncertainties involved in measurement of PON and  $\delta^{15}\text{N}$  the uncertainty in uptake rates arises due to overaddition of tracer (>10% of ambient concentration) and due to isotopic dilution (Dugdale and Goering 1967). The uncertainty due to over addition arises mainly from lack of analytical precision when the ambient nutrient concentrations are very low (McCarthy et al. 1992), especially in surface water. This results in enrichment of dissolved fraction with  $^{15}\text{N}$  from 50 to 100% and hence overestimation of uptake rate (Dugdale and Wilkerson 1986; Harrison et al. 1996; L'Helguen et al. 2002). During present study care was taken to minimise this uncertainty by adding the tracer as recommended by JGOFS protocol (~10nM range). However, the enrichment during the first station of SS-212 was more than 90% as there was no nitrate present in the surface layer. The addition of tracer causes the substantial increase in dissolved N concentration and in turn overestimate the uptake rate (Dugdale and Wilkerson 1986). The extent of overestimation for nitrate uptake at discrete depths during present study was estimated as suggested by MacIsaac and Dugdale (1972). The half saturation constant for Bay of Bengal was taken as 0.05 $\mu\text{M}$  which is a characteristic value of nitrogen poor oceanic waters (Kanda et al. 1985; McCarthy et al. 1992; Harrison et al. 1996) whereas for the Arabian Sea, it was taken as 1 $\mu\text{M}$ , typical for eutrophic waters (MacIsaac and Dugdale 1969; half saturation constant of 1.7 $\mu\text{M}$  has been reported for northwestern Arabian Sea by McCarthy et al. 1999). This exercise suggests that on an average the percentage of overestimation in the Bay of Bengal is <3% during SK-191 and <10% during SK-182. However, the

overestimation during Arabian Sea has been found to be relatively more (<5% during SK-186 and around 20% during SS-212). The effect of isotope dilution on uptake rate (Dugdale and Goering 1967) has not been considered as the incubation period was short (less than four hours) enough not to have effective dilution of initial isotopic enrichment, so as to affect the uptake rate significantly (Dugdale and Wilkerson 1986).

### **2.13 Quality Control**

Quality control was of utmost importance during the experiments. Go-Flo bottles were used to avoid trace metal contamination. The NALGENE bottles used for experiments were filled directly from the Go-Flo bottles. No carboys were used to store the water samples in order to avoid possible contamination. Bottles were thoroughly rinsed with the same water before collecting the samples. The samples were collected in low light conditions. Samples were covered with thick black cloth after the collection. During the tracer addition new pipette tips were used for each addition to avoid cross contamination. The samples were always kept in dark and were not exposed suddenly to light when taking out for incubation. These measures were taken to avoid possible light shock to the phytoplankton. Filtration was also done in an almost dark environment. During the filtration of the samples, only the sample to be filtered was taken out and rest of them were kept in dark. Different filtration cups and forceps were used for different tracers and natural samples. These cups were thoroughly rinsed with filtered seawater after filtering one sample. Once the whole filtration was over the polycarbonate NALGENE bottles were cleaned with 0.25N HCl and three times with Milli-Q water (Fitzwater et al. 1982) before the next experiment.

### **2.14 Physical and Chemical parameters**

Onboard measurements of various physical properties were carried out during both Arabian Sea as well as Bay of Bengal cruises. The primary physical properties measured were pressure, temperature and salinity using conductivity-temperature-depth profiler (CTD). The chemical components in the seawater such as dissolved oxygen and total dissolved inorganic carbon were measured by NIO, Goa during Bay of Bengal studies. The chemical constituent studies were not a priority in the Arabian Sea and hence no such measurements were carried out. However, Dr. S.G.P. Prabhu Matondkar of NIO, Goa, carried out the chlorophyll *a* measurements using fluorometric technique.

A Satlantic radiometer was operated during both cruises of Arabian Sea to monitor the upwelling and downwelling irradiance at different depths. Continuous profiles of temperature and chlorophyll was also obtained from sensors attached to the radiometer for the purpose. All sensors were well calibrated before the starting of the cruise. Quality of chemical and chlorophyll *a* measurements was monitored, by analysing suitable standard materials and repeat analyses.

**Chapter 3**  
**The Northeastern Arabian Sea**

---

---

### 3.1 Introduction

The Arabian Sea constitutes the northwestern part of the Indian Ocean. It is surrounded by the Asian and African continents to the north and west and the Indian subcontinent to the east. Assuming equator as its southern boundary, it encompasses an area of about  $6.2 \times 10^6 \text{ km}^2$  (Burkill et al. 1993). Although the Arabian Sea is one of the smaller ocean basins, its unique geographical setting transforms it into a perfect biogeochemical laboratory that contains different biogeochemical provinces such as eutrophic, oligotrophic and oxygen deficient environments. The uniqueness of the Arabian Sea is that it comes under the influence of seasonally reversing monsoonal wind forcing. The winds have the greatest influence in the biogeochemical cycling in the Arabian Sea. The winds over Arabian Sea blow from northeast (NE) during December to February (NE monsoon) and reverse direction during May and start blowing from the southwest (SW) direction (SW monsoon) persisting till August. The transition periods, October-November and March-May are known as Fall and Spring intermonsoons (Schott et al. 1990).

The monsoonal coupling between ocean and atmosphere is so intense that the seasonal shift in wind pattern causes semi-annual reversal of surface currents in the Arabian Sea basin (Figure 3.1). These changes lead to the greatest seasonal variability of biological productivity observed in any ocean basin in the world (Smith et al. 1998). In general, the most important characteristics of the Arabian Sea seasonal cycle of physical conditions are as follows (Barber et al. 2001):

1. Strong wind stress during the SW monsoon resulting in widespread upwelling and mixing.
2. Moderate strength, relatively cool and dry winds during the NE monsoon leading to evaporative cooling and subsequent convective mixing.
3. Weak winds and strong stratification due to surface layer heating during the spring and fall intermonsoons.

Apart from witnessing changes in physical and biogeochemical conditions in time, the Arabian Sea also exhibits considerable spatial variation that is not seen in any other ocean (Smith and Bottero 1977). Asymmetric monsoonal effect creates strong gradient in biogeochemical processes within the basin (Burkill et al. 1993). During the SW monsoon, a narrow, low level, atmospheric jet with exceptionally strong winds known

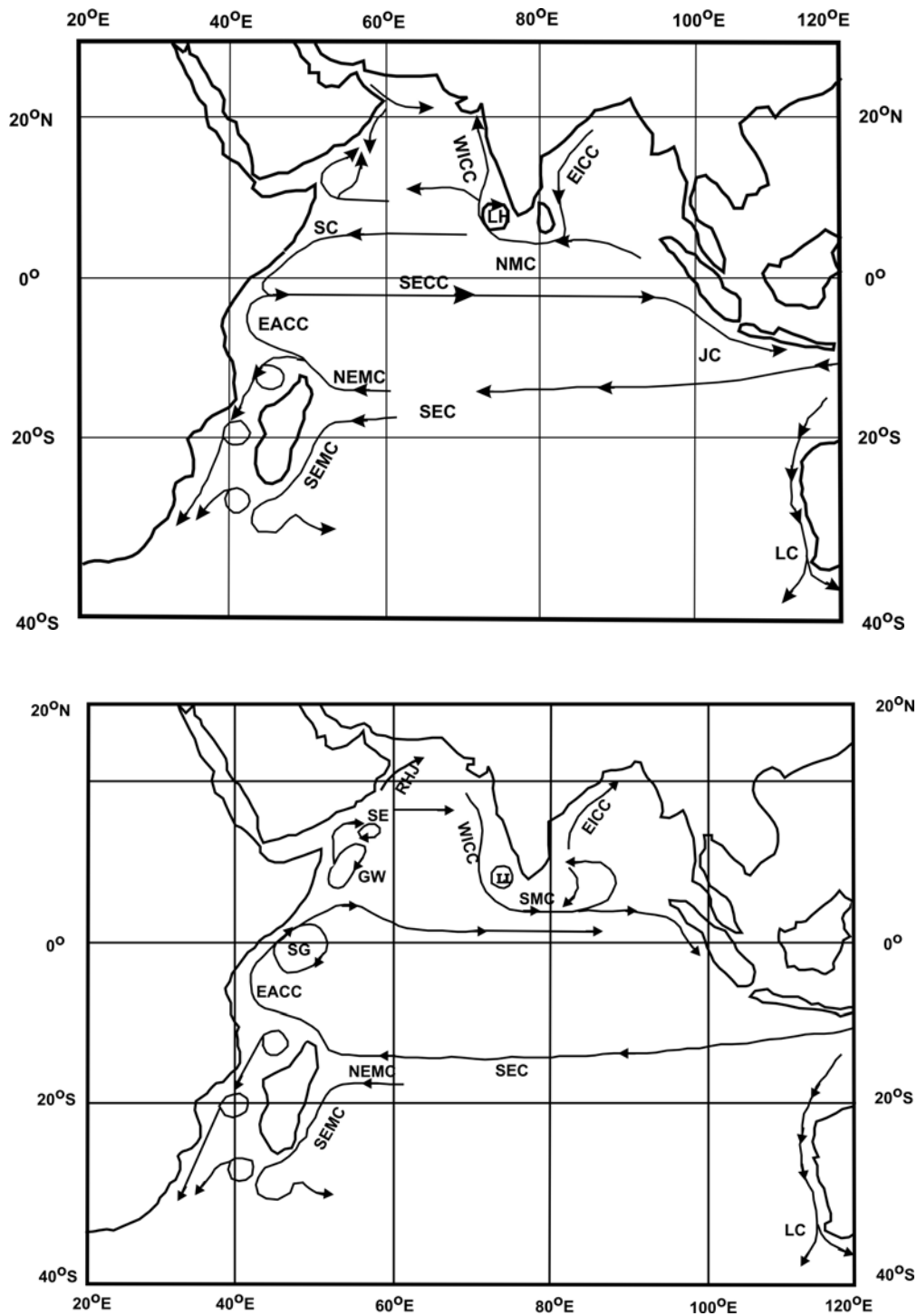


**Figure 3.1** A schematic representation of identified current branches during Northeast (top) and southwest (bottom) monsoon taken from Schott and McCreary Jr. (2001). Current branches indicated are the South Equatorial Current (SEC), South Equatorial Counter Current (SECC), Northeast and Southeast Madagascar Current (NEMC and SEMC), East African Coast Current (EACC), Somali Current (SC), Southern Gyre (SG), Great Whirl (GW), Socotra Eddy (SE); Ras al Hadd Jet (RHJ); West and East India Coastal Current (WICC and EICC), Laccadive High and Low (LH and LL), Southwest and Northeast Monsoon current (SMC and NMC); South Java current (JC) and Leeuwin Current (LC).

as the Findlater Jet (Findlater, 1974) causes strong gradients in the wind stress curl field (Figure 3.2). A positive wind stress curl drives open ocean upwelling (at the rate of about  $1-2 \times 10^{-3} \text{ cm s}^{-1}$ ) due to upward Ekman pumping to the NW of the Findlater Jet axis extending as far as 400km offshore (Smith and Bottero 1977). To the SE of the jet axis decreasing southwesterly wind causes negative wind stress curl (Hastenrath and Lamb 1979) that drives the surface water downward by Ekman pumping resulting into considerable deepening of mixed layer (Brock et al. 1991; Brock and McClain 1992;

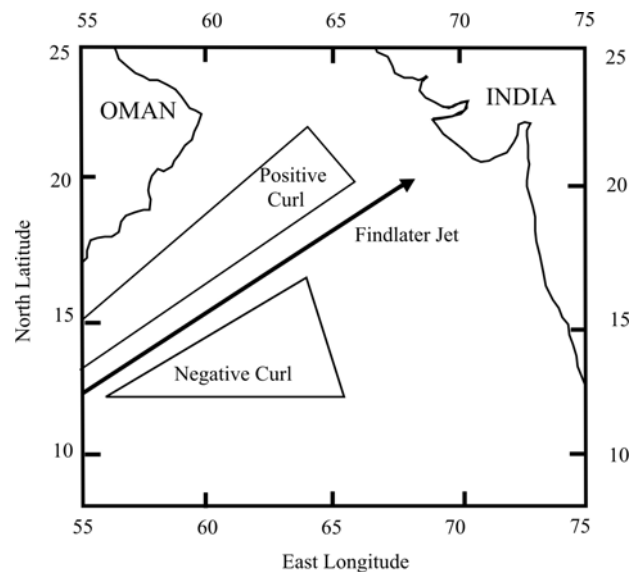


**Figure 3.2** Findlater jet along with region assumed to have positive and negative wind stress curl (Brock et al. 1991).

McCreary et al. 1996). Apart from the open ocean upwelling in the Arabian Sea, coastal upwelling driven by offshore Ekman divergence of surface water under the influence of winds parallel to the coast is also known (Smith and Bottero 1977). Coastal upwelling (at the rate of about  $3 \times 10^{-3} \text{ cm s}^{-1}$ ) is more pronounced off the coast of Oman and Somalia (Smith and Bottero 1977; Lee et al. 2000) however, a weaker upwelling is known to occur off southwest India (Wyrтки 1973). Upwelling is replaced by the convective mixing during NE monsoon in the Arabian Sea. The phenomena of upwelling and convective mixing bring enormous amount of nutrient rich deep water into the surface ocean, leading to increase in productivity and subsequently the cycling of nitrogen in the Arabian Sea.

Even before JGOFS, the Arabian Sea had been widely studied for its physical, chemical, geological and biological characteristics. However, the collective and thorough exploration of the Arabian Sea with well-defined objectives was performed

during the JGOFS period (1994-96). The main purpose of the JGOFS was to answer the following questions (Smith 2001):

1. Is the Arabian Sea a source or sink of carbon dioxide?
2. Is the Arabian Sea Mother Nature's iron experiment?
3. Do grazing zooplankton control carbon flux to the seabed?
4. Does the paleoceanographic record help us predict the ocean's response to climate change? and
5. What are the predominant physical processes of the Arabian Sea?

The present study concentrates mainly on the measurement of total and new production using  $^{15}\text{N}$  tracer technique along with natural nitrogen isotopic studies in the northeastern Arabian Sea. The following two subsections briefly discuss the productivity measurements carried out earlier in the region using  $^{14}\text{C}$  and  $^{15}\text{N}$  techniques followed by the work carried out during the present study.

### **3.2 $^{14}\text{C}$ based Productivity in the Arabian Sea**

Several observations for the total primary productivity in the Arabian Sea have been made (Ryther et al. 1966; Kabanova 1968; Krey 1973; Qasim 1977; Qasim 1982; Banse 1987), but in majority of the cases data have been averaged over coarse spatial and temporal domains, which is a serious limitation for a detailed process study. After the advent of satellite oceanography, greater insight into the annual changes in the phytoplankton productivity regimes have been observed, particularly using Coastal Zone Colour Scanner (CZCS) data (Banse and McClain 1986; Brock et al. 1991, 1993, 1994; Brock and McClain 1992). In addition to the JGOFS study (Savidge and Gilpin 1999 and Barber et al. 2001), earlier ship based studies include Owens et al. (1993) and Jochem et al. (1993).

Savidge and Gilpin (1999) have studied the size fractionated  $^{14}\text{C}$  based productivity in the Arabian Sea during two UK "ARABESQUE" cruises during the late SW Monsoon and autumn intermonsoon of 1994. During the late SW monsoon season, maximum productivity of  $3800 \text{ mgC m}^{-2} \text{ d}^{-1}$  (dominated by  $> 18\mu\text{M}$  fraction), distributed patchily, was observed in the coastal upwelling zone, whereas an average productivity of  $1500 \text{ mgC m}^{-2} \text{ d}^{-1}$  was observed elsewhere with the dominance of 0.2- $2\mu\text{M}$  fraction. During the autumn intermonsoon the productivity averaged around  $750 \text{ mgC m}^{-2} \text{ d}^{-1}$  with dominance of 0.2- $2\mu\text{M}$  size fraction. Ryther et al. (1966) have

reported a mean productivity of  $2230 \text{ mgC m}^{-2} \text{ d}^{-1}$  (ranging from  $840\text{-}6580 \text{ mgC m}^{-2} \text{ d}^{-1}$ ;  $n = 18$ ) for the Oman coastal upwelling zone (north of  $18^\circ\text{N}$ ) compared to  $3080 \text{ mgC m}^{-2} \text{ d}^{-1}$  reported for the same region by Savidge and Gilpin (1999). A decrease in the mean productivity to  $1550 \text{ mgC m}^{-2} \text{ d}^{-1}$  by Ryther et al., (1966) and  $2050 \text{ mgC m}^{-2} \text{ d}^{-1}$  by Savidge and Gilpin (1999) have been reported for region between  $16$  and  $18^\circ\text{N}$ . For the region between  $9$  and  $16^\circ \text{N}$  the average productivity of  $910 \text{ mgC m}^{-2} \text{ d}^{-1}$  by Savidge and Gilpin (1999) and  $1060 \text{ mgC m}^{-2} \text{ d}^{-1}$  by Ryther et al. (1966) have been reported.

Owens et al. (1993) have reported primary productivity variations from approximately  $500 \text{ mgC m}^{-2} \text{ d}^{-1}$  at the equator to  $300 \text{ mgC m}^{-2} \text{ d}^{-1}$  in the oligotrophic gyre in the central Arabian Sea, and  $> 2500 \text{ mgC m}^{-2} \text{ d}^{-1}$  in the upwelling region off the coast of Oman during September-October, 1986. They observed higher production in the regions where chlorophyll was more but could not find any significant statistical relationship to conclude that higher productivity was due to the presence of subsurface chlorophyll maximum at a number of stations.

Jochem et al. (1993) have studied the productivity regime and size structure of the phytoplankton during the spring intermonsoon of 1987, in the Arabian Sea. They found the integrated productivity to vary from  $1000$  to less than  $600 \text{ mgC m}^{-2} \text{ d}^{-1}$  near the coast of Oman with a maximum contribution from picoplankton ( $< 2 \mu\text{M}$ ). The mean productivity was around  $700 \text{ mgC m}^{-2} \text{ d}^{-1}$  for the central Arabian Sea with picoplankton as the dominant contributing fraction. Primary productivity of  $200\text{-}400 \text{ mgC m}^{-2} \text{ d}^{-1}$  was observed near the shelf off Pakistan.

The monsoon-driven variability in primary productivity and its regulation in the Arabian Sea were studied by Barber et al. (2001) in year 1995 as a part of the US JGOFS using the  $^{14}\text{C}$  technique. The study was carried out from the coast of Oman to the central Arabian Sea ( $65^\circ\text{E}$ ). According to this study, the SW Monsoon was the most productive season with an average value of  $1476 \pm 108 \text{ mgC m}^{-2} \text{ d}^{-1}$  followed by an unexpectedly high average productivity of  $1344 \pm 84 \text{ mgC m}^{-2} \text{ d}^{-1}$  during the NE Monsoon. However, the Barber et al. (2001) argue that high productivity observed during the SW Monsoon was less than that expected for a coastal upwelling region because of efficient grazing of diatoms by mesozooplankton. During the spring intermonsoon season, the Arabian Sea is considered to be oligotrophic; however, the observed productivity during this season by Barber et al. (2001) was much higher ( $1032 \pm 72 \text{ mgC m}^{-2} \text{ d}^{-1}$ ) than in other oligotrophic regions of the world such as the

tropical Pacific ( $348 \pm 24 \text{ mgC m}^{-2} \text{ d}^{-1}$ ) and the North Pacific gyre ( $384 \pm 96 \text{ mgC m}^{-2} \text{ d}^{-1}$ ). Overall, the annual mean productivity in the Arabian Sea in the year 1995 was observed to be  $1332 \pm 132 \text{ mgC m}^{-2} \text{ d}^{-1}$  that is roughly equal to that during the spring bloom of the North Atlantic ( $1284 \pm 276 \text{ mgC m}^{-2} \text{ d}^{-1}$ ). No gradient in productivity was observed from the coast to the open ocean. There was no evidence of light limitation, as expected, during NE Monsoon convective mixing or deep wind mixing during the SW monsoon.

Qasim (1982) has reported a very wide range of primary productivity for the northern Arabian Sea (north of  $15^\circ\text{N}$ ) varying from 13.0 to  $6010 \text{ mgC m}^{-2} \text{ d}^{-1}$  with an average value of  $835 \text{ mgC m}^{-2} \text{ d}^{-1}$ . He has also found the coastal areas to be more productive (average  $1329 \text{ mgC m}^{-2} \text{ d}^{-1}$ ) than the offshore areas ( $626 \text{ mgC m}^{-2} \text{ d}^{-1}$ ) and concluded that coastal water sustained more than 50% of the total production of the northern Arabian Sea. Qasim (1982) found that the Arabian Sea was most productive during the SW monsoon (average  $921 \pm 1140 \text{ mgC m}^{-2} \text{ d}^{-1}$ ); the productivity during NE monsoon ( $919 \pm 1030 \text{ mgC m}^{-2} \text{ d}^{-1}$ ) was less and during premonsoon ( $733 \pm 947 \text{ mgC m}^{-2} \text{ d}^{-1}$ ) was lesser. Qasim (1982) emphasised that northern Arabian Sea ( $\sim 1.7 \cdot 10^6 \text{ km}^2 \sim 25\%$  of total area) supports 50% ( $518 \cdot 10^6 \text{ tonnes C y}^{-1}$ ) of the total primary production of the Arabian Sea. However, Radhakrishna et al. (1978) have reported lower estimates of productivity from the same region.

The primary productivity study closest to the present study area (the northeastern Arabian Sea) was performed during the intermonsoon, NE monsoon and SW monsoon by Bhattathiri et al. (1996) as a part of the Indian JGOFS. The integrated production rates reported by Bhattathiri et al. (1996) varied between 193-199, 337-643 and  $770 \text{ mgC m}^{-2} \text{ d}^{-1}$  in the open ocean (along  $64^\circ\text{E}$ ) for the three seasons respectively whereas for the near coastal stations these values were 281-306, 200-807 and 440-1760  $\text{mgC m}^{-2} \text{ d}^{-1}$ . The seasonal variation in productivity was found to be consistent with the circulation patterns and associated nutrient levels.

Overall, available literature points towards the seasonal and geographical variation in the productivity regime of the Arabian Sea. In general, the SW monsoon has been found to be the most productive season followed by NE monsoon and intermonsoon. The reason cited for the SW monsoon and NE monsoon to be the productive seasons is the availability of nutrients in the surface layer due to vertical wind mixing during SW monsoon and convective mixing due to winter cooling during

NE monsoon. Geographically, the coastal locations such as off Oman are more productive than open ocean locations. The average productivity values reported for the Arabian Sea have been indexed in Table 3.1.

**Table 3.1**  $^{14}\text{C}$  based average total productivity values reported for different seasons and locations in the Arabian Sea.

	<b>Season</b>	<b>Region</b>	<b>Total Productivity (mgC m<sup>-2</sup> d<sup>-1</sup>)</b>
<b>Ryther et al. (1966)</b>	Late September- Early November	North of 18°N	2230
		16 and 18°N	1550
		9 and 16°N	1060
<b>Qasim (1982)</b>	Premonsoon SW monsoon NE monsoon	Northern Arabian Sea	733
			921
			919
<b>Owens et al. (1993)</b>	September-October	Equator	500
		Central Northern Indian Ocean	<300
		Off Coast of Oman	>2500
<b>Jochem et al. (1993)</b>	Spring Intermonsoon	Coast of Oman	1000-300
		Central Arabian Sea	700
		Shelf off Pakistan	200-400
<b>Bhattathiri et al. (1996)</b>	Premonsoon NE monsoon SW monsoon	Central and Eastern Arabian Sea	193-199
		Open Ocean Locations	337-643
			770
	Premonsoon NE monsoon SW monsoon	Coastal Locations	281-306
			200-807
			440-1760
<b>Savidge and Gilpin (1999)</b>	Late SW monsoon	NW Indian Ocean	1500
	Autumn Intermonsoon		750
<b>Barber et al. (2001)</b>	NE monsoon- January	Coast of Oman to 1000km offshore in Central Arabian Sea	1644
	NE monsoon- December		1056
	Intermonsoon- Spring		1032
	SW monsoon-Mid		1620
	SW monsoon-Late		1320
	Annual Mean		1332

### 3.3 <sup>15</sup>N based productivity in the Northwestern and the Central Arabian Sea

Results for <sup>15</sup>N based productivity (new and regenerated production) or nitrogenous nutrient uptake in the northwestern and central Arabian Sea have been reported by Owens et al. (1993), McCarthy et al. (1999), Watts and Owens (1999) and Sambrotto (2001). *No data for nitrogen based productivity has been reported from the eastern Arabian Sea till the present study.*

Owens et al. (1993) observed almost five-fold variation in the potential total nitrogen (Nitrate + Ammonium) assimilation ( $23.1 \text{ mmolN m}^{-2}\text{d}^{-1}$  for central Arabian Sea to  $96.7 \text{ mmol N m}^{-2}\text{d}^{-1}$  for off Oman coast) during September-October 1986 and found that the assimilation rates varied with primary production. The f-ratio varied from 0.09 in the oligotrophic region to as high as 0.92 in the upwelling region and showed a marked switch from a system dominated by ammonium assimilation in the oligotrophic region to nitrate-dominated in the upwelling region. Based on the high f-ratio Owens et al. (1993) concluded that a significant portion of the productivity would be available for higher trophic levels or sedimentation.

McCarthy et al. (1999) studied the nitrogen dynamics of the Arabian Sea during early and late NE monsoon of 1995. They found the higher abundance of all nitrogenous nutrients in the late phase of NE monsoon. McCarthy et al. (1999) have also reported the widespread suppressing effect of  $\text{NH}_4^+$  on  $\text{NO}_3^-$  uptake that was found to be 2-3 times more extreme during night than during day. They have reported low f-ratios, 0.15 (s.d. = 0.07, n= 15) and 0.13 (s.d. = 0.08, n=17) for early and late NE monsoon respectively and argued that the combined effect of high affinity for low concentration of  $\text{NH}_4^+$  and effect of  $\text{NH}_4^+$  concentration on  $\text{NO}_3^-$  uptake may be the possible reasons. McCarthy et al. (1999) also studied the effect of light on uptake of  $\text{NO}_3^-$  and  $\text{NH}_4^+$  in the Arabian Sea and concluded that  $\text{NO}_3^-$  utilization was more strongly influenced by light than  $\text{NH}_4^+$  utilization (only 20% of  $\text{NO}_3^-$  uptake occurred during night relative to 35% in the case of  $\text{NH}_4^+$ ). The higher uptake for  $\text{NH}_4^+$  relative to  $\text{NO}_3^-$  reflects either a higher contribution of heterotrophic activity to the aggregate rate of  $\text{NH}_4^+$  uptake or greater autotrophic potential to use  $\text{NH}_4^+$  in the absence of light. For the whole study area, the total nitrogen uptake during the late NE monsoon ( $\sim 26 \text{ mmolN m}^{-2}\text{d}^{-1}$ ) was higher than during the early NE monsoon ( $11 \text{ mmol N m}^{-2}\text{d}^{-1}$ ).

Watts and Owens (1999) reported nitrogen assimilation by phytoplankton that varied from 1.1 to 23.6 mmol N m<sup>-2</sup>d<sup>-1</sup> in the northwestern Indian Ocean during an intermonsoon period of 1994. They also reported ammonium to be the most preferred substrate.

Sambrotto (2001) reported nitrogen productivity and regeneration during the Spring Intermonsoon and the SW monsoon for the northern Arabian Sea. Overall, the new (nitrate) production varied from 0.1 to 13mmolN m<sup>-2</sup>d<sup>-1</sup>, whereas the f-ratio varied from 0.03 to 0.4. As expected, the onset of SW monsoon results in an increase in the nitrate uptake by an order of magnitude compared to the spring intermonsoon.

### **3.4 Chlorophyll *a*, nutrients and physical parameters during January 2003 in the Northeastern Arabian Sea**

#### **3.4.1 Chlorophyll *a***

Chlorophyll *a* concentrations were measured at six out of seven stations. The measurement could not be performed at PP7 due to sampling problems. During the study period the maximum integrated Chl *a* concentration of 68.5 mg m<sup>-2</sup> was found at PP2 (an open ocean station). For all other stations it varied within a range of 26.4 to 31.8 mg m<sup>-2</sup> (Figure 3.3-left panel). The surface Chl *a* was also maximum at PP2 where it was 1.15mg m<sup>-3</sup>. At all other stations it varied from 0.42 at PP4 (an open ocean station) to 0.7 mg m<sup>-3</sup> at PP6 (a coastal station). The vertical profiles of Chl *a* at different stations are shown in Figure 3.3-right panel. At PP1 there is decrease in Chl *a* from surface to 40m that increases again to show Chl *a* maximum at 55m, slightly more than that of the surface value (0.56 compared to surface value of 0.52 mg m<sup>-3</sup>). At PP2 the Chl *a* is slightly more than or around 1 mg m<sup>-3</sup> at most of the depths and decreases sharply after 50m to reach a lowest value of 0.39 mg m<sup>-3</sup> at 65m. There is no distinct Chl *a* max at PP2. Profile at PP3 shows a small subsurface Chl *a* minimum at 20m and again peaks up to remain almost uniform throughout the water column with a typical concentration of ~0.42 mg m<sup>-3</sup>. The range of variation at PP4 is between 0.41 to 0.52 mg m<sup>-3</sup> with a maximum at 50m. The Chl *a* concentration at PP5 shows a general increase with depth with a minimum value at the surface and a maximum at 65m (base of euphotic depth) whereas PP6 shows the trend opposite to PP5 with a general decrease with depth in Chl *a* concentration.

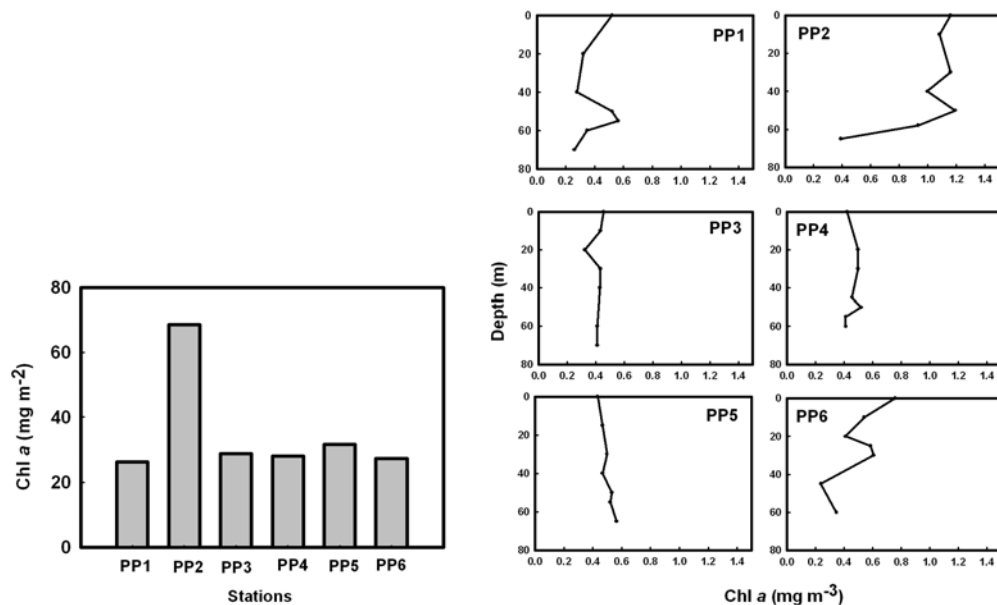


**Figure 3.3** Euphotic zone integrated concentration (left panel) and vertical profile (right panel) of Chlorophyll *a* at productivity stations during January 2003.

### 3.4.2 Nutrients

Samples from different stations were analysed for nitrate and ammonium concentrations using an autoanalyser. The integrated nitrate varied from as low as 5.2 mmol m<sup>-2</sup> at coastal station (PP7) to as high as 254 mmol m<sup>-2</sup> at open ocean station (PP4). Most of the stations had integrated nitrate around or more than 100 mmol m<sup>-2</sup>

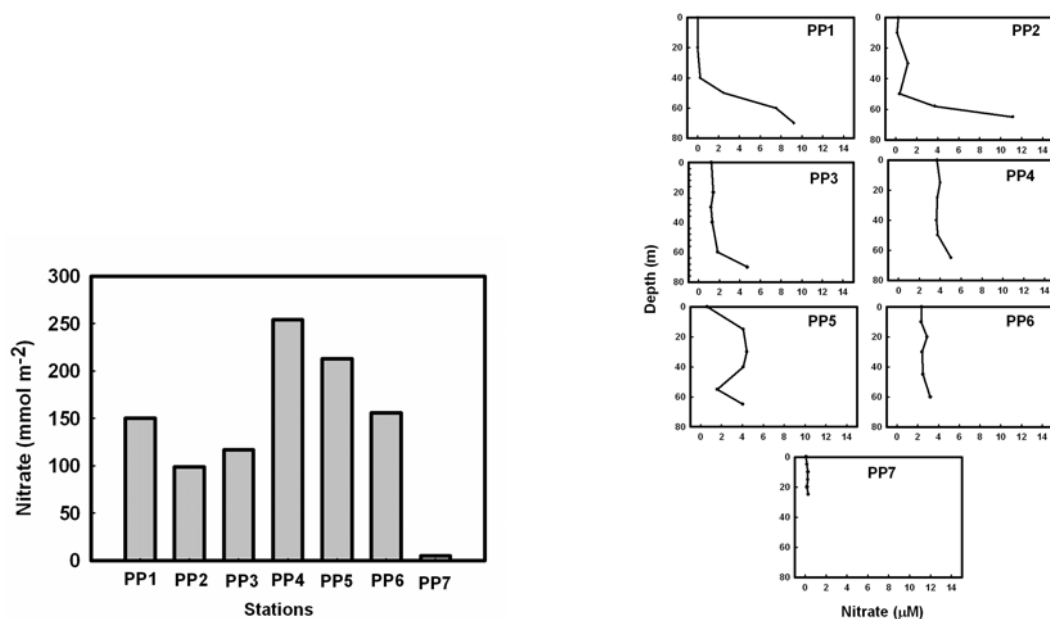


**Figure 3.4** The euphotic zone integrated (left panel) and vertical profile (right panel) of ambient nitrate at different stations during January 2003.

(Figure 3.4-left panel). The vertical profiles of nitrate at different stations are shown in Figure 3.4-right panel. PP1 and PP2 do not have much nitrate in the upper 50m of water column ( $<0.4\mu\text{M}$ ), but it increases to around 7 and  $11\mu\text{M}$  respectively around 65m. PP3 has nitrate more than  $1\mu\text{M}$  throughout the water column, it increases to  $3\mu\text{M}$  throughout at PP4. PP5 and PP6 also have almost uniform nitrate concentrations with 4 and  $\sim 2\mu\text{M}$  respectively at each depth. Again at the coastal station PP7, nitrate decreases significantly to around  $0.1\mu\text{M}$  (measurement was made only up to 25m, euphotic depth). The increased nitrate concentration at open ocean stations indicates the effect of winter cooling leading to deeper mixed layer depth and consequent enrichment of nitrate in the water column.

The integrated ammonium concentration during January in the northeastern Arabian Sea varied within a narrow range of 0.5 (PP7) to  $8.4\text{mmol m}^{-2}$  (PP4). The integrated ammonium concentration at different stations is shown in Figure 3.5 (left panel). The ammonium concentration during the study period was never more than  $0.3\mu\text{M}$  for any station within the euphotic zone and it was found below detection limit ( $0.01\mu\text{M}$ ) at several depths. At PP7 ammonium was almost absent through the top 20m of water column to reach  $0.05\mu\text{M}$  at bottom of euphotic zone. The depth profile of ammonium is shown in Figure 3.5 (right panel).

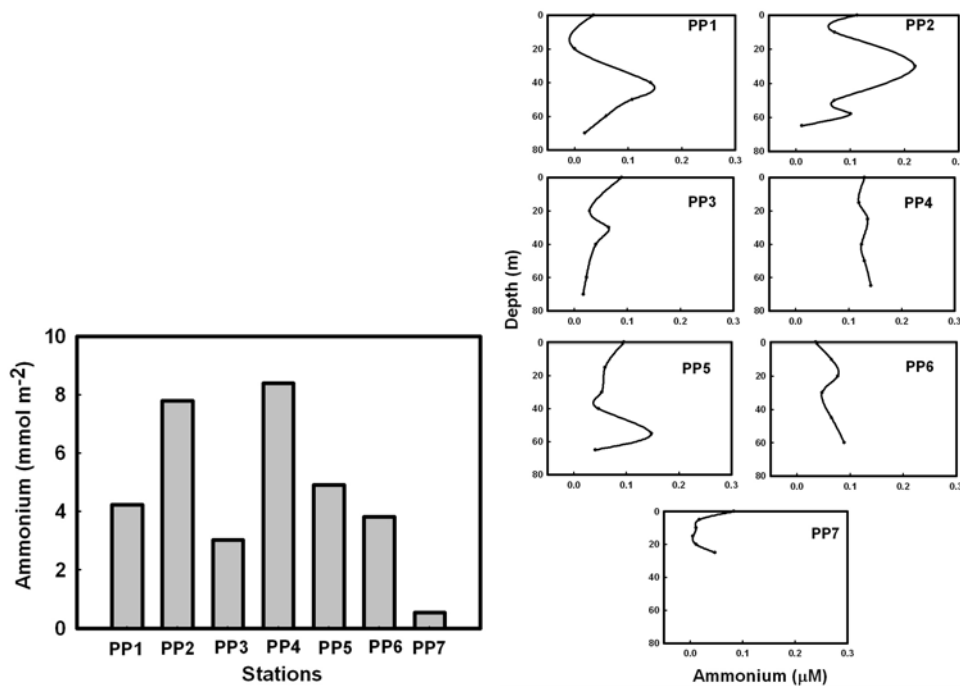


**Figure 3.5** The euphotic zone integrated (left panel) and vertical profile (right panel) of ambient ammonium at different stations during January 2003.

### 3.4.3 Hydrographic and meteorological conditions

The present study was conducted during the Asian winter monsoon. This period in the Arabian Sea witnesses a temperature difference of almost 5-6°C from the south to the north. The long-term average temperature during the month of January in the Arabian Sea is shown in Figure 3.6 (left-panel). During the study period sea surface temperature showed a general decrease from south to north, with maximum temperature of 28.6°C at one of the southernmost stations (PP1) and minimum of 23.9 °C at one of the northernmost stations i.e., Stn.11 (Figure 3.6-right panel). Decrease in temperature from the south to the north during winter is characteristic of the region and has been found to decrease at a rate of 0.5°C per degree latitude (Madhupratap et al. 1996).

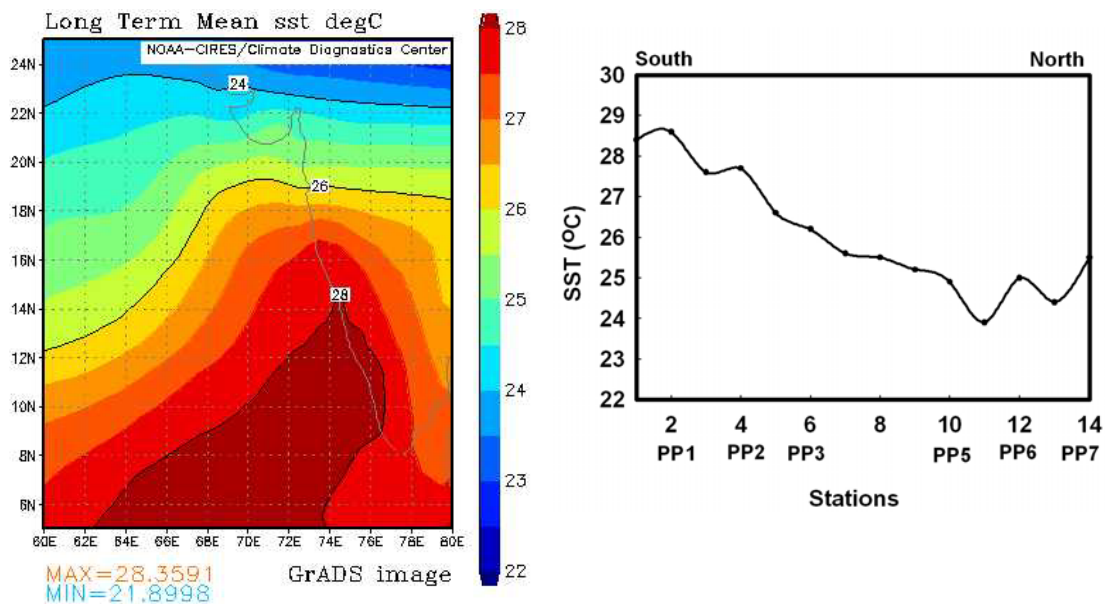


**Figure 3.6** The long-term average Sea surface Temperature (SST) of the Arabian Sea during January (left panel, Source: Climate Diagnostic Center, National Center for Environmental Prediction, USA) and SST at different stations at the time of sampling (right panel) during January 2003.

Similarly, the air temperature over the Arabian Sea also dropped from 29.2°C in the south to 24°C in the north during the study period (Figure 3.7-left panel). Long term average of air temperature during January is shown in Figure 3.7 (right panel). At most of the stations SST was higher than the air temperature by 0.6°C or more. Wind during January was north/northeasterly with an average speed of around 4ms<sup>-1</sup>. The average wind direction and speed during January is shown in Figure 3.8 (left-panel) and the

wind speed during sampling is shown in Figure 3.8 (right-panel). The surface pressure was the lowest at the start of the cruise (1012.5mb at Stn 1) and increased

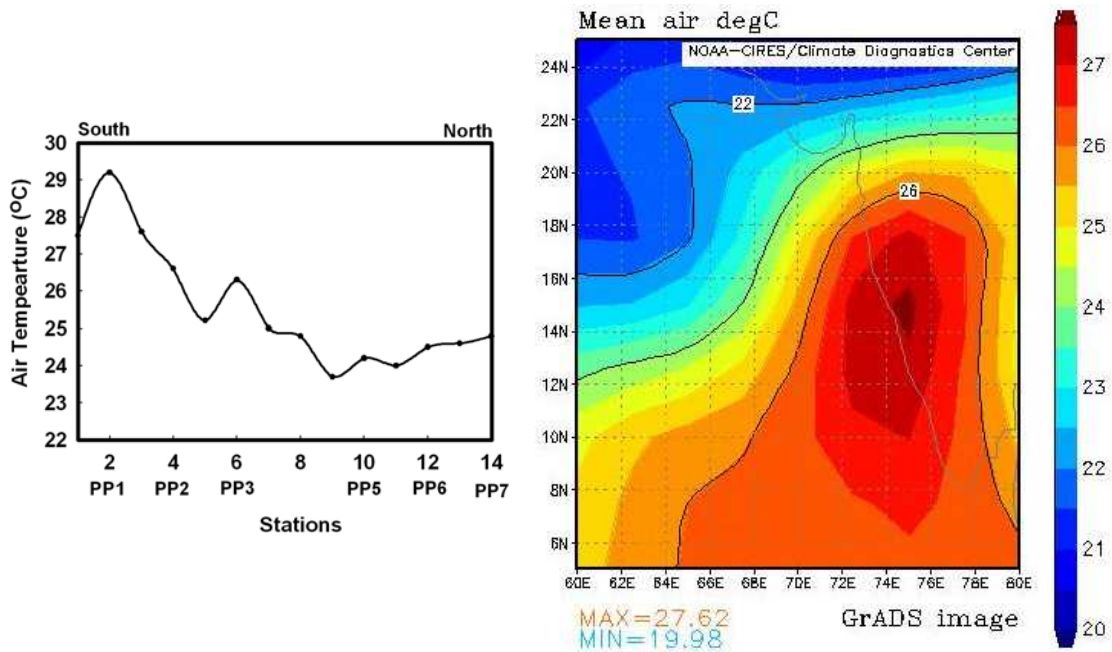


**Figure 3.7** Air temperature at different stations at the time of sampling (right panel) during January 2003 and the long-term average air temperature over the Arabian Sea during January (left panel, Source: Climate Diagnostic Center, National Center for Environmental Prediction, USA).

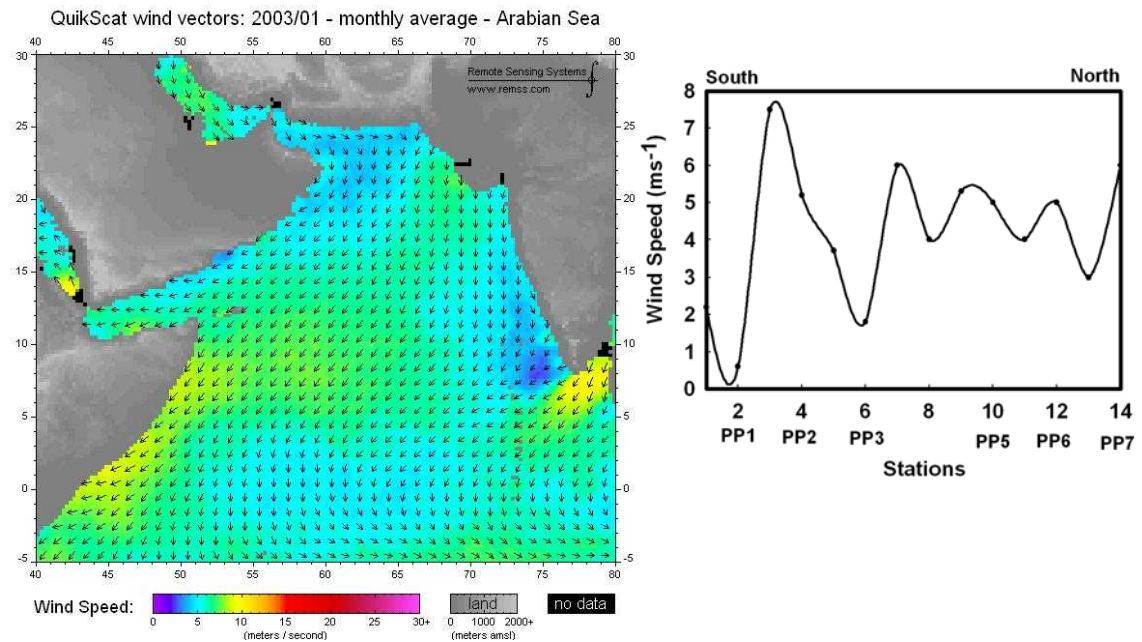


**Figure 3.8** The monthly average of wind speed and direction over Arabian Sea (left panel, Source: Quikscat) and wind speed measured at the time of sampling during January 2003.

gradually to reach a maximum of 1019mb at PP5 (Stn. 12). A sharp drop in atmospheric pressure was observed from Stn. 10 to Stn. 11 (1014.5 mb) to peak up again at stn. 12 (Figure 3.9). General increase in surface layer depth with uniform

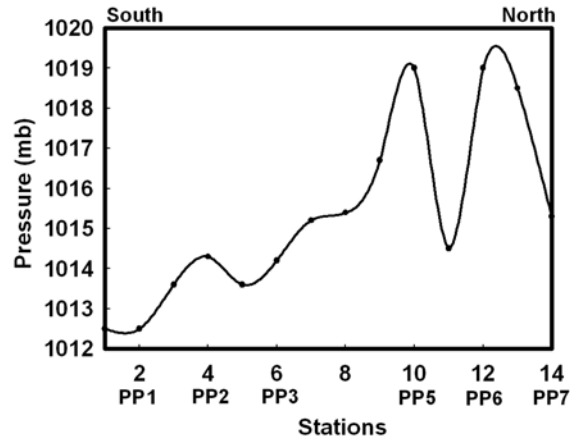


**Figure 3.9** Air pressure at the time of sampling during January 2003.

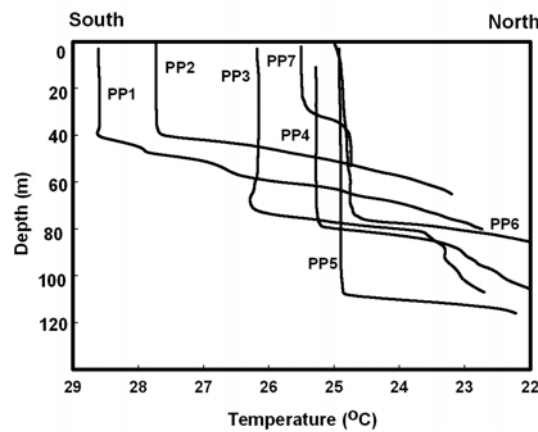


**Figure 3.10** Temperature profile at different stations obtained with Satlantic Radiometer during January 2003.

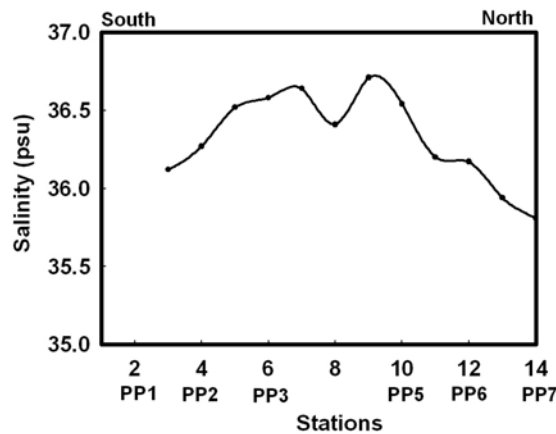


**Figure 3.11** Salinity variation from south to north at sampling time during January 2003.

temperature (henceforth as temperature based mixed layer or MLD) was observed from south to north with southern station PP1 at around 40m to 107m for one of northernmost (PP5~ stn.10) stations (Figure 3.10). The most dramatic increase in MLD was observed from PP2 (40m) to PP3 (70m). The average euphotic depth in the open ocean was 60m (maximum 70m at Stn.1 to minimum 53m at stn.10~PP5) that reduced to 25m at coastal station PP7 (stn. 14). Slight variation in surface salinity from south to north was observed during study period (Figure 3.11). The maximum salinity of 36.71 was observed at an open ocean station (stn. 9) whereas minimum was observed at coastal stn.14. (PP7).

### 3.5 $^{15}\text{N}$ based productivity study during January 2003

#### 3.5.1 Total Production

The present study concentrated mainly in the open ocean, where five out of seven were open ocean stations (PP1 to PP5) and two (PP6 and PP7) were coastal stations (off Gujarat). The rates of total N-uptake, integrated over the water column from the surface upto 1% light level (photic depth) span an order of magnitude over the study area and range from  $6.17 \text{ mmolN m}^{-2} \text{ d}^{-1}$  to  $65.4 \text{ mmolN m}^{-2} \text{ d}^{-1}$  (Figure 3.12). The highest rate has been measured at the second station (PP2), which is  $65.4 \text{ mmolN m}^{-2} \text{ d}^{-1}$  ( $\sim 5000 \text{ mgC m}^{-2} \text{ d}^{-1}$ ), one of the highest observed so far for the northeastern Arabian Sea.

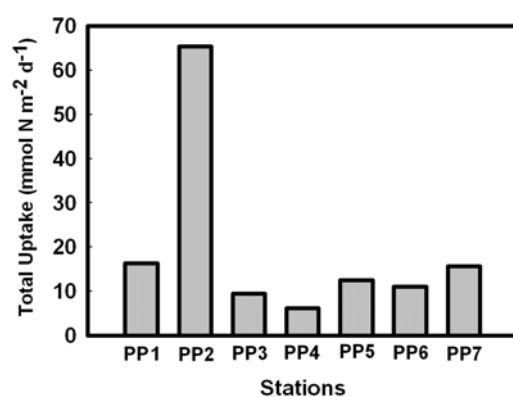


**Figure 3.12**  $^{15}\text{N}$  based total productivity (estimated as sum of nitrate, ammonium and urea uptakes) observed during present study.

However, total productivity as high as  $6010 \text{ mgC m}^{-2} \text{ d}^{-1}$  has been reported for coastal waters of the northern Indian Ocean during the premonsoon season (Qasim, 1982). Ryther et al. (1966) have also reported the productivity value as high as  $6580 \text{ mgC m}^{-2} \text{ d}^{-1}$  from the coastal area off Oman. The minimum rate of  $6.17 \text{ mmolN m}^{-2} \text{ d}^{-1}$  was

observed in the station PP4, also an open ocean station. No systematic spatial variability from south to north has been observed in the total uptake rates. Except PP2, uptake rates range from ~6 to 16 mmolN m<sup>-2</sup> d<sup>-1</sup> for the region. Total productivity during present study averages around 20 (±20)\* mmolN m<sup>-2</sup> d<sup>-1</sup> (~ 1590 mgC m<sup>-2</sup> d<sup>-1</sup>), which reduces to 12 (±3.8) mmolN m<sup>-2</sup> d<sup>-1</sup> (954 mgC m<sup>-2</sup> d<sup>-1</sup>) when PP2 is excluded. The average rate of total N-uptake for open ocean station is around 22(±24) mmolN m<sup>-2</sup> d<sup>-1</sup> (~1750 mgC m<sup>-2</sup> d<sup>-1</sup>) and comes down to 11 (±4.4) mmol N m<sup>-2</sup> d<sup>-1</sup> (~ 874 mgC m<sup>-2</sup> d<sup>-1</sup>) after excluding PP2. Two coastal stations studied off Gujarat averaged around 13.4(±3.2) mmol N m<sup>-2</sup> d<sup>-1</sup> (~1065 mgC m<sup>-2</sup> d<sup>-1</sup>). For the same region, Bhattathiri et al., (1996) have reported <sup>14</sup>C based total productivity varying from 337-643 mgC m<sup>-2</sup> d<sup>-1</sup> for the open ocean and upto 807 mgC m<sup>-2</sup> d<sup>-1</sup> (~ 10.1 mmol N m<sup>-2</sup> d<sup>-1</sup>) for the coastal locations during the same season. The average values reported here (excluding station PP2) are similar to the values reported by Bhattathiri et al. (1996). Since the PP2 has anomalously high value compared to other stations, the average value excluding PP2 will be considered as the representative value for the study region and the same will be used for comparison with other studies. Average total nitrogen uptake of 26 mmolN m<sup>-2</sup> d<sup>-1</sup> (ranging from 9.2 - 40 mmolN m<sup>-2</sup> d<sup>-1</sup>) and 11 mmolN m<sup>-2</sup> d<sup>-1</sup> (ranging from 3.9-24 mmolN m<sup>-2</sup> d<sup>-1</sup>) has been reported for the northwestern and central Arabian Sea during the month of January (same season as present study) and November respectively (McCarthy et al. 1999). Although of the same month, the value reported by McCarthy et al. (1999) for January is significantly higher than reported during the present study probably indicating higher nutrient availability due to convective mixing by winter cooling and effective utilization of the available nutrients by the phytoplankton in the northwestern and central Arabian Sea than the northeastern Arabian Sea. However, the average value reported by McCarthy et al. (1999) for the month of November is comparable with the average values of the present study. Highest value of productivity (40 mmolN m<sup>-2</sup> d<sup>-1</sup>) reported by McCarthy et al. (1999) for a central Arabian Sea station is considerably lower than the highest value for open ocean station of the present study. Watts and Owens (1999) have reported the average integrated assimilation rate of 8.3 mmolN m<sup>-2</sup> d<sup>-1</sup> for northwestern Arabian Sea during intermonsoon, which is significantly lower than the average values reported during present study. This shows that the northeastern Arabian Sea during NE monsoon is definitely more productive

---

\* Numbers in parentheses are geographical variabilities and not experimental uncertainties.

than the otherwise highly productive northwestern Arabian Sea during intermonsoon season. The values reported here are comparable to nitrogen uptake rates in the northeast Atlantic during July 1996 (Donald et al. 2001) but higher than the total productivity reported for equatorial Pacific Ocean along meridional section at 150°W during February-March (Dugdale et. al. 1992). The 'productivity normalised to Chlorophyll *a*' during the present study (spatially) averaged around 2.3 ( $\pm$  2.3) h<sup>-1</sup> which is well within the observed oceanic range.

### 3.5.2 New Production

As mentioned in the earlier chapter, nitrate uptake has been considered as new production during the present study. Barring station PP2, where new production has been found to be quite high (34.8 mmolN m<sup>-2</sup>d<sup>-1</sup> ~ 2766 mgC m<sup>-2</sup>d<sup>-1</sup>), it ranges from 1 (~ 80mgC m<sup>-2</sup>d<sup>-1</sup>) to 4.3mmolN m<sup>-2</sup> d<sup>-1</sup> (~342 mgC m<sup>-2</sup>d<sup>-1</sup>) (Figure 3.13). Overall new production for the region averages around 2.3( $\pm$ 1.1) mmolN m<sup>-2</sup> d<sup>-1</sup> (~183 mgC m<sup>-2</sup>d<sup>-1</sup>), but it increases to ~7( $\pm$ 12.3) mmolN m<sup>-2</sup> d<sup>-1</sup> (~ 557 mgC m<sup>-2</sup>d<sup>-1</sup>) when PP2 is taken into consideration. Open ocean locations average around 1.7( $\pm$ 0.61) mmolN m<sup>-2</sup> d<sup>-1</sup> (~ 135 mgC m<sup>-2</sup>d<sup>-1</sup>) whereas at two coastal stations average new production (3.4 $\pm$ 1.2 mmolN m<sup>-2</sup> d<sup>-1</sup> ~ 270 mgCm<sup>-2</sup>d<sup>-1</sup>) has been found to be twice that of open ocean average. The highest new production among the stations other than PP2, was observed at a coastal location closest to the coast (PP7).

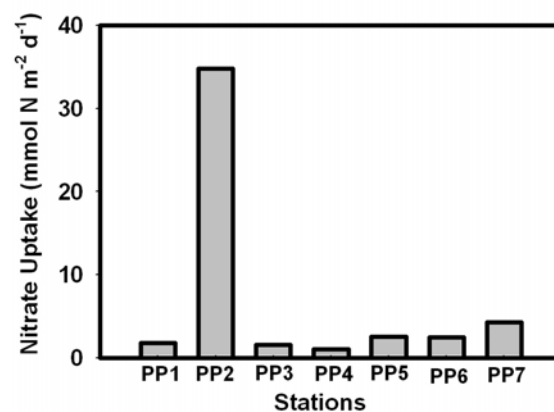


**Figure 3.13** New production observed at different locations during January 2003.

The average new production measured during the present study is less by ~1mmol Nm<sup>-2</sup> d<sup>-1</sup> from the average value reported by McCarthy et al. (1999) for nitrate uptake during January (3.2mmolN m<sup>-2</sup> d<sup>-1</sup>) but is more than average value reported for November (1.5

mmolN m<sup>-2</sup> d<sup>-1</sup>) for the northwestern and the central Arabian Sea. However, the average values reported by McCarthy et al. (1999) can be considered similar in magnitude to the present study as they fall within 1 standard deviation (1σ) of the present average value. The average nitrate uptake values reported by Sambrotto (2001) for different transects (coastal upwelling, Findlater Jet, Off India) during the SW monsoon and spring intermonsoon for the northern Arabian Sea are more (>3.1 mmolN m<sup>-2</sup> d<sup>-1</sup>) than the average new production reported during present study. But the average value for southeastern Arabian Sea (0.4 mmol N m<sup>-2</sup> d<sup>-1</sup>) is significantly less than the present average value. Watts and Owens (1999) have reported the average nitrate assimilation rate of 1.8 mmolN m<sup>-2</sup> d<sup>-1</sup> for the intermonsoon season of the northwestern Arabian Sea, which is comparable within 1σ of the present average value. The nitrate uptake in the NE Atlantic measured along a transect from 58°N to 37°N during July 1996 (Donald et al. 2001) is also within the upper limit (~3.5mmol Nm<sup>-2</sup>d<sup>-1</sup>) of the present study. However, the new production during the present study is higher than that reported for equatorial Pacific Ocean during February-March (Dugdale et al. 1992) and eastern Alboran Sea (L'Helguen et al. 2002). Total average nitrate uptake of 5.6 mmol N m<sup>-2</sup> d<sup>-1</sup> has been observed during Lagrangian experiments in the Iberian upwelling region by Joint et al. (2001) which is significantly higher than the present average value, but is comparable to off India (5.2 mmol N m<sup>-2</sup> d<sup>-1</sup>) nitrate uptake value, during spring intermonsoon and SW monsoon reported by Sambrotto (2001). One of

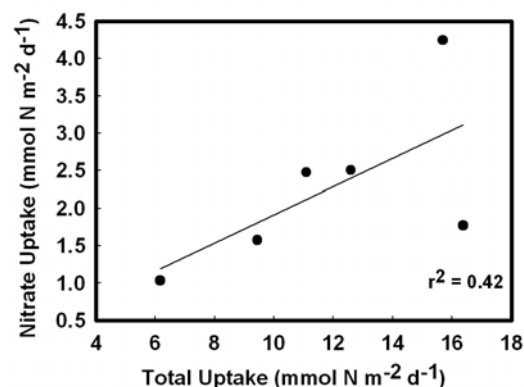


**Figure 3.14** Relationship between new and total production (excluding PP2) observed during January 2003 in the Arabian Sea.

the most important aspects of the new production result during present study is a general trend of spatial increase from south to north (i.e., from Goa to Gujarat). Also,

excluding PP2, there exists a fair correlation ( $r^2 = 0.42$ ; significant at 0.10 level) between new and total production during January (Figure 3.14). However, this correlation becomes very significant ( $r^2 = 0.98$ ) when PP2 is included. This is mainly due to very high total and new production at PP2 which falls far away from the rest of the stations basically transforming the regression into a two point regression, one being PP2 and second, the cluster of rest. Overall, it appears that new production during January 2003 in the northeastern Arabian Sea is well within the range for nitrate uptake obtained by other workers for northwestern and central Arabian Sea.

### 3.5.3 Regenerated production

The sum of  $\text{NH}_4$  and urea uptake has been considered as regenerated production. As in the case of new and total production, regenerated production was also the highest at PP2. The  $\text{NH}_4$  uptake at this station was found to be  $23.3 \text{ mmolN m}^{-2} \text{ d}^{-1}$ . Regenerated production at all the stations except PP2 is more than the new production. However, at PP2 new production ( $34.8 \text{ mmolN m}^{-2} \text{ d}^{-2}$ ) is significantly higher than the regenerated production indicating the more significant role played by nitrate than ammonium at this station. Except at PP2,  $\text{NH}_4$  uptake rate varied from 3.8 to  $10 \text{ mmolN m}^{-2} \text{ d}^{-1}$ , with an overall average of  $6.4(\pm 2.2) \text{ mmolN m}^{-2} \text{ d}^{-1}$  ( $8.8 \pm 6.7 \text{ mmolN m}^{-2} \text{ d}^{-1}$  including PP2). There is not much difference between the overall average  $\text{NH}_4$  uptake and the average  $\text{NH}_4$  uptake at open ( $6.7 \pm 2.7 \text{ mmolN m}^{-2} \text{ d}^{-1}$ ;  $10 \pm 7.7 \text{ mmolN m}^{-2} \text{ d}^{-1}$  after including PP2) and coastal ( $5.8 \pm 0.5 \text{ mmolN m}^{-2} \text{ d}^{-1}$ ) locations. The lowest  $\text{NH}_4$  uptake was observed at PP4, where nitrate uptake was also the lowest, whereas the second highest (PP2 being the first)  $\text{NH}_4$  uptake was observed at PP1. The values of regenerated production reported here are significantly lower than the average ammonium uptake rate ( $21.5 \text{ mmol N m}^{-2} \text{ d}^{-1}$ ) reported by McCarthy et al. (1999) for January of the northwestern Arabian Sea. The latter is comparable to the highest ammonium uptake rate (at PP2) reported during the present study. Except one station of McCarthy et al. (1999), where ammonium uptake is  $5.4 \text{ mmolN m}^{-2} \text{ d}^{-1}$ , all other stations have ammonium uptake more than that observed for any station of the present study (except anomalous PP2). Ammonium uptake during November for northwestern Arabian Sea averages around  $8.6 \text{ mmolNm}^{-2} \text{ d}^{-1}$  (McCarthy et al. 1999), which is comparable within the upper limit of the present study. Overall comparison of present study with McCarthy et al. (1999) suggests that the ammonium uptake and role of ammonium as a

nutrient is more prevalent in the northwestern Arabian Sea than the northeastern Arabian Sea during peak NE monsoon. However, the average ammonium uptake reported here is more than the average ammonium assimilation rate of  $3.7 \text{ mmolN m}^{-2} \text{ d}^{-1}$  reported by Watts and Owens (1999) for intermonsoon period in the northwestern Arabian Sea and the ammonium uptake rate ( $3.2 \text{ mmolNm}^{-2} \text{ d}^{-1}$ ) reported by Joint et al. (2001) for the Iberian upwelling during August.

Urea uptake during the present study is a conservative estimate and hence the minimum contribution of urea to the total production. Urea uptake obtained for the study period varied from 1.3 to  $7.3 \text{ mmolN m}^{-2} \text{ d}^{-1}$ . The overall average was found to be  $3.8 \text{ mmolN m}^{-2} \text{ d}^{-1}$  (including PP2) with an open ocean average of 3.63 and a coastal average of  $4.2 \text{ mmolN m}^{-2} \text{ d}^{-1}$  respectively. The average urea uptake observed by Watts and Owens (1999) for the northwestern Arabian Sea averages ( $1.6 \text{ mmolN m}^{-2} \text{ d}^{-1}$ ) less than half of that observed during the present study, with a minimum of  $0.5 \text{ mmolN m}^{-2} \text{ d}^{-1}$  near the Oman coast to a maximum of  $5.5 \text{ mmolN m}^{-2} \text{ d}^{-1}$  off India. The nitrate,  $\text{NH}_4$  and urea uptakes observed at different stations are shown in Figure 3.15.

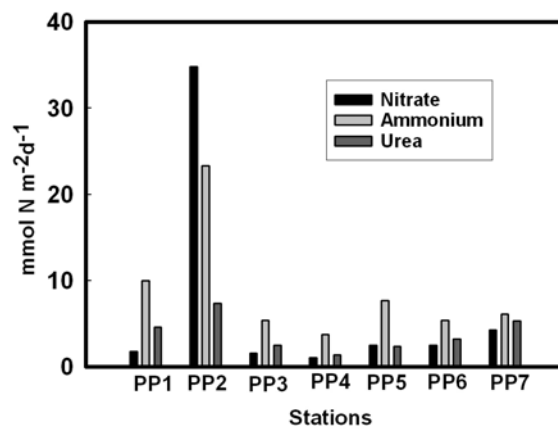


**Figure 3.15** New (nitrate uptake) and Regenerated (ammonium + urea uptake) production observed in the Arabian Sea during present study.

### 3.5.4 Rationale for the preference of ammonium over nitrate

At almost all stations during the present study  $\text{NH}_4$  was assimilated in preference to urea and  $\text{NO}_3$ , which is in agreement with the observations for the northwestern and the central Arabian Sea. This similarity in the relative preferences for different nitrogenous nutrients in the northwestern and the northeastern Arabian Sea indicates more or less the same nitrogen dynamics for both parts of the basin. The preference for reduced (recycled) forms of nitrogen such as  $\text{NH}_4$  (if available) relative to nitrate is well known

in marine and freshwater environments (Dugdale and Goering 1967; McCarthy and Eppley 1972; McCarthy et al. 1977; Glibert et al. 1982b; Paasche and Kristjansen 1982; Smith and Nelson 1990; Owens et al. 1991; Rees et al. 1995). The physiological reason for the preference of  $\text{NH}_4$  over  $\text{NO}_3$  is given in terms of higher energy requirement during assimilation of  $\text{NO}_3$ , as nitrate has to be transported and reduced before being consumed by the phytoplankton (McCarthy and Carpenter 1983). It is also known that large part of reduced nitrogen pool is consumed by the phytoplankton of size less than  $20\mu\text{m}$ . Size fraction study of productivity was not the aim of the present study and therefore estimation of phytoplankton in different size ranges was not carried out. However, high picoplankton densities, ranging upto  $45 \times 10^6$  cells  $\text{l}^{-1}$  has been observed during February near the present study area (Ramaiah et al. 1996) but their contribution in total productivity is not known. The nano- ( $2\text{-}18\mu\text{m}$  diameter) and Pico- ( $<2\mu\text{m}$  diameter) planktons fraction are known to constitute  $>75\%$  of productivity in the northwestern Arabian Sea (Watts and Owens 1999). Jochem et al. (1993) have found picophytoplankton dominating the phytoplankton productivity (48-76%) in the central Arabian Sea and off the Oman Coast. Owens et al. (1993) have also found in their study that phytoplankton less than  $5\mu\text{m}$  size were responsible for more than 75% of the phytoplankton production. Heterotrophic bacteria are also known to assimilate dissolved ammonium (Laws et al. 1985; Kirchman 1994) and if these bacteria form a significant portion of the total biomass, they could pose serious implications to new and regenerated production estimation by  $^{15}\text{N}$  tracer technique (Watts and Owens 1999). Pomroy and Joint (1999) have found a 10-30% contribution by heterotrophic bacteria during their study in northwestern Arabian Sea. The present study cannot estimate the effect of heterotrophic bacteria on ammonium uptake data for the same reason cited by Watts and Owens (1999) i.e., unknown fraction of bacterial abundance on the GF/F filter paper (pore size  $0.7\mu\text{m}$ ) used for present study and also the extent of dissolved inorganic nitrogen as an alternative source of nitrogen, if present. However, Ramaiah et al. (1996) have found higher bacterial densities (of about  $1 \times 10^9$  cell  $\text{l}^{-1}$ ) during the intermonsoon period than the southwest and winter monsoons. Therefore, the effect of bacteria may not be very prominent in ammonium assimilation during the present study or it would be less than that during the intermonsoon. However, it is necessary to study phytoplankton abundance in different size ranges and bacterial

abundance during the same cruise in order to ascertain their roles in the uptake of different nitrogen sources.

### 3.5.5 Vertical profiles of Nitrate and Ammonium Uptake

The vertical profiles of nitrate and ammonium uptake obtained by  $^{15}\text{N}$  technique are a function of light and nutrient concentrations at different depths. The vertical profile of nitrate uptake at different stations during January 2003 is shown in Figure 3.16. The nitrate uptake profile at almost all the stations suggests a subsurface uptake maximum varying between 5 and 40m from the surface. The general euphotic depth during the

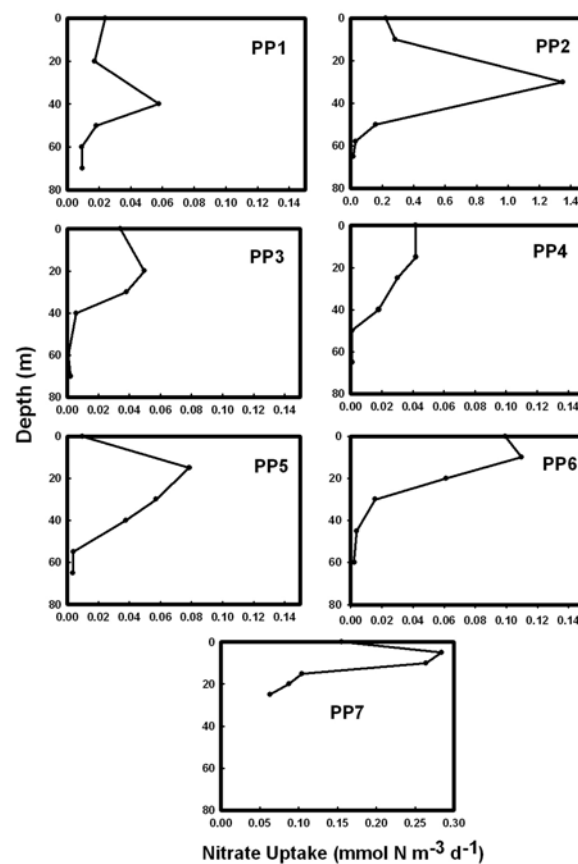


**Figure 3.16** Vertical profiles of nitrate uptake rates at discrete depths at different locations. The uptake profile is limited upto the measured euphotic depths.

study period was between 60-70m, except at PP7 where it was just 25m. So the uptake maxima in general fell within the 90 and 5% of surface light. At PP1 the maximum was at 40m with an uptake value of around  $0.06\text{mmolN m}^{-3}\text{d}^{-1}$ . This was the zone in the water column from where there was sharp increase in the nitrate concentration. The nitrate uptake did not stop at 1% light level ( $0.01\text{ mmolN m}^{-3}\text{d}^{-1}$ ) at this station. The

nitrate uptakes for all depths were highest at PP2 with surface uptake around  $0.2 \text{ mmol N m}^{-3} \text{ d}^{-1}$  and a maximum uptake of around  $1.4 \text{ mmol N m}^{-3} \text{ d}^{-1}$  at 30m. However, the nitrate profile of the station does not show very high values ( $<1.2 \mu\text{M}$  in top 50m of water column). The reason may be the rapid utilisation of nitrate in the water column by the phytoplankton as this station, characterised by very high biomass (Chl *a* varying between  $1\text{-}1.2 \text{ mg m}^{-3}$  with euphotic zone integrated value of  $68.5 \text{ mg m}^{-2}$ ). PP3 to PP6 show the uptake maxima in the top 20m of water column with the maximum uptake rate varying from  $0.04$  to  $0.11 \text{ mmol N m}^{-3} \text{ d}^{-1}$ . All these stations are characterised by higher uniform nitrate in the water column. The uptake profile of the coastal station PP7 shows relatively higher uptake rates at discrete depths than the open ocean stations with maximum at 5m with an uptake value of around  $0.28 \text{ mmol N m}^{-3} \text{ d}^{-1}$ . The uptake at the base of euphotic depth is also high (around  $0.06 \text{ mmol N m}^{-3} \text{ d}^{-1}$ ). However, the nitrate profile of the station does not suggest very high value (maximum  $0.28 \mu\text{M}$  at base of euphotic zone).

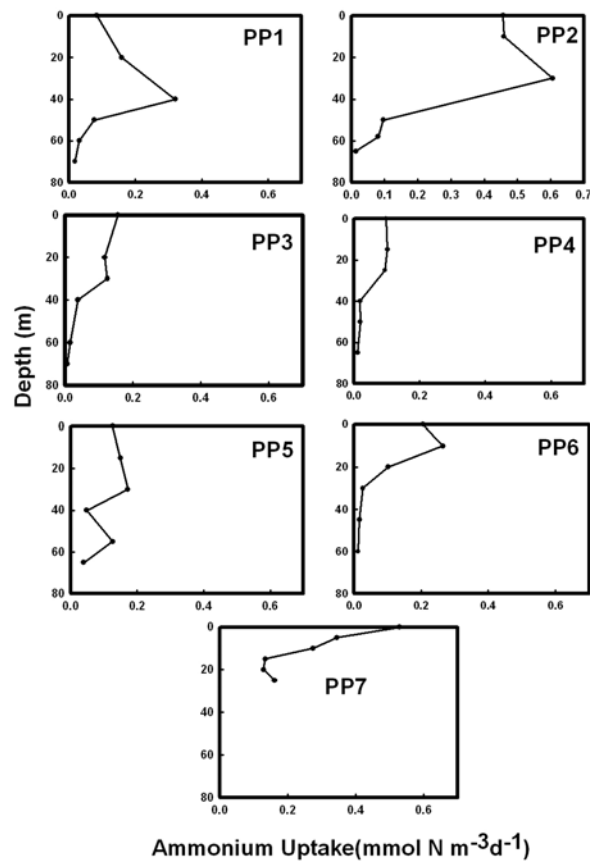


**Figure 3.17** Vertical profile of ammonium uptake rates at different depths at various locations. The uptake profile is limited upto measured euphotic depths as in the case of nitrate.

The vertical profile of ammonium uptake at different stations during January is shown in Figure 3.17. The ammonium uptake profiles do not show the subsurface maximum at all the stations as was the case in the nitrate uptake. PP1 shows subsurface maximum at 40m as in the case of nitrate uptake but with higher values ( $0.32\text{mmolN m}^{-3}\text{d}^{-1}$ ). The ammonium concentration in the water column was also maximum ( $0.14\mu\text{M}$ ) at that depth. PP2 also has the subsurface maximum ( $0.61\text{mmolN m}^{-3}\text{d}^{-1}$ ) at 30m, similar to nitrate uptake at this station. However, the maximum ammonium uptake at PP2 is only twice that of PP1 maximum value, whereas in the case of nitrate uptake, maximum at PP2 was around 23 times higher than maximum at PP1. The ammonium concentration at the depth of maximum ammonium uptake at PP2 was also found to be highest ( $0.22\mu\text{M}$ ) for the study region. PP3 and PP7 show maximum ammonium uptake at the surface with values  $0.15$  and  $0.52\text{mmolN m}^{-3}\text{d}^{-1}$  respectively and decrease with depth. PP5 shows two distinct maxima for ammonium uptake at 30 and 55m respectively, the second peak coinciding with the maximum ammonium concentration in the water column ( $0.14\mu\text{M}$ ). PP4 and PP6 show the maximum uptake at 15 and 10m respectively but these maxima do not coincide with maximum ammonium concentration in the water column as in other cases. The uptake of ammonium has not ceased completely at the base of the euphotic zone probably indicating the dark uptake of ammonium.

### **3.5.6 f-ratio during January 2003**

The f-ratio during the present study has been calculated as integrated nitrate uptake/total integrated (nitrate + ammonium + urea) uptake, where integration has been performed over the entire photic zone. f-ratio has been presented here in two different ways: first estimate does not include urea uptake and second estimate includes it (Figure 3.18). This has been done to estimate the effect of urea uptake on f-ratio as in most of the earlier studies f-ratio was expressed as nitrate uptake/(nitrate + ammonium) uptake, particularly because of lack of urea uptake measurements. Since the second estimate includes urea uptake that has been calculated assuming the absence of urea in the water column, it depicts the upper bound of f-ratio possible during the study period. When urea has not been taken into consideration, the overall variation in the f ratio is from 0.15 at PP1 to 0.60 at PP2 (0.11 and 0.53 respectively, after incorporating urea in the calculation). While discussing the average values of f-ratio for the region the PP2 has been excluded, due to its anomalously high value, as has been done in the case of

nitrate. Without urea, f-ratio during the month of January for the region averages around  $0.26(\pm 0.09)$  [ $0.31(\pm 0.15)$  after including PP2]. With urea, the f-ratio averages around  $0.19(\pm 0.06)$  [ $0.24(\pm 0.14)$  after taking PP2 into consideration]. Inclusion of urea leads to decrease in the overall average f-ratio. Without urea, the open ocean stations averages around  $0.21(\pm 0.04)$  [ $0.29(\pm 0.18)$  with PP2], whereas two coastal stations average around  $0.36(\pm 0.07)$ . The inclusion of urea leads to decrease in open ocean [ $0.16(\pm 0.03)$ ] as well as coastal stations [ $0.25\pm 0.03$ ] f-ratio. However, except PP2 and PP6, the f-ratios for all the stations are less than 0.32, indicating the relative importance of regenerated production over new production during this period. PP2, an open ocean location and PP6, a coastal location have f-ratios more than 0.4, implying that the new production is relatively more important at these two locations. The new, regenerated and total production along with f-ratio during the present study have been presented in Table 3.2.

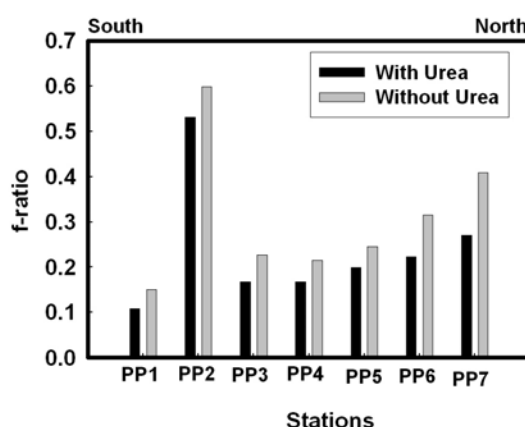


**Figure 3.18** f-ratio observed (with and without urea) during January 2003.

**Table 3.2**  $^{15}\text{N}$  based productivity and f-ratio estimates during January 2003 in the Arabian Sea.

Stn.	New Production Nitrate Uptake ( $\text{mmol N m}^{-2} \text{d}^{-1}$ )	Regenerated Production		Total Production ( $\text{mmol N m}^{-2} \text{d}^{-1}$ )	f-ratio	
		Ammonium Uptake ( $\text{mmol N m}^{-2} \text{d}^{-1}$ )	Urea Uptake ( $\text{mmol N m}^{-2} \text{d}^{-1}$ )		(With Urea)	(Without urea)
PP1	1.77	10.00	4.61	16.38	0.11	0.15
PP2	34.78	23.30	7.34	65.43	0.53	0.60
PP3	1.58	5.39	2.47	9.44	0.17	0.23
PP4	1.03	3.78	1.36	6.17	0.17	0.21
PP5	2.51	7.72	2.36	12.58	0.20	0.25
PP6	2.48	5.39	3.22	11.09	0.22	0.31
PP7	4.25	6.14	5.31	15.69	0.27	0.41

### 3.5.7 Effect of winter cooling on the f-ratio

Except at PP2, f-ratio in general shows an increasing trend from the south to the north (PP1  $\sim 0.15$  being the southernmost and PP6  $\sim 0.31$ , the northernmost). This can be explained in terms of the spatial variation in the sea surface temperature, air temperature, wind speed (atmospheric forcings) and mixed layer depth. During the study period winds were predominantly north/northeasterlies with an average speed of  $\sim 4\text{ms}^{-1}$ . However, the wind speed is too weak to induce significant offshore Ekman transport. Madhupratap et al. (1996) overrules Ekman transport due to the existence of a deep mixed layer in the region. Also, the suggested positive wind stress curl ( $< 1 \times 10^{-8}$  dyne  $\text{cm}^{-3}$ ) by the climate atlas over the region is too small to support the existence of deep MLD and higher nutrient in the surface layer together. Madhupratap et al. (1996) have shown through the computation of heat and freshwater (Evaporation-Precipitation) fluxes along  $64^\circ\text{E}$  that the northern Arabian Sea (north of  $10^\circ\text{N}$ ) experiences a net heat ( $\sim 30\text{Wm}^{-2}$ ) and freshwater losses ( $\sim 125\text{mm}$  per month) during the winter season. Further, a comparison of specific humidity during different months (Climate Atlas) suggests the prevalence of dry air (specific humidity  $\sim 10\text{g kg}^{-1}$ ) during winter over the northeastern Arabian Sea. Based on these observations Madhupratap et al. (1996) advocated that the northeast trade winds prevalent in the region during this season brings the cool, dry continental air causing an increase in the evaporation. During this period the evaporation in the region exceeds the precipitation and also the heat loss exceeds heat gain. This intensified evaporation leads to the cooling of surface water as a result of which the surface water of the northeastern Arabian Sea becomes denser. The increase in density causes the water to sink resulting in convective mixing. This whole process leads to a deepening of the mixed layer as observed, and consequent transport of nutrients from the base of the mixed layer and upper thermocline to the surface layer. The general increase in the nitrate concentration, new production and consequently the f-ratio from south to north observed during the present study suggests the influence of above mechanism. The increased mixed layer depth (MLD) also suggests a strong coupling between the surface and the subsurface layers. An examination of the column integrated nitrate reveals that the nitrate varies from as low as  $5.2\text{mmol m}^{-2}$  for PP7 (coastal station) to as high as  $254\text{mmol m}^{-2}$  for PP4 (open ocean station) with temperature based mixed layer of around  $80\text{m}$ . If it is assumed that the vertical upward flux of nitrate from below the photic zone is the dominant

component of newly available nitrate (Eppley et al. 1977), then the degree of coupling can also be deciphered by the f-ratio. Platt et al. (1992) have observed that the area where surface layers are strongly coupled with sub-surface layers will experience new production as a large fraction of the total production. Therefore the observed increase in new production and f-ratio from the south to the north clearly indicates the effect of winter cooling during January and may be interpreted as the biological response to the prevailing physical forcings.

### 3.5.8 Low f-ratio despite presence of nutrients in the water column

Excluding PP2 which has an anomalously high f-ratio, the relationship between f-ratio and the ambient euphotic zone integrated nitrate concentration levels reveals that the stations fall into two distinct groups (Figure 3.19-left panel): First group where stations are characterised by relatively low column integrated nitrate concentration ( $<150 \text{ mmol m}^{-2}$ ) which includes two southern stations PP1 and PP3 and one northern coastal station PP8. The second group includes the three northern stations that have column integrated nitrate more than  $150 \text{ mmol m}^{-2}$ . The regression analysis of both the groups yields  $r^2 = 0.99$ . This figure suggests a very clear negative relationship of f-ratio and integrated nitrate indicating that even at higher column nitrate the f-ratio can be low. The relationship observed is regardless of inclusion of urea uptake in the f-ratio calculation. The same negative relationship with  $r^2 = 0.61$  has been found between new production (excluding PP2) and euphotic zone integrated nitrate (Figure 3.19-right panel). This leads to the situation where nitrate is available in the water column but is

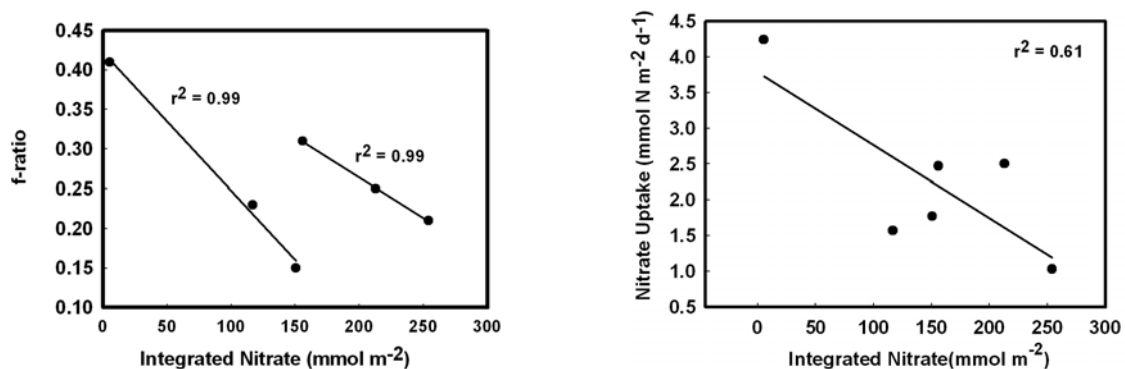


**Figure 3.19** The observed negative relationship between f-ratio and euphotic zone integrated nitrate (left panel) and new production-integrated nitrate (right panel) during present study.

not being utilized. Watts and Owens (1999) suggest two possible explanations for this kind of situation: First, the suppression of nitrate uptake in presence of ammonium that has been very commonly observed in the world oceans (Glibert et al. 1982b; Harrison et al. 1987; Jacques 1991; Owens et al. 1991; Rees et al. 1995, McCarthy et al. 1999). McCarthy et al. (1999) have observed that the effect of  $\text{NH}_4$  addition is most sensitive at  $\text{NO}_3$  concentrations less than  $1.0 \mu\text{mol kg}^{-1}$  and also relatively higher rates of  $\text{NO}_3$  uptake persisted at higher concentrations of ammonium. The second reason for nitrate being not utilized is the higher addition of  $^{15}\text{NH}_4$  tracer than required. Ideally, the concentration of enriched tracers added should be less than 10% of ambient concentration. Higher concentration of tracer added may artificially stimulate ammonium uptake in the presence of nitrate. However, during the present study, at times the addition was made more than 10% of ambient ammonium concentration but it was not large enough to stimulate the artificial uptake of ammonium. This is suggested by the very low correlation ( $r^2 \sim 0.006$ ) found when regression was performed between the percentage of  $\text{NH}_4$  addition relative to ambient and ammonium uptake rates at different depths at different stations. The third possibility could be the deterioration of light conditions due to deep mixed layer (Sambrotto 2001) and relative preference for ammonium in light limited conditions (McCarthy et al. 1999).

### **3.6 Chlorophyll *a*, nitrate and physical parameters during late February- early March 2003 in the Northeastern Arabian Sea**

Late February and early March in the Arabian Sea witnessed a phytoplankton bloom particularly at the three open ocean stations PP3, PP4 and PP5 (between  $19\text{-}21^\circ\text{N}$  and  $66\text{-}68^\circ\text{E}$ ). The genus of phytoplankton during the bloom was *noctiluca*.

#### **3.6.1 Chlorophyll *a***

In general, the euphotic zone integrated Chlorophyll *a* during late February-early March in the Arabian Sea was more than that observed during January, despite the fact that the euphotic depth, in general, was shallower than that of January. This is due to higher concentration of Chl *a* at different depths. The stations during this period can be divided into two categories: one with Chl *a* concentration less than  $40 \text{ mg m}^{-2}$  which includes three out of six stations (PP1: 36.6, PP2: 38.8 and PP6: 29.3  $\text{mg m}^{-2}$ ) and other with Chl *a* more than  $40 \text{ mg m}^{-2}$ . The second category includes stations (PP3: 45.1,

PP4: 52.5 and PP5: 45.3  $\text{mgm}^{-2}$ ) that were typical bloom stations. Seawater at these stations was virtually green (Figure 3.20-left panel). Even though these were bloom stations the Chl *a* concentrations at these stations were not of the same magnitude that was observed at PP2 during January (68.5  $\text{mg m}^{-2}$ ).

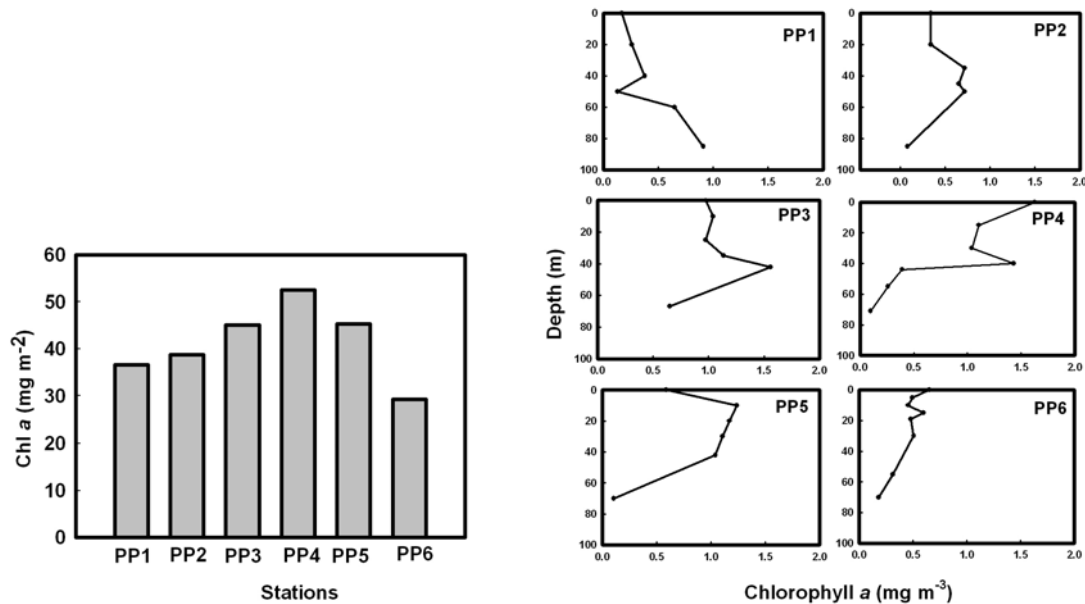


**Figure 3.20** Euphotic zone integrated (left panel) and vertical profiles (right panel) of Chlorophyll *a* at productivity stations during late February-early March 2003. The euphotic depth at three stations PP3, PP4 and PP5 were only 42m.

Vertical profiles of Chl *a* suggest varying patterns at different stations (Figure 3.20-right panel). The profile at PP1 shows a subsurface minimum at 50m ( $0.13 \text{mg m}^{-3}$ ). The maximum value has been observed at the base of the euphotic zone ( $0.91 \text{mg m}^{-3}$ ). PP2 shows a plateau of Chl *a* maximum between 35 and 50m with concentration around  $0.70 \text{mg m}^{-3}$ . PP3 shows higher Chl *a* throughout the photic zone ( $> 0.9 \text{mg m}^{-3}$ ) with a maximum at the base of photic zone i.e., 42m ( $1.5 \text{mg m}^{-3}$ ) whereas PP4 shows maximum Chl *a* at the surface ( $1.6 \text{mg m}^{-3}$ ) with another peak at 40m ( $1.4 \text{mg m}^{-3}$ ) and decreases to near zero at 70m. PP5 shows more than  $1.0 \text{mg m}^{-3}$  Chl *a* at the subsurface depths between 10 and 42m (euphotic depth) and decreases thereafter. PP6 has Chl *a* around  $0.5 \text{mg m}^{-3}$  in first 30m of water column to decrease to  $0.18 \text{mg m}^{-3}$  at base of euphotic zone (70m). The profiles of Chl *a* at bloom stations PP3-PP5 suggest the existence of chlorophyll well beyond the euphotic depth which is around 42m.

### 3.6.2 Nitrate

Among the nutrients, only nitrate could be measured during late February-early March. On an average, euphotic zone integrated nitrate was less than that observed during January (Figure 3.21-left panel). However, the maximum euphotic zone integrated nitrate during the present study (both January and late February-early March) has been observed at PP2 ( $537 \text{ mmol m}^{-2}$ ) of late February-early March. It is noteworthy that the integrated nitrate at bloom sustaining stations PP3, PP4 and PP5 were 22, 53 and  $132 \text{ mmol m}^{-2}$  respectively, which is very less compared to non bloom sustaining stations PP1 ( $174 \text{ mmol m}^{-2}$ ) and PP2 ( $537 \text{ mmol m}^{-2}$ ). This is because of shallower euphotic depths at bloom stations. However, one non bloom station (PP6) also shows very low integrated nitrate ( $24.9 \text{ mmol m}^{-2}$ ). The vertical profile of nitrate does not show much change in nitrate concentration within the euphotic zone at most of the stations (Figure 3.21-right panel). The nitrate at PP1 is below detection limit in the top 12m of water column and increases to  $2 \mu\text{M}$  around 40m and with a sharp increase from 60 to 85m ( $8 \mu\text{M}$ ). At PP2 also the water is almost devoid of nitrate in the first 20m but nitrate increases sharply downwards to reach to  $12 \mu\text{M}$  at the base of the euphotic zone at 85m. PP3 and PP4 show almost uniform nitrate in the euphotic zone with concentrations below 1 and  $2.2 \mu\text{M}$  respectively. PP5 shows the highest nitrate concentration in the top 20m ( $\sim 3.5 \mu\text{M}$ ) which goes down to  $2.1 \mu\text{M}$  at 40m. PP6 is characterized by a nitrate concentration of less than  $0.7 \mu\text{M}$  throughout the euphotic zone.

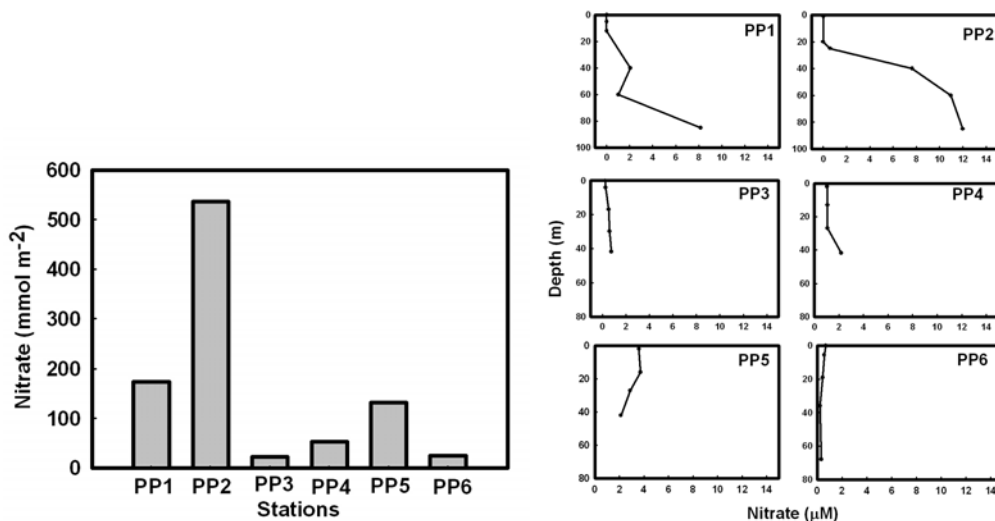


**Figure 3.21** The euphotic zone integrated (left panel) and vertical profiles (right panel) of ambient nitrate at different stations during late February-early March 2003.

One important difference between bloom and non bloom stations is the existence of nitrate in the top surface layer at bloom stations; non bloom stations are almost devoid of it in the top layer, where light is available in plenty for photosynthesis.

### 3.6.3 Hydrographic and meteorological conditions

The sea surface temperature pattern during the study period (late February-early March) was almost the same as in January i.e., decreasing SST from the south to the north as indicated by the long-term average temperature profile (Figure 3.22-left panel). However, a slight decrease in temperature ( $< 0.5^{\circ}\text{C}$ ) for a particular location from January to late February-early March can be observed by the long-term average SST data. SST measured during the sampling indicates the temperature variation between  $27.8^{\circ}\text{C}$  at the southernmost station (PP1) to  $24.7^{\circ}\text{C}$  at the northernmost station (PP5) (Figure 3.22-right panel). Air temperature over the study region also showed a

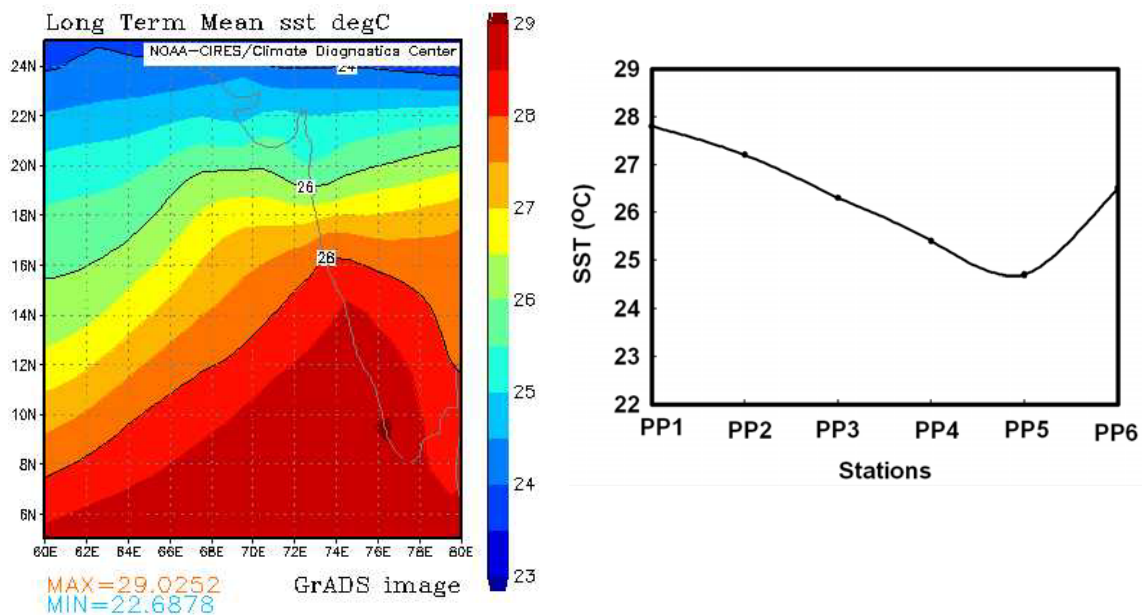


**Figure 3-22** The long-term average Sea Surface Temperature (SST) of the northeastern Arabian Sea for the study period (1-10 March) (left panel, Source: Climate Diagnostic Center, National Center for Environmental Prediction, USA) and SST at different stations at the time of sampling (right panel) during late February-early March 2003.

similar pattern of spatial variability from the south to the north (Figure 3.23). It varied from  $27.2^{\circ}\text{C}$  to southernmost station (PP1) to  $22.8^{\circ}\text{C}$  at northernmost station (PP5). Air temperature at all stations was less than that SST of that particular station. This difference was less for the southern stations ( $<0.5$ ) than the northern stations, where the

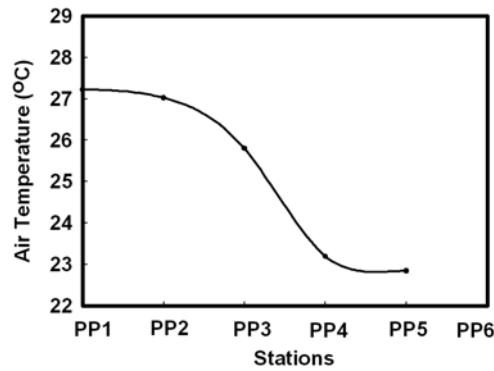


**Figure 3-23** Air temperature measured over the northeastern Arabian Sea during sampling. Data for PP6 is not available.

difference was around 2°C. Wind speed at the first two stations were around 4.01 and 2.74ms<sup>-1</sup>, typically in the range observed during January (Figure 3.24). Sea was also calm at these two sites. However, the wind speeds of more than 8ms<sup>-1</sup> were encountered at the rest of the stations and the sea was very choppy with sea state 4-5. The surface pressure increased from 1013mb at PP1 to a maximum of 1017mb at PP4

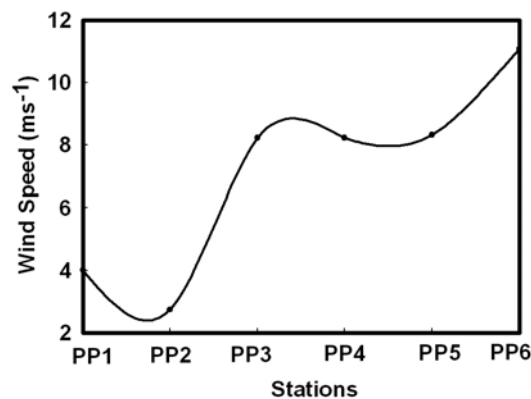


**Figure 3.24** Wind speed over the Arabian Sea during Late February-early March.

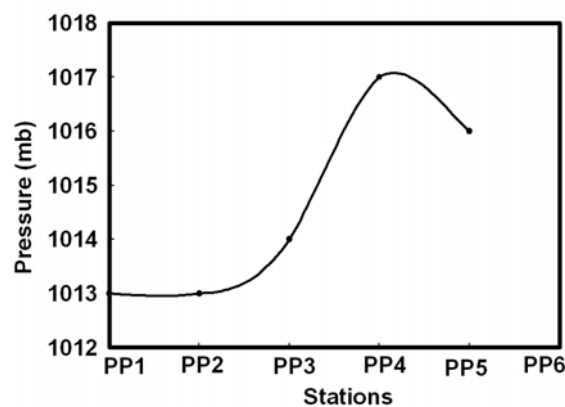


**Figure 3.25** Air Pressure during sampling time in the Arabian Sea. Measurement at PP6 could not be performed.

to decrease to 1016mb at PP5 (Figure 3.25). Euphotic depth at the first two stations (PP1 and PP2) was 85m that reduced to less than half (42m) at all three bloom stations (PP3-PP5) and again increased to 68m at the non bloom station PP6. The drastic decrease in euphotic depth at bloom stations was probably due to faster attenuation of light because of increased biomass. This perhaps led to an increase in the attenuation coefficient to  $0.1\text{m}^{-1}$ .

The most important feature of this cruise, which was strikingly different from January, was the temperature based mixed layer depth (MLD). The MLD for the first three stations (PP1-PP3) was not clearly defined and temp-depth profile shows a continuous decrease in temperature with slight undulations (Figure 3.26). This might

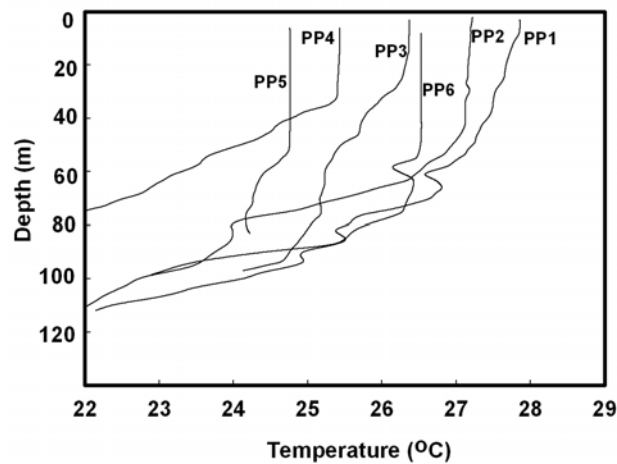


**Figure 3.26** Temperature profiles at different stations obtained with Satlantic Radiometer during Late February-Early March 2003.

be an indication of the varying degree of mixing with depth between cooler water and relatively warmer surface water. The cooler water might have been supplied from deeper sources or due to horizontal advection from a nearby region. Interestingly, depth-temperature profiles of stations PP4-PP6 is marked by relatively sharper decrease in temperature with depth, probably indicating a shallow mixed layer for these stations varying between 33-55m. Although SST at these locations is not drastically different from January, the MLD is markedly shallower compared to January (it was near 80m in the same region). The relatively shallow mixed layer at these locations persisted despite higher wind speed ( $8\text{ms}^{-1}$ ) indicating the limited role played by wind in the deepening of MLD in this period. Prasanna Kumar et al. (2001) in their study of physical forcing of biological productivity in Arabian Sea during NE monsoon have also observed that the formation of deep mixed layer during winter is not due to wind

mixing but is a result of winter cooling. Therefore, the shallowness in MLD from January to early March indicates the decrease in effectiveness of winter cooling in the region (cooling starts in December and persists till the end of February, Madhupratap et al. 1996).

One important source of nutrients to the study region could be the surface currents. However, the current known to flow from the southern to the northern Arabian Sea during winter is WICC (West India Coastal Current) whose strength decreases as it moves northward (400km wide at 10°N to 100 km wide near 22°N; Shetye et al. 1990). Moreover, WICC is a coastal current and is unlikely to supply nutrients at 19°N-68°E.

### **3.7 <sup>15</sup>N based productivity study during late February-early March 2003**

#### **3.7.1 Total Production**

<sup>15</sup>N based total productivity has been calculated as the sum total of nitrate uptake and conservative estimates of ammonium and urea uptakes (Figure 3.27). The total productivity varied from a minimum of 17mmolN m<sup>-2</sup> d<sup>-1</sup> (~ 1353mgC m<sup>-2</sup>d<sup>-1</sup>) at PP6 (a non bloom station) to maximum of 37.8mmolN m<sup>-2</sup> d<sup>-1</sup> (~ 3006mgC m<sup>-2</sup>d<sup>-1</sup>) at PP4 (a bloom station). Overall, the average total productivity during the study period was 26.3(±8.6)mmolN m<sup>-2</sup>d<sup>-1</sup> (~2090±687 mgC m<sup>-2</sup>d<sup>-1</sup>). The average total productivity at non-bloom stations was 22.3±4.7mmolN m<sup>-2</sup>d<sup>-1</sup> whereas at bloom stations it was 30.2±10.9mmolN m<sup>-2</sup>d<sup>-1</sup>. The high spatial variability for bloom stations was because of relatively low total productivity at PP5 (17.8mmolN m<sup>-2</sup> d<sup>-1</sup>) compared to the other two stations, where it was 35.1 (PP3) and 37.8mmolN m<sup>-2</sup> d<sup>-1</sup> (PP4) respectively. The average total productivity reported here is more than twice of the average total productivity reported for the month of January (11.9mmol Nm<sup>-2</sup>d<sup>-1</sup>) during the same study. However, it is comparable to the average value (25.8mmolN m<sup>-2</sup>d<sup>-1</sup>) reported by McCarthy et al. (1999) for the northwestern Arabian Sea during the NE monsoon (January) and is thrice higher than the average value (8.3mmolN m<sup>-2</sup>d<sup>-1</sup>) reported by Watts and Owens (1999) for intermonsoon season in the northwestern Arabian Sea. McCarthy et al. (1999) values are based on nitrate and ammonium uptake only and urea uptake was not considered in their total productivity estimation. Inclusion of uptake by urea would lead to a higher total productivity than reported and hence the actual total productivity during the experiments of McCarthy et al. (1999) may be higher than

reported. One major difference between McCarthy et al. (1999) and present study is the contribution of nitrate and ammonium uptakes to total productivity. The maximum contribution to the total productivity budget during present study is due to nitrate uptake whereas McCarthy et al. (1999) have found the maximum contribution by the ammonium component. This difference is clearly evident in the f-ratios of the respective studies. One possible reason could be species composition.

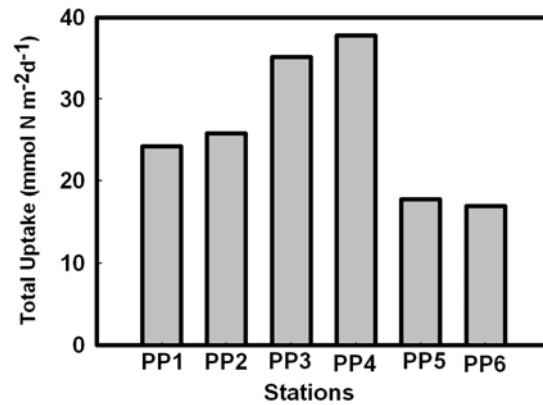


**Figure 3.27** <sup>15</sup>N based total productivity during late February-early March 2003 expressed as the sum of nitrate uptake and conservative estimates of ammonium and urea uptakes.

### 3.7.2 Regenerated Production

Due to lack of ambient ammonium and urea concentrations, a conservative estimate of regenerated production was made during late February-early March, assuming the absence of ammonium and urea in the water column (Figure 3.28). Ammonium uptake varied within a narrow range of 6.2 at PP5 to 9mmolN m<sup>-2</sup> d<sup>-1</sup> at PP3 with an average

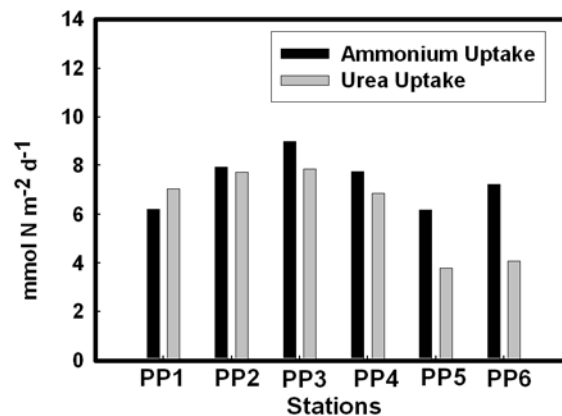


**Figure 3.28** Components of regenerated production (ammonium and urea uptake). Both ammonium and urea uptake estimates are conservative.

value of  $7.4 (\pm 1) \text{ mmolN m}^{-2} \text{ d}^{-1}$  for the region. There is not much difference between the average values of ammonium uptakes at bloom ( $7.6 \text{ mmolN m}^{-2} \text{ d}^{-1}$ ) and non bloom ( $7.1 \text{ mmolN m}^{-2} \text{ d}^{-1}$ ) sustaining stations. Since the assumption for ambient nutrient is same for all the stations, it can be inferred from the ammonium uptake estimates that there was no major relative difference in ammonium uptake from one station to another. However, the ammonium uptake observed by McCarthy et al. (1999) in the northwestern Arabian Sea during late NE monsoon showed a wide variation with a minimum value of  $5.4 \text{ mmolN m}^{-2} \text{ d}^{-1}$  in the central part to  $37 \text{ mmolN m}^{-2} \text{ d}^{-1}$  at the northern part. Watts and Owens (1999) have also reported ammonium uptake variation ranging from 0.1 to  $11.8 \text{ mmolN m}^{-2} \text{ d}^{-1}$  for the northwestern Arabian Sea.

Conservative estimates for urea uptake varied from a minimum of  $3.8 \text{ mmolN m}^{-2} \text{ d}^{-1}$  at PP5 to a maximum  $7.8 \text{ mmolN m}^{-2} \text{ d}^{-1}$  at PP3, both being bloom stations. The average urea uptake for the region worked out to be  $6.2 (\pm 1.8) \text{ mmolN m}^{-2} \text{ d}^{-1}$ . There is no difference between the average urea uptake of bloom ( $6.2 \text{ mmolN m}^{-2} \text{ d}^{-1}$ ) and non bloom ( $6.2 \text{ mmolN m}^{-2} \text{ d}^{-1}$ ) stations. However, urea uptake estimates from the northwestern Arabian Sea show variations from 0 to a maximum of  $5.6 \text{ mmolN m}^{-2} \text{ d}^{-1}$  (Watts and Owens 1999).

### 3.7.3 New production

Euphotic zone integrated new production during late February-early March (Figure 3.29) in the northeastern Arabian Sea ranges from  $5.7 \text{ mmolN m}^{-2} \text{ d}^{-1}$  ( $454 \text{ mgC m}^{-2} \text{ d}^{-1}$ ) at a non-bloom station (PP6) to  $23.2 \text{ mmolN m}^{-2} \text{ d}^{-1}$  ( $1846 \text{ mgC m}^{-2} \text{ d}^{-1}$ ) at a bloom station (PP4). The average column new production was found to be  $12.7 (\pm 6.7) \text{ mmolN m}^{-2} \text{ d}^{-1}$  ( $\sim 1009 \text{ mgC m}^{-2} \text{ d}^{-1}$ ) that is more than five times the new

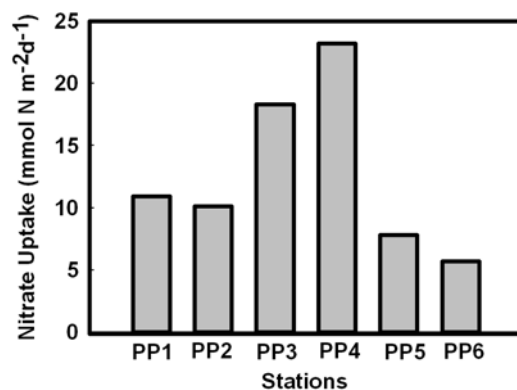


**Figure 3.29** New production observed at different locations during late February-early March in the northeastern Arabian Sea.

production observed during January ( $2.3 \text{ mmolN m}^{-2}\text{d}^{-1}$ , excluding PP2). The average new production at bloom stations is  $16.4 (\pm 7.8) \text{ mmolN m}^{-2}\text{d}^{-1}$  ( $\sim 1307 \text{ mgC m}^{-2} \text{d}^{-1}$ ) that is almost twice the average new production at non bloom stations ( $8.9 \text{ mmolN m}^{-2}\text{d}^{-1}$   $\sim 710 \text{ mgC m}^{-2}\text{d}^{-1}$ ). There is no systematic spatial trend in the new production as was the case during January. At PP5 the euphotic zone integrated chlorophyll *a* concentration was one of the highest ( $45 \text{ mg m}^{-2}$ ) with a typical (bloom station) euphotic depth of 42m but surprisingly the new production ( $7.8 \text{ mmolN m}^{-2}\text{d}^{-1}$ ) is far below the other two bloom stations where it was 18.3 (PP3) and  $23.2 \text{ mmolN m}^{-2} \text{d}^{-1}$  (PP4) respectively. On the basis of integrated column new production the stations during late February-early March could be divided into three different groups: PP1 and PP2 with new production around  $10 \text{ mmolNm}^{-2}\text{d}^{-1}$ ; PP3 and PP4 with new production more than  $18 \text{ mmolN m}^{-2} \text{d}^{-1}$ , representative of bloom condition in the

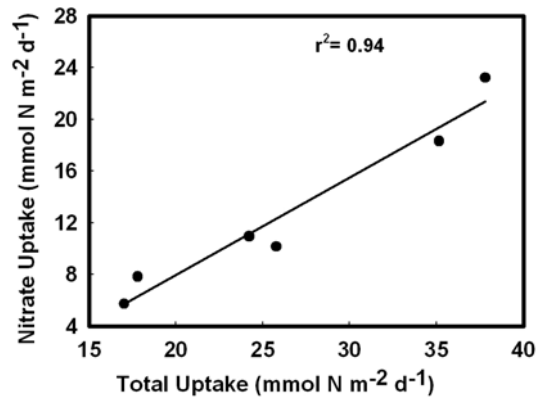


**Figure 3.30** Observed relationship between new and total production in the Arabian Sea during late February and early March 2003.

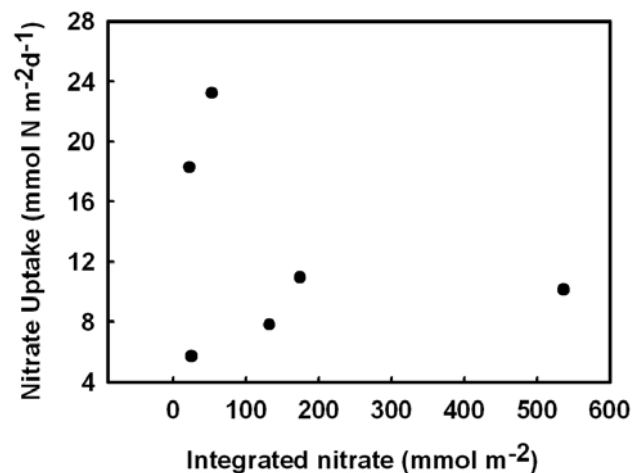


**Figure 3-31** Relationship between new production and euphotic zone integrated nitrate observed in the Arabian Sea during late February and early March 2003.

region and PP5 and PP6 with new production less than  $8 \text{ mmolN m}^{-2} \text{ d}^{-1}$ . The values reported here are the highest estimates of new production reported for the region so far. Watts and Owens (1999) reported a maximum nitrate uptake of  $9.8 \text{ mmolN m}^{-2} \text{ d}^{-1}$  off India during the intermonsoon. McCarthy et al. (1999) reported a maximum nitrate uptake of  $7.2 \text{ mmol N m}^{-2} \text{ d}^{-1}$  off Oman followed by 6.8 and  $5.6 \text{ mmol N m}^{-2} \text{ d}^{-1}$  in the central Arabian Sea (along  $65^\circ\text{E}$ ) during NE monsoon. No earlier data exists for comparison in the northeastern Arabian Sea. However, based on the higher values observed by Watts and Owens (1999) off India and McCarthy et al. (1999) in the central Arabian Sea, it can be speculated that the eastern Arabian Sea also has a potential for high new production, as evident during the present study. There is a very strong correlation ( $r^2 = 0.94$ ) between the new and total production during late February-early March (Figure 3.30) and is significantly better than that observed during January. This significant relationship may be because of a very high dependence of total production on the new production. During January the contribution of regenerated production to the total production was significant leading to poor new-total production relationship. However, no particular relationship is observed between the euphotic zone integrated column nitrate and new production (Figure 3.31) indicating the former to be a poor indicator of new production. It also signifies that the availability of nitrate in the water column is not the only criterion for high new production. Significant nitrification could also be taking place, but this needs to be verified.

#### **3.7.4 Vertical profiles of nitrate uptake**

The vertical profiles of nitrate uptake at different locations during late February-early March are shown in Figure 3.32. As expected, the uptake rates at different depths were quite high during late February-early March compared to January, which was less than  $0.08 \text{ mmolN m}^{-3} \text{ d}^{-1}$  for most of the stations. The first three stations PP1, PP2 and PP3 show a typical subsurface uptake maximum. PP1 and PP2 show uptake maxima of 0.40 and  $0.27 \text{ mmolN m}^{-3} \text{ d}^{-1}$  respectively at a depth of 40m that moves upward to 17m with a maximum value of  $0.83 \text{ mmolN m}^{-3} \text{ d}^{-1}$  at PP3. A profile similar to that at PP3 has been observed at PP5 with an uptake maximum of  $0.35 \text{ mmolN m}^{-3} \text{ d}^{-1}$  at 16m depth. The maximum uptake at PP4 has been observed at the surface ( $1.11 \text{ mmolN m}^{-3} \text{ d}^{-1}$  - this is also the maximum uptake at any particular depth during late February-early March) and is nearly the same till 13m, to decrease drastically to  $0.05 \text{ mmolN m}^{-3} \text{ d}^{-1}$  at

27m. The upward shift in depths of maximum uptake rate at PP3, PP4 and PP5 compared to the two earlier stations may be because of light limitation at deeper

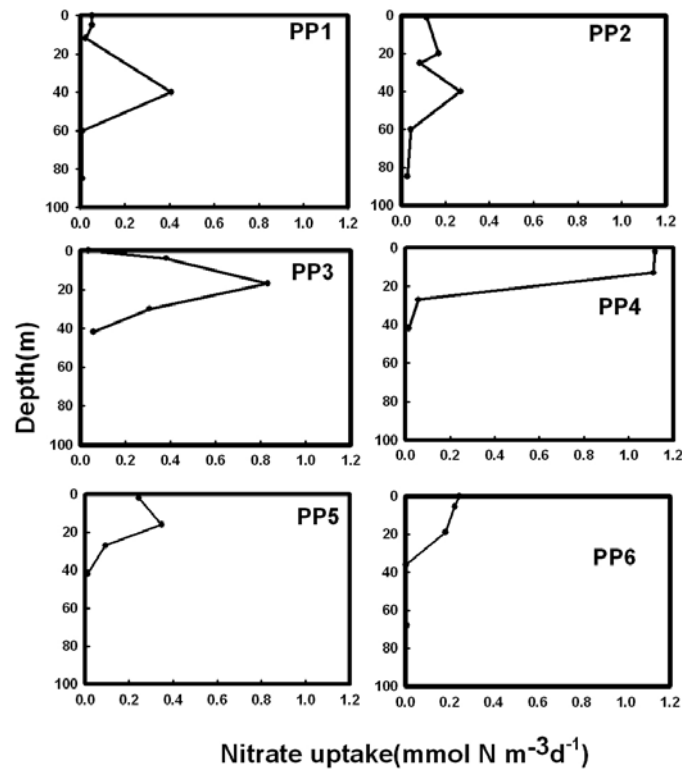


**Figure 3.32** Vertical profiles of nitrate uptake rates at various locations in the northeastern Arabian Sea during late February-early March 2003. The uptake profile is limited upto the measured euphotic depths.

depths due to abundant biomass at the surface as they are bloom stations. However, the maximum uptake rate at surface has also been observed at PP6, a non-bloom station, but the rate of uptake is significantly less.

### 3.7.5 f-ratio

Since the f-ratio has been calculated using the conservative estimates of ammonium and urea uptakes, the values presented here represent the upper bound (Figure 3.33). The f-ratio averages around 0.60 ( $\pm 0.10$ ) without urea, which decreases by 25% ( $0.45 \pm 0.09$ ) when urea is included into the calculation. These values are in sharp contrast to the average f-ratio (0.12 and 0.15) reported by McCarthy et al. (1999) during late and early NE monsoon and by Watts and Owens (1999) during intermonsoon (0.28) for the northwestern Arabian Sea. The average f-ratio of bloom sustaining stations is  $0.65 \pm 0.10$  without urea which decreases to  $0.52 \pm 0.09$  (by 20%) with urea. The average f-ratio of the three non-bloom stations is significantly lower

( $0.54 \pm 0.09$  without urea and  $0.39 \pm 0.06$  with urea; a decrease by 27%) than the average bloom station value. No particular relationship has been observed between f-ratio and the integrated nitrate and follows the same pattern as new production-integrated nitrate relationship. The new, regenerated and total production along with f-ratio observed during late February-early March is indexed in Table 3.3.

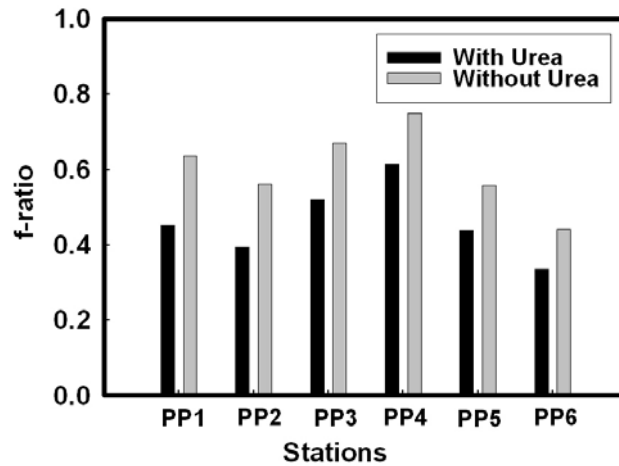


**Figure 3.33** f-ratios observed (with and without urea) in the northeastern Arabian Sea during the present study.

**Table 3.3**  $^{15}\text{N}$  based productivity and f-ratio estimates during late February-early March 2003 in the Arabian Sea.

Stn.	New Production			Total Production (mmol N m <sup>-2</sup> d <sup>-1</sup> )	f-ratio	
	Nitrate Uptake (mmol N m <sup>-2</sup> d <sup>-1</sup> )	Ammonium Uptake (mmol N m <sup>-2</sup> d <sup>-1</sup> )	Urea Uptake (mmol N m <sup>-2</sup> d <sup>-1</sup> )		(With Urea)	(Without urea)
PP1	10.94	6.22	7.04	24.21	0.45	0.63
PP2	10.13	7.92	7.72	25.78	0.39	0.56
PP3	18.30	8.99	7.84	35.14	0.52	0.67
PP4	23.22	7.73	6.85	37.81	0.61	0.75
PP5	7.81	6.19	3.78	17.80	0.43	0.55
PP6	5.71	7.22	4.08	17.02	0.33	0.44

### 3.7.6 Source of nutrients for the sustenance of the bloom

Compared to January, the average new and total productions during late February-early March were more than five and two fold respectively. The source of the nutrients during January was deeper nitrate due to convective mixing as indicated by deeper

MLD. However, there seems to be no such continuous supply of nitrate during late February-early March, as MLD has been observed to be shallow, particularly at the three bloom sustaining stations. The supply of nutrients due to advection from the first three stations (PP1-PP3) may be a potential source, as undulating MLD profile at these stations suggests supply of relatively cooler water. However, this supply does not seem to be strong enough to sustain a bloom as suggested by relatively low productivity at these stations. During January deeper nitrate is known to get entrained in the water column. Nitrate residence time in the water column was calculated from the January data of the region by dividing the column nitrate with the nitrate uptake rate. It was more than 50 days at most of the stations except at PP2 and PP7, where it was around 2 days (Figure 3.34). The residence time for nitrate reported here presents a minimum estimate as it ignores any additional nitrate supplied during the day. A residence time less than 1 day has been suggested to be indicative of nutrient limited productivity

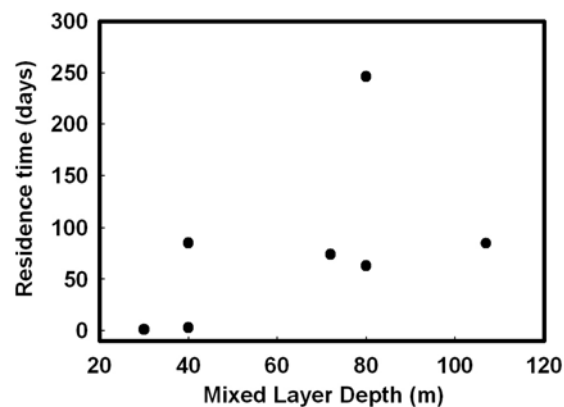


**Figure 3.34** Relationship between the temperature based mixed layer depth and the residence time of nitrate in the water column estimated for January.

while a value significantly greater than one day indicates growth under nutrient replete conditions (Sambrotto 2001). Present data suggest nutrient replete conditions in the northeastern Arabian Sea during January at all stations. Residence time does not show any particular relationship with MLD and seems to be independent of it. The residence time suggests that if the same rate of removal due to nitrate uptake by phytoplankton continues the nitrate in the water column will remain at least for 50 days. However, the surface layer of ocean is not a closed system and nutrients will continuously be introduced as long as MLD is deeper and winter cooling is effective. Also the nitrate uptake by the phytoplankton may also increase as the effectiveness of winter cooling

decreases. The nutrients introduced in the water column during January do not get efficiently consumed probably because of degraded light condition due to deeper mixing. However, the nutrients entrained in the water column have to be eventually consumed and is probably utilised during February-early March when the MLD becomes shallow due to the waning winter cooling. The available nitrate along with increased light conditions possibly leads to the development of a bloom. Hence, there seems to be a time lag between the nutrient entrainment and peak biomass development as has been reported by Banse and English (1993). This condition in the Arabian Sea is similar to high latitude spring blooms that do not deplete surface nitrate unless there is a sustained period where the mixed layer is less than half the critical depth (Sambrotto et al. 1986). Therefore, the nutrients entrained in the water column during January seem to be a more important source along with advected nutrients for the bloom development in the northeastern Arabian Sea.

### **3.8 Natural Isotopic Composition of Surface Suspended Matter**

Particulate organic matter (POM), which mainly consists of phytoplankton in the euphotic zone of the open ocean, plays an important role in marine nitrogen and carbon cycles (Saino and Hattori 1980). Due to its significant vertical transport, it enables the ocean to remove carbon dioxide from the surface layer and, in turn, from the lower atmosphere, to the deeper parts of the ocean or settle permanently as sediment on the ocean floor. The study of the nitrogen isotope ratio  $^{15}\text{N}/^{14}\text{N}$  of POM provides an insight into the availability and utilization of nutrients such as nitrate, ammonia and urea in the euphotic zone. Several studies in this regard have been done in different parts of the world ocean (Saino and Hattori 1980; Saino and Hattori 1987; Rau et al. 1991; Calvert et al. 1992; Altabet 1996). Similar studies in ocean sediments have been used for the reconstruction of past changes in surface ocean nutrient utilization (Altabet and Francois 1994, Farrell et al. 1995). In addition, sediment trap material has also been analysed in some cases (Schafer and Ittekkot 1995). To better understand the nitrogen isotope systematics in the ocean sediments and sediment trap material, it is essential to measure directly the nitrogen isotopes in surface POM to either verify whether surface  $\delta^{15}\text{N}$  is faithfully transmitted down to the sediment column or to quantify the isotopic modification, if any (Altabet et al. 1991; Buesseler 1991).

The nitrogen isotopic composition ( $\delta^{15}\text{N}$ ) of naturally occurring land derived particulate matter has been reported to have lower values (1.5-2.5‰; Miyake and Wada 1967), while the  $^{15}\text{N}$  content in the marine realm has a strong dependence on source isotopic composition and has been reported to vary significantly (Saino and Hattori 1980; Altabet 1996; Wada and Hattori 1991; Rau et. al. 1998). The phytoplankton  $\delta^{15}\text{N}$  averages around 7 ‰ while zooplankton and fishes, which are at higher trophic levels in the food web, have values around 10 ‰ and 15 ‰ respectively (Wada and Hattori 1976).

These variations in  $\delta^{15}\text{N}$  of particulate organic nitrogen (PON) are caused by fractionation of isotopes during various biogeochemical transformations and biological processes. The processes mainly responsible for such variations are  $\text{N}_2$  fixation, denitrification, nitrification and nitrate assimilation. Also, during the uptake of dissolved nitrogen in eutrophic waters, phytoplankton prefers  $^{14}\text{N}$  to  $^{15}\text{N}$  (Wada and Hattori 1978). Denitrification leads to  $^{15}\text{N}$  enrichment of the remaining nitrate while nitrification causes enrichment of  $^{15}\text{N}$  in the ammonia pool (Mariotti et al. 1984). Isotopic fractionation up to 20 ‰ has been found due to denitrification (Miyake and Wada 1971; Cline and Kaplan 1975; Liu and Kaplan 1989), nitrification (Miyake and Wada 1971) and nitrate assimilation (Wada et al. 1971). Fixation of atmospheric nitrogen is known to lower the  $\delta^{15}\text{N}$  values of PON because of the depleted source (atmospheric nitrogen  $\sim 0$  ‰); the areas with lower  $\delta^{15}\text{N}$  may thus be attributed to  $\text{N}_2$  fixation. However, a different view (Altabet 1988) is that lower  $\delta^{15}\text{N}$  could also be caused by the preferential removal of  $^{15}\text{N}$  enriched matter by sinking material, leading to a depletion of  $^{15}\text{N}$  in the remaining suspended matter. In addition,  $\delta^{15}\text{N}$  also depends on species, physiology and rate of growth of plankton (Montoya and McCarthy 1995).

One of the aims of the present study was to investigate the possible change in natural isotopic composition of nitrogen in particulate organic nitrogen (PON) of surface suspended matter from January to March. The aim was also to reconstruct the possible nutrient regime shift or change in utilisation behaviour of nutrients by the phytoplankton. For this purpose the Arabian Sea surface water was filtered to estimate the particulate organic nitrogen content in the suspended matter and its natural nitrogen isotopic composition ( $\delta^{15}\text{N}$ ) during both January and late February-early March.

### 3.8.1 January

The samples were collected at 13 different locations, which included 9 open ocean location (Stn.2 to Stn.10) and 4 coastal locations (Stn. 11 to Stn. 14). Overall, the PON content varied widely ranging from 0.16  $\mu\text{M N}$  at station 8, which was an open ocean station to 2.10 $\mu\text{M N}$  at station 13, a coastal station. Overall, PON averaged around 1.04 ( $\pm 0.47$ ) $\mu\text{M N}$ . The PON at open ocean locations varied from 0.16 to 1.27 $\mu\text{M N}$  averaging around 0.90( $\pm 0.41$ )  $\mu\text{M N}$ , whereas at coastal stations variation was between 0.89 to 2.1 $\mu\text{M N}$  with relatively higher average value of 1.35 ( $\pm 0.52$ ) $\mu\text{M N}$ . Among the open ocean stations, there is a clear demarcation in PON concentration, where the first four stations have PON more than 1 $\mu\text{M N}$  with an average of 1.23 $\mu\text{M N}$ . The rest of the open ocean locations have PON less than 1  $\mu\text{M N}$ , averaging around 0.64 $\mu\text{M N}$ .

The nitrogen isotopic composition of PON also shows a wide variation in the region during this month with minimum of 1.7‰ at station 7, which is an open ocean location, to 7.5‰ at station 13, a coastal location. Interestingly, PON concentration at station 13 is also a maximum during the whole study period. No systematic spatial pattern was observed in  $\delta^{15}\text{N}$ . Overall, the  $\delta^{15}\text{N}$  averaged around 4.7 ( $\pm 1.7$ )‰. The average  $\delta^{15}\text{N}$  for open ocean locations was around 4.4 ( $\pm 1.5$ )‰ and no clear demarcation was observed as in the case of open ocean PON content. The  $\delta^{15}\text{N}$  of coastal locations averaged around 5.3 ( $\pm 2.2$ )‰. Barring three locations during the study period (Stations 3, 7 and 12) the  $\delta^{15}\text{N}$  was around or more than 4‰ during January.

### 3.8.2 Late February- Early March

During this period, only five stations were sampled for natural isotopic variation study. All the five stations sampled were open ocean stations. The PON content during this period varied from 1.0 to 2.25  $\mu\text{M N}$  with an average value of 1.6( $\pm 0.5$ ) $\mu\text{M N}$ . The  $\delta^{15}\text{N}$  varied from 7 to 11‰ with an average of 9.4( $\pm 1.7$ )‰. The PON content and  $\delta^{15}\text{N}$  for both the cruises is listed in Table 3.4.

A plot of  $\delta^{15}\text{N}$  and PON content for the two cruises reveals a positive relationship between the two with  $r^2 = 0.41$ (Figure 3.35). No significant ( $r^2 = 0.14$ ) relationship has been observed between the surface nitrate and  $\delta^{15}\text{N}$  (Figure 3.36) for both the months. In general, this relationship is expected to have a strong negative correlation, as the nitrate concentration increases  $\delta^{15}\text{N}$  should decrease. Such a

relationship is common in a region like the southern ocean where nitrate concentration is very high. The observed poor relationship may be because of low nitrate concentrations and limited number of nitrate measurements. The most

**Table 3.4** PON content and nitrogen isotopic composition in surface suspended matter during January and late February-early March 2003. Cruise number given in bracket. In bold are the bloom stations.

Month	Stations	PON ( $\mu\text{M N}$ )	$\delta^{15}\text{N}$ ( $\text{‰}$ )
<b>January</b> <b>(SK-186)</b>	2	1.61	6.7
	3	1.06	2.7
	4	0.99	4.6
	5	1.27	5.8
	6	0.75	3.8
	7	0.79	1.7
	8	0.16	5.1
	9	0.65	4.7
	10	0.86	4.6
	11	1.20	5.7
	12	0.89	2.3
	13	2.10	7.5
	14	1.21	5.6
	<b>Late February- Early March</b> <b>(SS-212)</b>	2	1.04
<b>3</b>		2.25	10.6
4		1.61	10.9
5		2.00	8.1
6		1.13	7.0

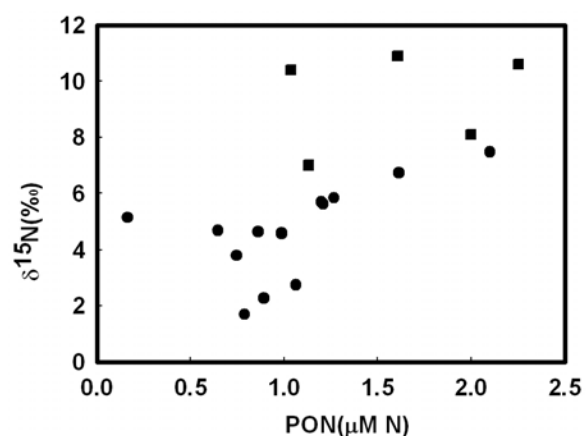


**Figure 3.35** Relationship between  $\delta^{15}\text{N}$  and PON during both cruises. Circles and squares represent January and late February-early March respectively.

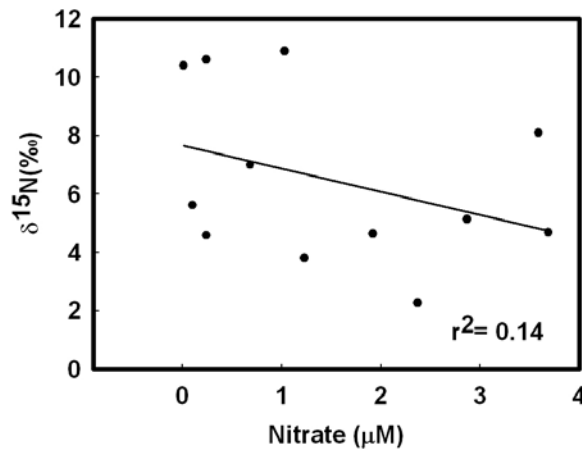


**Figure 3.36** Relationship between  $\delta^{15}\text{N}$  and  $\text{NO}_3$  concentration during both cruises.

noticeable and significant result of the present study is the overall increase in  $\delta^{15}\text{N}$  of the region during late February-early March. As stated earlier, during this period, study was undertaken for the open ocean only, a comparison of  $\delta^{15}\text{N}$  of open ocean locations of January to Feb-March reveals an average increase of  $\sim 5\%$ , which is highly significant. A significant increase of  $0.7\mu\text{M N}$  in PON content has also been observed from January to Feb-March.

### 3.8.3 Possible reasons for increased $\delta^{15}\text{N}$

This increase in  $\delta^{15}\text{N}$  point towards the change in nutrient source or the fractionation pattern of the phytoplankton from one month to another. The significant increase in  $\delta^{15}\text{N}$  of PON during late February-early March is possible under three circumstances: (A) the overall increase in the nitrogen isotopic composition of source ( $\delta^{15}\text{N}$ ) nutrient taken up by the phytoplankton. (B) Change in the fractionation during uptake by the phytoplankton, while maintaining the same  $\delta^{15}\text{N}$  of nutrient during both periods, and (C) a combination of both (A) and (B). However, the explanation for the mechanism of increased  $\delta^{15}\text{N}$  of nutrient is dependent upon its source. Very high new production during early March suggests nitrate to be the principal source of nutrient. As mentioned in the previous section the source of nitrate during early March could be deeper nitrate or nitrate already present in the water column, which entrained during January due to the deeper mixed layer. However, the temperature based shallow mixed layer at the last three stations during early March suggests only a remote possibility of nitrate supply from deeper layers at these sites. However, the undulating and continuously sloping mixed layer at the first three stations suggests the supply of cooler water. This supply

may be from deeper layers or due to advection from nearby region where the effect of winter cooling has not completely vanished and is still getting deeper nitrate. During the present discussion the contribution from both the above mentioned sources and consequent  $\delta^{15}\text{N}$  enrichment of PON would be explored. If the nutrient source during both the months is deeper nitrate, the dramatic change in  $\delta^{15}\text{N}$  of nitrate is possible only when there is intensification in denitrification process in the intermediate waters of the study region leading to an increase in the  $\delta^{15}\text{N}$  of the supplied nitrate. However, if the nitrate already entrained in the surface layer is assumed to be the only source, the continuous use of available nitrate might probably leave the remaining pool enriched enough to explain the observed variation. The following subsections explore possible explanations based on both the above arguments.

#### **A. Denitrification in the Arabian Sea**

Although most part of the open Arabian Sea is well oxygenated, an acute depletion of oxygen occurs at intermediate depths (100-500m), particularly in the eastern and the central Arabian Sea. Reason for this depletion is the consumption of oxygen during the decomposition of organic matter sinking below the euphotic zone. This transition from 'oxic' to 'anoxic' condition at mid depths prompts the facultative bacteria, responsible for decomposition of organic matter, to switch over to nitrate ions that are the next most abundant source of free energy, for the decomposition of organic matter (Richards 1965; Naqvi 1994). The reduction of nitrate to molecular nitrogen with nitrite as one of the intermediate products is known as denitrification. The Arabian Sea is known for intense depletion of oxygen at intermediate depths with concentration often below the threshold value (1.2-3.85 $\mu\text{M}$ ; Broenkow and Cline 1969) required for the initiation of denitrification (Devol 1978). Since, nitrite ( $\text{NO}_2^-$ ) is one of the intermediate products in the denitrification process; its concentration within the water column provides the measure of denitrification. The distribution of  $\text{NO}_2^-$  has been used to demarcate the geographical boundaries of denitrification zone; bounding the denitrification zone by 0.2 $\mu\text{M}$  contour, the total area affected by denitrification in the Arabian Sea has been estimated to be around  $1.37 \times 10^6 \text{ km}^2$  (Naqvi 1991). The rate of denitrification ranges between 20-30  $\text{Tg N yr}^{-1}$  when computed using physico-chemical and between 24-33  $\text{Tg N yr}^{-1}$  using biochemical techniques respectively (Naqvi 1987; Naqvi and Shailaja 1993). The variation in the denitrification intensity based on seasonal scale has been

observed (Naqvi et al 1990) in the Arabian Sea. During the southwest monsoon, a subsurface poleward undercurrent (Shetye et al. 1990) supplies oxygen and nitrate to the eastern Arabian Sea, suppressing the denitrification process. However, this feature is absent during the northeast monsoon i.e., the present study period.

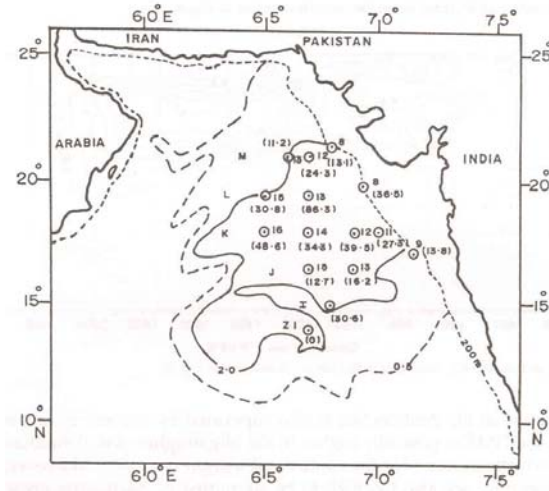


**Figure 3.37** Geographical limits of the Arabian Sea denitrification zone delineated by Naqvi (1991). The area of present study falls within the zones of highest denitrification.

The area of present study undergoes intense denitrification (Figure 3.37) and modifies the isotopic composition of nitrate with a great deal which is the source nutrient for the phytoplankton.

### **Possible role of denitrification to explain the observed variation**

During the process of denitrification  $^{14}\text{NO}_3$  is used up faster than  $^{15}\text{NO}_3$ , resulting in the remaining nitrate getting enriched in  $^{15}\text{NO}_3$ . Thus, denitrification leaves a strong imprint upon the isotopic composition of the remaining nitrate (Cline and Kaplan 1975; Liu and Kaplan 1989). The fractionation for this process is given as  $\alpha_{\text{denitrification}} = \frac{^{15}\text{R}}{^{14}\text{R}}$  where  $^{15}\text{R}$  and  $^{14}\text{R}$  are rates of denitrification for  $^{15}\text{NO}_3$  and  $^{14}\text{NO}_3$  respectively. This can also be represented as  $\epsilon_{\text{denitrification}} = (1-\alpha)*1000$ . Brandes et al. (1998) have estimated  $\epsilon_{\text{denitrification}}$  in the central Arabian Sea using two different models and found it ranging from  $22\pm 3$  (advection-diffusion model) to  $25\pm 4$  (reaction-diffusion model) using an initial nitrate isotopic composition of 6‰.

It is well known from discussions earlier that denitrification leads to the enrichment of the remaining nitrate, which eventually acts as a source for phytoplankton. But why is there so much difference in  $\delta^{15}\text{N}$  of PON from January to March? Are they signatures of intensification of denitrification at intermediate depths

between these two months, which eventually have caused the nitrate  $\delta^{15}\text{N}$  to get enriched from January to March? Banse (1984) have observed the suppression of denitrification during winter due to the supply of oxygen to the upper part of the oxygen minimum zone as a result of enhanced diffusion due to deepening of the mixed layer. The lowering of SST to  $24^\circ\text{C}$  and deepening of mixed layer up to 107m have been observed in the northern stations in the month of January during the present study. This might have helped in reducing the denitrification leading to lower  $\delta^{15}\text{N}$  values of nitrate during January, which is reflected in the  $\delta^{15}\text{N}$  of PON. Such situations were not as prolific as January during the study period in late February-early March as the effect of winter cooling was waning. The mixed layer during this period was also shallow at a few stations. These conditions suggest that the environment during late February-early March was not so supportive of convective mixing and hence the decrease in the aeration of deeper layers. This might have lead to increase in the intensity of denitrification and consequent increase in  $\delta^{15}\text{N}$  of nitrate.

### Intensification of denitrification

Brandes et al. (1998) have estimated the vertical profile of  $\delta^{15}\text{N}$  of nitrate in the Central Arabian Sea for three different periods (September, January and April). The September and January profile exhibited the highest  $\delta^{15}\text{N}$  value of 15‰ at 350m while April profile increased only upto 10.5‰ (Figure 3.38). However, they have observed a

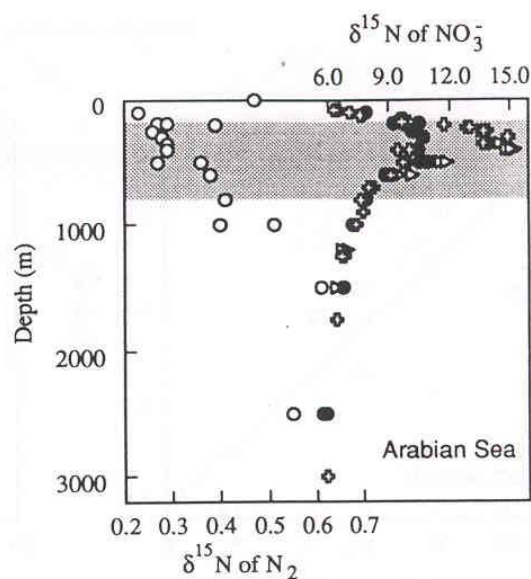


**Figure 3.38** Isotopic composition of nitrate (filled circles, open triangles, and crosses) and nitrogen gas (open circles) with depth as observed by Brandes et al. (1998) for the central Arabian Sea.

decrease in  $\delta^{15}\text{N}$  of nitrate (6‰) at 80m. The reason proposed by Brandes et al. (1998) for the reduced  $\delta^{15}\text{N}$  observed at 80m is the dilution of heavy isotope signatures of nitrate supplied from subsurface layer through upwelling and vertical mixing in the Arabian Sea by lighter isotopes added due to nitrogen fixation. Going with the arguments of Brandes et al. (1998) and assuming that there is similar level of dilution of nitrate isotopic composition at around 80m by nitrogen fixation in the Arabian Sea, which is a potential nutrient source, and assuming the same fractionation factor for both months during uptake of nitrate by phytoplankton, the discussion point towards the potential increase in  $\delta^{15}\text{N}$  of nitrate due to the intensification of denitrification from January to March.

### **Dilution of deeper nitrate**

Another possible explanation could be the following. Assuming that there was no intensification in denitrification from January to March and the  $\delta^{15}\text{N}$  of nitrate produced in the denitrification layer remains same (say 15‰) along with the fractionation behaviour of the planktons during the uptake of nitrate. If most nutrient input to the surface layer was from the suboxic layer; the observed  $\delta^{15}\text{N}$  of PON points towards the requirement of surface light nitrate input for dilution as the deeper nitrate is significantly enriched. The resulting discrepancy of 5‰ in PON can be explained by the varying degree of dilution of enriched nitrate due to nitrogen fixation in the surface layer. The dilution during January will be more than that for late February-early March to explain the required level of  $\delta^{15}\text{N}$  of nitrate. To estimate the level of dilution during both the months the highest value of  $\delta^{15}\text{N}$  of PON of respective months would be considered as the  $\delta^{15}\text{N}$  of ambient nitrate available for uptake assuming that these values of  $\delta^{15}\text{N}$  are reflection of the  $\delta^{15}\text{N}$  of nitrate consumed without fractionation. These values during January and late February-early March were 7.5 and 11‰ respectively, and represent the minimum values for nitrate during these two months assuming no significant spatial variation. The January value (7.5‰) is closer to the known  $\delta^{15}\text{N}$  of nitrate in world ocean (~5‰; Miyake and Wada 1967). The dilution level required to obtain the 7 and 11‰ can be obtained by simple isotopic mass balance:

$$15x + (1-x)*5 = 7.5 \text{ (January) and } 15x + (1-x)*5 = 11 \text{ (March)}$$

Where  $x$  is the proportion of deeper nitrate and  $(1-x)$  is fraction of required dilution by lighter nitrate. 5 and 15‰ are the assumed isotopic composition of natural and deeper nitrate respectively. From this equation it is quite clear that the 75% of dilution would be required during January whereas only 30% required during late February-early March. The mechanism suggested for dilution is the nitrogen fixation.

### **Change in the fractionation behaviour of phytoplankton**

Third scenario may be of a situation where there is same denitrification intensity and level of dilution with varying fractionation pattern. Assuming that the  $\delta^{15}\text{N}$  of nitrate in the denitrification layer is 15‰ that undergoes similar dilution in the surface layer such that the isotopic composition changes to 11‰. This 11‰ nitrate will be acting as source during both months. The observed difference of 5‰ now can be explained by different degree of fractionation during uptake in January and March, to reach the observed isotopic composition from the same source. This depends upon the pool of available nitrate to the phytoplankton. If the pool is large, the phytoplankton can have the luxury of discriminating against  $^{15}\text{N}$  to reach the desirable  $\delta^{15}\text{N}$  level. However, such a scenario is not possible when there is a dearth of nitrate in the surface layer and the phytoplankton have to take up whatever is available and the nitrate isotopic composition is directly reflected in the PON. The nitrate concentration in surface water of the open Arabian Sea during these two months suggest the abundant nitrate (average  $\sim 1.8\mu\text{M}$ ) during January whereas its dearth (average  $\sim 0.3\mu\text{M}$ ) during February except at one station where it was  $3.5\mu\text{M}$ . This high nitrate concentration during January and lower concentration during late February-early March indicate the flexibility for phytoplankton to fractionate during January, and not during March; consequently, reflecting lower and higher  $\delta^{15}\text{N}$  values during January and late February-early March respectively. The  $\delta^{15}\text{N}$  of PON is known to depend also on phytoplankton species, physiology and rate and phase of growth of phytoplankton (Montoya and McCarthy 1995).

However, all the above explanations are based on the assumption that the deeper nitrate is essentially the source. This is quite understandable during January when MLD is more than 80m and convective mixing due to winter cooling maintains the high nitrate concentration in the water column. However, this does not seem to hold good directly at all stations during late February-early March, when the MLD was

found to be shallow (at three stations) despite high wind speeds in the region ( $>8 \text{ ms}^{-1}$ ). However, as mentioned earlier, supply due to advection from nearby regions with deeper MLD is a possible source during late February-early March. But surprisingly during late February-early March *noctiluca* bloom ( $>40 \text{ mg Chl } a \text{ m}^{-2}$  in the euphotic zone) was observed during the study period. Where does the nutrient in the surface layer to support a bloom during late February-early March come from? Apart from nitrate due to advection, another possibility is the supply of nitrate due to turbulent diffusion across the thermocline; however, it is highly unlikely that the amount of nutrients required to sustain a bloom could be supplied due to diffusion.

### **B. Utilization of nitrate present in the surface layer**

One important possibility of the nutrient availability during late February-early March is the inefficient utilization of the nitrate introduced in the water column during January. It is interesting to note that the euphotic zone integrated nitrate concentration in the water column at most of the stations during January was more than  $150 \text{ mmol m}^{-2}$  but the average new production was only  $\sim 2.3 \text{ mmol N m}^{-2} \text{ d}^{-1}$ . However, the integrated euphotic zone column nitrate during March was only around  $80 \text{ mmol m}^{-2}$  but the average new production was as high as  $13 \text{ mmol N m}^{-2} \text{ d}^{-1}$ . These facts clearly indicate that the nutrients entrained in the water column due to convective mixing during January did not get consumed much and mostly remained there in the water column. Assuming the surface layer of the ocean as closed system and nitrate with initial isotopic composition ( $\delta_o$ ) of 7‰ as the source for phytoplankton during January, the isotopic composition of remaining nitrate ( $\delta$ ) will keep on changing with the consumption of the substrate pool (i.e., fraction of substrate remaining,  $f$ ) according to well known relationship:

$$\delta = \delta_o + \epsilon * \ln(f) \quad \text{where, } \epsilon = (\alpha - 1) * 1000; \alpha \text{ is fractionation factor.}$$

Assuming that the isotopic composition of nitrate available during late February-early March is 11‰ and taking  $\epsilon = -5‰$  (general value assumed for fractionation; Waser et al. 1998) the  $f$  from the above equation comes to be 0.4. It reveals that at the start of the uptake during late February-early March 60% of the nitrate introduced in the water column during January had already been consumed. If we take  $\epsilon = -9‰$  as in some cases (Rau et al. 1998) only 40% of the nitrate was consumed and rest 60% was available for further consumption (Figure 3.39).

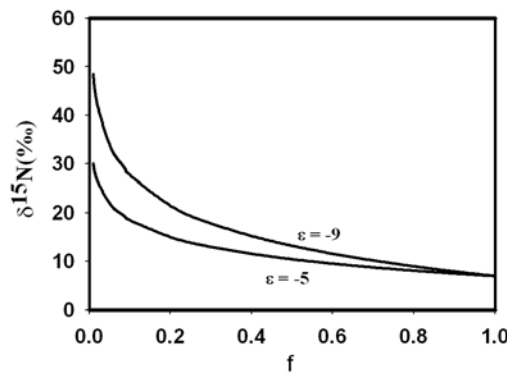


**Figure 3.39** Relationship between fraction of remaining nitrate ( $f$ ) and its isotopic composition for different fractionation factors.

### 3.9 Conclusions

The present study was an attempt to understand and quantify the new production in the northeastern Arabian Sea during NE monsoon and compare it with the other, well explored, northwestern parts of the Arabian Sea. The effect of winter cooling on new production and on the natural nitrogen isotopic composition of suspended matter also formed a major part of the present study. The following are the most important findings of the present work:

- There exists a systematic dependence of new production on the winter cooling phenomenon in the northeastern Arabian Sea.
- The new production and  $f$ -ratio appear to increase from the south to the north.
- There appears to be a lag between the entrainment of nutrient in the water column and development of bloom in the northeastern Arabian Sea.
- The new production during bloom period in late February-early March was found to be five fold more than the new production in January.
- Ammonium was the preferred substrate during January whereas nitrate was during late February-early March.
- The inclusion of conservative urea uptake into the calculation reduces the  $f$ -ratio.
- The nitrogen isotopic composition of suspended particulate matter increases by  $\sim 5\text{‰}$  from January to February indicating the shift in the nutrient regime.

# **Chapter 4**

## **The Bay of Bengal**

---

---

## 4.1 Introduction

The Bay of Bengal (BOB) is a semi enclosed tropical basin located in the northeastern part of the Indian Ocean touching the eastern boundary of the Indian Subcontinent. BOB is also partially connected to the Pacific through the Australasian seaways, thus exchanging physical, chemical and biological properties. BOB covers an area of  $2.2 \times 10^6 \text{ km}^2$  and constitutes 0.6% of the world ocean (LaFond 1966). Like the extensively studied Arabian Sea, BOB also experiences seasonal changes in climate and surface circulation due to the Asian monsoon system, resulting in heavy rainfall during the SW monsoon in the Indian Subcontinent (Ramage 1971). On an average, the annual rainfall over the BOB is in excess of 2m (Gill 1982) and precipitation has been reported in excess of evaporation (Venkateswaran 1956). The fresh water discharge into BOB due to all major Indian rivers, particularly the Ganges-Brahmaputra system, reaches a maximum during SW monsoon (Figure 4.1). BOB receives fairly large quantities of fresh water from the Indian rivers ( $1.6 \times 10^{12} \text{ m}^3 \text{ yr}^{-1}$  compared to  $0.3 \times 10^{12} \text{ m}^3 \text{ yr}^{-1}$  to the Arabian Sea, Subramanian 1993) exerting a strong influence on the surface water circulation and stratification of the sea surface (Shetye et al. 1991; Shetye et al. 1996). This riverine input of freshwater in BOB also causes significant variations in the salinity, which varies from 35 psu in the open Bay to as low as 20 psu in the coastal regions during the SW monsoon (La Violette 1967; Prasanna Kumar et al. 2002). The river water also brings a lot of nutrients and thus, is a major source of nutrients such as  $\text{SiO}_2$ , nitrate and phosphate. The supply of  $\text{SiO}_2$  by major Indian rivers like Ganga and Brahmaputra to the Bay has been estimated to be 1.5% ( $133 \times 10^9 \text{ mol yr}^{-1}$ ) of the total annual riverine input of  $\text{SiO}_2$  to the world ocean (Sarin et al. 1989). BOB receives 10% of the total dissolved phosphorus flux of the world ocean by the Ganga-Brahmaputra-Meghna river system (Datta 1999). However, the reported nitrate concentration is not as high as that of silica in the Bay (DeSousa et al. 1981). Also, the Ganga-Brahmaputra river system alone supplies a significant part of its average annual sediment load of  $1.1 \times 10^9$  tonnes (Milliman and Syvitski 1992), and forms the largest deep sea fan of the world. In general, the circulation pattern in BOB is controlled by the equatorial Indian Ocean effects, atmospheric forcings and fresh water inputs (Schott and McCreary 2001). During premonsoon, BOB circulation is characterized by a well developed anticyclonic gyre and a poleward western boundary current known as the East India Coastal Current (EICC, Shetye et al. 1993). During the

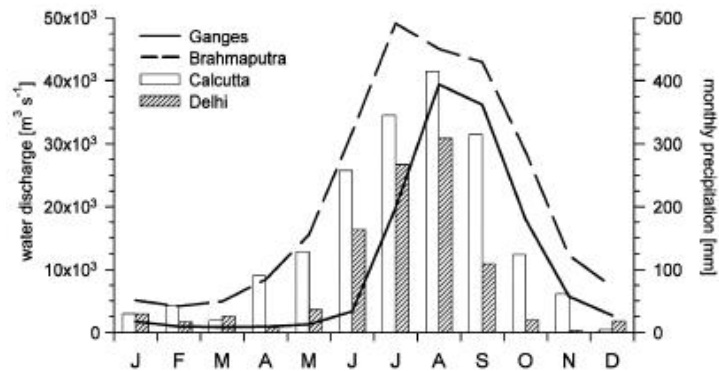


**Figure 4.1** Mean monthly water discharge of Ganges (averaged over 1985-1992) and Brahmaputra (averaged over 1969-1975) and mean monthly precipitation at Delhi and Calcutta (averaged over 1994-1997). Source: Unger et al. (2003).

summer monsoon, there is a reversal of the circulation pattern with a southward current along the coast (Shetye et al. 1996). Coastal upwelling has also been reported in BOB, but much less in intensity than in the Arabian Sea (Shetye et al. 1991, 1993), and is known to be hampered due to surface stratification (Shetye et al. 1991). Overall, BOB represents a magnificent natural laboratory to study the effect of freshwater fluxes due to seasonally changing and interacting continental and oceanic processes on the marine ecosystem and material cycling.

The present study in the Bay of Bengal concentrates mainly on the  $^{15}\text{N}$  based new production measurements, *which is the first of its kind in the BOB*. It also concentrates on the natural nitrogen isotopic variability in suspended matter. The discussion on BOB in the subsequent sections will be in the following sequence:

- Experiments related to the effect of concentration and incubation time on the uptake rate of nutrients.
- $^{15}\text{N}$  based new and total production during the postmonsoon.
- $^{15}\text{N}$  based new and total production during the premonsoon.
- Natural isotopic composition of suspended matter.
- Productivity estimates using remotely sensed data.

## 4.2 Effect of tracer concentration and incubation time on the uptake rate of nutrients

The mechanism by which the nutrient is supplied and the kinetics of the utilization of the dissolved inorganic nitrogen play a critical role in determining the productivity, size

structure, and species succession of phytoplankton in the world ocean (Harrison et al. 1996). Dugdale (1967) proposed a theoretical framework for nitrogen uptake by phytoplankton at steady state. Generally, uptakes of both nitrate and ammonium follow the Michaelis-Menten expression for enzyme kinetics. Michaelis-Menten expression is concentration dependent and a hyperbola describes the relationship between the concentration of nitrate (or ammonium) and its uptake; however, exceptions to this exist (MacIsaac and Dugdale 1969). Nitrate uptake estimates have been made in different regions of the world ocean (Dugdale et al. 1992; McCarthy et al. 1999; Watts and Owens 1999; Sambrotto 2001; L'Helguen et al. 2002; Rees et al. 2002). These are based on the incorporation of 'trace' addition of  $^{15}\text{N}$ -labelled  $\text{NO}_3$  into phytoplankton during incubation experiments. The details of the experimental procedure followed in these studies are somewhat variable; e.g. time of incubation could vary between 2 and 24 hours (the latter, when dark incubation is included). Though in general, the JGOFS protocol (JGOFS 1996) is followed, a number of questions arise regarding these procedures for uptake at low-level concentrations. These are: (a) what is the effect of duration of the incubation on the uptake rate of nutrients by the phytoplankton? Are there significant variations within the time of 2-4 hours as recommended by the JGOFS protocol? (b) What is the effect on the uptake rate of the substrate concentration added? (c) f-ratio, the ratio of new to total production (Eppley and Peterson 1979), has been calculated by different workers (Wafar et al. 1995; Watts and Owens 1999) for different oceans but what happens to the f-ratio in cases (a) and (b)? (d) The JGOFS protocol suggests simulated *in-situ* incubation for  $^{15}\text{N}$  uptake experiments for durations of 2 to 4 hours. Longer incubation times could lead to problems such as increased regeneration of ammonium and urea, which will also be taken up along with nitrate. However, primary productivity (PP) experiments using  $^{14}\text{C}$  are preferably done *in-situ* for 12 hours (e.g., Madhupratap et al. 2003). To facilitate comparison of PP measured and new production estimated from  $^{15}\text{N}$  experiments, it is essential to know whether the results of *in situ* and simulated *in-situ* incubation experiments (using  $^{15}\text{N}$ ) from dawn to dusk are comparable.

The intention of the present study was to investigate the above questions based on  $^{15}\text{N}$  uptake experiments performed for very low concentration of nutrients in the surface waters of the Bay of Bengal (BOB). Although the number of experiments during this study is limited, the idea was to have a first hand investigation of the  $\text{NO}_3$  and  $\text{NH}_4$  uptake behaviour and to explore the possible signature of inhibitory effects of

NH<sub>4</sub> on NO<sub>3</sub> uptake in the natural plankton assemblages of the Bay of Bengal. Our objective was also to investigate if N uptake in very small concentration can be expressed by traditional saturation kinetics. Sampling was done during Sep-Oct 2002 onboard ORV Sagar Kanya. The tracers used for experiments were 99 atom% <sup>15</sup>N enriched sodium nitrate, ammonium chloride and urea procured from SIGMA-ALDRICH. Details of the individual experiments are discussed below.

#### **4.2.1 Material and Methods**

##### **Experiment 1**

The aim of this experiment was to observe the variations in the uptake rates of different N-species due to varying durations of incubation. The JGOFS protocol was followed: surface water samples were collected (at 17° 56' 33.1" N, 87° 54' 38.6" E) in one litre Polycarbonate NALGENE bottles, pre-washed to avoid contamination. Samples were divided into three sets of four bottles each for nitrate, ammonium and urea tracers. In each bottle, a constant amount of 0.01 µM of the respective tracer was added. After the tracer addition, samples were kept for incubation at 10.00 Hrs, in a deck incubator with flowing surface seawater (from 5m depth). No neutral density filters were used as the samples were from the sea surface. Every hour one bottle from each set was taken out of the incubator and filtered on precombusted (4hr @ 400°C) Whatman GF/F filters under low vacuum. The samples were dried and kept for further mass spectrometric analysis.

##### **Experiment 2**

This experiment was intended to determine uptake rate variations of different nitrogenous species by the phytoplankton due to varying concentrations of the substrates. For this experiment too, surface water samples were collected (at 20° 0' 15.0" N, 87° 59' 36.4" E) in one litre bottles and divided into three sets of four each. But the concentration added in different bottles of each set was different. The concentrations added were 0.01, 0.02, 0.03 and 0.04 µM of the respective tracers in different bottles of the respective sets. These amount to 9%, 18%, 27% and 36% respectively of the nitrate concentration in the surface waters. For ammonium and urea, these are much in excess of the ambient concentrations (see section 2.4). Incubation was done on deck for four hours symmetrical to local noon i.e., from 10.00 to 14.00

Hrs. Running seawater maintained the temperature during incubation. Neutral density filters were not used, as in experiment 1. After incubation, the samples were filtered and preserved for analysis as described earlier.

### **Experiment 3**

To estimate the differences in the uptake rates due to deck and in-situ incubations, samples were collected (at 14° 0' 17.2" N, 80° 59' 54.9" E) from surface, 20, 40 and 60 metres depth and transferred to six one litre bottles from each depth. Three bottles were used for in-situ and the other three for deck experiments for each of the three different tracers. In the case of urea and ammonium, the ambient concentration measurements could not be performed due to logistic problems; however they were estimated indirectly using zooplankton biomass. The euphotic zone in the Bay of Bengal is well oxygenated; the expected ambient ammonium and urea concentrations here are low, hence, a constant concentration of 0.01 $\mu$ M for ammonium and 0.03 $\mu$ M for urea was added for all the four depths. No literature exists for the relationship between oxygen and ammonium concentration for the Bay of Bengal. However, US JGOFS data for Arabian Sea suggests absence of ammonium in surface layers where water is well oxygenated as in the Bay of Bengal. An attempt to add less than 10 % of ambient concentrations was made in the case of nitrate, which lead to the addition of 0.03, 0.02, 0.03 and 0.6  $\mu$ M for surface, 20, 40 and 60 m samples. A secchi disk was used to measure the light attenuation with depth. It was found that light was less than 1% of the surface value at ~60 m depth. Further, Chl *a* concentrations were near zero below this depth. The light conditions for the deck incubation were simulated using well calibrated neutral density filters and also the continuous flow of seawater from 5m depth was maintained in order to maintain the temperature. The neutral density filters used were such that equivalent depths were 4, 41, 55 and 77m. The incubation was done for 12 hours (from dawn to dusk) in both cases and subsequently, the samples were filtered and preserved for analysis.

In all three experiments above duplicate analysis was made wherever possible

#### **4.2.2 Physical conditions and nutrients at the experimental stations**

The salinities at the stations of experiment 1 and 2 were 29.2 and 28.1 psu and are

affected by fresh water influx. However at the site of experiment 3 surface salinity was 33.4 psu. The riverine inputs are a potential source of nutrients, such as phosphate and silica to the Bay. Also, BOB is a cyclone-prone region and these events churn up the sea, injecting nutrients into the surface layer especially during the post monsoon season. Sea surface temperature (SST) varied from 28.2 to 30.1°C. SST along with other meteorological and hydrodynamic parameters at the experimental stations is listed in Table 4.1. The ambient nitrate concentration required for the uptake calculation was measured by column reduction technique (Strickland and Parson, 1972). These values are also listed in Table 4.1. Ammonium and urea concentrations have been calculated as follows: The regeneration of ammonium and urea by zooplankton is well known (Mullin et al. 1975; Jawed 1973). Mesozooplankton biomass in this season in BOB ranged from 0.1 to 1.1 ml.m<sup>-3</sup>.

**Table 4.1** Physical parameters at the experimental stations.

Parameter	Experiment 1	Experiment 2	Experiment 3
Latitude (°N)	~18	~20	~14
Longitude (°E)	~88	~88	~81
Wind speed (m/s)	6	4	4
Pressure (mbar)	1008	1008	1010
Air Temperature (°C)	>31	29	27.5
SST (°C)	29	28.9	30
surface Salinity (PSU)	29.2	28.1	33.4
MLD (m)	3	6	24
Chlorophyll-a (mg/m <sup>2</sup> )	15	13	15
surface Nitrate(μM)	0.07	0.11	0.16
PON (μM)	1.04	1.2	1.08

Based on the equations given by Wiebe et al. (1975) the zooplankton biomass was converted into dry weight and using the average ammonium and urea excretion rates of 0.59 and 0.32 mg at-N (g dry wt)<sup>-1</sup> d<sup>-1</sup>, the release rates were calculated for 12 hour residence time of zooplankton in mixed layer (Wafar et al. 1986). According to this calculation, the ammonium and urea concentrations near the station of experiment-3 were found to be 0.014 and 0.004μM respectively. Considering the uncertainties involved in the equations used for the calculation, the above values could well be near zero.

### 4.2.3 Results and Discussion

#### Experiment 1

**UREA:** Results from experiment 1 suggest that both specific uptake rate and the uptake rate are the highest for N-uptake from urea (Figure. 4.2) in the nutrient poor waters of the Bay. This observation is similar to that of Rees et al. (2002), who observed urea to be the most preferred substrate in the oligotrophic North Sea. However our value for the average uptake rate from urea is only one third of the value obtained by Rees et al. (2002) for a similar concentration of the substrate added. The specific uptake rate for urea increases for incubation times more than 2 hours, but declines for incubation times greater than 3 hours. This significant decline is also exhibited by the uptake rate for urea. Uptake rates range from a maximum of  $2.48 \mu\text{mol N m}^{-3}\text{h}^{-1}$  to a minimum of  $1.56 \mu\text{mol N m}^{-3}\text{h}^{-1}$ . These values are comparable in magnitude with values obtained by others elsewhere (McCarthy et al. 1999; Cochlan and Bronk 2001).

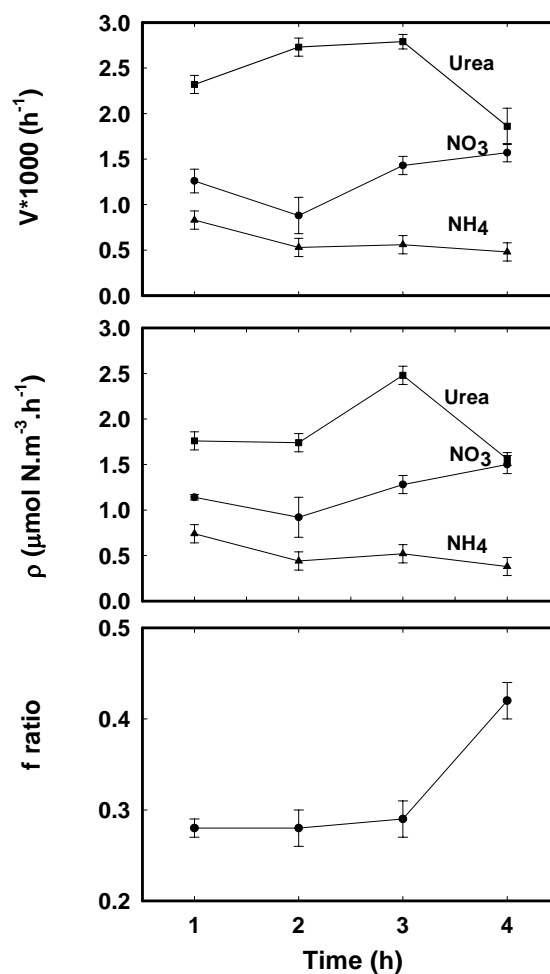


**Figure 4.2** The result of experiment 1 showing variation in specific uptake rate (top panel), uptake rate (middle panel) and f-ratio (bottom panel) with increase in the duration of incubation from 1 to 4h.

**AMMONIUM:** In the case of ammonium, where constant addition of 0.01  $\mu\text{M}$  was made, both specific uptake rate and uptake rate decreased slightly for incubation time more than 1 hour, and remained constant for higher incubation times (Figure 4.2). The uptake rate for ammonium showed a maximum of nearly  $0.74 \mu\text{molN m}^{-3}\text{h}^{-1}$  and a minimum of  $0.38\mu\text{molN m}^{-3}\text{h}^{-1}$ . These values are comparable to those reported by Rees et al. (2002) for ammonium uptake rate in the oligotrophic North Sea, extrapolated to the same substrate concentration. It is known that in ammonium poor waters, ammonium is taken up as soon as it becomes available (Glibert et al. 1982b). For example phytoplankton growing in ammonium deprived cultures can assimilate ammonium at a much faster rate compared to their growth rate (McCarthy and Goldman 1979).

**NITRATE:** The specific uptake rates and uptake rates for nitrate lie between those of urea and ammonium. The uptake rate remains nearly the same for incubation times upto 2 hours, but for 3 and 4 hour incubations, it is slightly higher (Figure 4.2). The uptake rate varies within a narrow range of  $0.92$  to  $1.5 \mu\text{mol N m}^{-3}\text{h}^{-1}$ , values comparable to those obtained by Rees et al. (2002) for North Sea waters.

These changes in the uptake rates of different N-species as a function of time are reflected in the f-ratio as well. The f-ratio [defined as the ratio of the uptake rate of  $\text{NO}_3^-$  and uptake rates of ( $\text{NO}_3 + \text{NH}_4 + \text{Urea}$ )] almost follows the pattern of  $\text{NO}_3$  uptake rate. There is a significant increase in the f-ratio for incubation times greater than 3 hours, from 0.29 to 0.42. This is partly due to the significant decrease ( $2.48$  to  $1.56 \mu\text{mol m}^{-3}\text{h}^{-1}$ ) of the urea uptake rate.

The change in uptake rates of individual N-species within four hours of incubation indicates the high demand for ammonium in the initial hours so that ammonium may become limited in the third and fourth hours due to a rapid initial uptake. In contrast, the uptake of nitrate is less prominent in first two hours but rises in the third and fourth hours. This may be because unlike reduced species such as urea and ammonium, nitrate has to be reduced in the cells before uptake, which therefore has a larger time constant. The effect of these variations on f-ratio is notable. It appears that f-ratio may be underestimated if incubation is done only for two hours, f-ratio at this stage in this water was found to be 0.28. However the result after four hours of incubation shows an f-ratio of 0.42. This may be because of the higher uptake rate for

nitrate in later hours of incubation. The f-ratio after four hours of incubation is one and a half times more than that observed after two hours. Harrison et al. (1996) have reported a linear tracer uptake over a 3 hour incubation period during time-course experiment performed in the Canary Basin. However, Goldman and Glibert (1983) suggested that the estimates of parameters could change with incubation time reflecting different biogeochemical processes: short term incubations (minutes) assess membrane transport processes, whereas long incubations (hours) assess macromolecular synthesis (Wheeler et al. 1982).

## **Experiment 2**

As seen in the case of experiment 1, urea seems to be the most preferred substrate in this water, in general. When concentration added is  $0.01\mu\text{M}$  for all the three tracers, the rate of uptake after four hours of incubation is the highest for nitrate followed by urea (Figure.4.3). But when the concentration of substrate added is increased, the specific uptake as well as uptake rate for urea becomes higher.

There is a significant increase in sp. uptake rate from  $0.0024$  to  $0.0062\text{ h}^{-1}$  when the concentration of urea added increased from  $0.01$  to  $0.04\mu\text{M}$ . The uptake rate of urea also increased from  $2.3$  to  $7.3\mu\text{molN m}^{-3}\text{h}^{-1}$ . There is a significant linear correlation between the urea-N uptake rate ( $y_u$ ) and the substrate concentration ( $x_u$ ):  $y_u = 1.88x_u + 0.004$  ( $r^2 = 0.88$ ).

Ammonium closely follows the pattern exhibited by the urea; however, the sp. uptake rate and uptake rate values are less than that for urea. The sp. uptake rate varies from  $0.0014$  to  $0.0044\text{ h}^{-1}$  when ammonium concentration added increased from  $0.01$  to  $0.04\mu\text{M}$ . Uptake rate varies from  $1.3$  to  $5.6\mu\text{molN m}^{-3}\text{h}^{-1}$ . There exists a significant linear correlation between the ammonium-N uptake rate ( $y_a$ ) and the substrate concentration ( $x_a$ ):  $y_a = 2.07x_a - 0.002$  ( $r^2 = 0.55$ ). Similar linear correlations for ammonium and urea uptakes have been reported by Rees et al. (2002). The slopes reported by them are lower possibly because their experiments pertain to a plankton bloom, whereas ours do not.

Nitrate shows a completely opposite trend of what has been observed in the cases of ammonium and urea. The specific uptake rate and uptake rate for nitrate decreases with increase in concentration. It shows maximum values when nitrate addition was  $0.01\mu\text{M}$ . It shows a marginal change in uptake rate when concentration

changed from 0.02 to 0.03  $\mu\text{M}$ , however it drops down when concentration added is increased to 0.04 $\mu\text{M}$ . There is a significant negative correlation between the nitrate-N uptake rate ( $y_n$ ) and the substrate concentration ( $x_n$ ):  $y_n = -0.76x_n + 0.05$  ( $r^2 = 0.86$ ).

The f-ratio almost reflects the change in nitrate uptake rate. It shows maximum value of 0.47 when nitrate uptake rate is maximum i.e., when concentration added to the sample is 0.01 $\mu\text{M}$ . It shows minimum value of nearly 0.10 for 0.04  $\mu\text{M}$  addition, because at this concentration the nitrate uptake rate drops down.

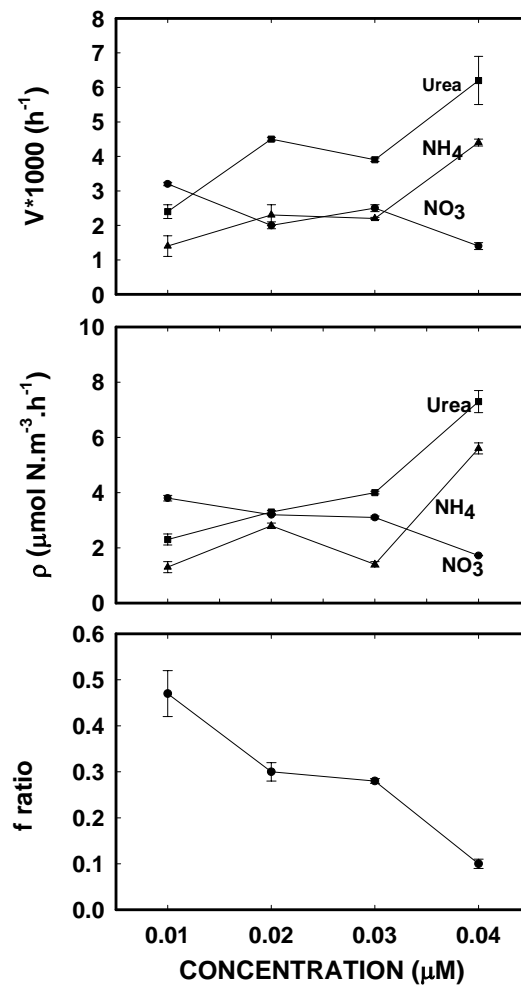


**Figure 4.3** The result of experiment 2 showing variation in the specific uptake rate (top), uptake rate (middle) and f-ratio (bottom) with increase in the substrate concentration.

The results of the present study were examined to determine whether the traditional saturation kinetics model (Michaelis-Menten equation) was followed or not at present nanomolar level experiment. Ammonium and urea uptakes, in general, were found to have a positive correlation with the concentration but could not be represented by a

typical hyperbolic function as in Harrison et al. (1996). The main reason could be the range up to which experiment was done. During present study, the maximum addition of tracer was done up to 40nM whereas Harrison et al. (1996) have gone upto substrate levels of 2000nM. Since, the required hyperbolic curve could not be traced because of the above reasons, the half saturation constant could not be determined reliably during present study.

At lower concentration level (with an incubation time of four hours), the uptake rate for nitrate is more but as the concentration of substrate increases, the uptake rates for ammonium and urea are higher. The reason for the decrease in the nitrate uptake for a higher concentration may be the build up of ammonium due to its regeneration in the bottle (Glibert et al. 1982b). This ammonium might be preferred for uptake leading to an increase in the concentration of glutamine on reduction, known to suppress the synthesis of the enzyme needed for reduction of nitrate and hence suppression of its uptake (Dortch 1990; Flynn et al. 1997; Flynn 1998). Suppression of nitrate uptake in the presence of ammonium has been observed earlier in the Arabian Sea (McCarthy et al. 1999). Wheeler and Kokkinakis (1990) have shown that an extremely low level of  $\text{NH}_4$  is capable of significant inhibition of  $\text{NO}_3$  uptake (50% reduction of nitrate uptake at  $\text{NH}_4$  concentrations of 50-200nM). However, contradictory reports do exist: Wheeler and Kokkinakis (1990) have observed almost complete  $\text{NO}_3$  inhibition at  $\text{NH}_4$  concentrations of 100-300nM, whereas Harrison et al. (1996) have rarely observed a complete inhibition even at  $\text{NH}_4$  concentrations of 2000nM. Harrison et al. (1996) in the experiment where  $^{14}\text{NH}_4$  was added to bottles containing  $^{15}\text{NO}_3$  found that the simultaneous uptake of unlabelled nitrogen ( $^{14}\text{NH}_4$ ) during incubation dilutes the isotope ratio in the PON and results in an underestimate of nitrate uptake rate (Collos 1987) and consequently the overestimation of  $\text{NO}_3$  uptake inhibition. It is not very clear why the effect of the nitrate suppression should be more at a relatively higher  $\text{NO}_3$  concentration than at a lower concentration during present study. However, Conway (1977) suggested inhibition to be the greatest under nutrient replete conditions and the least when phytoplankton are N-starved. The present nutrient level, however, cannot be classified as nutrient replete; but there may be a relative increase in the suppression effect with increased concentration. Price et al. (1994) have found that in the  $\text{NO}_3$  rich equatorial pacific ambient ammonium level (150nM) alone may have reduced nitrate uptake by half. Harrison et al. (1996) have suggested that if  $\text{NH}_4$  level were ~10nM (likely in the Bay of Bengal) inhibition of nitrate uptake by ambient ammonium levels

would have averaged 15-20% at oceanic stations. The f-ratio during the present study decreases drastically with increase in the substrate concentration. To circumvent this effect it is important to add tracers in a level less than 10% of the ambient concentration to get a reasonably correct estimate of the f ratio.

If the above results are extrapolated to in-situ conditions, as long as the surface nutrients are close to zero as observed, a small amount of extraneous input can increase the new production. If the extraneous input is used up quickly enough, then the conditions are restored for further uptake as and when nutrient pulses are introduced. On the other and, if the extraneous input is relatively large, the initial surge in new production may not be sustained at a high level for prolonged periods. This is in contrast to the observation of Rees et al. (2002), who observed a linear increase in the nitrate uptake rate with substrate concentration. However, it is worth noting that their experiments were conducted on a coccolith bloom, whereas the waters of the Bengal seldom known to support a bloom.

It is interesting to compare the uptake and specific uptake rates of the 4 hour incubations at 0.01  $\mu\text{M}$  nitrate addition from the two experiments above (see Table 4.2). Values obtained in the second station (experiment 2) are significantly larger than those from the first (experiment 1). However it is to be noted that there is no significant difference in the f-ratios. Table 4.1 shows that the environmental conditions are more or less same on both the days. The reason for the difference in uptake rates, therefore, may be attributed to the difference in available light levels on these two days. On the day of the first experiment, the sky was intermittently overcast (during the incubation period), whereas on the day of the second experiment, it was bright and sunny. Day to day variations in uptake rates can be quite significant depending on cloudiness, in the Bay of Bengal. Gomes et al. (2000) have observed column productivity significantly affected by cloudiness in the Bay.

**Table 4.2** Comparison of specific uptake and uptake rates at two different stations for 4 h incubation at 0.01 $\mu\text{M}$  concentration. Uncertainty based on duplicate measurements given in parentheses.

Tracer	Experiment 1		Experiment 2	
	Sp. Uptake rate *1000 ( $\text{h}^{-1}$ )	Uptake rate $\mu\text{mol N m}^{-3} \text{h}^{-1}$	Sp. Uptake rate *1000 ( $\text{h}^{-1}$ )	Uptake rate $\mu\text{mol N m}^{-3} \text{h}^{-1}$
Nitrate	1.57(0.1)	1.5(0.1)	3.2(0.05)	3.8(0.1)
Ammonia	0.48(0.1)	0.38(0.1)	1.4(0.3)	1.3(0.2)
Urea	1.86(0.2)	1.56(.07)	2.4(0.3)	2.3(0.2)

### Experiment 3

The nitrogen uptake rates from ammonium (triangle), urea (square) and nitrate (circle) are plotted as a function of depth in Figure 4.4 both for deck (filled symbols) and in-situ (open symbols) incubations. Results of the deck experiments are plotted such that the depths correspond to the light levels provided, rather than the actual depths from which the water samples were taken. The analytical uncertainties in the calculated uptake rates are shown as error bars corresponding to one standard deviation. It is seen that the surface values (2 to 4 m depth) are the same for in situ and deck incubations, within errors. Ammonium uptake rates are the lowest and do not vary much with depth in both in-situ and deck experiments. Urea uptake rates are also in agreement within two standard deviation for the in-situ and interpolated deck values for corresponding depths. Only at 20 and 40 m depths the nitrate uptake rates are significantly higher in the in-situ case relative to the interpolated deck values. In region such as the Bay of Bengal one would expect a subsurface maximum in the nitrate uptake rate, which is seen in the in-situ experiment, but is absent in deck experiment. Two possible reasons for this discrepancy could be (a) The deck incubation were probably carried out at a higher temperature (of water at 5m depth) than the actual temperature at 20, 40 and 60m depths (the mixed layer was only 5m, Table 4.1); (b) Sample heterogeneity and (c) The light cut off was more than that required for the depths of incubation of the in-situ experiment.

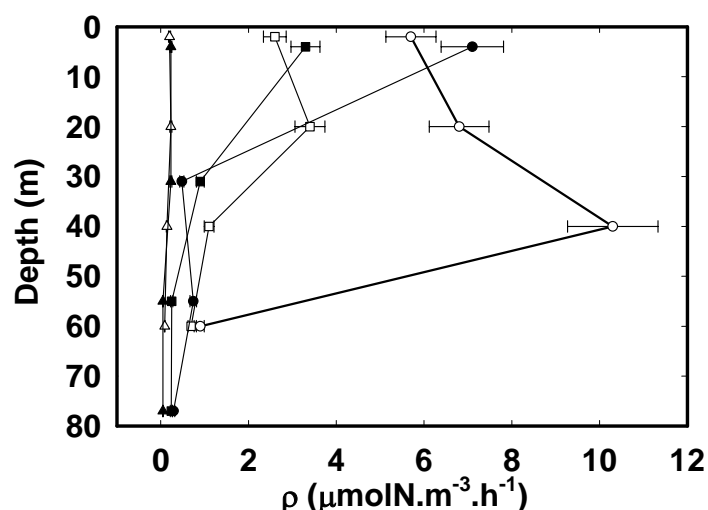


**Figure 4.4** Comparison of uptake results obtained from in-situ and simulated in-situ experiments. In situ nitrate, ammonium and urea uptake are indicated by open circle, triangle and square respectively. Simulated in-situ nitrate, ammonium and urea uptake are indicated by filled symbols.

The column-integrated values for the productivity (taking C/N Redfield ratio as 6.6) obtained by us were  $519 \text{ mg C m}^{-2} \text{ d}^{-1}$  and  $251 \text{ mg C m}^{-2} \text{ d}^{-1}$  respectively for in-situ and deck incubations. In the same location primary production was measured using  $^{14}\text{C}$  method for the same depths during the previous day (same mean solar radiation  $\sim 100 \text{ mW/cm}^2$  on both days). This value  $\sim 218 \text{ mgC m}^{-2} \text{ d}^{-1}$ , is closer to our deck incubation value. Use of 6.6 for C/N ratio might be questionable as variations have been reported (Rees et al. 2002) for C: N consumption rates. However, here we use statistical average of 6.6 observed for organic matter in this region.

Another experiment to check the effect of incubation during different intervals in a day was performed during premonsoon cruise (SK-191) at two different locations-PP2 and PP7. At both the stations the surface water samples were collected early in the morning (before sun rise) in 9 one litre NALGENE bottles. The three bottles were incubated from 600 to 1000 Hrs. after adding  $0.01 \mu\text{M}$  of each tracer (nitrate, ammonium and urea). The rest six were kept in dark. At 1000 Hrs., another three were incubated till 1400 Hrs. followed by next three from 1400 to 1800 Hrs. The samples were filtered and dried as soon as incubation was over. The results obtained from this study show a similar trend at both the stations. The specific uptake rate during morning (600 to 1000 Hrs) is higher for all the tracers (except urea at PP7) and remain same for noon (1000 to 1400 Hrs) and evening (1400 to 1800 Hrs) intervals (Figure 4.5). The most striking is the very high specific uptake rate for nitrate during morning interval at both the stations, which decreases drastically at noon and evening intervals. One possible reason for reduction in specific uptake rate during noon and evening intervals may be the storage of phytoplankton for a longer time in the bottles. However, these are preliminary results, which need to be repeated in future cruises.

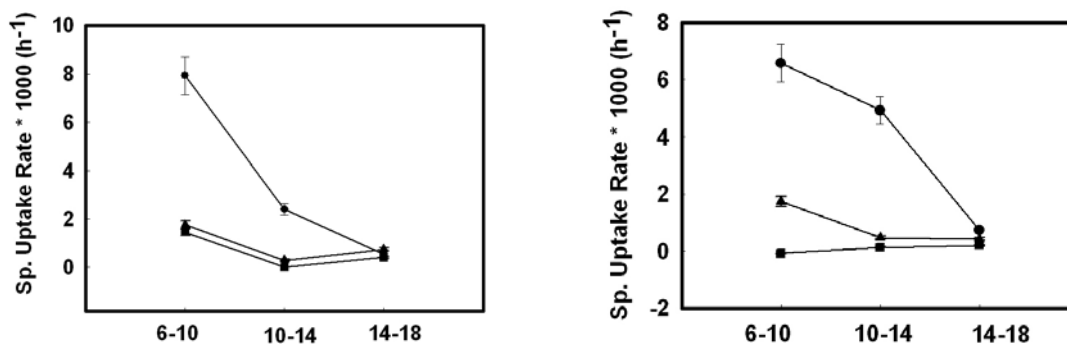


**Figure 4.5** The specific uptake rate at PP2 (left) and PP7 (right) for the incubation at different intervals during a day. The x-axis denotes the different intervals.

### 4.3 Earlier measurements of $^{14}\text{C}$ based Productivity and Chl *a* in the Bay of Bengal

As mentioned earlier, the Bay of Bengal has not received much scientific attention compared to the Arabian Sea. The ongoing Bay of Bengal process studies (BOBPS) is an attempt to evaluate the biogeochemical characteristics of the Bay. A few measurements exist regarding the total primary productivity, which show a random distribution over space and time. Qasim (1977) observed that surface production in the Bay is higher than Arabian Sea due to low light intensities whereas column production is higher in the Arabian Sea. Nair et al. (1973) have reported primary productivity values varying from  $3.0\text{-}8.7\text{ g C m}^{-2}\text{ d}^{-1}$  for inshore waters of the east coast of India during the SW monsoon. Radhakrishna et al. (1978) have reported the variability in the primary productivity (PP) values for the off shore regions from  $129.99$  to  $329.45\text{ mgC m}^{-2}\text{ d}^{-1}$  (av.  $219\text{ mgC m}^{-2}\text{ d}^{-1}$ ) and  $49.66$  to  $606.37\text{ mgC m}^{-2}\text{ d}^{-1}$  (av.  $315.43\text{ mgC m}^{-2}\text{ d}^{-1}$ ) for the slope region along the western margin of the Bay during August-September 1976. Bhattathiri et al (1980) have reported  $180\text{-}2200\text{ mgC m}^{-2}\text{ d}^{-1}$  (av.  $740\text{ mgC m}^{-2}\text{ d}^{-1}$ ) for offshore and  $120\text{-}3410\text{ mgC m}^{-2}\text{ d}^{-1}$  (av.  $1280\text{ mgC m}^{-2}\text{ d}^{-1}$ ) for the slope region along the Indian side for August-September 1978 and concluded that primary production of the Bay is not less than that reported for the Arabian Sea. Most recently Gomes et al. (2000) have studied the productivity and Chl *a* concentration for the three seasons in the BOB for both off shore and inshore regions. Average depth integrated Chl *a* values for inshore stations have been reported to be  $30.4$ ,  $165$  and  $26.2\text{ mg m}^{-2}$  while for offshore stations it was found to be  $18.8$ ,  $97.0$ ,  $27.6\text{ mg m}^{-2}$  for presouthwest, southwest and northeast monsoon respectively. Whereas the average depth integrated primary productivity for the above mentioned three seasons were  $1.05$ ,  $0.55$  and  $0.44\text{ gC m}^{-2}\text{ d}^{-1}$  for inshore waters, for the offshore waters these values were found to be less, averaging around  $0.16$ ,  $0.30$  and  $0.30\text{ gC m}^{-2}\text{ d}^{-1}$ . Apart from the above mentioned average values Gomes et al. (2000) have also reported Chl *a* and production rates as high as  $53\text{ mg m}^{-2}$  and  $4.5\text{ gC m}^{-2}\text{ d}^{-1}$  for presouthwest monsoon (March-April), which they attribute to nutrient laden cooler waters brought to the surface by poleward flowing east India coastal current. The high Chl *a* but low productivity value reported for summer monsoon has been attributed to light limitation due to intense cloud cover over BOB during this season. Madhupratap et al. (2003) have reported poor surface Chl *a* in open ocean ( $0.06\text{-}0.28\text{ mg m}^{-3}$ ) and in the coastal region ( $0.06\text{-}0.16\text{ mg m}^{-3}$ ) of

BOB during the summer monsoon 2001. Column integrated PP has been reported between 90-220 mgC m<sup>-2</sup> d<sup>-1</sup> in the off shore stations, which lie along 88°E. Relatively higher values have been reported along shelf stations that fall in the range of 328-520 mgC m<sup>-2</sup> d<sup>-1</sup>.

#### **4.4 Chlorophyll *a*, nitrate and physical parameters during the postmonsoon (September-October) 2002**

##### **4.4.1 Chlorophyll *a***

NIO colleagues (Dr. N. Ramaiah and others) measured the Chl *a* concentration during the cruise up to 120m, regardless of the euphotic depth, which averaged around 60m. The Chl *a* integrated over 120m water column varied from a maximum of 23.3 mg m<sup>-2</sup> at PP1 to a minimum of 8.65mg m<sup>-2</sup> at PP9 (Figure 4.6-left panel). No significant difference has been observed when Chl *a* was integrated up to euphotic depth (20.9mg m<sup>-2</sup> at PP1 and remains the same at PP9), implying the presence of significant portion of Chl *a* within the euphotic zone. Overall the average Chl *a* is 15.2(± 4.3) mg m<sup>-2</sup> for the region during the study period that reduces to 13(±3.5) mg m<sup>-2</sup> when integrated only over the euphotic depth. There is no significant difference between offshore (PP1-PP4) and shelf (PP5-PP9) stations and average around 16.7(±4.4) and 14(±4.4) mgm<sup>-2</sup> and reduce to 14.1(±4.6) and 12.1(±2.7) mg m<sup>-2</sup> respectively after column integration only upto the euphotic depth. The depth profiles of Chl *a* (Figure 4.6-right panel) at different stations show typical subsurface Chl *a* maxima varying between 10 and 60m. Chl *a* profile at PP1 suggests two subsurface Chl *a* maxima at 10 and 40m with a value 0.42 mg m<sup>-3</sup> that decreases to less than 0.08mg m<sup>-3</sup> below 60m. PP2 shows Chl *a* maxima at 60m with value half that of maximum at PP1 (0.21mg m<sup>-3</sup>), it decreases to less than 0.1mg m<sup>-3</sup> after 80m. PP3 shows a broad peak between 10 and 20m whereas PP4 has peak at 40m. The maximum Chl *a* at these two stations are the same (0.28mg m<sup>-3</sup>), that drops to less than 0.1mg m<sup>-3</sup> after 60m. PP5, PP7 and PP8 show Chl *a* maxima at 40m with increasing concentrations of 0.24, 0.35 and 0.43 mg m<sup>-3</sup> respectively. PP5 and PP7 show a drastic decrease in the concentration from 40 to 60m (<0.04mg m<sup>-3</sup>) whereas PP8 shows a concentration less than 0.1 mg m<sup>-3</sup> only after 80m. PP6 is the only station that has a maximum Chl *a* at surface (0.77mg m<sup>-3</sup>) with maximum concentration observed for any depth during study period. It could be visually observed that at this station the surface water was green, unlike other stations.

However, the concentration decreases sharply at 10m ( $0.25 \text{ mg m}^{-3}$ ) and reaches less than  $0.1 \text{ mg m}^{-3}$  at 60m.

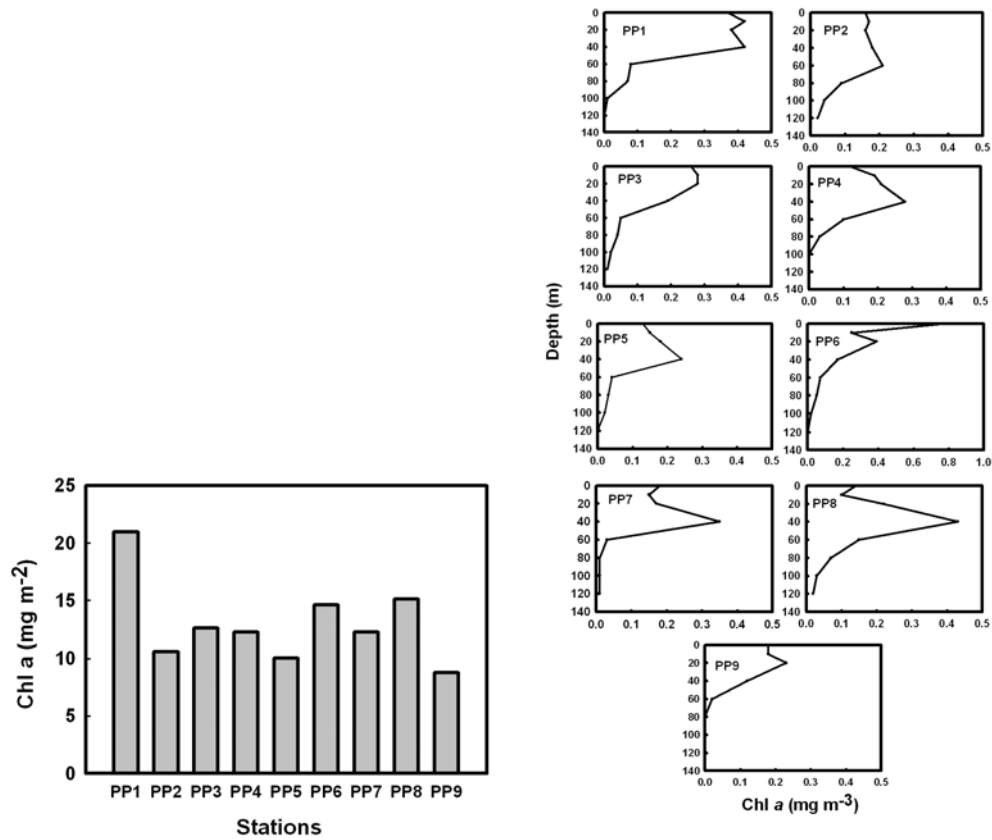


**Figure 4.6** Euphotic zone integrated (left) and vertical profiles of Chl *a* at different productivity stations (right) in the Bay of Bengal during postmonsoon (SK-182).

#### 4.4.2. Nitrate

Euphotic zone integrated nitrate concentration (Figure 4.7-left panel) during the study period for the region averaged around  $340 \text{ mmol m}^{-2}$  with a wide variation from minimum of  $\sim 46 \text{ mmol m}^{-2}$  at PP6 to maximum of  $\sim 625 \text{ mmol m}^{-2}$  at PP9, both shelf stations. The average euphotic zone nitrate concentrations at offshore and shelf stations are 261 and  $402 \text{ mmol m}^{-2}$  respectively. However, the variations within the offshore ( $60 \text{ mmol m}^{-2}$  at PP3 to  $572 \text{ mmol m}^{-2}$  at PP4) and shelf stations ( $46 \text{ mmol m}^{-2}$  at PP6 to  $625 \text{ mmol m}^{-2}$  at PP9) are quite large. Depth profiles of nitrate (Figure 4.7-right panel) at different stations suggest the top 20m to be almost devoid of nitrate. However, the nitrate concentration increases drastically between 20 and 60m depending upon the location. PP1 shows  $< 0.2 \mu\text{M}$  for top 20m but increases to  $9.61 \mu\text{M}$  at 40m and  $13.86 \mu\text{M}$  at 60m. The nitrate concentrations at PP2 and PP3 are below detection limit for the top 10m and 40m respectively, and increase gradually at PP2 ( $0.2$  and  $1.27 \mu\text{M}$

at 20 and 40m respectively) and drastically at PP3 ( $5.58\mu\text{M}$  at 60m). Again at PP4 nitrate is below detection limit in the top 10m but increases to  $5.89$  and  $21.16\mu\text{M}$  at 20 and 60m. The nitrate at shelf locations (PP5 to PP9) is always more than detection limit even in the surface waters. Interestingly, at all shelf locations (except at PP6) the nitrate in the top 20m is always less than  $1.13\mu\text{M}$  but increases sharply from 20 to 40m ( $14.82$ ,  $16.73$ ,  $5.36$  and  $21.09\mu\text{M}$  at PP5, PP7, PP8 and PP9 respectively). These increased concentrations at depths lead to a higher column nitrate in the euphotic zone. At PP6 the increase in nitrate concentration is gradual to reach to  $7.35\mu\text{M}$  at 60m.

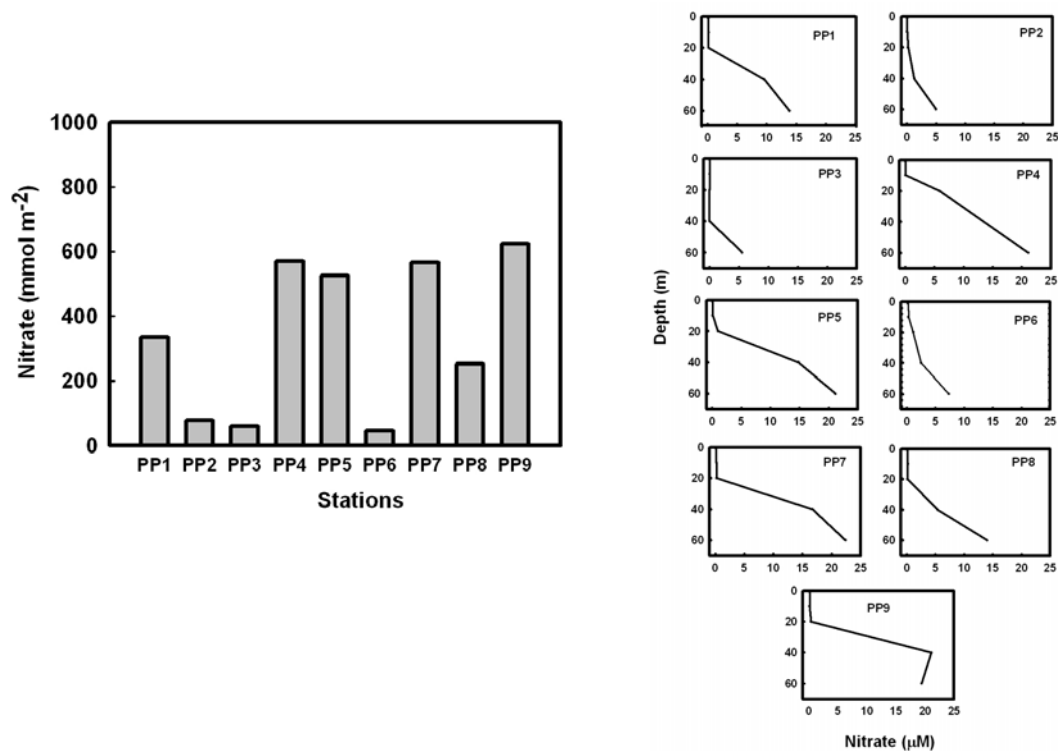


**Figure 4.7** Euphotic zone integrated (left) and vertical profiles of nitrate at different productivity stations (right) in the Bay of Bengal during postmonsoon (SK-182).

#### 4.4.3 Hydrographic and meteorological conditions

As mentioned earlier, freshwater input causes a significant spatial variation in the salinity of the surface Bay during and after the monsoon (Figure 4.8-top left). The salinity during the study period varies from 20.92 psu at PP7 (Stn.18, a shelf station) to 34.59 psu at PP1 (Stn. 3, an offshore station). The salinity for the offshore locations decreases from south to north from a maximum of 34.59 psu at PP1 (Stn.3) to a minimum of 28.40 psu at the northern Stn. 13. Shelf stations show wide variation from a maximum of 33.92 psu at the southern part (Stn. 23) to a minimum of 20.92 at PP7

(Stn. 18). The salinity structure of the Bay during the study period clearly indicates the terrestrial influence (i.e., fresh water) on shelf stations and the northernmost offshore stations. Sea surface temperature (Figure 4.8-top right) along the offshore varies marginally from 28.2 (Stn. 2 and Stn. 3) to 29°C (Stn. 12) from the south to the north, whereas for shelf locations it does not show any trend and varies from 28.9 (Stn. 14) to 30.1°C (Stn. 19). The mixed layer depths (MLD) for the study period show a wide variation from a maximum of 64m at Stn.5 to a minimum of 2m at Stn. 17 (Figure 4.8-bottom left). Freshwater stratifies the surface layer leading to low MLD at stations

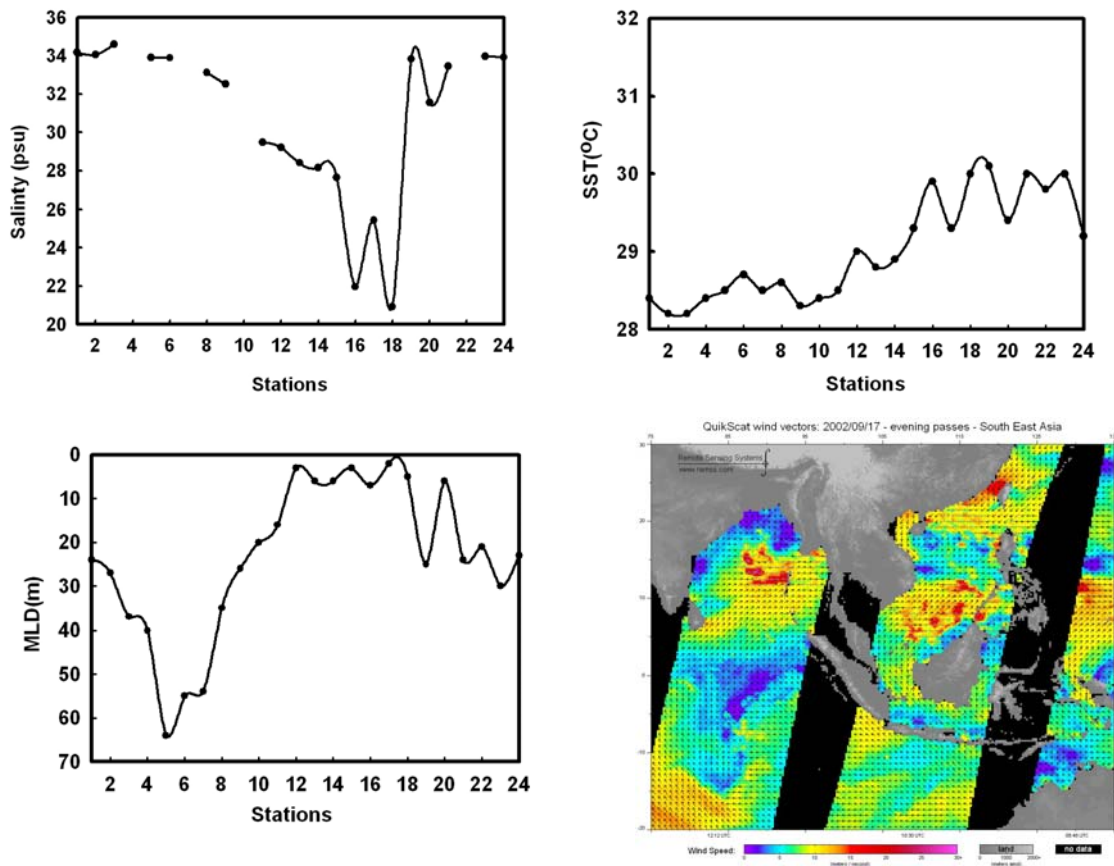


**Figure 4.8** The spatial distribution of salinity (top left), SST (top right), MLD (bottom left) and typical wind speed (17<sup>th</sup> Sep 2002, bottom right) during (SK-182).

with low salinity. The MLD for offshore stations increases from Stn.1 (24m) to Stn 5 (64m) but starts decreasing further northward and shoals up to 3 and 6m at Stn. 12. and Stn.13 respectively. MLD at the northern shelf stations (Stn. 14 to Stn. 20) is less than 10m except at Stn. 19 (25m) and increases southward to reach between 20 and 30m. Bay of Bengal is known for frequent cyclonic activity during the postmonsoon season (Sep-Dec.) that is understood to be one of the predominant factors that bring nutrients from deeper to the surface Bay by churning the ocean. Data from Indian

Meteorological department shows that 25 and 15% of the total cyclones in the BOB occur during September-October and April-May respectively (Das 1995). However, no specific cyclone was encountered during the study period but wind with relatively higher speed was prevalent in the area during the beginning of the study (Figure 4.8-bottom right).

## 4.5 $^{15}\text{N}$ based productivity study during postmonsoon 2002

### 4.5.1 Total Production

Total productivity during the present study has been estimated as the sum of nitrate uptake rate and conservative estimates of ammonium and urea uptake rates. Overall, the total productivity varies almost an order of magnitude with a maximum value of  $10.99 \text{ mmolN m}^{-2} \text{ d}^{-1}$  ( $\sim 873 \text{ mgC m}^{-2} \text{ d}^{-1}$ ) at PP2, an offshore station to  $1.17 \text{ mmolN m}^{-2} \text{ d}^{-1}$  ( $\sim 93 \text{ mgC m}^{-2} \text{ d}^{-1}$ ) at the southernmost shelf station, PP9 (Figure 4.9-left panel). The average total production for the study region is  $4 (\pm 3.14) \text{ mmolNm}^{-2} \text{ d}^{-1}$  ( $\sim 318 \text{ mgC m}^{-2} \text{ d}^{-1}$ ). The total production based on  $^{14}\text{C}$  technique observed during the same cruise had a similar average value of around  $300 \text{ mgC m}^{-2} \text{ d}^{-1}$ . However, these values are greater than the average values reported for the summer monsoon 2001 (Madhupratap

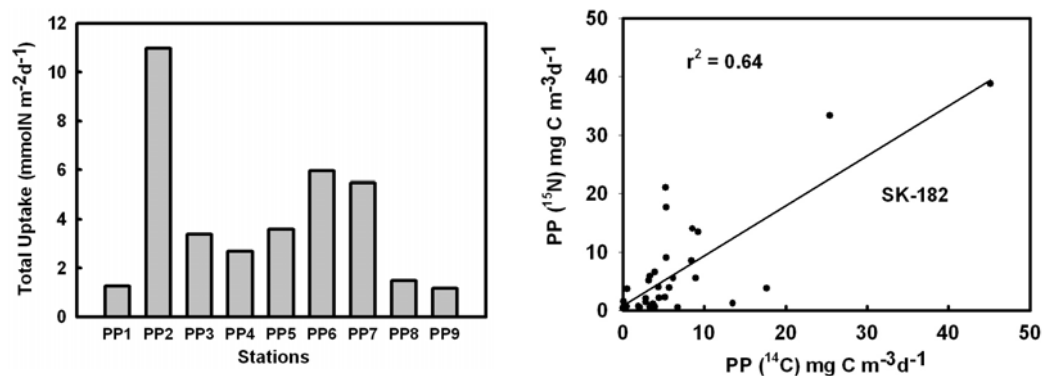


**Figure 4.9** The euphotic zone integrated total column productivity (left) and relationship with  $^{14}\text{C}$  based productivity (right), during postmonsoon 2002 (SK-182).

et al. 2003). The offshore locations average around  $4.58 (\pm 4.36) \text{ mmolN m}^{-2} \text{ d}^{-1}$  ( $\sim 364 \text{ mgC m}^{-2} \text{ d}^{-1}$ ) whereas shelf locations average around  $3.54 (\pm 2.21) \text{ mmolN m}^{-2} \text{ d}^{-1}$  ( $\sim 280 \text{ mgC m}^{-2} \text{ d}^{-1}$ ). The biomass-normalised productivity (P/B) has been obtained by dividing the productivity ( $\text{mgC m}^{-3} \text{ h}^{-1}$ ) with the measured Chl ( $\text{mg m}^{-3}$ ) at discrete depths at all the stations and it averages around  $2.4 (\pm 3.3) \text{ h}^{-1}$ . A similar exercise performed with simultaneous  $^{14}\text{C}$  based productivity measurements by NIO scientists yields an average

value quite similar ( $2.2 \pm 2.3 \text{ h}^{-1}$ ) to the  $^{15}\text{N}$  based measurements. The maximum value in both the cases has been found at the surface of PP7, where it is  $15.2$  and  $11.8 \text{ h}^{-1}$  using the  $^{15}\text{N}$  and  $^{14}\text{C}$  methods respectively. The depth wise  $^{14}\text{C}$  (denoted by  $x$ ) and  $^{15}\text{N}$  (denoted by  $y$ ) based total productivity values are well correlated:  $y = 0.85x + 0.82$ , with linear correlation coefficient of  $0.80$ , significant at  $0.005$  level ( $n = 34$ ) (Figure 4.9-right panel). The slope of  $0.85$  implies that on an average the  $^{15}\text{N}$  based total productivity is less than that based on  $^{14}\text{C}$  by  $\sim 15\%$ . However, this could be due to the analytical uncertainties associated with both the methods and therefore the two methods during study period appear to yield consistent results.

#### 4.5.2 New Production

New production (the nitrate uptake rate) in the region during the study period averages around  $2.61 (\pm 2.77) \text{ mmolN m}^{-2} \text{ d}^{-1}$  ( $\sim 207 \text{ mgC m}^{-2} \text{ d}^{-1}$ ). It varies from a maximum of  $8.85 \text{ mmolN m}^{-2} \text{ d}^{-1}$  ( $\sim 703 \text{ mgC m}^{-2} \text{ d}^{-1}$ ) at the offshore station, PP2, to a minimum of  $0.17 \text{ mmolN m}^{-2} \text{ d}^{-1}$  ( $\sim 13 \text{ mgC m}^{-2} \text{ d}^{-1}$ ) at a southern shelf station, PP8 (Figure 4.10-left panel). The average new production for offshore stations is  $3.06 (\pm 3.89) \text{ mmolN m}^{-2} \text{ d}^{-1}$  ( $\sim 243 \text{ mgC m}^{-2} \text{ d}^{-1}$ ) mainly because of very high new production observed at PP2. The average new production reduces to  $1.13 \text{ mmolN m}^{-2} \text{ d}^{-1}$  when PP2 is omitted. The variation in the new production at shelf locations is from  $0.17$  at PP8 to  $4.48 \text{ mmolN m}^{-2} \text{ d}^{-1}$  at PP6. The new production averages around  $2.26 (\pm 1.91) \text{ mmolN m}^{-2} \text{ d}^{-1}$  ( $\sim 180 \text{ mgC m}^{-2} \text{ d}^{-1}$ ), similar to the offshore stations. Depth profiles of nitrate uptake at various locations during the study period suggest the general absence of subsurface maxima except at PP2 and PP4 where an uptake maximum has been observed at  $20\text{m}$  (Figure 4.10-right panel). Based on the maximum uptake observed at any depth, stations may be divided into two categories: first where the maximum uptake rate is less than or equal to  $0.1 \text{ mmolN m}^{-3} \text{ d}^{-1}$  and second, greater than that value. Except PP2, PP6 and PP7, all the rest fall in the first category. At PP1 the maximum uptake is at surface ( $0.01 \text{ mmolN m}^{-3} \text{ d}^{-1}$ ) and decreases with depth to reach almost one tenth of the surface value at  $60\text{m}$ . PP2 shows a maximum uptake of  $0.22 \text{ mmolN m}^{-3} \text{ d}^{-1}$  at  $20\text{m}$  that remains almost the same at  $40\text{m}$ , to decrease sharply at  $60\text{m}$  ( $0.008 \text{ mmolN m}^{-3} \text{ d}^{-1}$ ). PP3 and PP5 have maximum uptake at the surface ( $\sim 0.10 \text{ mmolN m}^{-3} \text{ d}^{-1}$ ) that decreases with depth to reach almost  $0.001 \text{ mmolN m}^{-3} \text{ d}^{-1}$  at  $40\text{m}$ . PP4 shows a maximum at  $20\text{m}$  ( $0.05 \text{ mmolN m}^{-3} \text{ d}^{-1}$ ) and decreases at  $40\text{m}$  and peaks up again at  $60\text{m}$ . PP6 and PP7 show maximum uptake values of  $0.40$  and  $0.33 \text{ mmolN m}^{-3} \text{ d}^{-1}$  respectively at the

surface, which decreases sharply at 15 and 20m respectively. The uptake rate at the surface at PP6 is the highest for any depth during the study period. The maximum uptake at PP8 (0.008 mmolN m<sup>-3</sup> d<sup>-1</sup>), which is at surface, is the lowest of all maximum values during the study period. Again, PP9 shows a maximum uptake at the surface, and decreases sharply with depth.

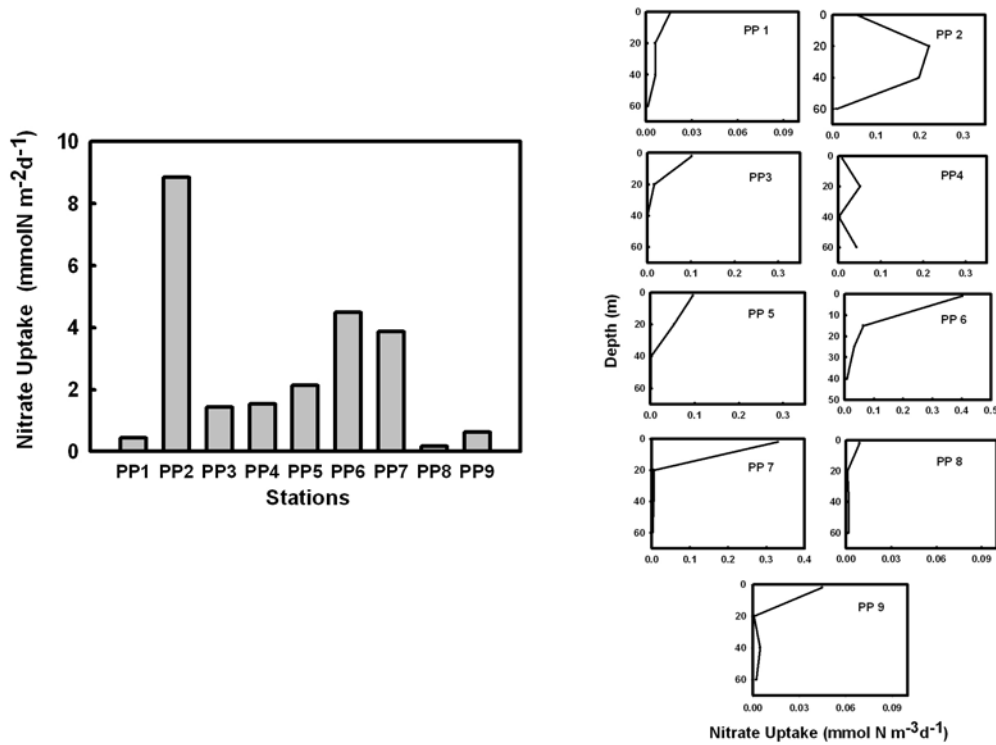


**Figure 4.10** The euphotic zone column integrated nitrate uptake (left panel) and depth profile of nitrate uptake at different stations (right panel) in the Bay of Bengal (SK-182).

The maximum uptake observed at the surface during present study agrees with the observations by Qasim (1977) and Radhakrishna (1978), that the surface productivity (1m depth) in the Bay of Bengal (4.9 tonnes carbon km<sup>-2</sup> yr<sup>-1</sup>) is greater than the Arabian Sea (3.9 tonnes carbon km<sup>-2</sup> yr<sup>-1</sup>), but reverse is the case for column productivity. The reason offered for this difference is the greater cloud cover over Bay of Bengal (Annual range ~ 4.1-5.1 oktas) compared to the Arabian Sea (Annual range ~ 1.5-3.7 oktas). They argue that the cloud cover present over the Bay attenuates the excess light intensity that would otherwise reach the sea surface and result in photoinhibition of plankton in surface water as in the Arabian Sea. Another reason cited for the higher surface production in the Bay of Bengal is significant nitrogen and phosphorus brought by runoff and rainfall into the Bay of Bengal; the runoff can dilute

the upper 25m of the Bay by 5% (Qasim 1977) without influencing the waters below this depth.

### 4.5.3 Regenerated Production

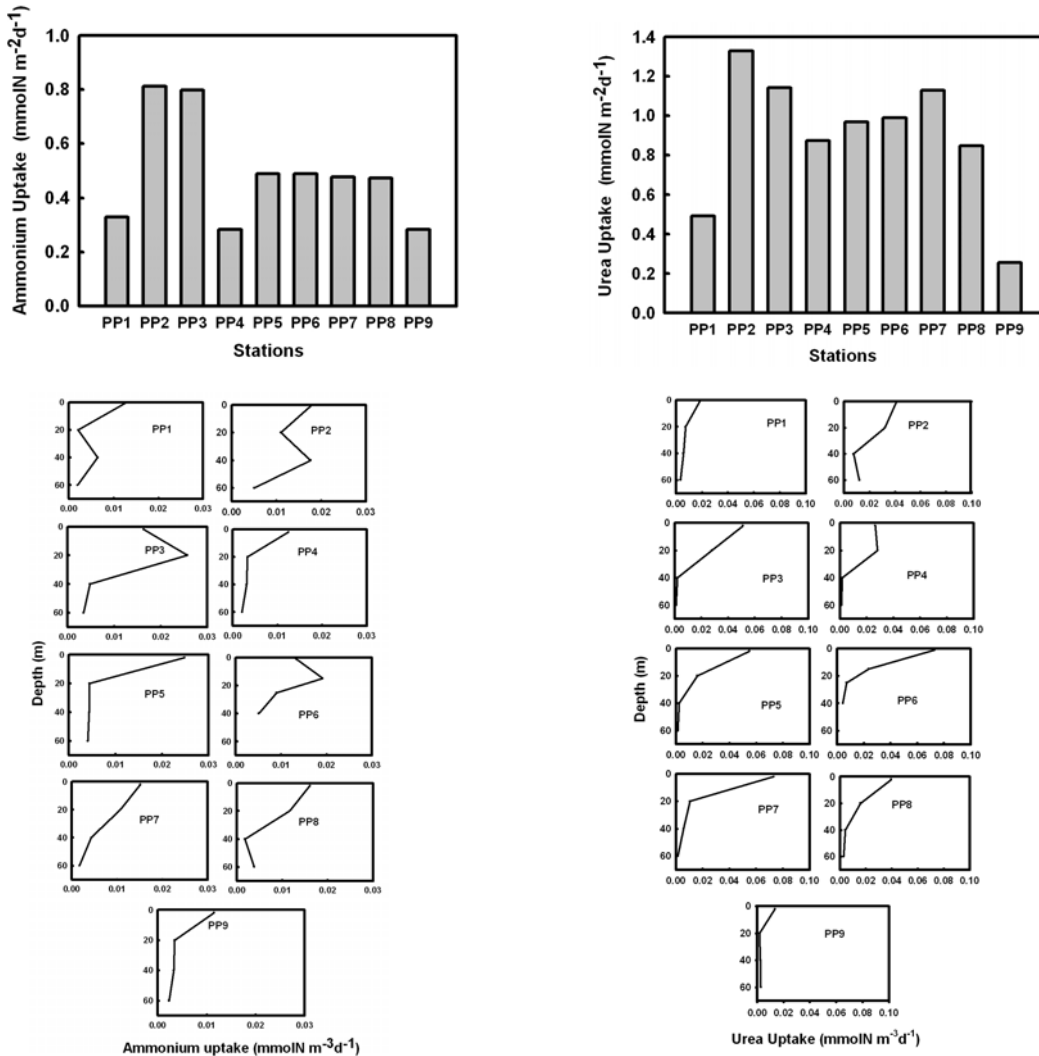


**Figure 4.11** Euphotic zone integrated column uptake of ammonium (top left) and urea (top right). Depth profiles of ammonium uptake (bottom left) and urea uptake (bottom right) are also shown for Bay of Bengal (SK-182).

As mentioned earlier the regenerated production during present study has been estimated as sum of conservative estimates of ammonium and urea uptake. This provides the lower limit of regenerated production, and can help in estimating the relative potential of ammonium and urea uptakes at different stations. Ammonium uptake during the study period is less than 1 mmolN m<sup>-2</sup>d<sup>-1</sup> and varies from 0.28 mmol N m<sup>-2</sup> d<sup>-1</sup> (~23 mgC m<sup>-2</sup>d<sup>-1</sup>) at southern shelf station PP9 to a maximum of 0.81mmol N m<sup>-2</sup> d<sup>-1</sup> (~ 64 mgCm<sup>-2</sup>d<sup>-1</sup>) at the offshore station PP2 (Figure 4.11-top left). The overall

average for the study region is  $0.49(\pm 0.20)$   $\text{mmolNm}^{-2}\text{d}^{-1}$  ( $\sim 40 \text{ mgCm}^{-2}\text{d}^{-1}$ ) with an offshore average of  $0.56(\pm 0.29)$   $\text{mmolN m}^{-2} \text{d}^{-1}$  ( $\sim 44\text{mgCm}^{-2}\text{d}^{-1}$ ) and shelf average of  $0.44(\pm 0.09)$   $\text{mmolNm}^{-2}\text{d}^{-1}$  ( $\sim 35\text{mgCm}^{-2}\text{d}^{-1}$ ). Depth profiles of ammonium uptake (Figure 4.11-bottom left) at a majority of stations (except PP3 and PP6) show a maximum uptake at the surface with the majority of values less than  $0.018\text{mmolN m}^{-3}\text{d}^{-1}$  except at PP5, where it is the maximum ( $0.024 \text{ mmolN m}^{-3}\text{d}^{-1}$ ). PP3 and PP6 are the two stations showing subsurface ammonium uptake maxima of  $0.025$  and  $0.02\text{mmolN m}^{-3}\text{d}^{-1}$  at 20 and 15m depths respectively. Urea uptake for the study period ranges from a minimum of  $0.26\text{mmol m}^{-2}\text{d}^{-1}$  at PP9 to a maximum of  $1.33 \text{ mmolN m}^{-2}\text{d}^{-1}$  at PP2 with an overall average of  $0.89 (\pm 0.33)$   $\text{mmol N m}^{-2} \text{d}^{-1}$  ( $\sim 71\text{mgCm}^{-2} \text{d}^{-1}$ ), almost twice the average ammonium uptake (Figure 4.11-top right). The offshore region averages around  $0.96 (\pm 0.36)$   $\text{mmolN m}^{-2} \text{d}^{-1}$  whereas shelf locations average around  $0.84(\pm 0.34)$   $\text{mmol N m}^{-2} \text{d}^{-1}$ . Depth profiles of urea uptake (Figure 4.11-bottom right) show a maximum at the surface at all stations unlike ammonium and nitrate where a few stations show a subsurface maximum. The maximum surface uptake ranged from  $0.07\text{mmolN m}^{-3}\text{d}^{-1}$  at PP6 and PP7 to  $0.01\text{mmolN m}^{-3}\text{d}^{-1}$  at PP9.

#### 4.5.4 f-ratio

f-ratio, estimated as the ratio of integrated nitrate uptake to total integrated uptake, provides an upper bound of f-ratio in the region. It varies from minimum of 0.11 at PP8 to maximum of 0.81 at PP2 with an overall average of  $0.54(\pm 0.22)$  (Figure 4.12-left

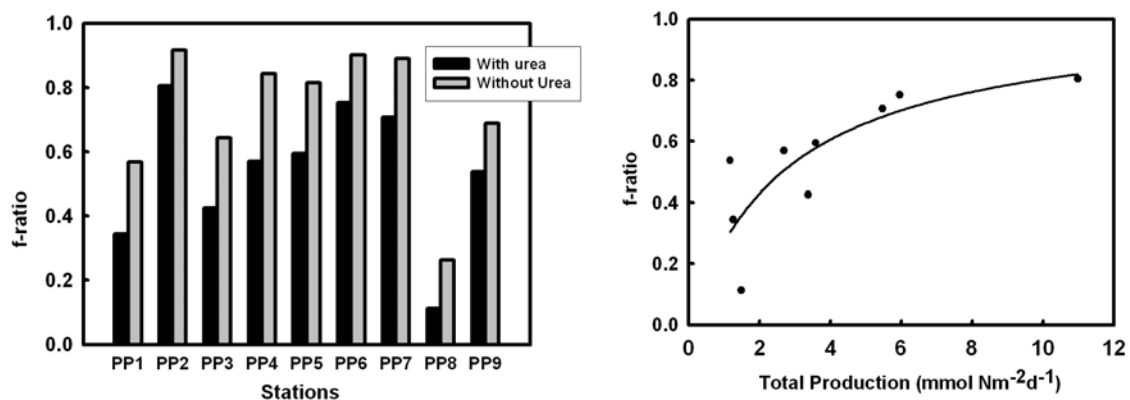


**Figure 4.12** The upper bound of f-ratio (left) and relationship between f-ratio and total production during post monsoon in the Bay of Bengal.

panel). Interestingly, the f-ratio in both the offshore and shelf locations averages around 0.54 implying that the Bay of Bengal can at best transfer about half the total production to the deep during the postmonsoon season. Exclusion of urea from the calculation of f-ratio (for the sake of comparison with some Arabian Sea estimates, where urea uptake was not measured by earlier workers) shows an average increase in f-ratio by ~ 47%. The relationship between total production and f-ratio during the study period is best represented by a hyperbola ( $f\text{-ratio} = [1.02(\pm 0.24) * \text{total production}] / [2.78(\pm 1.59) + \text{total production}]$ ) indicating a higher f-ratio for a higher total production emphasizing the substantial role played by nitrate in the total production (Figure 4.12-right panel).

## 4.6 Chlorophyll *a*, nitrate and physical parameters during the premonsoon (April-May 2003)

### 4.6.1 Chlorophyll *a*

The euphotic zone integrated Chl *a* concentration during the premonsoon in the Bay of Bengal varies from 8.65 mg m<sup>-2</sup> at the offshore station PP1, to 42.35mg m<sup>-2</sup> at a shelf station PP7 (Figure 4.13-left panel). Locations on the offshore transect show increasing integrated Chl *a* from the south to the north with maximum concentration at

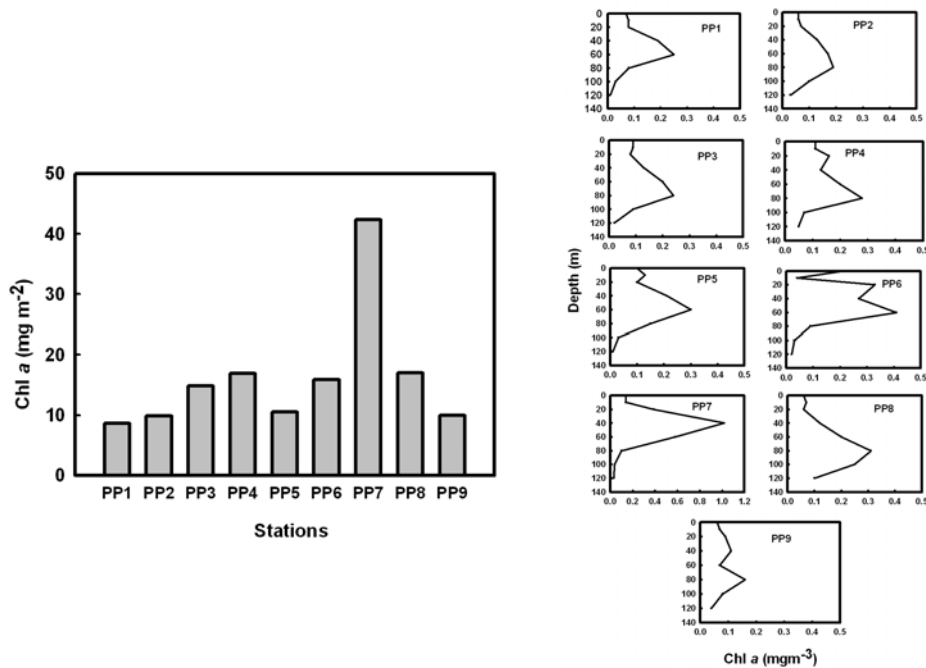


**Figure 4.13** Euphotic zone integrated (left) and vertical profiles of Chl *a* at different productivity stations during premonsoon (right) in the Bay of Bengal (SK-191).

northernmost station PP4 ( $16.95\text{mg m}^{-2}$ ). There has been a significant decrease in Chl *a* concentration at PP1 compared to the postmonsoon season ( $20.95\text{ mg m}^{-2}$ ) whereas Chl *a* at PP3, PP4 and PP5 increased during the premonsoon. Among the shelf locations the variations in Chl *a* is more than four fold with a minimum at the southernmost station, PP9 ( $9.95\text{mg m}^{-2}$ ), and a maximum at PP7. The integrated Chl *a* at PP7 is the highest observed during the study period. Almost all shelf stations show an increase in the euphotic zone integrated Chl *a* compared to the postmonsoon. Depth profiles of Chl *a* at all stations show subsurface Chl *a* maxima varying between 40 and 80m that is deeper than subsurface Chl *a* maxima observed during post monsoon (20-60m) (Figure 4.13-right panel). This may be due to relatively deeper euphotic depth ( $\sim 60\text{-}100\text{m}$ ) during premonsoon compared to postmonsoon ( $\sim 60\text{m}$ ). PP1 and PP5 show maximum Chl *a* of  $0.25$  and  $0.30\text{ mg m}^{-3}$  respectively at 60m, to decrease to  $0.01\text{ mgm}^{-3}$  at 120m. Majority of stations (PP2, PP3, PP4, PP8 and PP9) show Chl *a* maxima at 80m with values varying between  $0.31\text{mg m}^{-3}$  (PP8) and  $0.16\text{mg m}^{-3}$  (PP9). PP6 shows two subsurface Chl *a* peaks at 20 and 60m with values  $0.33$  and  $0.41\text{mg m}^{-3}$  respectively. PP7 shows peak at 40m with maximum Chl *a* for any depth during present study ( $1.02\text{mg m}^{-3}$ ).

#### 4.6.2 Nitrate

The euphotic zone integrated nitrate concentration during the premonsoon for the region shows wide variations from a minimum of  $78\text{mmol m}^{-2}$  at PP5 to maximum of  $1622\text{ mmol m}^{-2}$  at PP7, both being shelf stations. PP6 and PP8 show relatively moderate concentrations of  $153$  and  $113\text{ mmol m}^{-2}$  whereas PP9 has nitrate concentration as high as  $490\text{mmol m}^{-2}$  (Figure 4.14-left panel). Among the offshore stations, PP3 shows the highest nitrate concentration of  $625.5\text{ mmol m}^{-2}$  whereas PP1 has the minimum concentration of  $189\text{ mmol m}^{-2}$ . Comparison with the postmonsoon data indicates a decrease in the euphotic zone integrated nitrate at two offshore locations (PP1 and PP4), and increase at another two (PP2 and PP3). Nitrate concentrations at shelf locations, except PP7, normally show a decrease compared to postmonsoon. Depth profiles of nitrate during premonsoon suggest that the nitrate level has never declined below the detection limit in the surface layer, a case which was frequent at offshore locations during postmonsoon (Figure 4.14-right panel). The

nitrate concentration, in general, has always been more than  $0.2\mu\text{M}$  in the top 40m at any location in the study region and starts increasing thereafter. Another difference

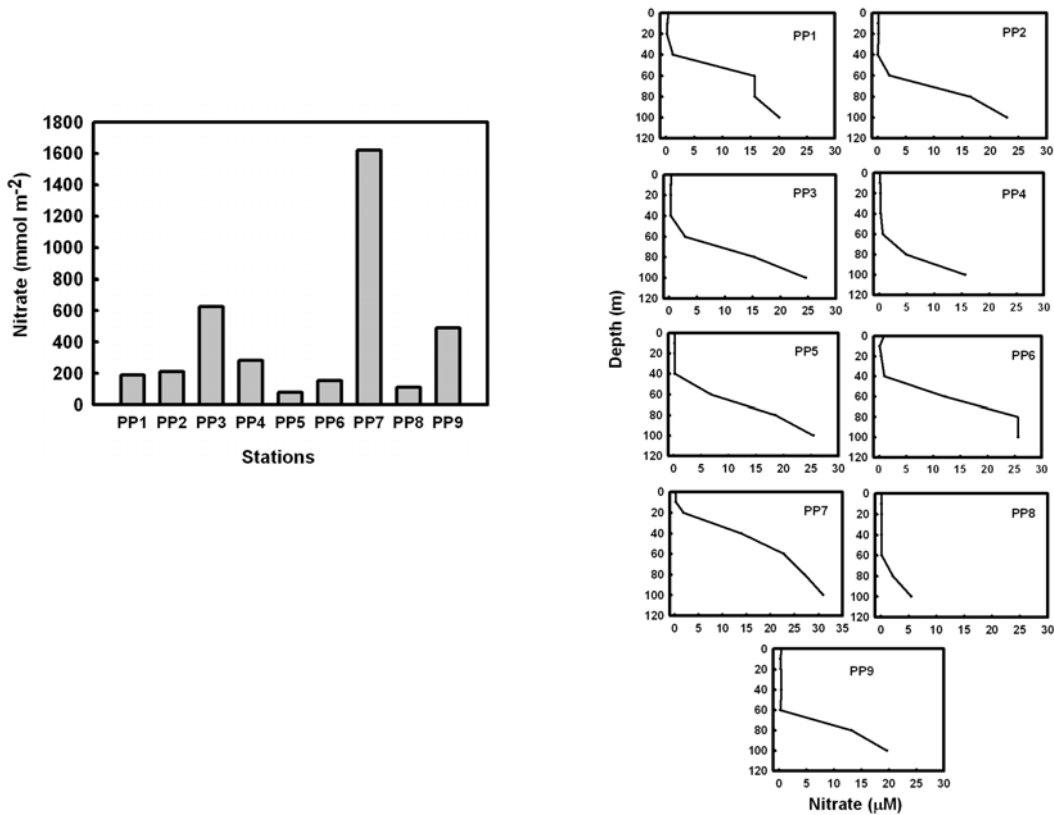


**Figure 4.14** Euphotic zone integrated (left) and vertical profiles of nitrate at different productivity stations (right) during premonsoon in the Bay of Bengal (SK-191).

between post and premonsoon nitrate profile is the change in nitrate concentration with depth. During postmonsoon nitrate shows a sharp increase between 10 and 40m (actual depth varying with location) whereas during the premonsoon it seems to occur between 40 and 60m, except at PP7 where it shows an increase after 10m only. The reason for relatively higher euphotic zone integrated nitrate at most of the stations during postmonsoon is the higher concentration at 40 and 60m depth despite the absence or less concentration at the top. However, during premonsoon nitrate is present throughout the euphotic zone but not as high as postmonsoon values at 40 and 60m.

#### 4.6.3 Hydrographic and meteorological Conditions

The hydrographic and meteorological conditions of the Bay of Bengal during premonsoon are different from those during postmonsoon. The main difference is in terms of reduced freshwater influx from the rivers and is evident from the difference in

the observed surface salinity variation during the two seasons. Overall, salinity varies in a narrow range of 34.23 psu at Stn. 21 to 32.47 psu at Stn. 10 compared to wide variation of 34.59 to 20.92 psu during postmonsoon (Figure 4.15-top left). The northern offshore locations (Stn.11 to Stn.13) where salinity was less than 30psu (28.40-29.47psu) during postmonsoon has reached more than 32.89psu (32.89-33.33psu) during premonsoon. The shelf stations (Stn.14 to Stn.18) showing very low salinity during the postmonsoon (28.15-20.92 psu) exhibit salinity as high as 32.94-33.84 psu. However, the southern shelf (Stn19-Stn.23) as well as offshore stations (Stn1-Stn.9) do not show much change in salinity. In fact, the southernmost offshore stations are more saline (by up to 1.6 psu) during postmonsoon than premonsoon.

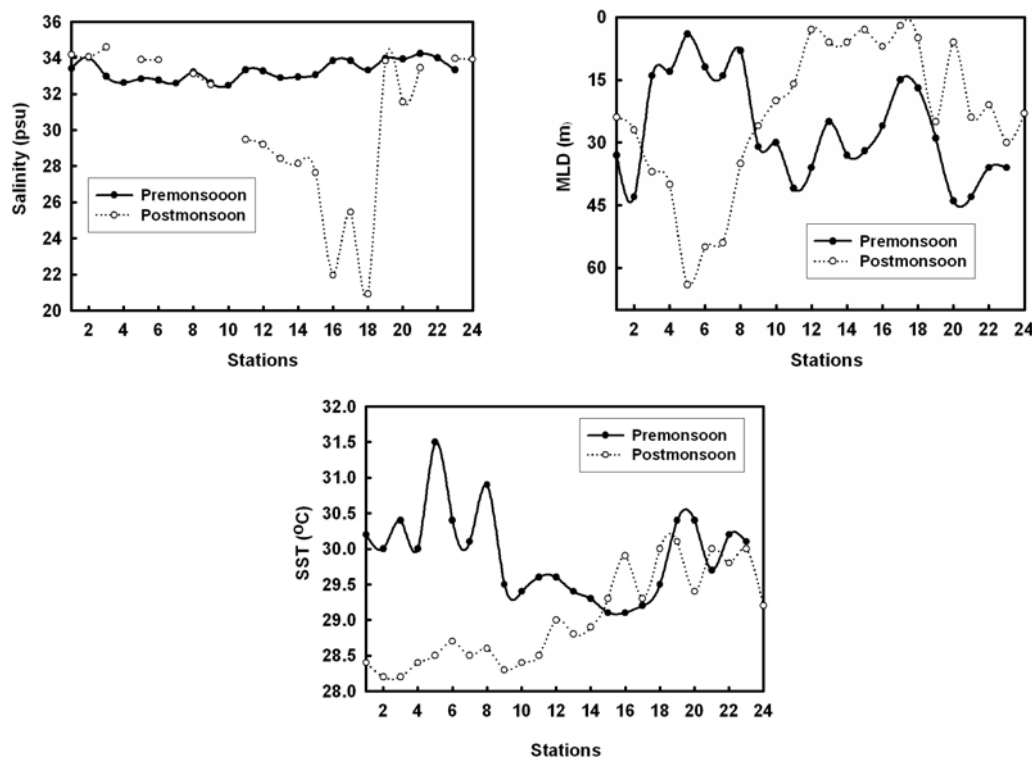


**Figure 4.15** Comparison of Salinity (top left), MLD (top right) and SST (bottom) during pre and postmonsoon in the Bay of Bengal.

The rise in salinity from postmonsoon to premonsoon is a direct manifestation of the decrease in river runoff and hence the terrestrial influence. This rise in salinity (~ density) leads to a reduction in the stratification of the surface, evident from the increased mixed layer depths (MLD) at stations normally influenced by riverine discharge. MLD of 2-7m (Stn.12-Stn.18) during postmonsoon deepened to more than 25m (Stn. 12-Stn.16) and 15m (Stn.17 and Stn.18) during the premonsoon (Figure

4.15-top right). Overall, MLD during the premonsoon varies from 4m at the offshore stn. 5 to 44m at the shelf Stn. 20. The first two offshore stations show relatively deeper MLD of 33 and 43m respectively to shoal up to 4m at Stn.5. This deepens northward to reach 8m at Stn.8. From Stn. 9 onwards MLD is always more than 25m except at Stn 17 and Stn. 18 where it shoals up to nearly 15m. However, the comparison of MLD for the two seasons shows the reversal of pattern for offshore and shelf locations. In general, the MLD during postmonsoon was deeper for offshore ocean and shallower for shelf locations that has reversed during premonsoon. Overall the variation in SST during premonsoon is from 31.5°C at Stn.5 to 29.1°C at Stn. 15 and 16 (Figure 4.15-bottom). SST during premonsoon is more by 1-3°C than postmonsoon at offshore locations whereas shelf locations fall in a similar range during both the seasons (within  $\pm 1^\circ\text{C}$ ).

## **4.7 $^{15}\text{N}$ based productivity study during premonsoon 2003**

### **4.7.1 Total Production**

In general, total productivity during the premonsoon is higher than the postmonsoon. It varies from 1.93mmolNm<sup>-2</sup>d<sup>-1</sup> (~154 mgC m<sup>-2</sup>d<sup>-1</sup>) at an offshore station PP1 to 12.27 mmolNm<sup>-2</sup>d<sup>-1</sup> (~975 mgCm<sup>-2</sup>d<sup>-1</sup>) at the shelf station PP6 (Figure 4.16-left panel). Overall, it averages around 7.23( $\pm 4.17$ )mmolNm<sup>-2</sup>d<sup>-1</sup> (~575 mgC m<sup>-2</sup>d<sup>-1</sup>) for the study region against the 4mmolNm<sup>-2</sup> d<sup>-1</sup> during the postmonsoon. The total productivity for both the offshore and shelf transects have increased from the post to the premonsoon. In the offshore transect total productivity varies from a minimum at PP1 to a maximum of 11.17mmolNm<sup>-2</sup> d<sup>-1</sup> at PP4 with an average of 5.33( $\pm 4.08$ ) mmolNm<sup>-2</sup> d<sup>-1</sup> (~424 mgC m<sup>-2</sup>d<sup>-1</sup>). Shelf locations show variations from 3.56 mmolNm<sup>-2</sup>d<sup>-1</sup> at PP5 to a maximum at PP6 averaging around 8.75( $\pm 3.97$ ) mmolNm<sup>-2</sup>d<sup>-1</sup> (696 mgCm<sup>-2</sup>d<sup>-1</sup>). One important difference between the post and the premonsoon is the higher average productivity for the offshore transect than the shelf transect observed during postmonsoon has reversed during premonsoon, probably indicating the shift in the availability of nutrients. Productivity measurements performed using the <sup>14</sup>C technique during the same cruise yields an average value around 300mgC m<sup>-2</sup>d<sup>-1</sup>, significantly less than that obtained using <sup>15</sup>N technique. The main difference between results obtained using two techniques during present study has been found at one offshore location (PP4) and two shelf locations (PP8 and PP9) where total productivity obtained

by  $^{14}\text{C}$  is significantly lower than that by the  $^{15}\text{N}$  technique. Significant differences in the results obtained using the two techniques has also been observed in the Arabian Sea (Watts and Owens 1999). The productivity normalised to biomass (P/B) obtained during present study is higher than that for the postmonsoon possibly due to optimum light conditions. The average value during present study is  $4.5\text{h}^{-1}$  compared to  $2.4\text{h}^{-1}$  during postmonsoon with maximum value of  $13.7\text{h}^{-1}$  in the subsurface waters of PP9. The relationship of the productivity values observed at discrete depths using  $^{14}\text{C}$  (x) and  $^{15}\text{N}$  (y) techniques ( $y = 0.94x + 3.64$ ) has deteriorated ( $n = 54$ ; linear correlation coefficient  $r = 0.36$ ) compared to the postmonsoon (Figure 4.16-right panel). The  $^{14}\text{C}$  based results are preliminary and need to be re-checked.

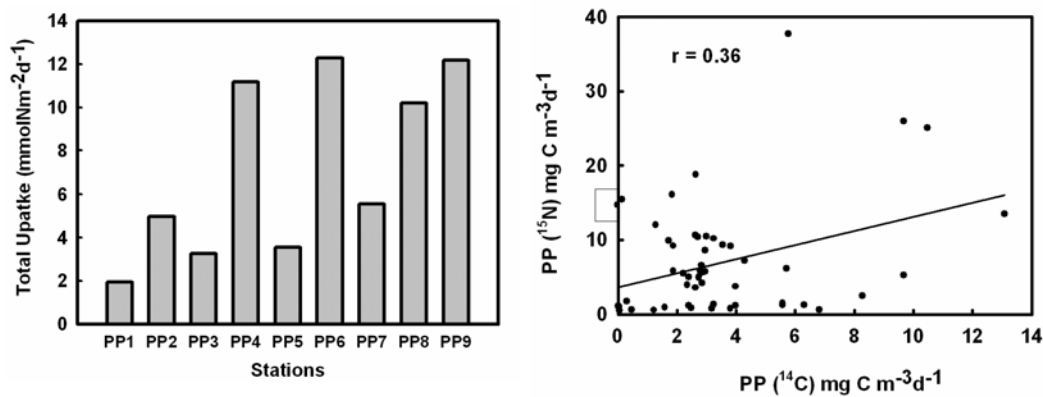


**Figure 4.16** The euphotic zone integrated total column productivity (left) and relationship with  $^{14}\text{C}$  based productivity (right) during the premonsoon.

#### 4.7.2 New Production

As in the case of total productivity, new production during the premonsoon was also higher than that in the postmonsoon and ranged from a minimum of  $0.98\text{mmolNm}^{-2}\text{d}^{-1}$  ( $\sim 78\text{mgCm}^{-2}\text{d}^{-1}$ ) at an offshore station PP1 to  $10.67\text{mmolNm}^{-2}\text{d}^{-1}$  ( $\sim 849\text{mgCm}^{-2}\text{d}^{-1}$ ) at PP6, a shelf station. Overall, new production for the region during the premonsoon averages around  $5.44(\pm 3.66)\text{mmolNm}^{-2}\text{d}^{-1}$  ( $\sim 433\text{mgCm}^{-2}\text{d}^{-1}$ ), that is almost twice the average value observed during the postmonsoon ( $2.61\text{mmolNm}^{-2}\text{d}^{-1}$ ) (Figure 4.17-left panel). The variation at offshore locations is from as low as  $0.98\text{mmolNm}^{-2}\text{d}^{-1}$  at the southernmost PP1 to  $8.46\text{mmolNm}^{-2}\text{d}^{-1}$  at the northernmost PP4 with an average of  $3.57(\pm 3.39)\text{mmolNm}^{-2}\text{d}^{-1}$  ( $\sim 284\text{mgCm}^{-2}\text{d}^{-1}$ ). The difference between the average new production for the offshore transects during the two seasons is not significant (premonsoon higher only by  $0.5\text{mmolNm}^{-2}\text{d}^{-1}$ ). The shelf locations show variations

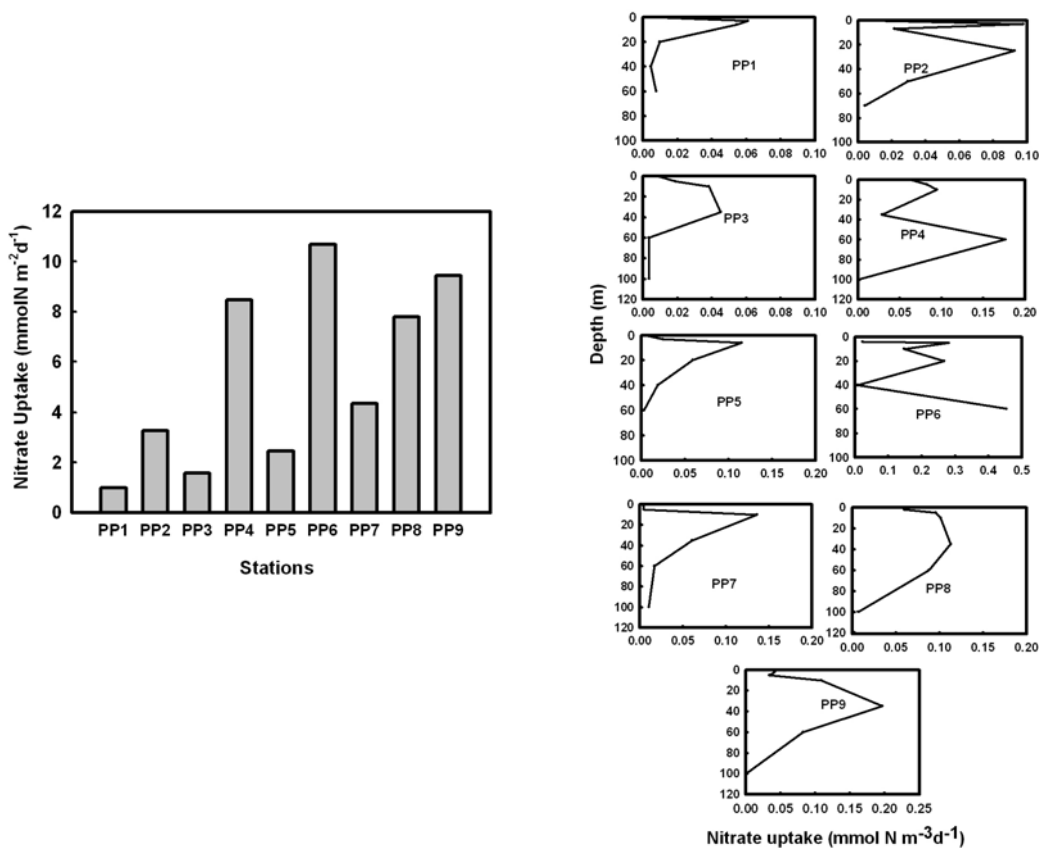


**Figure 4.17** The euphotic zone column integrated nitrate uptake (left panel) and depth profiles of nitrate uptake at different stations (right panel) during premonsoon in the Bay of Bengal (SK-191).

from  $2.46 \text{ mmolN m}^{-2}\text{d}^{-1}$  at PP5 to  $10.67 \text{ mmolN m}^{-2}\text{d}^{-1}$  at PP6 with an average of  $6.94 \text{ mmolN m}^{-2}\text{d}^{-1}$  ( $\sim 552\text{mgCm}^{-2}\text{d}^{-1}$ ). Average values of the shelf transect exhibit new production during the premonsoon to be thrice that of the postmonsoon indicating an increased rate of supply and more efficient use of nitrate during the premonsoon season. The presence of nitrate throughout the water column and increased P/B during premonsoon may be the reasons for this increased new production. In general, the depth profiles of nitrate uptake for the premonsoon is also different from those of postmonsoon, where the maximum uptake was at the surface. The nitrate uptake profiles during the premonsoon show subsurface uptake maxima at all the stations indicating the photoinhibition at surface Bay as suggested by Qasim (1977) and Radhakrishna et al. (1978) for the surface Arabian Sea (Figure 4.17-right panel). Although the euphotic depth during the study was between 60-100m the subsurface uptake maxima occur between 3 and 60m. Three out of four offshore stations (except PP4) fall in the category where maximum uptake is less than  $0.10\text{mmolN m}^{-3}\text{d}^{-1}$ . All

shelf stations have uptake maxima of more than  $0.10 \text{ mmolN m}^{-3}\text{d}^{-1}$ . PP1, PP5 and PP7 are the stations where uptake maxima lie in the top 10m (3, 6 and 10m, respectively) with values 0.06, 0.11, and  $0.13 \text{ mmolN m}^{-3}\text{d}^{-1}$  respectively, and the uptake does not cease completely at the euphotic depth. PP2, PP4 and PP6 are the stations that show more than one subsurface maximum. PP2 shows uptake maxima at 3 and 25m with values  $0.09\text{mmolN m}^{-3}\text{d}^{-1}$ . PP4 shows uptake maxima at 10 and 60m with values 0.09 and  $0.17\text{mmolN m}^{-3}\text{d}^{-1}$  and decreases sharply to cease at 100m. PP6 shows the maximum value at the base of the euphotic zone ( $0.45\text{mmolN m}^{-3}\text{d}^{-1}$ ), that is the maximum for any depth during the study period. The Chl *a* concentration at that depth is also maximum ( $0.41\text{mgm}^{-3}$ ). Apart from this, PP6 also has two peaks at 5 and 20m ( $0.28\text{mmol N m}^{-3}\text{d}^{-1}$ ). PP3, PP8 and PP9 show uptake maxima at 35m with values 0.04, 0.11 and  $0.19\text{mmolN m}^{-3}\text{d}^{-1}$ . The uptake during postmonsoon was almost negligible below 40m (20m at some) at most of the stations whereas significant uptake was observed between 40 and 100m at most of the stations during premonsoon. This might be one of the reasons for higher column new production during the postmonsoon.

#### 4.7.3 Regenerated Production

Sum of the conservative estimates of ammonium and urea uptake rates has been considered as regenerated production, as during the postmonsoon. Compared to the postmonsoon, there is an increase in the ammonium component of the regenerated production whereas the urea component has decreased slightly. Ammonium uptake varies from a minimum of  $0.67\text{mmolN m}^{-2}\text{d}^{-1}$  at PP1 to a maximum of  $1.80\text{mmolN m}^{-2}\text{d}^{-1}$  at PP4, both offshore stations (Figure 4.18-top left). Overall, the ammonium uptake averages around  $1.18(\pm 0.39) \text{ mmolN m}^{-2}\text{d}^{-1}$  ( $\sim 94\text{mgC m}^{-2}\text{d}^{-1}$ ) compared to  $0.49(\pm 0.20) \text{ mmolN m}^{-2}\text{d}^{-1}$  during the postmonsoon. The offshore stations average around  $1.11(\pm 0.48) \text{ mmolN m}^{-2}\text{d}^{-1}$  ( $\sim 88 \text{ mgCm}^{-2}\text{d}^{-1}$ ) whereas shelf locations average around  $1.24(\pm 0.34) \text{ mmolN m}^{-2}\text{d}^{-1}$  ( $\sim 99\text{mgCm}^{-2}\text{d}^{-1}$ ). Depth profiles of ammonium uptake are similar to those of nitrate uptake (Figure 4.18-bottom left). They also show a subsurface uptake maximum that shifts between 3 and 35m depending on the location. However, the uptake rate never exceeds  $0.034\text{mmol Nm}^{-3}\text{d}^{-1}$  for any depth at any station. PP1 shows maximum at 20m ( $0.025\text{mmol Nm}^{-3}\text{d}^{-1}$ ), to drop sharply at 40m. PP5 also has a maximum at 20m ( $0.027\text{mmol Nm}^{-3}\text{d}^{-1}$ ) but also shows another similar peak at 3m. PP3, PP4 and PP7 have maximum uptakes at 10m ( $0.022, 0.028$  and  $0.021$

mmol Nm<sup>-3</sup>d<sup>-1</sup> respectively) and decrease downwards. However, the uptake rates at these stations do not cease completely even at the bottom of euphotic zone. PP2 has a prominent peak at 25m (0.022 mmolNm<sup>-3</sup>d<sup>-1</sup>). Both PP8 and PP9 have a maximum uptake rate of ~0.025 mmol Nm<sup>-3</sup>d<sup>-1</sup> at 35m. Urea uptake during the study period for the region averages around 0.60(±0.32) mmolN m<sup>-2</sup>d<sup>-1</sup> that is slightly less than the premonsoon value of 0.89 mmolN m<sup>-2</sup>d<sup>-1</sup> (Figure 4.18- top right). The offshore

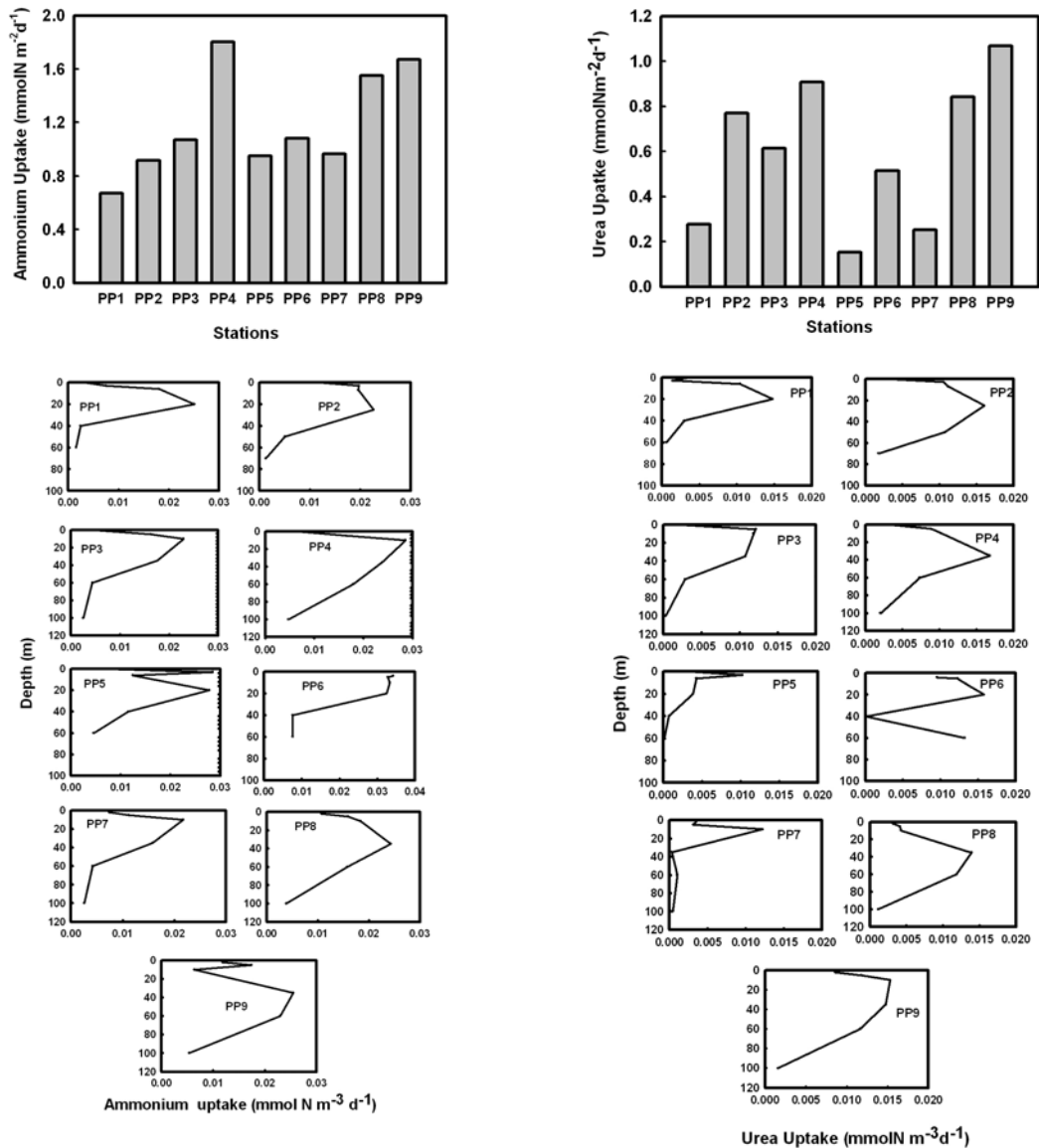


**Figure 4.18** Euphotic zone integrated column uptake of ammonium (top left) and urea (top right) during premonsoon. Depth profiles of ammonium uptake (bottom left) and urea uptake (bottom right) during same season are also shown.

transect averages around 0.64 (±0.27) mmolN m<sup>-2</sup>d<sup>-1</sup> whereas shelf transect averages 0.56(±0.38) mmolN m<sup>-2</sup>d<sup>-1</sup>. Depth profiles of urea uptake also follow the pattern shown by nitrate and ammonium uptake (Figure 4.18-bottom right). At all the stations

subsurface uptake maxima exist between 3 and 35m and uptake rate never exceeds  $0.016\text{mmolN m}^{-3}\text{d}^{-1}$ . PP6 exhibits the pattern observed during nitrate uptake where the uptake rate peaks at the base of euphotic zone ( $\sim 60\text{m}$ ) where Chl *a* concentration is also maximum.

#### 4.7.4 f-ratio

The f-ratio during premonsoon has also been calculated as described earlier (nitrate uptake/total uptake) and hence provides the upper bound of the f-ratio at the respective stations. The estimated f-ratio during premonsoon varies from a minimum of 0.50 at PP1 to maximum of 0.87 at PP6 implying that at best 50 to 87% of the total productivity can be exported to deeper layers under steady state (Figure 4.19-left panel). However, the average f-ratio estimated for the entire region has increased to  $0.70(\pm 0.12)$  during premonsoon as compared to 0.54 during the postmonsoon. The f-ratio for offshore transect averages around  $0.60(\pm 0.12)$  whereas for the shelf transect it averages  $0.77(\pm 0.06)$ . During postmonsoon the average f-ratio for both shelf and offshore stations was same (0.54) whereas during premonsoon shelf stations have

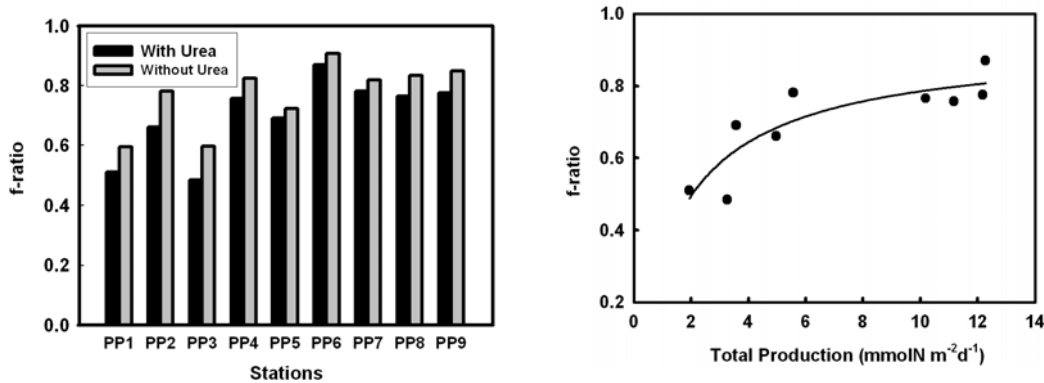


**Figure 4.19** The upper bound of f-ratio (left) and relationship between f-ratio and total production during pre monsoon in the Bay of Bengal (SK-191).

significantly higher f ratios than the offshore stations. This is mainly due to the increased column new production in the offshore transect due to the reasons discussed earlier. One important difference observed during pre and postmonsoon is the change in f-ratio when urea is excluded from the calculation. During the postmonsoon the exclusion of urea lead to an average increase in f-ratio by 47% whereas this increase was only around 11% during premonsoon. The relationship between total production

and f-ratio can be represented by hyperbola as during postmonsoon (Figure 4.19-right panel):  $f\text{-ratio} = [0.91(\pm 0.06) * \text{total production}] / [1.7(\pm 0.55) + \text{total production}]$ . This is indistinguishable from the postmonsoon relationship within the associated uncertainties. The observed hyperbolic relationship between f-ratio and total production in the Bay of Bengal can be used for estimating the fraction of total production, which has potential to sink down to the deeper layers.

#### **4.8 Implications of the new production measurements in the Bay of Bengal**

The average rate of photosynthetic fixation of carbon by marine phytoplankton (primary productivity) is more than a factor of two higher in the Arabian Sea than in the Bay of Bengal (Madhupratap et al. 2003). However, the time averaged sediment trap data indicate that on the basin scale, the downward flux of organic carbon in the Arabian Sea is not proportionately higher than that of the Bay of Bengal, except for the upwelling region in the northwestern Arabian Sea. Our experiments done in two different seasons consistently show a high new production (averaging around  $2.6 \text{ mmolN m}^{-2} \text{ d}^{-1}$  during postmonsoon and  $5.4 \text{ mmolN m}^{-2} \text{ d}^{-1}$  during premonsoon) and a linear relationship with total production (Figure 4.20); which could be one of the reasons for relatively higher downward organic carbon flux in the moderately productive Bay. Hence, such oceanic regions may play a more significant role in removing the excess anthropogenic  $\text{CO}_2$  from the atmosphere, than considered so far. The new production measurements in the Bay of Bengal during present study have helped to understand a few long standing paradoxes related to the Bay on basin scale. The following are the most important:

##### **Reason for comparable downward organic carbon fluxes in the Arabian Sea and the Bay of Bengal:**

Major international scientific programmes such as JGOFS (Joint Global Ocean Fluxes Study), aimed at assessing the role of oceans as source/sink of atmospheric carbon dioxide, concentrated mostly on highly productive regions of the oceans, e.g., Arabian Sea (Smith 2001). Intense upwelling during summer and convective mixing due to surface cooling in winter enhance the productivity of the Arabian Sea (Madhupratap et al. 1996). In contrast, the limited studies carried out for the adjacent Bay of Bengal

suggest it to be less productive because of the cloud cover and stratification of the surface layers by copious freshwater discharge from rivers draining the Indian sub-continent, inhibiting vertical mixing and the supply of nutrients from below (Prasanna Kumar et al. 2002). Although there is some seasonal and geographical variability, the typical average  $^{14}\text{C}$  based productivity in the Arabian Sea is around  $1200 \text{ mgC m}^{-2} \text{ d}^{-1}$ , (Barber et al. 2001), whereas in the Bay it is about  $300 \text{ mgC m}^{-2} \text{ d}^{-1}$  (Madhupratap et al. 2003), despite comparable numerical abundances of phytoplankton (Sawant and Madhupratap 1996). In contrast, sediment trap data from both these regions (Table 4.3) show that on an average, the annual downward flux of organic carbon in the Bay of Bengal is not significantly less than that of the Arabian Sea (Ittekkot 1991; Haake et al. 1993; Unger et al. 2003). Exceptions do exist; e.g., sediment traps placed near

**Table 4.3** Time-averaged fluxes of organic carbon ( $\text{gC.m}^{-2}\text{yr}^{-1}$ ) in sediment traps, 1000 m above sea floor (values in parentheses are from the shallow trap, 1000 m below the sea surface). Traps were distributed east-west in the Arabian Sea and north-south in the Bay of Bengal (Ittekkot 1991; Haake et al. 1993; Unger et al. 2003; Honjo et al. 1999; Lee et al. 1998).

<b>ARABIAN SEA</b>				
<b>Stations</b>	<b>Latitude (°N)</b>	<b>Longitude (°E)</b>	<b>Flux (<math>\text{gC m}^{-2}\text{y}^{-1}</math>)</b>	<b>Data averaged over (yrs)</b>
WAST	16° 20'	60° 30'	3.2	4
CAST	14° 31'	64° 46'	1.9	3
EAST	15° 31'	68° 43'	2.1	4
MS1	17° 41'	58° 51'	3.8	1
MS2	17° 24'	58° 48'	5.6	1
MS3	17° 12'	59° 36'	5.3	1
MS4	15° 20'	61° 30'	3.6	1
MS5	10° 00'	65° 00'	1.3	1
<b>BAY OF BENGAL</b>				
NBBT-N	17° 27'	89° 36'	2.86(3.11)	10
NBBT-S	15° 32'	89° 13'	2.38 (2.38)	10
CBBT	13° 09'	84° 22'	2.7 (2.6)	10
SBBT	04° 28'	87° 19'	2.27(2.5)	10

the upwelling sites by US JGOFS (particularly traps MS2 and MS3) have observed higher organic carbon fluxes (Honjo et al. 1999; Lee et al. 1998)]. The most important question was to understand the possible reasons for the comparable downward organic carbon fluxes in highly productive Arabian Sea and moderately productive Bay of Bengal. One possible explanation to this observation is the ballast hypothesis whereby

organic carbon is ballasted into the deep by the high lithogenic flux from rivers, which form aggregates with the former (Ittekkot 1991). However, the annual lithogenic flux in the Bay decreases sharply from the north to the central shallow trap ( $21.89 \text{ g m}^{-2}$  to  $9.37 \text{ g m}^{-2}$ , by 57%), whereas the organic carbon flux ( $3.59 \text{ g m}^{-2}$  to  $2.6 \text{ g m}^{-2}$ ) does not show a corresponding reduction. It decreases only by 26%. (Ittekkot et al. 1991). Further, time series data from two shallow traps in the north ( $17^\circ 27' \text{ N}$  and  $15^\circ 32' \text{ N}$ ) show that the annual lithogenic flux decreased from  $14.5$  to  $8.7 \text{ g m}^{-2}$  (by 40%), while organic matter flux decreases from  $5.6$  to  $4.3 \text{ g m}^{-2}$  (by 23%; Unger et al. 2003). However, the annual carbonate flux increases from north to south ( $12.5$  to  $13 \text{ g m}^{-2}$ ), probably compensating for decrease in lithogenic fluxes, as the possibility of other mineral matters acting as ballast have been reported (Hedges et al. 2001). However, apart from the efficient transfer mechanism there has to be the availability of organic matter to form the aggregate, particularly for southern region in the Bay, which is far from the influence of possible organic matter contribution by rivers. Independent estimates of new production based on nitrogen uptake performed during present study has helped to understand this in a better way, because, under steady state, new production is considered theoretically equal to the export production (Eppley and Peterson 1979). Eppley et al. (1983) have suggested that new production and particle sinking are coupled over longer (annual) time scales. Consistent higher new production of  $4 \text{ mmol N m}^{-2} \text{ d}^{-1}$  ( $\sim 318 \text{ mgC m}^{-2} \text{ d}^{-1}$ ) observed during two different seasons in the Bay of Bengal indicates its significant role in the observed organic carbon flux on the time scales of sediment traps data. The higher new production observed may be responsible for the higher downward flux of organic carbon in the Bay of Bengal despite moderate overhead productivity.

#### **Reason for reduced $\text{pCO}_2$ in surface Bay of Bengal:**

Despite having some seasonal sinks, the oceanic region between  $10$  and  $25^\circ \text{N}$ , in general, is considered to be a source of atmospheric  $\text{CO}_2$  (Broecker et al. 1986; Takahashi 1989). However, data on the air-sea exchange of  $\text{CO}_2$  for the northern Indian Ocean in general, and Bay of Bengal in particular, are not adequate in space and time. So far, very little data exists for the Bay (Kumar et al. 1992; George et al. 1994). The study carried out by Kumar et al. (1996) during the presouthwest monsoon and the northeast monsoon of 1991 reveals that a large area of the Bay is characterized by  $\text{pCO}_2$  levels far below the atmospheric value ( $\sim 350 \text{ } \mu\text{atm}$ ). This effect was found to be

more prominent during northeast monsoon when air-sea  $p\text{CO}_2$  gradient sometimes exceeds  $100 \mu\text{atm}$ . Kumar et al. (1996) guessed that the cause for the low  $p\text{CO}_2$  in the Bay could be physical as well as biological processes. One important physical parameter known to decrease the  $p\text{CO}_2$  level is salinity due to its effect on solubility of  $\text{CO}_2$ , dissociation constants for carbonic, boric and other weak acids and the concentration of boric acid in seawater (Takahashi et al. 1993). However, Kumar et al (1996) have shown that the salinity can lower the  $p\text{CO}_2$  to a maximum of only  $\sim 30 \mu\text{atm}$  which was about 25% of the highest recorded  $p\text{CO}_2$  drawdown and therefore surmised that biological activity should account for the rest of the observed  $p\text{CO}_2$  decrease i.e., due to moderately high new production sustained by external nutrients brought in by rivers and/or atmospheric deposition. The higher new production estimates during present study has proved the conjecture of Kumar et al. (1996) for low  $p\text{CO}_2$  in surface Bay. However, the nutrient source is probably not exactly as predicted.

#### **Contribution to the development of Oxygen Minimum Zone in the Bay:**

Oxygen Minimum Zone (OMZ) has been observed between 100-500 m in the Bay of Bengal. Its presence in ocean is usually explained by the utilization of oxygen due to decomposition of organic matter brought into the deeper water from the surface. This explanation holds good for the Arabian Sea where the overhead productivity is high and the degradation of organic matter settling down consumes dissolved oxygen, leading to the existence of OMZ and denitrification zones (Olson et al. 1993). But the existence of OMZ in the Bay of Bengal, where the overhead productivity is less is indeed puzzling. There may be two possible reasons for this. First, higher residence time of the deeper waters of the Bay due to lack of ventilation caused by presence of low density waters on the top (ventilation is also limited due to the closure of the basin by the continent in the north), leading to the constant use of sub surface oxygen by the organic matter, even if it is small in magnitude. Secondly, higher f-ratio i.e., high new production may be responsible as the fraction of organic matter going to deeper waters is more than that previously believed and the available oxygen is getting consumed in decomposition of these organic matter leading to formation of OMZ.

#### **4.9 Relationship between new and total production: possible implication**

Results of nitrate, ammonium and urea uptakes for both the seasons at nine stations discussed earlier are shown in Table 4.4. The nitrate uptake (new production) has been estimated after consideration of ambient concentration, whereas the ammonium and urea uptakes are conservative estimates. From Table 4.4 it is seen that the f-ratio (calculated here as nitrate uptake / total uptake) is in general very high (mean upper bound  $\sim 0.65$ ), regardless of season and the proximity to the coast. Since f-ratio has been calculated using conservative ammonium and urea uptakes, it provides the upper limit of the f-ratio for the region. This is significantly higher than the values (mean  $< 0.3$ ) reported for the highly productive northwestern Arabian Sea for intermonsoon season (Watts and Owens 1999). However, the data of Watts and Owens (1999) take into account the ambient ammonium concentration and may go up when conservative estimates are taken. Using the average Redfield ratio (C/N) of 6.6, we convert the total nitrogen uptake to carbon uptake; the total productivity in the Bay of Bengal was found to vary from 90 to 870  $\text{mgC m}^{-2} \text{d}^{-1}$  during September-October 2002, with an average value of 318  $\text{mgC m}^{-2} \text{d}^{-1}$ . The total productivity during April-May 2003 varied from 154 to 975  $\text{mgC m}^{-2} \text{d}^{-1}$  with an average of 575  $\text{mgC m}^{-2} \text{d}^{-1}$ . Also, the new production during April-May 2003 (overall average  $\sim 433$  with shelf region average of 552 and offshore average of 284  $\text{mgC m}^{-2} \text{d}^{-1}$ ) is higher than that of September-October 2002 (overall average  $\sim 207$  with shelf region averaging around 180 and offshore around 243  $\text{mgC m}^{-2} \text{d}^{-1}$ ). These values are comparable to the new production off India,  $400 \pm 160$   $\text{mgC m}^{-2} \text{d}^{-1}$  reported for the Arabian Sea (Sambrotto 2001). However, these values reported here are somewhat higher than the productivity ( $^{14}\text{C}$  tracer method) reported for this region (40 to 502  $\text{mgC m}^{-2} \text{d}^{-1}$ ) during the peak summer monsoon (July, 2001; Madhupratap et al. 2003). The reason for this discrepancy could be two fold: first, the increase in mean cloudiness during the summer monsoon season over the BOB (i.e., less light available for photosynthesis), which is known to affect the productivity in this region (Gomes et al. 2000). Second reason could be the cyclones, which are very frequent in the Bay during the postmonsoon season (September-December) and can bring nutrients to the surface by churning up the ocean and hence increase the productivity.

**Table 4.4** The nitrate, ammonium and urea uptake rates in the Bay of Bengal during post and premonsoon

	Stations	Nitrate (mmolN m <sup>-2</sup> d <sup>-1</sup> )	Nitrate (mgC m <sup>-2</sup> d <sup>-1</sup> )	Ammonium (mmolN m <sup>-2</sup> d <sup>-1</sup> )	Ammonium (mgC m <sup>-2</sup> d <sup>-1</sup> )	Urea (mmolN m <sup>-2</sup> d <sup>-1</sup> )	Urea (mgC m <sup>-2</sup> d <sup>-1</sup> )	Total (mmolN m <sup>-2</sup> d <sup>-1</sup> )	Total (mgC m <sup>-2</sup> d <sup>-1</sup> )	f-ratio
<b>Post</b> monsoon	PP1	0.43	34.40	0.33	26.21	0.49	39.22	1.26	99.82	0.34
	PP2	8.85	703.32	0.81	64.47	1.33	105.64	10.99	873.44	0.81
	PP3	1.44	114.35	0.80	63.48	1.14	90.82	3.38	268.65	0.43
	PP4	1.53	121.77	0.28	22.51	0.87	69.45	2.69	213.73	0.57
	PP5	2.13	169.61	0.49	38.74	0.97	76.96	3.59	285.32	0.59
	PP6	4.48	356.45	0.49	38.70	0.99	78.62	5.96	473.77	0.75
	PP7	3.87	307.81	0.48	37.84	1.13	89.81	5.48	435.45	0.71
	PP8	0.17	13.33	0.47	37.47	0.85	67.35	1.49	118.15	0.11
	PP9	0.63	49.87	0.28	22.56	0.26	20.40	1.17	92.83	0.54
Average										
Overall		2.61	207.88	0.49	39.11	0.89	70.92	4.00	317.91	0.54
Offshore		3.06	243.46	0.56	44.17	0.96	76.28	4.58	363.91	0.54
Shelf		2.26	179.41	0.44	35.06	0.84	66.63	3.54	281.10	0.54
<b>Pre</b> monsoon	PP1	0.99	78.37	0.67	53.38	0.28	22.03	1.93	153.78	0.51
	PP2	3.28	260.67	0.91	72.68	0.77	61.22	4.96	394.57	0.66
	PP3	1.58	125.64	1.07	84.94	0.61	48.72	3.26	259.30	0.48
	PP4	8.46	672.85	1.80	143.29	0.91	72.12	11.17	888.26	0.76
	PP5	2.47	195.99	0.95	75.45	0.15	12.19	3.57	283.63	0.69
	PP6	10.68	848.98	1.08	86.02	0.51	40.80	12.27	975.80	0.87
	PP7	4.35	345.57	0.96	76.69	0.25	19.98	5.56	442.25	0.78
	PP8	7.80	619.78	1.55	123.31	0.84	66.91	10.19	809.99	0.77
	PP9	9.44	750.13	1.67	133.01	1.07	85.03	12.18	968.17	0.77
Average										
Overall		5.45	433.11	1.19	94.31	0.60	47.67	7.23	575.08	0.70
Offshore		3.58	284.38	1.11	88.57	0.64	51.02	5.33	423.98	0.60
Shelf		6.94	552.09	1.24	98.90	0.57	44.98	8.75	695.97	0.78

There is a very significant correlation between new (y) and total production (x):  $y = 0.88x - 0.89$  (coefficient of determination,  $r^2 = 0.99$ ) in the Bay of Bengal. The relationship remains significant ( $r^2=0.96$ ) but with a small decrease in the slope,

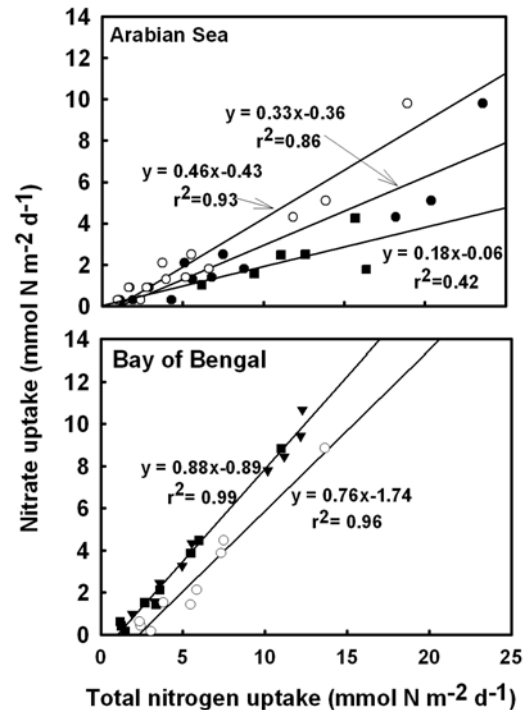


**Figure 4.20** Relationship between total and new production. Top panel represents the Arabian Sea data from Watts and Owens (1999) where filled circles are the original data, open circles are the recalculated conservative estimates and squares are Arabian Sea data of the present study (SK-186). In the bottom panel, rectangles are for Sep-Oct 2002, triangles for Apr-May 2003 and circles are for Sep-Oct 2002 after taking into account the ambient ammonium estimated from zooplankton biomass.

when ammonium concentration from zooplankton regeneration is considered for September-October 2002 (Figure 4.20). Data for the Arabian Sea (Watts and Owens 1999) also show such a correlation, but with some scatter:  $y = 0.33x - 0.36$  ( $r^2 = 0.86$ ). However, this relationship improves ( $y = 0.46x - 0.43$ ;  $r^2 = 0.93$ ) when the conservative estimates (i.e., no ambient ammonium) were considered. During this calculation the average ammonium concentration was taken as  $0.13\mu\text{M}$  (Woodward et al. 1999; where the nutrient data of their study are presented). Interestingly, in both the seas, the x-intercept, i.e. minimum amount of regenerated production in the total absence of extraneous nitrate supply is  $\sim 1 \text{ mmolN m}^{-2} \text{ d}^{-1}$  (equivalently  $\sim 80 \text{ mgC m}^{-2} \text{ d}^{-1}$ ). Based on the regression of Watts and Owens (1999) data and present data for the Bay of Bengal, the f-ratio ( $= y/x$ ) can be expressed as  $\alpha (1-1/x)$  (as the slope and intercept being roughly equal numerically, in both cases), where x is the total

production and  $\alpha$  is the slope of the straight-line in (x, y) plot. It is apparent that when x tends to large values, there is a limit to the f-ratio, given by the slope,  $\alpha$ . Thus, available limited data suggest that in the Bay of Bengal, the f-ratio can be as high as 0.88 while in the Arabian Sea it can be at best  $\sim 0.46$  during intermonsoon. The Arabian Sea data of the present study during NE monsoon (January) also agrees with the above argument where the f ratio in general is less than 0.41 except at PP2 where it is anomalously high (0.60). However, the upper bound of f-ratio estimated for early March could go as high as 0.61 at the bloom station PP4.

#### **4.10 Possible nutrient sources to the Bay of Bengal**

Different sources and mechanisms of nutrients supply to the Bay of Bengal and their effect on productivity have not been thoroughly investigated as in the case of the Arabian Sea and the situation here is partly speculative. The present section discusses the different possible sources of nutrient supply to the Bay of Bengal required to sustain the observed new production.

##### **Terrestrial Sources**

One important source of nutrients to the Bay of Bengal is the adjacent land, particularly due to the river water discharge, which has been speculated to have an enormous influence on biogeochemical processes in the Bay of Bengal (Ittekkot 1991). However, no systematic data exists to quantify the riverine contribution to the nutrient pool of the Bay despite the fact that almost all the major rivers of the Indian subcontinent, except the Indus and the Narmada, drain into the Bay of Bengal. These rivers are expected to bring a large pool of nutrients with them. Curiously, actual measurements from the shelf to offshore in the surface Bay does not show significant presence of nitrate (De Sousa et al. 1981). The nitrogen flux into the Bay was indirectly calculated by Kumar et al. (1996) using the global flux of water ( $37.4 \times 10^{12} \text{ m}^3 \text{ yr}^{-1}$ ; Martin and Whitfield 1983) and nitrogen ( $50 \times 10^{12} \text{ gN yr}^{-1}$ ; Duce et al. 1991) in world rivers to the ocean assuming the Indian rivers deliver nitrate in the same proportion to the total water flux. It was found to be  $2.17 \times 10^{12} \text{ gN yr}^{-1}$ . If the fresh water is assumed to spread over a total area of the Bay ( $2.2 \times 10^{12} \text{ m}^2$ ; LaFond 1966), the above calculated influx works out to be  $2.68 \text{ mgN m}^{-2} \text{ d}^{-1}$ . Another possible contribution to the nitrate pool of the Bay is by atmospheric deposition, which has been proposed to play a crucial role in regulating

the productivity of ocean (Jickells 1998). The contribution to the nitrogen pool of the Bay through atmospheric wet deposition has been reported to be around  $1.53 \text{ mgN m}^{-2} \text{ d}^{-1}$  (Kumar et al. 1996) using an annual precipitation rate of 2m over BOB (Tomczak and Godfrey 1994) and an average combined nitrogen concentration of  $20 \mu\text{M}$  in rainwater. This calculation shows total external input of nitrogen to the Bay as  $4.21 \text{ mgN m}^{-2} \text{ d}^{-1}$ . However, another estimate for the external nitrogenous inputs to the Bay has been given by Schafer et al. (1993) and is on the relatively higher side. According to them, the fluvial input (particulate and dissolved) has been estimated to be  $5.2 * 10^{12} \text{ gN yr}^{-1}$ , which amounts to  $6.36 \text{ mgN m}^{-2} \text{ d}^{-1}$  after taking into account the areal extent of the Bay. The atmospheric input values are based on the cruises carried out during spring and autumn 1988 and have been divided into nitrogen inputs in the form of ammonium and nitrate compounds (dry and wet deposition). Total nitrogen input from the atmosphere in the form of ammonium compounds has been reported to be around  $3.74 \text{ mgN m}^{-2} \text{ d}^{-1}$  ( $3.70 \text{ mgN m}^{-2} \text{ d}^{-1}$  as wet deposition and  $0.04$  as dry deposition) whereas in the form of nitrate deposition to be  $2.5 * 10^{12} \text{ gN yr}^{-1}$  ( $\sim 3.09 \text{ mgNm}^{-2} \text{ d}^{-1}$ ). These values are the upper estimates provided by Schafer et al. (1993). Therefore, the total maximum atmospheric nitrogen input works out to be  $6.83 \text{ mgN m}^{-2} \text{ d}^{-1}$ , which is of the same order of magnitude as the fluvial input; thus the total extraneous nitrogen (fluvial + atmospheric) to the Bay is around  $13.19 \text{ mgN m}^{-2} \text{ d}^{-1}$  ( $\sim 0.94 \text{ mmol N m}^{-2} \text{ d}^{-1}$ ). However, all may not be in bioavailable form, particularly the particulate component contributed by rivers. Our results for the two seasons show average new production of  $4 \text{ mmolN m}^{-2} \text{ d}^{-1}$ ; therefore, estimated nitrogen inputs from rivers and atmosphere can at best supply only around 20% of the total required nitrogenous inputs (<10% by the estimates of Kumar et al. 1996). The rest 80% of the required nitrogen has to come from the supply of nitrate from the deeper waters.

### **Cyclonic Churning**

The shallow nitracline in the Bay of Bengal (Madhuratap et al. 2003) might have allowed the nitrate to come up to the surface, especially when aided by churning due to cyclonic winds in the postmonsoon season. These cyclones stir up the surface Bay and thus supply the nutrients from below. The formation of localized intense blooms and also the intensification of bloom generated by anticyclonic gyre are known due to cyclonic activity in this region (Vinaychandran and Mathew 2003). Also, the stratification due to freshwater discharge, which prevents the upwelling of nutrients in

the Bay, reduces towards the south and is not strong enough to prevent nutrients to come up to the surface (Vinaychandran et al. 2002). At the beginning of study period the wind speed more than 20m/s over the Bay had been encountered (Figure 4.8-bottom right; Qscat wind speed data; <http://www.ssmi.com/qscat/>). Furthermore, in 2002 the monsoon was somewhat weaker (80% of long term mean rainfall over India, see [www.tropmet.res.in](http://www.tropmet.res.in)), leading perhaps to less than normal stratification of the surface Bay. It is seen from Figure 4.8-bottom left that the mixed layer depths are generally higher for the offshore stations than the shelf stations for September-October 2002. As discussed earlier the nitrate concentration in the Bay increases sharply below 40 and 60m, the stations with mixed layer depth more than 40m (average euphotic depth was ~ 60m) shows higher new production (PP2 during September-October 2002 and PP8 during April-May 2003), probably indicating the coupling between surface and subsurface layers.

### **Surface Currents**

The higher new production in the Bay at shelf stations during April-May 2003 may be attributed to the presence of a poleward surface current along the western boundary of the Bay of Bengal. This current, known as EICC is active at north of 10°N that brings cooler, more saline water with nutrients to the surface (Shetye et al. 1993). Shetye et al. (1993) have also proposed that this poleward current is the western boundary current of anticyclonic subtropical gyre which is best developed during March-April, and decays only by June, which includes the study period. Gomes et al. (2000) have also observed the increase in productivity in the coastal region due to EICC.

Moreover, another reason could be the higher uptake rates observed at deeper depths (~ 40m) during premonsoon season where nutrients are available in plenty (average ~7μM) along with the light (euphotic zone ~80m). Since the euphotic zone was more than 80m and mixed layer was thin, as often the case during the intermonsoon period, the upper part of the thermocline with high nutrient levels fell well within the euphotic zone leading to higher uptake rates at depths more than 40m (Figure 4.17). In such a condition photosynthetic rate several fold higher than that at sea surface has been reported earlier (Pollehne et al. 1993).

### **Upwelling**

Another mechanism that can bring nutrients to the surface is upwelling, a major cause of the high biological productivity in the Arabian Sea. The nutrient rich waters upwelled off Somalia and Arabia are advected laterally out of the upwelling region and contribute to productivity in the Central Arabian Sea (Prasanna Kumar et al. 2001). However, Bay of Bengal lacks such intense upwelling except for a 40 km wide band along the western margin that has been found to be the result of local longshore wind stress (Shetye et al. 1991). This upwelling has been observed during southwest monsoon and disappears northward as this phenomenon is overwhelmed by the enormous freshwater influx from Ganga-Brahmaputra rivers. Therefore, upwelling does not seem to be a prominent nutrient source during the study period.

### **Convective mixing**

Cooling of surface waters by the northeasterly winds during the northeast monsoon has been suggested (Shetye et al. 1996). Winter cooling of surface water in the month of January has also been reported (Murty et al. 1998). However, this winter cooling does not lead to convective mixing as in the case of Arabian Sea (Madhupratap et al. 1996). Mixing is again prevented due to the presence of low salinity water in the upper layer.

### **Eddies**

Presence of thermocline oscillations and cold-core eddy signatures during summer 2001 have been reported (Madhupratap et al. 2003). These eddies could pump cold water and nutrients from below to upper subsurface waters. But such eddies are usually capped by surface freshwater layer and are unable to surface, thus perhaps not contributing significantly to the surface nitrate pool.

### **Submarine ground water discharge**

Another potential nutrient supply to the Bay of Bengal may be from submarine groundwater discharge. An annual subsurface discharge from Bengal Basin to the Bay of  $1.5 \pm 0.5 \times 10^{11} \text{ m}^3 \text{ yr}^{-1}$ , which is  $\sim 10\%$  of Ganga-Brahmaputra riverine flux to the Bay, has been reported (Dowling et al. 2003). The depth of discharge is more than 30m. However, the nitrate in groundwater sampled from domestic wells in Bangladesh shows large variations ranging from 1 to 191  $\mu\text{mol/kg}$ , with most of the wells showing

nitrate less than detection limit. Taking a conservative 10  $\mu\text{mol/kg}$  as the mean concentration, this would lead to a total annual nitrogen flux of  $1.5 \times 10^9$  mol N,  $\sim 1\%$  of the surface flux of nitrogen (Kumar et al. 1996) from rivers. Thus, available limited data do not clearly advocate the submarine discharge to be the substantial source of nutrient in the surface Bay of Bengal. Further studies are required for better quantification.

Cyclonic churning, therefore appears to be the best candidate to explain the high new production.

#### **4.11 Natural Nitrogen Isotopic Composition of Suspended Matter**

The importance of the study related to the natural isotopic composition of nitrogen in suspended matter has already been discussed in the previous chapter. In the Bay of Bengal the stations studied are divided into two transects: one along the  $88^\circ\text{E}$  longitude (Stn.1-Stn.13), defined here as offshore stations (transect) and the other parallel to the Indian coast (Stn. 14 to Stn.24) as the shelf stations (transect).

##### **4.11.1 Surface suspended matter**

In the Bay of Bengal, it has been observed that the average surface particulate organic nitrogen (PON) concentration during postmonsoon ( $\sim 1.41 \mu\text{M N}$ ) is nearly twice that of premonsoon ( $0.71 \mu\text{M N}$ ). During the postmonsoon the difference in average shelf ( $1.31 \mu\text{M N}$ ) and offshore ( $1.49 \mu\text{M N}$ ) surface PON is around  $0.18 \mu\text{M N}$ , which is significant. The same is not true for the premonsoon season, where it averages  $0.74 \mu\text{M N}$  for shelf and  $0.69 \mu\text{M N}$  for offshore locations. During the study period, a maximum surface PON of  $2.5 \mu\text{M N}$  has been observed at Stn.15 (postmonsoon), which is the nearest to the coast with the shallowest water column depth of 620m. The  $\delta^{15}\text{N}$  values of surface PON for both pre and postmonsoon season range from 2 to 7.6 ‰ and fall in the general range of known oceanic  $\delta^{15}\text{N}$  for PON. The overall  $\delta^{15}\text{N}$  of surface PON averages around 4.1‰ for postmonsoon and around 4‰ for premonsoon season, which agree within analytical error. There is a significant difference of 1.5‰ between average  $\delta^{15}\text{N}$  of offshore (4.8‰) and shelf (3.3‰) stations during postmonsoon (Table 4.5). However, no such difference has been observed for the

samples collected during premonsoon, (where both average around 4‰). There is no significant latitudinal variation in  $\delta^{15}\text{N}$  during either season. There exists a significant

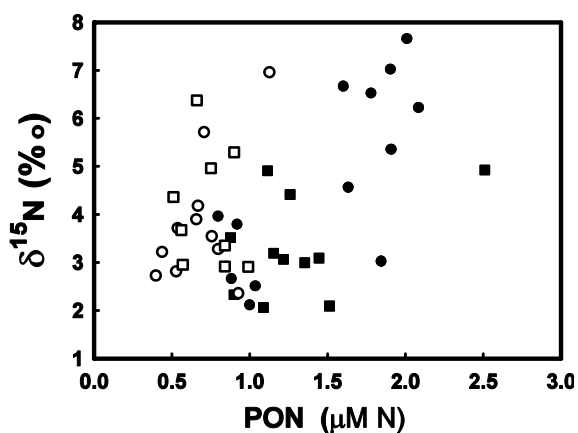


**Figure 4.21** The relationship between  $\delta^{15}\text{N}$  and PON during post (filled circles and squares represent offshore and shelf stations) and premonsoon (open circle and squares represent offshore and shelf stations).

**Table 4.5** PON content and  $\delta^{15}\text{N}$  of surface suspended matter observed during pre and post monsoon in the Bay of Bengal.

Stations	Premonsoon		Postmonsoon	
	$\delta^{15}\text{N}(\text{‰})$	PON ( $\mu\text{M}$ )	$\delta^{15}\text{N}(\text{‰})$	PON ( $\mu\text{M}$ )
1	3.2	0.44	6.7	1.60
2	2.8	0.53	5.3	1.91
3	3.9	0.66	7.6	2.01
4	N.A	N.A	2.1	1.00
5	N.A	N.A.	3.8	0.92
6	4.2	0.67	4.0	0.80
7	5.7	0.71	6.5	1.78
8	3.5	0.76	7.0	1.91
9	3.7	0.54	2.7	0.89
10	2.7	0.40	6.2	2.09
11	7.0	1.13	3.0	1.85
12	3.3	0.80	2.5	1.04
13	2.3	0.93	4.6	1.64
14	N.A	N.A	3.1	1.22
15	5.3	0.90	4.9	2.51
16	5.0	0.75	3.0	1.35
17	2.9	0.84	3.1	1.45
18	3.4	0.84	2.1	1.51
19	3.7	0.56	4.9	1.12
20	3.0	0.57	2.3	0.90
21	2.9	0.99	2.1	1.09
22	6.4	0.66	3.2	1.15
23	4.4	0.51	3.5	0.88
24	N.A	N.A.	4.4	1.26

positive linear correlation between PON and  $\delta^{15}\text{N}$  (Figure 4.21) during the postmonsoon ( $r^2 = 0.42$ ,  $n=24$ ,  $p = 0.005$ ;  $\delta^{15}\text{N} = 2.35*\text{PON} + 0.78$ ) and vanishes during premonsoon ( $r^2 = 0.09$ ;  $\delta^{15}\text{N} = 2.01*\text{PON} + 2.52$ ). During the postmonsoon shelf stations show less variability and data points lie in the lower regime i.e., low PON- low  $\delta^{15}\text{N}$  zone. On the other hand, the offshore stations show two clusters of data points, one with low PON-low  $\delta^{15}\text{N}$  which averages around 3.0‰ and other with high PON-high  $\delta^{15}\text{N}$  with an average of 5.8‰. During the premonsoon no clear cut distinction exists between  $\delta^{15}\text{N}$  of PON in shelf and offshore ocean transects.

In oceanic environments, PON is mainly derived from phytoplankton, microzooplankton, bacteria and detritus. The nitrogen isotopic signature of PON in suspended matter depends on the isotopic fractionation associated with its formation, and in turn upon the isotopic composition of inorganic form of dissolved nitrogenous sources (such as  $\text{NO}_3^-$ , 3-7‰;  $\text{NH}_4^+$ , 6-8‰; and atmospheric  $\text{N}_2$ , 0‰; Miyake and Wada 1967) available for the utilization by phytoplankton. The variation in  $\delta^{15}\text{N}$  of PON reveals the utilization of different nitrogen sources by phytoplankton as these sources have distinct isotopic compositions. Microscopic study suggested absence of *Trichodesmium* during the postmonsoon, while diatoms were found to be the dominant species. However, there were sporadic occurrences of *Trichodesmium* during the premonsoon but it did not dominate in terms of N contribution to the PON. Our  $\delta^{15}\text{N}$  data also precludes the possibility of significant  $\text{N}_2$  fixation in the Bay of Bengal, as the cyanobacteria *Trichodesmium*; a well-known  $\text{N}_2$  fixer, generates PON with a  $\delta^{15}\text{N}$  value (0.6‰) nearer to the atmospheric  $\text{N}_2$  in equilibrium with seawater (Emerson et. al. 1991).  $\delta^{15}\text{N}$  values around -2 to 0‰ has also been reported for cyanobacteria *Trichodesmium* (Minagawa and Wada 1986). All our  $\delta^{15}\text{N}$  data are above the required value for an area dominated by  $\text{N}_2$  fixers.

For the purpose of discussion, stations in the Bay may be classified into two based on the surface salinity of the stations. The first includes the stations with salinity less than 32psu (the six shelf stations and three offshore stations during postmonsoon; Figure 4.22) and second includes the stations with surface salinity more than 32psu (all the rest). The former are influenced by the riverine discharge whereas the latter are not. The salinity and  $\delta^{15}\text{N}$  of suspended PON (Figure 4.22) for the two seasons indicate that when salinity is low (<32 psu), the  $\delta^{15}\text{N}$  is consistently on the

lower side (2-3‰) (except at one location each in shelf and offshore region, which have  $\delta^{15}\text{N}$  values of 4.9 and 4.6‰ respectively). The rivers draining the BOB bring a lot of terrestrial organic as well as detrital material (Unger et al. 2003). The consistent low

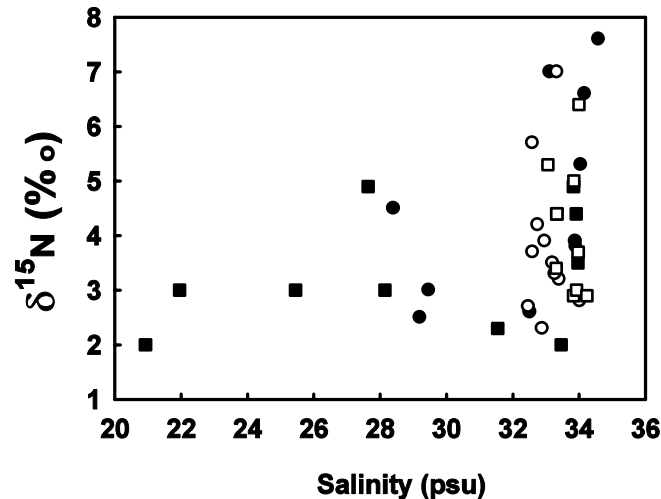


**Figure 4.22** The relationship between salinity and  $\delta^{15}\text{N}$  for post (filled circles and squares represent offshore and shelf stations) and premonsoon (open circle and squares represent offshore and shelf stations).

$\delta^{15}\text{N}$  suggests that isotopic signature of PON at these locations have been influenced by terrestrial inputs. Terrestrial particulate matter, brought by major rivers, might have diluted the overall  $\delta^{15}\text{N}$  signal of PON, although there exists no literature regarding the  $\delta^{15}\text{N}$  of such particulate matter draining into the Bay. But, the naturally occurring land derived materials are known to have low  $\delta^{15}\text{N}$  (mean of 2.5‰ for terrestrial organic matter, Sweeney et al. 1978; and 1.5‰ for terrestrial detrital component, Mariotti et al. 1984). Also, the C: N values in suspended matter during postmonsoon at locations under terrestrial influence have been found to be relatively higher (9.5, 9.3 and 8.2 at stations 12, 16 and 18 respectively) compared to stations without influence (5, 3.4, 4.6, 6.2 and 6.4 for stations 3, 6,9,20 and 23 respectively), indicating the contribution of continental inputs at these stations.

The stations, which are not influenced by riverine discharge, show a wide isotopic variability (2-7.6‰). However, high average  $\delta^{15}\text{N}$  of surface suspended matter (5.3 ‰ for offshore stations during postmonsoon and 4‰ for both offshore and shelf stations during premonsoon) have been observed for these stations. Since these locations are unaffected by the terrestrial influence the variability observed may be

attributed to the two possible reasons: first, uptake of regenerated ammonium (Wada and Hattori 1976); and second, supply of nitrate from deeper waters due to the presence of shallow nitracline, which is between 50-100m (Prasanna Kumar et al. 2002). In the former case, regenerated ammonium produced by excretion of zooplankton and heterotrophs in the surface layer has been considered as a source. In most oceanic regions, ammonium is the preferred substrate and normally does not accumulate in the surface layer (Mino et al. 2002). Soon after regeneration of ammonium, it is rapidly taken up by the algae; there is little time for isotopic fractionation and the  $\delta^{15}\text{N}$  of ammonium is imprinted in PON without much modification. Unfortunately,  $\delta^{15}\text{N}$  of ammonium in the BOB has not been measured to directly assess the role of ammonium on  $\delta^{15}\text{N}$  of PON. Values in the range of 6-8‰ have been reported for ammonium in other oceans (Miyake and Wada 1967). However, indirect estimation of degree of contribution of ammonium in  $\delta^{15}\text{N}$  of PON may be obtained from the new production (Dugdale and Goering 1967) measurements in the region (Kumar et al. 2004). If the new production is less, there could be a prominent effect of the regenerated ammonium on the  $\delta^{15}\text{N}$  of PON. But in the Bay of Bengal, in general, high new production has been observed during present study in both post (average  $\sim 2.6 \text{ mmolN m}^{-2} \text{ d}^{-1}$ ) and pre (average  $\sim 5.4 \text{ mmolN m}^{-2} \text{ d}^{-1}$ ) monsoon. Therefore, regenerated ammonium is likely to have played a limited role in observed  $\delta^{15}\text{N}$  of PON. However, significant ammonium contributions cannot be ruled out for three locations in the open ocean during postmonsoon and at one location during premonsoon, where values higher than 6‰ have been observed.

The nitrate from deeper water is a known source of nutrients in the Indian Ocean for phytoplankton (Vinaychandran and Mathew 2003); however, its possible imprint on  $\delta^{15}\text{N}$  of PON and related fractionation mechanism could only be estimated if the nitrate  $\delta^{15}\text{N}$  is known. But, as in the case of ammonium, nitrate  $\delta^{15}\text{N}$  has also not been measured in the Bay.  $\delta^{15}\text{N}$  values of 3-7‰ have been reported for nitrate in deeper waters lacking significant column denitrification as in the Bay (Miyake and Wada 1967; Cline and Kaplan 1975). The average value reported here for  $\delta^{15}\text{N}$  of PON in offshore waters during both post and premonsoon seasons (5.3 and 4‰) are found to be of similar magnitude. However, the observed variability can be explained in two different ways: first, the rapid uptake of the nitrate without fractionation and second, the fractionation of nitrate during uptake by the phytoplankton. In the first scenario, the

consumption of nitrate has to be fast enough for little or no isotopic fractionation and the original  $\delta^{15}\text{N}$  of nitrate would be reflected in the  $\delta^{15}\text{N}$  of PON (Altabet and McCarthy 1985; Wada and Hattori 1991). In this case, complete consumption of nitrate from the surface would be expected. The offshore stations during postmonsoon show a virtual absence of nitrate from the surface, implying its complete consumption. However, there is variability (2.1 to 7.6‰) in the  $\delta^{15}\text{N}$  of PON at these offshore stations despite undetectable ambient nitrate. Out of the thirteen stations, ten have  $\delta^{15}\text{N}$  ranging from 3 and 7.6‰, falling in the range of  $\delta^{15}\text{N}$  for oceanic nitrate as mentioned earlier. This variability in  $\delta^{15}\text{N}$  of PON indicates the possibility of change in isotopic composition of source nitrate.  $\delta^{15}\text{N}$  for 3 stations falls below 3‰ and cannot be explained by the complete consumption argument, discussed above.

The  $\delta^{15}\text{N}$  at premonsoon locations varies from 2.7 to 7‰ with relatively higher surface nitrate concentration (0.2 to 1.1  $\mu\text{M}$ ). This availability of nitrate pool in the surface water suggests that the phytoplankton have the luxury of discriminating in favour of  $^{14}\text{N}$  during uptake. The exact mechanism by which these nutrients reach the surface in the open Bay during premonsoon is a subject of speculation. However, nitrate for shelf locations during premonsoon might have been supplied by the EICC acting north of about 10°N. The EICC is best developed during March-April and decays only by June (Shetye et al. 1993).

As mentioned earlier,  $\delta^{15}\text{N}$  of suspended matter in BOB varies from 2 to 7.6‰, falling in the known oceanic range (-5 to +15‰; Wada and Hattori 1991). However, the latter is known to fall in different ranges depending on the nitrogen source and fractionation by the phytoplankton. Table 4.6 compares a few recent studies of  $\delta^{15}\text{N}$  in suspended matter of the world ocean. Rau et al. (1998) observed values in the Monterey Bay varying between 1.3 to 7.6‰, similar to the range observed during present study. Mino et al. (2002) have studied near surface waters along 50°N to 50°S in the Atlantic Ocean and the values ranged from -0.8 to 5.4‰. The negative relationship between  $\delta^{15}\text{N}$  of PON and nitrate concentration as observed by Rau et al. (1998) and Mino et al. (2002) was not observed during present study. Relatively higher values (4-6‰) observed by Mino et al. (2002) have been attributed to the rapid consumption of nitrate from deeper waters as found in a few open ocean stations during the postmonsoon of the present study.

Overall, the  $\delta^{15}\text{N}$  values of PON in the surface waters observed in the Bay may be explained in terms of mixing between (i) the terrestrial particulate matter with low  $\delta^{15}\text{N}$ , which has mostly influenced the six shelf locations and three offshore locations during postmonsoon, and (ii) marine phytoplankton, which has mainly inherited the  $\delta^{15}\text{N}$  of nitrate from deeper waters. However, the phytoplankton have a wide spectrum of values because of two extremes: one due to uptake of nitrate without fractionation (highest  $\delta^{15}\text{N}$ ) and other with high degree of fractionation (lowest  $\delta^{15}\text{N}$ ).

**Table 4.6**  $\delta^{15}\text{N}$  of particulate organic nitrogen in surface suspended matter from different oceanic regions of the world.

Oceanic regions	$\delta^{15}\text{N}$ (‰)	References
Southern Ocean		
Subantarctic zone	~1	Lourey et al. (2003)
Polar Frontal zone	0 to -4	Lourey et al. (2003)
Atlantic Ocean	-0.8 to 5.4	Mino et al. (2002)
Monterey Bay	1.3 to 7.6	Rau et al. (1998)
Sargasso Sea (annual Av)	0.2	Altabet (1988)
Northeastern Indian Ocean	2.1 to 10.1	Saino and Hattori (1980)
Bay of Bengal	2 to 7.6	Present Study

#### 4.11.2 Depth profiles of $\delta^{15}\text{N}$ of suspended matter

Depth related changes in nitrogen isotopic composition have been used as an indicator of particle transformations in ocean (Altabet 1988). Figure 4.23 presents the vertical profiles of  $\delta^{15}\text{N}$  and PON for premonsoon season at different locations in the Bay of Bengal. The profile is upto 300m or more, except for Stn.3, where it is only up to 100m. Average  $\delta^{15}\text{N}$  of PON in the top 60m for all the stations varies between 1.9 (Stn. 14) to 4.9‰ (Stn.16) with an average of around 3.6‰. Below 60m,  $\delta^{15}\text{N}$  increases with depth and reaches an average value of 5.9 ( $\pm 1.1$ )‰ at 300m. For the offshore stations the average top layer (60m)  $\delta^{15}\text{N}$  shows a decreasing trend from south to north with a maximum of 4.5‰ for southernmost station (Stn. 3) and minimum of 2.9‰ for northern station (Stn.12).  $\delta^{15}\text{N}$  also shows subsurface minima between 10 to 60 m varying with location. PON, in general, decreases with depth showing subsurface maxima within the euphotic zone. Top layer (60m) average of PON is  $\sim 0.7\mu\text{M N}$  that

decreases to  $\sim 0.3 \mu\text{M N}$  at 300m. The depth distribution of  $\delta^{15}\text{N}$  in suspended matter is in agreement with the general pattern observed in the world ocean i.e., it increases with depth and appears to be ubiquitous feature (Saino and Hattori 1980; Altabet and McCarthy 1985; Saino and Hattori 1985; Altabet and McCarthy 1986; Saino and

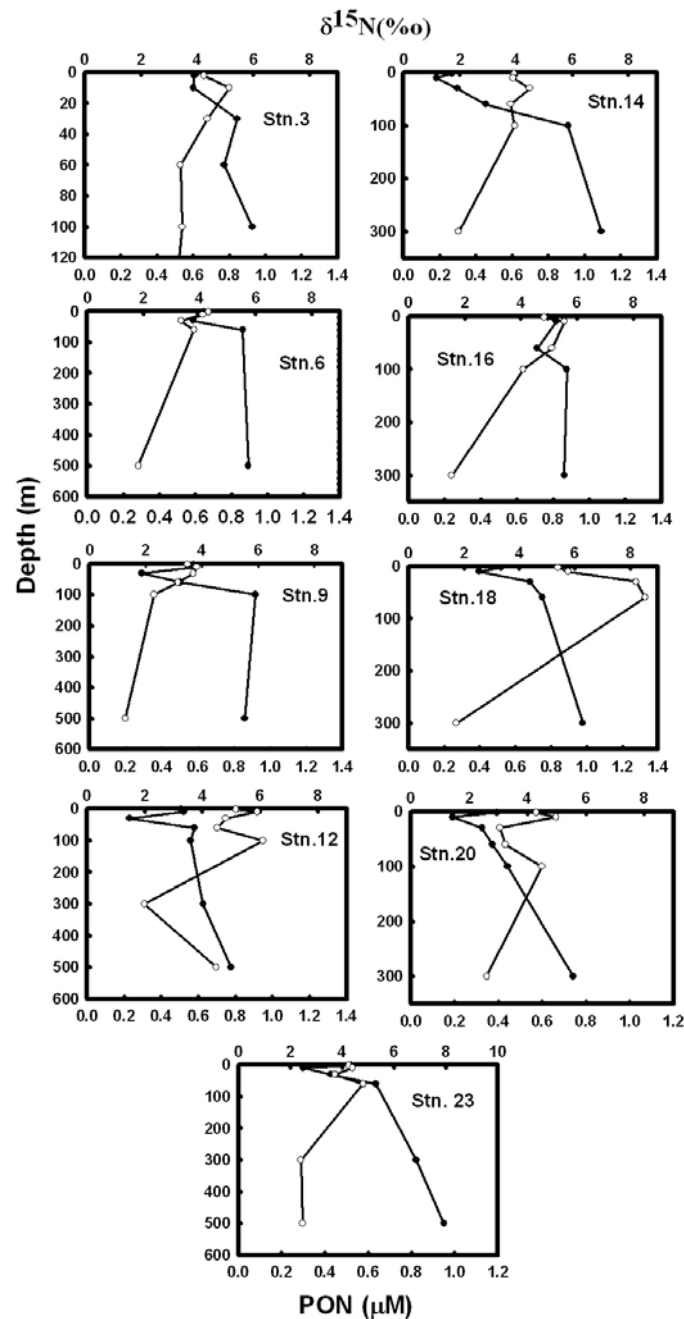


**Figure 4.23** The depth profiles of  $\delta^{15}\text{N}$  and PON during premonsoon in Bay of Bengal at different stations. The filled and unfilled circles indicate  $\delta^{15}\text{N}$  and PON respectively.

Hattori 1987; Altabet 1988). At most locations there is an increase in  $\delta^{15}\text{N}$  below 60m. This increase is from 0.21 to around 4‰ between 60 and 300m depending upon the

stations. High  $\delta^{15}\text{N}$  below euphotic depth has been observed mainly due to two reasons: (1) progressive decomposition of suspended matter itself causing the preferential release of  $^{14}\text{N}$  leaving the remaining PON enriched in  $^{15}\text{N}$ , in other words, release of dissolved nitrogen depleted in  $^{15}\text{N}$  during decomposition. The increased  $\delta^{15}\text{N}$  below the euphotic depth has been correlated with decreasing concentration and has often been cited as evidence for isotopic fractionation during the destruction of suspended particulate matter (Altabet and McCarthy 1986; Saino and Hattori 1980; Saino and Hattori 1985). This decrease in PON with depth has been observed during present study. (2) Production of suspended matter due to fragmentation of sinking particles below the euphotic depth (Bacon et al. 1985). These sinking particles are enriched in  $\delta^{15}\text{N}$  by 3-4 ‰ relative to suspended particle in euphotic zone because these particles are formed mainly as a by-product of zooplankton feeding, causing an increase in  $\delta^{15}\text{N}$  with each trophic step (DeNiro and Epstein 1981). The difference in  $\delta^{15}\text{N}$  between suspended and sinking PON ( $\Delta\delta^{15}\text{N}$ ) has been proposed as a measure of number of trophic steps linking primary production to the export of particulate organic matter from the euphotic zone as sinking particles (Altabet 1988).  $\Delta\delta^{15}\text{N}$  of 0 has also been observed by Altabet et al. (1991) during bloom conditions where phytoplankton aggregate and sink directly without trophic transfer. However, the variation in isotope ratio in biogeochemical processes are closely related to physico chemical conditions like water circulations, light, salinity and temperature etc. There is no data regarding  $\delta^{15}\text{N}$  of sinking particles for the Bay of Bengal at 300 or 500m depths. However,  $\delta^{15}\text{N}$  values for sinking particles are expected to increase with depth but lesser than the suspended particles (Altabet et al. 1991). The sediment traps placed at around 2000m in the Bay show  $\delta^{15}\text{N}$  variation in the range of 2.2-6.2 ‰ (Schafer and Ittekkot 1995). But  $\delta^{15}\text{N}$  of deep sinking particles (~2000m) is known to be less as it starts decreasing below 500m (Saino and Hattori 1987; Altabet et al. 1991). Based on this argument the  $\delta^{15}\text{N}$  of sinking particles around 300m in the present study area should be around 6‰. However, extensive interconversion of sinking and suspended particles through disaggregation and reaggregation also homogenize the  $\delta^{15}\text{N}$  signal between the two (Bacon et al. 1985); but Altabet et al. (1991) have observed that suspended and sinking particles do not extensively interact in the ocean as proposed earlier. Saino and Hattori (1980) have found  $\delta^{15}\text{N}$  as high as ~12‰ at 300m depth in the far eastern Indian Ocean. However our data suggest the average value of ~6‰ for the Bay of Bengal at

the same depth. This may be due to the high sinking rate of particles in the Bay allowing it lesser time for degradation. Here, the particle removal to the deep sea occurs in the form of large aggregates formed by the interaction of organic and mineral matter introduced from external sources like rivers and wind. This increases their density and consequently the settling rate in water column (Ittekkot 1991). Minima in the  $\delta^{15}\text{N}$  of PON within the surface layer as reported by Saino and Hattori (1980), has been observed during present study too, possibly due to the isotopic fractionation during nitrate uptake in light limited conditions.

#### **4.12 Primary productivity estimation using IRS P4 OCM**

Due to their broad and synoptic coverage remotely sensed images of ocean colour are considered important for spatial extrapolation of local data collected from ships in ocean biogeochemical studies (Platt and Sathyendranath 1993). These are also the only practical means for monitoring the spatial and seasonal variation of near surface phytoplankton that is essential for studying ocean primary productivity, global carbon and other biogeochemical cycles. During present study an attempt has been made to quantify the primary productivity using IRSP4 OCM (Indian Remote Sensing Satellite P4 Ocean Colour Monitor) data.

The main objective of the ocean colour remote sensing is the quantitative estimation of the oceanic constituents (such as chlorophyll, suspended matter, yellow substances etc.) from the spectral nature of the solar radiation backscattered from the ocean waters. Only the visible portion ( $\lambda \sim 400\text{-}670\text{nm}$ ) of the solar spectrum penetrates into the water and undergoes absorption and multiple scattering due to a series of interactions with suspended (phytoplankton, sediment etc.) and dissolved (DOM etc.) matter present. A small portion of this visible radiation is scattered out of the water and is detected by ocean colour sensor. These radiances are detected in a set of suitably selected wavelengths and the concentrations of oceanic constituents are estimated using a variety of empirical, semi-empirical and analytical algorithms.

##### **IRSP4 OCM (Oceansat-1)**

IRS P4 (Oceansat-1) was launched by the Indian Space Research Organization (ISRO) on May 26, 1999 with the objectives of gathering systematic data sets for

oceanographic, coastal and atmospheric applications. The satellite is placed in a near circular, sun-synchronous orbit at an altitude of 720km with the local time of equatorial crossing in the descending node at 1200hrs  $\pm$ 10minutes. This satellite carries two oceanographic payloads: the Ocean Colour Monitor (OCM) and Microwave Scanning Multi-frequency Radiometer (MSMR). OCM makes measurement of radiances in different spectral bands that relate to concentrations of phytoplankton pigments, suspended matter and coloured dissolved organic matter in coastal and oceanic waters and also the marine atmospheric aerosol parameters. The technical characteristics of IRS P4 are given in Table 4.7.

**Table 4.7** The technical specifications of IRS P4 OCM.

Parameters	Specifications	Applications
Spectral Range	404-882nm	
No. of Spectral bands	8	
Wavelength Range	nm	
Channel 1	404-423(414.2)	Yellow substance and turbidity
Channel 2	431-451(441.4)	Chlorophyll absorption maxima
Channel 3	475-495 (485.7)	Chlorophyll and other pigments ( $< 1.5\text{mg m}^{-3}$ )
Channel 4	501-520 (510.6)	Chlorophyll and other pigments ( $> 1.5\text{mg m}^{-3}$ )
Channel 5	547-565(556.4)	Suspended sediments (Away from Chlorophyll and Gelbstoff)
Channel 6	660-677(669.0)	Second Chlorophyll absorption maxima
Channel 7	749-787(768.6)	O <sub>2</sub> absorption R-branch
Channel 8	847-882(865.1)	Aerosol optical thickness
Satellite Altitude	720km	
Spatial Resolution	360 X 236m	
Swath	1420km	
Repetivity	2 days	
Quantisation	12 bits	
Equatorial crossing time	12 noon	
Along track steering	20°	
Camera MTF	> 0.2	
Transmission Frequency	X-Band	
Data rate	20.8 kbps	
SNR	>500	

#### 4.12.1 OCM data processing for Oceanic constituents

OCM data was processed using an in house software package developed at the Space Applications Centre, Ahmedabad (Chauhan et al. 2001). The main steps involved in the processing for the retrieval of oceanic parameters are:

1. Atmospheric correction i.e., retrieval of water leaving radiance in visible bands.
2. Implementation of bio-optical algorithm to normalised water leaving radiance data for estimating the chlorophyll concentration.

### **Atmospheric correction**

The radiation detected by sensor is a mixture of the radiation emerging from water (water leaving radiance) and the solar radiation backscattered by the air molecules (Rayleigh scattering) and the aerosols (Mie scattering) in the atmosphere. The part of the radiation contributed due to the back scattering by air molecule and aerosols is known as atmospheric path radiance and constitutes more than 85% of the radiance at Top of the Atmosphere (TOA). Therefore the radiance detected by ocean colour sensor at TOA in the wavelength  $\lambda$  can be split as (Doerffer 1992):  $L_t(\lambda) = L_a(\lambda) + L_r(\lambda) + t_d(\lambda) * L_w(\lambda)$

Where,  $L_t$  = Sensor detected radiance

$L_a$  = aerosol path Radiance

$L_r$  = Rayleigh path radiance

$L_w$  = water leaving radiance

$t_d$  = Atmospheric diffuse transmittance

The main idea of the atmospheric correction is to get rid of atmospheric path radiance for which OCM is equipped with two channels in infrared wavelength (channels 7 and 8) where ocean appears dark due to high infrared absorption by water. The radiation detected by OCM in these two bands is mainly due to scattering in the atmosphere and is used for estimating the atmospheric scattering contribution in lower wavelengths ( $\lambda < 700\text{nm}$ ) that is removed from sensor radiances through the atmospheric correction procedure (Gordon and Wang 1994). The atmospherically corrected water leaving radiances are subsequently utilised for the estimation of oceanic constituents using suitable bio-optical algorithms. Cloud screening algorithm is also applied on the OCM data prior to atmospheric correction procedure where albedo in Channel 8 (865nm) is computed and if found  $> 1.1\%$ , the pixel is masked as cloudy.

### **Chlorophyll *a* algorithm**

A variety of bio-optical algorithms for estimating Chlorophyll (C) and Chlorophyll and Phaeopigments (C+P) from ocean radiance data have been developed and most of them

are empirical equations derived by statistical regression of radiance versus Chlorophyll. During the present study, the empirical algorithm proposed by O'Reilly et al. (1998) known as Ocean Chlorophyll 2 or OC2 for processing SeaWiFS ocean colour data, has been used. O'Reilly et al. (1998) have proposed this algorithm after a comprehensive evaluation of a large number of semi-analytical and empirical bio-optical algorithms for the data collected from different sources and different global locations. OC2 captures the inherent sigmoidal relationship between  $R_{rs490}/R_{rs555}$  band ratio and the Chlorophyll concentration (C) Where  $R_{rs}$  is remote sensing reflectance. The simple and reversible functional form used by OC2 as well as its statistical and graphical results were superior to other formulations evaluated. The algorithm takes the following mathematical form:

$$C \text{ (mg m}^{-3}\text{)} = 10^{*(0.319 - 2.336*R + 0.879*R^2 - 0.135*R^3)} - 0.071$$

For  $0.01 \text{ mg m}^{-3} \leq C \leq 50 \text{ mg m}^{-3}$ .  $R = \log_{10} [R_{rs490}/R_{rs555}]$ .

#### **Algorithm for diffused attenuation coefficient (K)**

The following algorithm has been used for the calculation of the diffused attenuation coefficient K (490):

$$K(490) = 0.022 + 0.100 * [L_{wn}(443)/L_{wn}(555)]^{-1.30} \text{ (Muller and Charles 1994)}$$

Where  $L_{wn}$  is the water leaving radiance in the second and the fifth bands. K (490) has been computed by assuming case I waters where changes in phytoplankton biomass is considered to be the most important factor for the changes in optical properties of seawater.

#### **4.12.2 Estimation of Primary production**

Models for estimating primary productivity range from relatively simpler (empirical) to complex (spectral). During the present study non-spectral irradiance model proposed by Platt and Sathyendranath (1993) has been used with the following assumptions:

- \*Biomass is uniform throughout the upper mixed layer depth.
- \*Ignores spectral structure of irradiance.
- \*Sinusoidal variation of surface irradiance.

This model takes the mathematical form where water column primary production is proportional to the biomass (B), assimilation number ( $P_m^B$ ) and day length (D) and

inversely proportional to attenuation coefficient ( $K$ ) and is also a function of the normalised irradiance.

$$\int_{Z,T} P \sim [(B * P_m^B * D) / K] * f(I_0^m * \alpha^B / P_m^B)$$

Where,  $I_0^m$  is noon irradiance at sea surface and  $\alpha^B$  is the initial slope of photosynthesis-light curve.  $P_m^B$  and  $\alpha^B$  are called P-I parameters and are characteristic of given water mass.

The solution of the above equation is given in terms of fifth order polynomial and the whole equation is expressed as:

$$P_{Z,T} = [(B * P_m^B * D) / K] * \sum_{x=1}^5 \Omega_x (I^m)^x$$

After putting the weights ( $\Omega_x$ ) for  $x=1$  to 5 the equations takes the form:

$$P_{Z,T} = [(B * P_m^B * D) / K] * [0.610305 * I_m - 0.089251 * I_m^2 + 0.0081477 * I_m^3 - 0.00037427 * I_m^4 + 0.0000066103 * I_m^5]$$

Where,  $I_m = (I_0 * \alpha^B / P_m^B) * [e^{-K*Z1} - e^{-K*Z2}]$  and  $Z1$  and  $Z2$  are surface and mixed layer depth.

The parameters required in the model for the calculation and their sources are the following:

- Biomass (**B**) obtained using the OC2 model discussed above.
- Diffused attenuation Coefficient (**K**) obtained using the above model.
- Day Length (**D**) and
- Photosynthetically active Radiation (**I<sub>0</sub>**) for the desired days of year has been estimated using Bird's Clear Sky spectral irradiance model (Bird 1984) with adjustments by Sathyendranath and Platt (1988).
- **Z1** is the surface whereas **Z2** is the mixed layer depth taken from monthly mixed layer depth chart (Hasternath and Greisher 1989).
- The P-I parameters (**P<sub>m</sub><sup>B</sup>** and **α<sup>B</sup>**) are characteristics of water types and change over season and phytoplankton species. Assimilation number (**P<sub>m</sub><sup>B</sup>**) represents a point where photosynthesis becomes independent of light whereas the initial slope of photosynthesis-light curve (**α<sup>B</sup>**) is a measure of the effectiveness of phytoplankton in using the available light for photosynthesis. These two are obtained by generating a curve by a photosynthesis-light experiment, where a

sample of water containing phytoplankton are inoculated with a tracer for oxygen or carbon and incubated in a light gradient for a certain time period. To the best of our knowledge, no measurement of P-I parameter exists for the Bay of Bengal. During the present calculation  $P_m^B = 3.0 \text{ mg C (mg Chl)}^{-1} \text{ h}^{-1}$  and  $\alpha^B = 0.1 \text{ mg C (mg Chl)}^{-1} \text{ h}^{-1} (\text{Wm}^{-2})^{-1}$  has been used as in the case of the Arabian Sea (Brock et al. 1994).

#### 4.12.3 Discussion

The primary productivity maps have been generated for the study period (September-October 2002 and April-May 2003) in the Bay of Bengal. The maps obtained for the relatively cloud free days are shown in Plates 1 and 2. In general, the total productivity varied from 100 to 1500  $\text{mg C m}^{-2} \text{ d}^{-1}$ . The upper limit of productivity was mainly seen in the coastal waters (red colour). Chauhan et al. (2001) have shown that the OC2 algorithm when applied on OCM data works quite well for open ocean ( $r^2 = 0.85$ ; rms = 0.175  $\text{mg m}^{-3}$ ) whereas it was not found satisfactory in the sediment laden case-2 waters (coastal water). This adds to a high level of uncertainty to the primary productivity estimation in coastal waters. However, in general, the error in Chlorophyll determination by OCM data has been around 35% for the range 0.01-10  $\text{mg m}^{-3}$  (Prakash et al. 2001) and hence this is the minimum error for productivity values also. The productivity maps during September-October show the cloud cover over the Bay that diminishes at the beginning of October. The cloud cover over the Bay seems to be a permanent feature that is evident during April-May 2003 also, particularly in the coastal region. Pixel-wise examination of the productivity values suggests a general overestimation of productivity by remote sensing data compared to insitu values. The overestimation is more during September-October than April-May where insitu values are relatively higher. Figure 4.24 shows the log-log plot of insitu and OCM generated productivity values. When OCM data of same day as insitu experiment is not available due to difference in insitu experiment and OCM pass, the value of last or next OCM pass has been taken. The same exercise has been done for cloudy pixels. The OCM productivity to represent the insitu location has been estimated by taking the average of 3X3 pixels around the exact location. The Figure 4.24 indicates the overestimation of primary productivity by more than 40% at most of the locations by OCM, particularly during September-October. The observed overestimation in productivity is due to the

sum of errors involved in estimation of bio-optical and assumed P-I parameters. The P-I parameter value taken for calculation seems to be higher for the Bay of Bengal. The value taken is actually of summer period for the Arabian Sea and is known to overestimate productivity in the intermonsoons. Changes in P-I parameters ( $\alpha^B = 0.06 \text{ mg C (mg Chl)}^{-1}\text{h}^{-1} (\text{Wm}^{-2})^{-1}$ ) leads to a significant decrease in productivity value indicating the role of assumed high P-I parameter as one of the reasons for overestimation. The insitu determination of P-I parameters would greatly enhance the accuracy of productivity estimation by OCM data; however, P-I parameters are still scarce in the Arabian Sea and Bay of Bengal leading to significant errors in productivity estimation by algorithms using OCM data. Our measurements of new production and the linear relationship between new and total production can be used with improved algorithms in the Bay of Bengal to generate new production maps in the future.

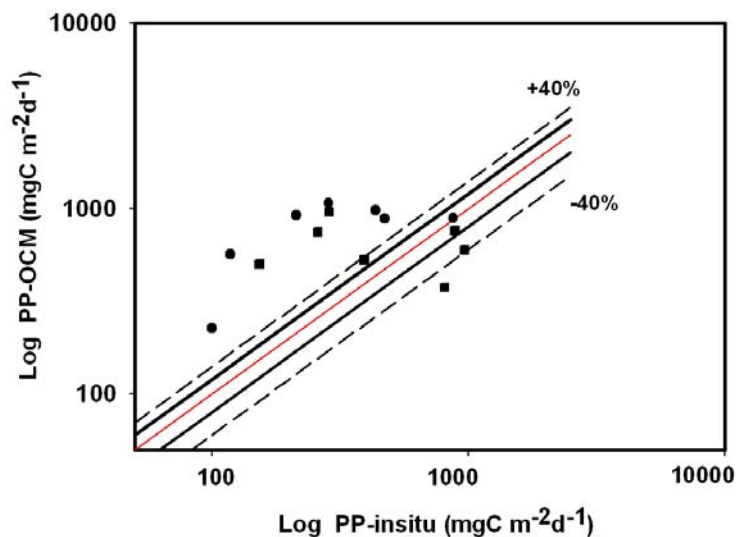
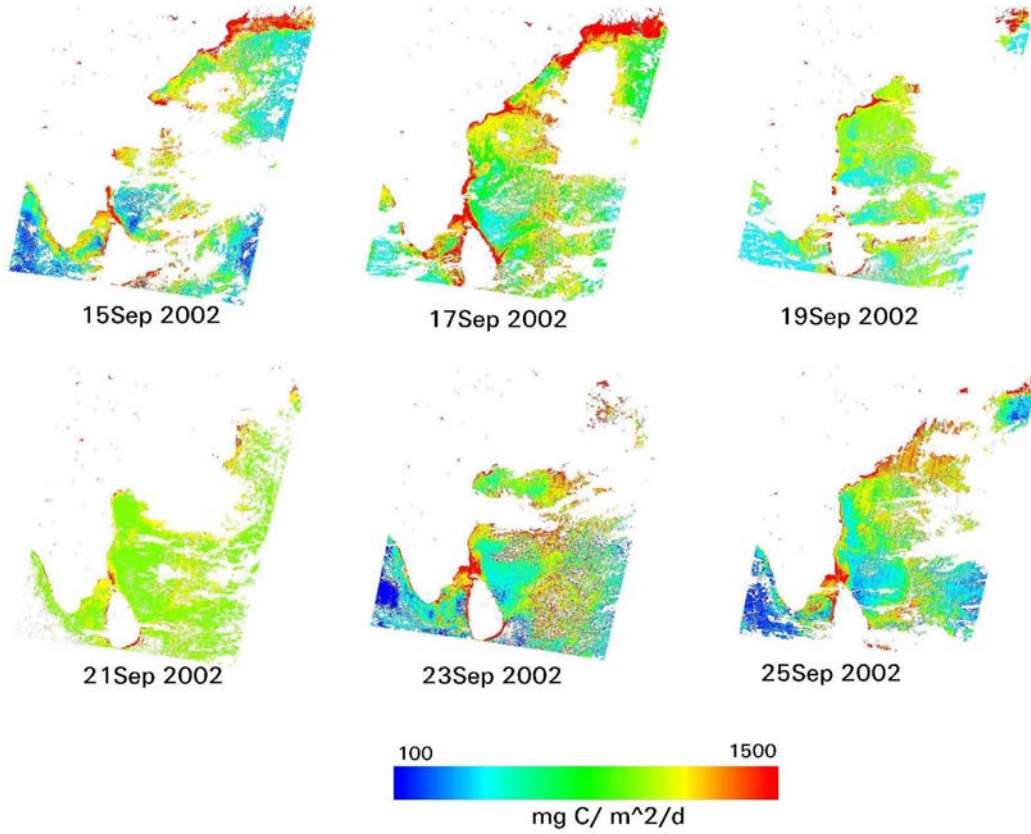


**Figure 4.24:** The Log-Log plot of euphotic zone integrated insitu primary productivity estimated by <sup>15</sup>N technique and corresponding climatological mixed layer integrated OCM values. The circles and squares represent September-October 2002 and March-April 2003 respectively.

Primary Productivity Map of the Bay of Bengal



Primary Productivity Map of the Bay of Bengal

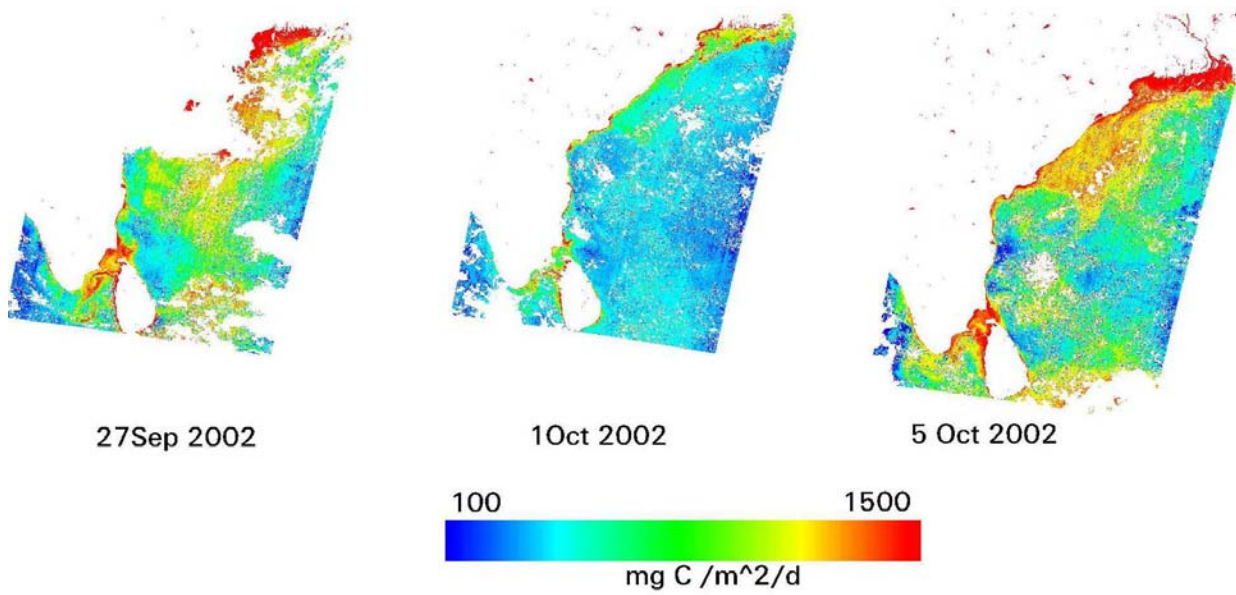
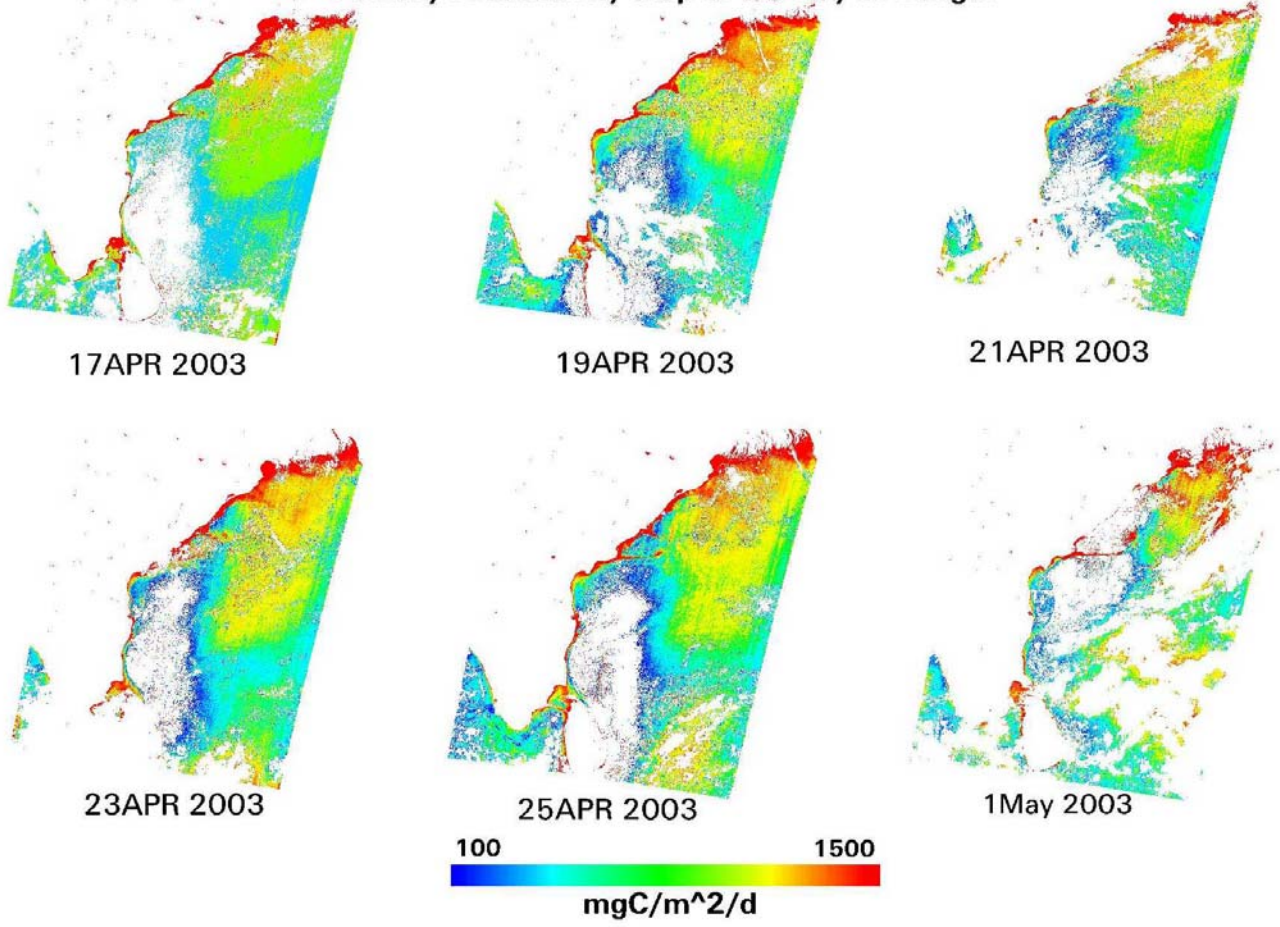


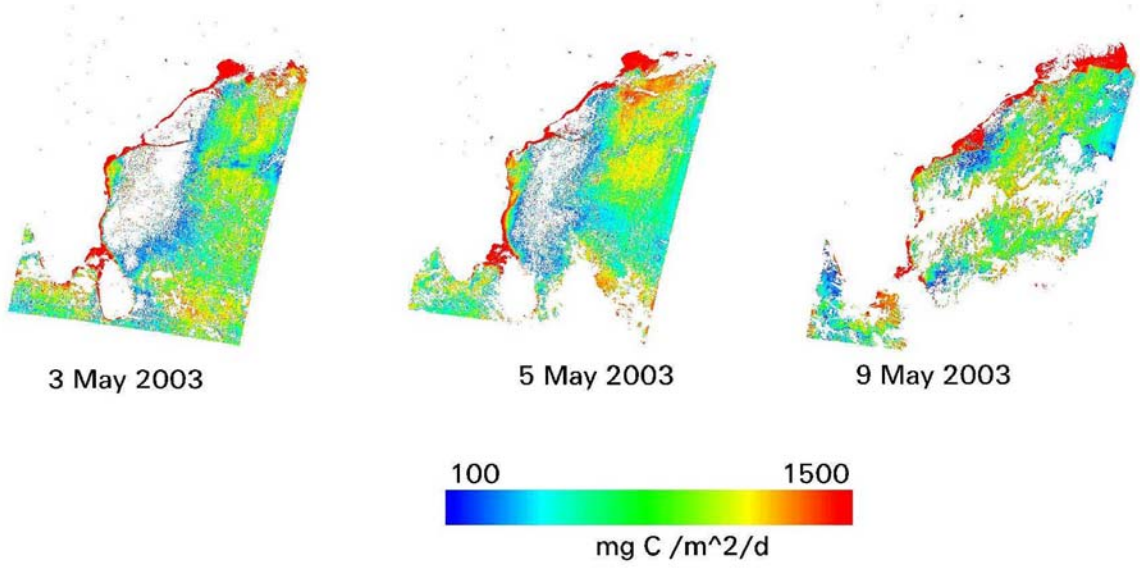
**PLATE 1**

**PLATE 2**

**Primary Productivity Map of the Bay of Bengal**



**Primary Productivity Map of the Bay of Bengal**



#### 4.13 Conclusions

The main aim of the present study in the Bay of Bengal was to estimate new production in different seasons. The natural nitrogen isotopic variabilities in suspended sediments and its fate at depth along with uptake experiments were also an important part of the work. The main results of the study are as follows:

- The new production measurements in the Bay of Bengal consistently show fairly high values, which average around  $2.6 \text{ mmol N m}^{-2} \text{ d}^{-1}$  during the postmonsoon and  $5.4 \text{ mmol N m}^{-2} \text{ d}^{-1}$  during the premonsoon.
- The average new production during premonsoon is more in the shelf area than in the offshore, contrary to that observed during the postmonsoon, reflecting the shift in the nitrate availability in the Bay.
- The observed higher new production in the Bay could also be one of the reasons for observed high organic carbon fluxes in the sediment trap.
- The observed high new production could be the reason for observed low  $\text{pCO}_2$  in the surface Bay of Bengal and OMZ.
- $\delta^{15}\text{N}$  of the surface PON in the Bay during postmonsoon shows a signature of mixing between continental and marine inputs.
- $\delta^{15}\text{N}$  of PON increases with depth as in the case of other oceans; however, the increase is lower than in the eastern Indian Ocean, indicating the role of high settling rates of sinking particles in the Bay.
- New production, in general, may be underestimated if incubation time is less than four hours.

**Chapter 5**  
**Summary and**  
**Scope for future work**

---

---

## **5.1 Important findings of this study**

The present study has added new data that can lead to better understanding of carbon fixing potential of the northern Indian Ocean. **For the first time**, new production and natural isotopic variability of nitrogen have been measured in the Bay of Bengal and the northeastern Arabian Sea. In addition, some uptake experiments and the estimation of primary productivity using IRSP4 data has provided insights into the experimental procedure and parameters to be adopted for the region. The important results that have emerged from this study and their implications are summarized below:

### **5.5.1 New production in the Bay of Bengal**

The results obtained from the estimation of new production in the Bay of Bengal during the present study have emphasized the role of moderately productive oceans in the global carbon and nitrogen cycles. An ocean basin, such as the Bay of Bengal, is capable of high new production, and thus can be efficient in removing the atmospheric CO<sub>2</sub> on longer time scales. The results obtained so far have the following possible implications:

#### **Reason for comparable organic carbon flux observed in sediment traps**

The average rate of photosynthetic fixation of carbon by marine phytoplankton is more than a factor of two higher in the Arabian Sea than in the Bay of Bengal. Although there is some seasonal and geographical variability, the typical average <sup>14</sup>C based productivity in the Arabian Sea is around 1200 mgC m<sup>-2</sup> d<sup>-1</sup>, (Barber et al., 2001), whereas in the Bay it is about 300 mg C m<sup>-2</sup> d<sup>-1</sup> (Madhupratap et al., 2003). However, the time averaged sediment trap data indicate that on the basin scale, the downward flux of organic carbon in the Arabian Sea is not proportionately higher than that of Bay of Bengal, except for the upwelling region in the north-west. The experiments done in two different seasons discussed earlier consistently show relatively higher new production (averaging around 2.6 mmolN m<sup>-2</sup> d<sup>-1</sup> during postmonsoon and 5.4 mmol N m<sup>-2</sup> d<sup>-1</sup> during premonsoon) and could be one of the reasons for relatively higher downward organic carbon flux in the moderately productive Bay. One explanation for this observation is the "ballast hypothesis", whereby organic carbon is ballasted into the deep by the high lithogenic flux from rivers, which form aggregates with the former (Ittekkot 1991). However, independent estimates of new production based on nitrogen

uptake during present study have helped to understand this in a better way, because, new production and particle sinking are coupled over longer time scales (Eppley et al. 1983). Consistent higher new production observed during two different seasons in the Bay indicates its role in the observed organic carbon flux on the time scales of sediment traps data. Hence, such oceanic regions may play a more significant role in removing the excess anthropogenic CO<sub>2</sub> from the atmosphere, than believed so far.

### **Reasons for reduced pCO<sub>2</sub> in surface Bay of Bengal**

Limited earlier data regarding the air-sea exchange of CO<sub>2</sub> for the northern Indian Ocean in general, and Bay of Bengal in particular reveals that a large area of the Bay is characterized by pCO<sub>2</sub> levels far below the atmospheric value (~350 μatm). This effect was found to be more prominent during northeast monsoon when air-sea pCO<sub>2</sub> gradient sometimes exceeds 100 μatm. Kumar et al. (1996) predicted that cause for the low pCO<sub>2</sub> in the Bay could be physical as well as biological processes. One such important physical parameter known to decrease the pCO<sub>2</sub> level is salinity, however, Kumar et al, (1996) have shown that the salinity can lower the pCO<sub>2</sub> by a maximum of ~30 μatm, which was about 25% of the highest recorded pCO<sub>2</sub> drawdown, and therefore predicted that biological activity should account for most of the observed pCO<sub>2</sub> decrease by sustaining moderately high new production. New production during April-May 2003 (overall average~ 433 with shelf region average of 552 and offshore average of 284 mg C m<sup>-2</sup> d<sup>-1</sup>) and September-October 2002 (overall average~ 207 with shelf stations averaging around 180 and offshore region around 243 mgC m<sup>-2</sup> d<sup>-1</sup>) observed during present study in the Bay of Bengal is indeed higher and comparable to the new production off India, 400±160 mg C m<sup>-2</sup> d<sup>-1</sup> reported for the Arabian Sea. Therefore, the present study successfully verifies the earlier conjecture put forward to explain the low pCO<sub>2</sub> in the surface Bay.

### **Contributing to development of Oxygen Minimum Zone in the Bay**

Presence of OMZ in ocean is usually explained by the utilization of oxygen due to decomposition of organic matter brought into the deeper water from surface that holds good for the productive Arabian Sea. But the existence of OMZ in the Bay of Bengal, where the overhead productivity is moderate, is puzzling. The present study provides one possible explanation. Due to the observed high new production in the Bay the flux

of material going to the deeper waters could be more than that previously believed and this higher flux could be responsible for consuming the available dissolved oxygen for the decomposition, leading to the formation of OMZ.

### **5.5.2 Results from uptake experiment**

The mechanism through which nutrients are supplied and the kinetics of dissolved inorganic nitrogen utilization play a critical role in determining the productivity, size structure, and species succession of phytoplankton in the world ocean. During the present study, experiments were performed to examine the effect of concentration and time on the uptake rate of different nitrogenous species, which lead to the following results.

New production may be underestimated if the incubation time is less than four hours. Incubation done for different time periods (one to four hours) after adding the enriched tracers for nitrate, ammonium and urea revealed that the uptake rate for nitrate remained the same for the first two hours but increased after the end of fourth hour (from 0.92 to 1.5  $\mu\text{mol m}^{-3}\text{h}^{-1}$ ). However, for ammonium, it decreased after one hour and remained the same for higher incubation times (0.74 to 0.38  $\mu\text{mol N m}^{-3}\text{h}^{-1}$ ). The urea uptake declined after the third hour (2.48 to 1.56  $\mu\text{mol N m}^{-3}\text{h}^{-1}$ ). These variations in uptake rates of different N-species lead to change in the f-ratio from 0.29 (after two hours) to 0.42 (after four hours).

An opposite trend has been observed for the case where tracer addition significantly higher than 10% of the ambient concentration was made. When the concentration of tracer was varied (keeping the incubation time constantly four hours), the uptake rate for both urea [ $y = 1.88x + 0.004$  ( $r^2 = 0.88$ )] and ammonium [ $y = 2.07x - 0.002$  ( $r^2 = 0.55$ )] showed a positive relationship with substrate concentration (x). However, nitrate uptake [ $y = -0.76x + 0.05$  ( $r^2 = 0.86$ )] showed a negative correlation. The f-ratio changed from 0.47 to 0.10 when tracer added was increased from 0.01 to 0.04  $\mu\text{M}$ .

### **5.5.3 Natural isotopic composition of nitrogen in suspended matter of the Bay of Bengal**

The first systematic measurements of  $\delta^{15}\text{N}$  in surface suspended matter of shelf as well as northern offshore Bay of Bengal shows signatures of mixing between continental inputs and marine sources. Dilution by the organic and detrital continental material

brought in by rivers leads to a consistently lower  $\delta^{15}\text{N}$ , evident from the relationship between surface salinity and  $\delta^{15}\text{N}$ .  $\delta^{15}\text{N}$  values of surface PON of open ocean locations during both seasons, and also at coastal locations during premonsoon suggest nitrate from deeper waters to be a predominant source of nutrients to the phytoplankton. The depth profiles of  $\delta^{15}\text{N}$  of PON during the premonsoon season at nine different locations are in agreement with the observed trend in the world ocean i.e., they increase with depth. This increase in  $\delta^{15}\text{N}$  is by maximum around 4‰ between top 60m and 300m, which is lower than that observed in the far eastern Indian Ocean, indicating the role of higher sinking rates of particles ballasted by aggregates of organic and mineral matter in BOB. The particulate organic nitrogen content decreases with depth as expected.

#### **5.5.4 Total productivity comparison with IRSP4 data**

Primary productivity was calculated using indigenous satellite data during the present study. However, lack of P-I parameters in the Bay of Bengal and errors in retrieval of oceanic constituents from satellite data led to overestimation of total production. Comparison of the  $^{15}\text{N}$  based total production and total production obtained from IRSP4 data reveals the overestimation of satellite based production by more than 40%.

#### **5.5.5 New and regenerated production in the Northeastern Arabian Sea**

The new and regenerated production in the northeastern Arabian Sea has been estimated for the first time during present study. At almost all the stations during January  $\text{NH}_4$  was assimilated in preference to urea and  $\text{NO}_3$ . This preference may be because of higher energy requirement during the assimilation of  $\text{NO}_3$ . Overall variation in the f ratio is from 0.15 to 0.60 and the inclusion of urea uptake rates in the calculation leads to a decrease in the overall average f-ratio by almost 27%.

#### **Effect of winter cooling on new production and f-ratio during January**

New production and f- ratio, in general, show increasing trends from the south (off Goa) to the north (off Gujarat), clearly depicting the systematic effect of intensification of winter cooling. Northeast trade winds prevalent in the region during this season bring the cool, dry continental air causing an increase in the evaporation and heat loss from the surface water. This intensified evaporation leads to surface cooling and consequent increase in the density, causing the surface water to sink setting up

convective mixing. This whole process leads to a deepening of the MLD and consequent transport of nutrients from the base of the mixed layer and upper thermocline to the surface to increase the new production. The increased MLD also suggests a strong coupling between the surface and subsurface layers.

Negative relationship between f-ratio and integrated nitrate has been observed during the month of January indicating that even at higher column nitrate, the f-ratio can be low, probably due to the inefficient utilization of nitrate. This situation can arise because of suppression of nitrate uptake by the presence of ammonium or because of higher addition of  $^{15}\text{NH}_4$  tracer. However, during the present study the ammonium addition has not been found to be a possible reason. The third possibility could be the deterioration of light condition due to the deep mixed layer and a relative preference for ammonium in light limited conditions.

#### **Increased new production during late February-early March bloom and nutrients for its sustenance**

The average column new production during March has been found to be more than five times the new production observed during January; however, there is no systematic spatial variability in the new production as was the case during January. The f-ratio (upper bound) in the region averages around 0.60 ( $\pm 0.10$ ) and inclusion of urea uptake rate into the calculation decreases it by almost a similar fraction (25%) as during January. The observed increase in new production may be due to lateral advection of nutrients from the first three stations or it may be sustained by the nutrient that entrained during January. The nitrate residence time for the nitrate entrained during January at most of the stations was more than 50 days suggesting that if the same rate of removal due to nitrate uptake by phytoplankton continues, the nitrate in the water column will remain at least for 50 days. This nitrate might have sustained the bloom during February-March, once the light conditions became optimum due to the waning effect of winter cooling.

#### **5.5.6 Natural isotopic composition of nitrogen in the suspended matter of the Arabian Sea**

The nitrogen isotopic composition of the surface suspended matter has been estimated during the January and early March in the Arabian Sea. Most noticeable and significant is the overall increase by  $\sim 5\text{‰}$  in  $\delta^{15}\text{N}$  of the surface suspended matter in the region

from January to March. Similarly, a significant increase of  $0.7\mu\text{M N}$  in PON content has also been observed. This increase in the isotopic composition of PON during March is possible due to an overall increase in the nitrogen isotopic composition of source ( $\delta^{15}\text{N}$ ) nutrient taken up by the phytoplankton or due to a change in the fractionation behaviour of the phytoplankton, while maintaining the same  $\delta^{15}\text{N}$  of nitrate during both periods. The analysis of nutrient regime suggests that if the deeper nitrate is the source during both months, the observed increase may be indicative of intensified denitrification leading to an isotopic enrichment of the source nitrate. And if the nitrate entrained during the January is the source, the continuous uptake by the phytoplankton might have led to an isotopic enrichment observed during March.

## **5.2 Scope for future work**

The Arabian Sea and the Bay of Bengal provide magnificent environments to understand the complexity of carbon and nitrogen cycles and their isotopes. These two adjacent basins are endowed with significantly different marine environments. On the one hand, the Bay can be studied for the effect of fresh water input on marine realm, while the Arabian Sea offers highly productive regions and denitrification zones to study the biogeochemistry of nitrogen and its isotopes. An attempt has been made during present study to cover a few biogeochemical aspects of nitrogen and its isotopes, the present study can be improved and new research can be pursued in this field. Based on the limitations faced during present study, the following could be areas of potential future research:

### **(A) Thorough understanding of nutrient regime in the Arabian Sea and Bay of Bengal.**

One of the major limitations of the present work is the non-availability of the ambient ammonium and urea concentrations leading to conservative estimates of regenerated production (except for January in the Arabian Sea). Arabian Sea is one of the most studied basins in the world but the knowledge of ambient ammonium and urea concentrations remains limited, particularly in the northeastern Arabian Sea. There is no data for ammonium and urea in the Bay of Bengal, to best of our knowledge. The thorough understanding of nutrient regime in these two basins, particularly in the Bay

of Bengal, can provide immense information about the regenerated production and its seasonal and spatial variability.

**(B) Study of nutrient inputs by rivers**

The nutrients brought in by rivers are known to affect the ecosystem of coastal waters. Bay of Bengal receives a huge amount of freshwater influx, potentially bringing a lot of nutrients; but a thorough knowledge of the amounts of nutrients such as nitrogen and phosphorus brought in by major rivers to the Bay is lacking, which could have provided important insights into the role these extraneous nutrients play in sustaining new production. Nitrogen and oxygen isotope based studies to infer the source of nutrients, particularly nitrate, for the rivers like Ganga and Brahmaputra during their journey from source to the ocean could be a challenging area of research.

**(C) Study of Atmospheric input of nutrients**

The dry and wet deposition of nutrients to the ocean and its role in modifying the productivity has gained momentum in recent years due to its significant contribution particularly to the oceanic regime closer to landmass (Kouvarakis et al. 2001). The Arabian Sea and Bay of Bengal have the potential to receive the atmospheric inputs particularly during monsoon periods. The increased frequency of atmospheric sampling in these basins can enhance our present understanding of nutrient inputs by atmospheric deposition.

**(D) The isotopic composition of nitrate and ammonium**

The knowledge of isotopic composition of seawater nitrate and ammonium is very essential to thoroughly understand the nutrient utilization behaviour in the marine environment. It would help in finding a better explanation of the observed variability in the isotopic composition of suspended matter and related fractionation patterns along with identifying the source of nutrients. Only one vertical profile for the isotopic composition of nitrate exists in the Arabian Sea (Brandes et al. 1998). However, there are no such measurements for ammonium. No such studies have been done in the Bay of Bengal either. The thorough study of nutrient concentrations along with their isotopic compositions would make a challenging and very significant study to take up.

**(E) The P-I parameter evaluation**

As mentioned in the earlier chapter, knowledge of exact P-I parameters for the Bay of Bengal and the Arabian Sea during different seasons would provide an opportunity to develop the primary and new production maps for the region and would help in estimating the carbon fixing potential of the region on larger temporal and spatial scales with better accuracy using satellite data.

# References

---

---

- Allen C.B.**, Kanda J. and Laws E.A. (1996) New production and photosynthetic rates within and outside a cyclonic mesoscale eddy in the North Pacific subtropical gyre, *Deep-Sea Res.*, 43, 917-936.
- Altabet M.A.** and McCarthy J.J. (1985) Temporal and spatial variations in the natural abundance of  $^{15}\text{N}$  in PON from warm core ring, *Deep-Sea Res., Part A*, 32, 755-772.
- Altabet M.A.** and McCarthy J.J. (1986) Vertical patterns in  $^{15}\text{N}$  abundance in PON from the surface waters of warm core rings, *J Mar. Sci.*, 44, 185-201.
- Altabet M.A.** (1988) Variations in nitrogen isotopic composition between sinking and suspended particles: Implications for nitrogen cycling and particle transformation in the open ocean, *Deep-Sea Res., Part A*, 35, 535-554.
- Altabet M.A.**, Deuser W.G., Honjo S. and Stienen C. (1991) Seasonal and depth-related changes in the source of sinking particles in the North Atlantic, *Nature*, 354, 136-139.
- Altabet M.A.** and Francois R. (1994) The use of nitrogen isotopic ratio for reconstruction of past changes in the surface ocean nutrient utilization, In: *Carbon Cycling in the Glacial Ocean: Constraints on the Ocean's Role in Global Change* (Eds) Zahn, R., Kaminski, M.A., Labeyrie, L., and Pederson, T. F., 281-306, Springer-Verlag, New York.
- Altabet M.A.** (1996) Nitrogen and carbon isotopic tracers of the source and transformation of particles in the Deep-Sea, In: *Particle Flux in the Ocean* (Eds) Ittekkot, V., Schafer, P., Honjo, S., and Depetris, P.J., 155-184, John Wiley, New York.
- Asper V.L.** and Smith W.O. (1999) Particle fluxes during austral spring and summer in the southern Ross Sea (Antarctica), *J. Geophys. Res.*, 104, 5345-5360.
- Bacon M.P.**, Huh C.A., Flerer A.P. and Deuser W.G. (1985) Seasonality in the flux of natural radionuclides and plutonium in the deep Sargasso Sea, *J. Mar. Res.*, 44, 185-201.
- Banse K.** (1984) Overview of the hydrography and associated biological phenomena in the Arabian Sea, off Pakistan, In: *Marine geology and oceanography of Arabian Sea and coastal Pakistan* (Eds) Haq B.U. and Milliman J.D., 271-303, Van Nostrand Reinhold Co., New York.
- Banse K.** and McClain (1986) Winter blooms of phytoplankton in the Arabian Sea as observed by the coastal zone color scanner, *Mar. Ecol. Progr. Ser.*, 34, 201-211.
- Banse K.** (1987) Seasonality of phytoplankton chlorophyll in the central and northern Arabian Sea, *Deep-Sea Res. I*, 34, 713-723.

- Banse K** (1992) Grazing, temporal changes of phytoplankton concentrations and the microbial loop in the open sea, In: Primary Productivity and Biogeochemical Cycles, (Eds) Falkowski P. and Woodhead A.D., 409-440, Plenum, New York.
- Banse K. and English D.C.** (1993) Revision of satellite-based phytoplankton pigment data from the Arabian Sea during the northeast monsoon, *Mar. Res.*, 2, 83-103.
- Barber R.T.** (1992) Introduction to the WEC88 cruise: An investigation into why the equator is not greener, *J. Geophys. Res.*, 97, 609-610.
- Barber R.T., Murray J.W. and McCarthy J.J.** (1994) Biogeochemical interactions in the equatorial Pacific, *Ambio*, 23, 62-66.
- Barber R.T., Sanderson M.P., Lindley S.T., Chai F., Newton J., Trees C.C., Foley D.G. and Chavez F.P.** (1996) Primary productivity and its regulation in the equatorial Pacific during and following the 1991-92 El Niño, *Deep-Sea Res. II*, 43, 933-969.
- Barber R.T., Marra J., Bidigare R.C., Codispoti L.A., Halpern D., Johnson Z, Latasa M., Goericke R. and Smith S.L.** (2001) Primary productivity and its regulation in the Arabia Sea during 1995, *Deep-Sea Res. II*, 48, 1127-1172.
- Bender M., Ducklow H., Kiddon J., Marra J. and Martin J.** (1992) The carbon balance during the 1989 spring bloom in the North Atlantic Ocean, 47°N, 20°W, *Deep-Sea Res.*, 39, 1707-1725.
- Ben-Yaakov S., Ruth E. and Kaplan I.R.** (1974) Calcium carbonate saturation in northeastern Pacific: *In situ* determination and geochemical implications, *Deep-Sea Res.*, 21, 229-2243.
- Berger W.H., Fisher K., Lai C. and Wu G.** (1987) Oceanic productivity and organic carbon flux, *Scripps Institution of Oceanography reference 87(30)*, 1-67.
- Bhattathiri P. M. A., Devassy V. P. and Radhakrishna K.** (1980) Primary production in the Bay of Bengal during southwest monsoon of 1978, *Mahasagar- Bulletin of the National Institute of Oceanography*, 13, 315-323.
- Bhattathiri P. M. A., Pant A., Sawant S., Gauns M., Matondakar S. G. P. and Mohanraju R.** (1996) Phytoplankton production and chlorophyll distribution in eastern and central Arabian Sea in 1994-1995, *Curr. Sci.*, 71, 857-862.
- Bird R.E.** (1984) A simple, solar spectral model for direct normal and diffuse horizontal irradiance, *Solar Energy*, 32, 461-471.
- Blackmer A.M. and Bremner J.M.** (1977) Nitrogen Isotope discrimination in denitrification of nitrate in soils, *Soil Biol. Biochem.*, 9, 73-77.
- Brandes J.A., Devol A.H., Yoshinari T., Jayakumar T.A. and Naqvi S.W.A.** (1998) Isotopic composition of nitrate in the central Arabian Sea and eastern tropical north Pacific: a tracer for mixing and nitrogen cycles, *Limnol. Oceanogr.*, 43, 1680-1689.

- Bremner J.M.** and Blackmer, A.M. (1981) Terrestrial nitrification as a source of atmospheric nitrous oxide, In: Denitrification, Nitrification, and atmospheric nitrous oxide (Ed) Delwiche C.C., Wiley, New York.
- Brock J.C.**, McClain C.R., Luther M.E. and Hay W.W. (1991) The phytoplankton bloom in the northwestern Arabian Sea during the southwest monsoon of 1979, *J. Geophys. Res.*, 96,20 623-20642.
- Brock J.C.** and McClain C.R. (1992) Interannual variability in phytoplankton blooms observed in the northwestern Arabian Sea during the Southwest monsoon, *J. Geophys. Res.*, 97, 733-750.
- Brock J.**, Sathyendranath S. and Platt T. (1993) Modelling the seasonality of subsurface light and primary production in the Arabian Sea, *Mar. Ecol. Prog. Ser.*, 101,209-221.
- Brock J.**, Sathyendranath S. and Platt T. (1994) A model study of seasonal mixed layer primary production in the Arabian Sea, *Proc. Ind. Acad. Sci. (Earth Planet. Sci.)*, 103 (2), 163-176.
- Broecker W.S.** (1982) Glacial to interglacial changes in ocean chemistry, *Progr. Oceanogr.*, 11, 151-197.
- Broecker W.S.**, Ledwell J.R., Takahashi T., Weiss R., Merlivat L., Memery L., Peng T.H., Jahne B. and Munnich K.O. (1986) Isotopic versus micrometeorologic ocean CO<sub>2</sub> fluxes: A serious conflict, *J. Geophys. Res.*, 91, 10517-10527.
- Broenkow W. W.** and Cline J.D. (1969) Calorimetric determination of dissolved oxygen at low concentrations, *Limnol. Oceanogr.*, 14,450-14,454.
- Bronk D.A.**, Glibert P.M. and Ward B.B. (1994) Nitrogen uptake, dissolved nitrogen release and new production, *Science*, 265, 1843-1846.
- Buesseler K.O.** (1998) The decoupling of production and particulate export in the surface ocean, *Global Biogeochem. Cycle*, 12, 297-310.
- Buesseler K.O.** (1991) Do upper-ocean sediment traps provide an accurate record of particle flux? *Nature*, 353, 420-423.
- Buesseler K.O.**, Bacon M.P., Cochran J.K. and Livingstone H.D. (1992) Carbon and nitrogen export during the JGOFS North Atlantic bloom experiment estimated from <sup>234</sup>Th: <sup>238</sup>U disequilibria, *Deep-Sea Res.*,39,115-1137.
- Burkill P.H.**, Mantoura R.F.C. and Owens N.J.P. (1993) Biogeochemical cycling in the northwestern Indian Ocean: a brief overview, *Deep-Sea Res. II*, 40, 643-649.
- Calvert S. E.**, Nielsen B. and Fontugne M.R. (1992) Evidence from nitrogen isotope ratios for enhanced productivity during formation of eastern Mediterranean sapropels, *Nature*, 359,223-225.

**Capone D.G.**, Zehr J.P., Paerl H.W., Bergman B. and Carpenter E.J. (1997) *Trichodesmium*, a Globally significant marine Cyanobacterium, *Science*, 276, 1221-1229.

**Capone D.G.** (2001) Marine nitrogen fixation: What's the fuss? *Current opinion in microbiology*, 4, 341-348.

**Chauhan P.**, Nagur C. R. C., Mohan M., Nayak S. and Navalgund, R. R., (2001) Surface Chlorophyll *a* distribution in Arabian Sea and Bay of Bengal using IRS P4 OCM satellite data, *Curr. Sci.*, 80 (2), 127-129.

**Cline J.D.** and Kaplan I.R. (1975) Isotopic fractionation of dissolved nitrate during denitrification in the eastern tropical North Pacific Ocean, *Mar. Chem.*, 3, 271-299.

**Cochlan W.P.** and Bronk D.A. (2001) Nitrogen uptake kinetics in Ross Sea, Antarctica, *Deep-Sea Res. II*, 48, 4127-4153.

**Cole J.J.**, Pace M.L. and Fidlay S. (1988) Bacterial production in fresh and saltwater ecosystems: a cross system overview, *Mar. Ecol. Prog. Ser.*, 43, 1-10.

**Collos Y.** (1987) Calculation of  $^{15}\text{N}$  uptake rates by phytoplankton assimilating one or several nitrogen sources, *Int. J. Rad. Appl. Instrum., Part A*, 275-282.

**Conway H.L.** (1977) Interaction of inorganic nitrogen in the uptake and assimilation by marine phytoplankton, *Mar. Biol.*, 39, 221-232.

**Cullen J.J.** (1991) Hypotheses to explain high nutrient, low chlorophyll conditions in the open sea, *Limnol. Oceanogr.*, 36, 1578-1599.

**Das P.K.** (1995) *The monsoons*, 219, National Book Trust, New Delhi.

**Datta D.K.** (1999) Dissolved phosphate in the Ganges-Brahmaputra-Meghna river system in the Bengal Basin, Bangladesh, *Mitteilungen aus dem Geologisch - Palaontologischen Institut der Universitat Hamburg*, SCOPE/UNEP Sonderband 82, 131-138.

**Delwiche C.C.** (1970) The nitrogen Cycle, *Scientific American*, 223, 136-147.

**Delwiche C.C.** (1981) The nitrogen cycle and nitrous oxide, In: *Denitrification, Nitrification, and atmospheric nitrous oxide* (Ed) Delwiche C.C., Wiley, New York.

**DeNiro M.J.** and Epstein S. (1981) Influence of diet on the distribution of nitrogen isotopes in animals, *Geochim. Cosmochim. Acta*, 45, 341-351.

**DeSousa S. N.**, Naqvi S. W. A. and Reddy C. V. G. (1981) Distribution of nutrients in the western Bay of Bengal, *Ind. J. Mar. Sci.*, 10, 327-331.

**Devol A.H.** (1978) Bacterial oxygen uptake kinetics as related to biological processes in oxygen deficient zones of the oceans, *Deep-Sea Res.*, 25, 137-146.

- DiTullio G.R.** and Laws E.A. (1991) Impact of an atmospheric-oceanic disturbance on phytoplankton community dynamics in the North Pacific Central Gyre, *Deep-Sea Res.*, 38, 1305-1329.
- Doerffer R.** (1992) Imaging spectroscopy for detection of chlorophyll and suspended matter, In: *Imaging Spectroscopy: Fundamentals and Prospective Applications* (Eds) Toselli F. and Bodechtel J., 215-257, Kluwer Academic Publisher.
- Donald K.M.**, Joint I., Rees A.P., Woodward E.M.S. and Savidge G. (2001) Uptake of carbon, nitrogen and phosphorus by phytoplankton along the 20°W meridian in the NE Atlantic between 57.5°N and 37°N, *Deep-Sea Res. II*, 48, 873-897.
- Dore J. E.** and Karl D. M. (1996) Nitrification in the euphotic zone as a source of nitrite, nitrate, and nitrous oxide at station ALOHA, *Limnol. Oceanogr.*, 41, 1619-1628.
- Dortch Q.** (1990) The interaction between ammonium and nitrate uptake in phytoplankton, *Mar. Ecol. Progr. Ser.*, 61, 183-201.
- Dowling C.B.**, Poreda R.J. and Basu A.R. (2003) The ground water geochemistry of Bengal Basin: Weathering, chemisorption, and trace metal flux to the oceans, *Geochim. Cosmochim. Acta*, 67(12), 2117-2136.
- Duce et al.** (1991) The atmospheric input of trace species to the world ocean, *Global Biogeochem. Cycles*, 5, 193-259.
- Ducklow H.W.** and Harris R. (1993) Introduction to the JGOFS North Atlantic Bloom Experiment, *Deep-Sea Res. II*, 40, 1-8.
- Ducklow H.W.** (1995) Ocean Biogeochemical fluxes: New production and export of organic matter from the upper ocean, *Rev. Geophys.*, Supplement, 1271-1276.
- Ducklow H.W.** (1999) The bacterial content of the oceanic euphotic zone, *Fems. Microbiol. Ecol.*, 30,1-10.
- Dugdale R.C.** (1967) Nutrient limitation in the sea: Dynamics, identification, and significance, *Limnol. Oceanogr.*, 12, 685-695.
- Dugdale R.C.** and Goering J.J. (1967) Uptake of new and regenerated forms of nitrogen in primary productivity, *Limnol. Oceanogr.*, 12, 196-206.
- Dugdale R.C.** and Wilkerson F.P. (1986) The use of <sup>15</sup>N to measure nitrogen uptake in eutrophic oceans; experimental considerations, *Limnol. Oceanogr.*, 31, 673-689.
- Dugdale R.C.**, Wilkerson F.P., Barber R. T. and Chavez F.P. (1992) Estimating new production in the Equatorial Pacific Ocean at 150° W, *J. Geophys. Res.*, 97, 681-686.
- Emerson S.P.**, Quay P., Stump C., Wilbur S. and Knox M. (1991) O<sub>2</sub>, Ar, N<sub>2</sub> and <sup>222</sup>Rn in surface waters of subarctic ocean: net biological O<sub>2</sub> production, *Global Biogeochem. Cycles*, 5, 49-69.

- Emerson S.**, Quay P. and Wheeler P.A. (1993) Biological productivity determined from oxygen mass balance and incubation experiments, *Deep-Sea Res.*, 40, 2351-2358.
- Emerson S.**, Quay P., Karl D., Winn C., Tupas L. and Landry M. (1997) Experimental determination of organic carbon flux from open Ocean surface waters, *Nature*, 389, 951-954.
- Eppley R.W.**, Sharp J.H., Renger E.H., Perry M.J. and Harrison W.G. (1977) Nitrogen assimilation by phytoplankton and other microorganism in the surface waters of the central North Pacific Ocean, *Mar. Biol.*, 39, 111.
- Eppley R.W.** and Peterson B.J. (1979) Particulate organic matter flux and planktonic new production in the deep ocean, *Nature*, 282, 677-680.
- Eppley R.W.**, Renger E.H. and Betzer R.R. (1983) The residence time of particulate organic carbon in the surface layer of the ocean, *Deep-Sea Res.*, 30, 311-323.
- Falkowski P.G.**, Laws E.A., Barber R.T. and Murray J.W. (2003) Phytoplankton and their role in primary new and export production, In: *Ocean Biogeochemistry* (Ed) Fasham M.J.R., 99-121, Springer, Heideberg.
- Farrell J.W.**, Pederson T.F., Calvert S.E. and Nielsen B. (1995) Glacial-interglacial changes in nutrient utilization in equatorial Pacific Ocean, *Nature*, 377, 514-517.
- Field C.**, Behrenfeld M., Randerson J. and Falkowski P. (1998) Primary production of the biosphere: integrating terrestrial and oceanic components, *Science*, 281, 237-240.
- Findlater J.** (1974) The low-level cross equatorial air current of the western Indian Ocean during the northern summer, *Weather*, 29, 411-416.
- Fitzwater S.E.**, Knauer G.A. and Martin J.H. (1982) Metal contamination and its effects on primary production measurements, *Limnol. Oceanogr.*, 27, 544-551.
- Flynn K.J.**, Fasham M. J. R. and Hipkin C.R. (1997) Modelling the interactions between ammonium and nitrate uptake in marine phytoplankton, *Philosophical Transactions of London B* 352, 1625-1645.
- Flynn K.J.** (1998) Estimation of kinetic parameters for the transport of nitrate and ammonium into marine phytoplankton, *Mar. Ecol. Prog. Ser.*, 169, 13-28.
- Fogel M.L.** and Cifuentes L.A. (1993) Isotope fractionation during primary production, In: *Organic Geochemistry*, (Eds) Engel M.H. and Macko S.A., 73-98, Plenum Press, New York.
- Francois R.**, Altabet M.A. and Burkle L.H. (1992) Glacial to interglacial changes in surface nitrate utilization in the Indian Sector of the Southern Ocean as recorded by sediment  $\delta^{15}\text{N}$ , *Paleoceanography*, 7, 589-606.

**Frost B.W.** and Franzen N.C. (1992) Grazing and iron limitation in the control of phytoplankton stock and nutrient concentration: A chemostat analogue of the Pacific equatorial upwelling zone, *Mar. Ecol. Prog. Ser.*, 83, 291-303.

**Galloway J.N.** et al. (2004) Nitrogen Cycles: past, present and future, *Biogeochemistry*, 1-73.

**George M.D.**, Kumar M.D., Naqvi S.W.A., Banerjee S., Narvekar P.V., De Sousa S.N. and Jayakumar D.A. (1994) A study of the carbon dioxide system in the northern Indian Ocean during premonsoon, *Mar. Chem.*, 47, 243-254.

**Gill A.E.** (1982) *Atmosphere-Ocean dynamics*, Academic Press, New York, 662.

**Glibert P.M.**, Lipschultz F., McCarthy J. J. and Altabet M. A. (1982a) Isotope dilution models of uptake and remineralization of ammonium by marine plankton, *Limnol. Oceanogr.*, 27, 639-650.

**Glibert P.M.**, Biggs D.C. and McCarthy J.J. (1982b) Utilization of ammonium and nitrate during austral summer in the Scotia Sea, *Deep-Sea Res.*, 29, 837-850.

**Goldman J.C.** and Glibert P.M. (1983) Kinetics of inorganic nitrogen uptake by phytoplankton, In: *Nitrogen in the marine environment*, (Eds) Carpenter E.J. and Capone D.G., 233-274, Academic.

**Gomes H. R.**, Goes J. I. and Saino T. (2000) Influence of physical processes and fresh water discharge on seasonality of phytoplankton regime in the Bay of Bengal, *Cont. Shelf Res.*, 20, 313-330.

**Gordon H.R.** and Wang M. (1994) Retrieval of water leaving radiance and aerosol optical thickness over the oceans with SeaWiFS: A preliminary algorithm, *Appl. Optics*, 33, 443-452.

**Haake B.**, Ittekkot V., Rixen T., Ramaswami V., Nair R. R. and Curry W. B. (1993) Seasonality and interannual variability of particle fluxes to the deep Arabian Sea, *Deep-Sea Res. I*, 40, 1323-1344.

**Handley L.L.** and Raven J.H. (1992) The use of natural abundance of nitrogen isotopes in plant physiology and ecology, *Plant Cell Environ.*, 15, 965-985.

**Hansell D.A.**, Whitledge T.E. and Goering J.J. (1993) Patterns of nitrate utilization and new production over the Bering -Chukchi Shelf, *Cont. Shelf Res.*, 13, 601-627.

**Hansen J.**, Johnson D., Lacis A., Lebedeff S., Lee P., Pind D. and Russel G. (1981) Climate impact of increasing atmospheric carbon dioxide, *Nature*, 213, 957-966.

**Harrison W.G.** (1980) Nutrient regeneration and primary productivity in the sea, In: *Primary productivity in the Sea*, (Ed) Falkowski P.G., Plenum, 433-460.

**Harrison W.G.**, Platt T. and Lewis M.R. (1987) f-ratio and its relationship to ambient nitrate concentration in coastal waters, *J. Plankton Res.*, 9, 235-248.

- Harrison W.G.**, Harris L.R. and Irwin B.D. (1996) The kinetics of nitrogen utilization in the oceanic mixed layer: nitrate and ammonium interactions at nanomolar concentrations, *Limnol. Oceanogr.*, 41, 16-32.
- Hastenrath S.** and Lamb P.J. (1979) *Climate Atlas of the Indian Ocean*, University of Wisconsin Press.
- Hastenrath S.** and Greishar L.L. (1989) *Climatic Atlas of the Indian Ocean. Part III: Upper Ocean structure* (University of Wisconsin press) 247.
- Heaton T.H.E.** (1986) Isotopic studies of nitrogen pollution in the hydrosphere and atmosphere: a review, *Chem. Geol. (Iso. Geo. Sect.)*, 5, 87-102.
- Hedges J.I.**, Baldock J.A., Gelinas Y., Lee C., Peterson M. and Wakehams S.G. (2001) Evidence for non selective preservation of organic matter in sinking marine particles, *Nature*, 409, 801-804.
- Holland H.D.** (1970) Ocean water, nutrients and atmospheric oxygen, *Proceedings of the international symposium on hydrogeochemistry and Biogeochemistry, Tokyo*, 68-81.
- Holm-Hansen O.** and Mitchell B.G. (1991) Spatial and temporal distribution of phytoplankton and primary production in the western Bransfield Strait region, *Deep-Sea Res.*, 38, 961-980.
- Honjo S.**, Spencer D.W. and Gardner W.D. (1992) A sediment trap intercomparison experiment in the Panama Basin, *Deep-Sea Res.*, 39, 333-358.
- Honjo S.** and Manganini S.J. (1993) Annual biogenic particle fluxes to the interior of the North Atlantic Ocean studied at 34°N, 21°W and 48°N, 21°W, *Deep-Sea Res. II*, 40, 587-607.
- Honjo S.**, Dymond J., Prell W. and Ittekkot V. (1999) Monsoon-controlled export fluxes to the interior of the Arabian Sea, *Deep-Sea Res. II*, 46, 1859-1902.
- Houghton J.T.** et al. (2001) *Climate change 2001: The scientific basis*, Cambridge University Press, New York.
- Hubner H.** (1986) Isotope effect of nitrogen in the soil and biosphere, In: *Handbook of Environmental Isotope Geochemistry*, (Eds) Fritz P. and Fontes J.C., The Terrestrial Environment, vol. 2b, 361- 425.
- Huntley M.**, Karl D.M., Niller P. and Holm-Hansen O. (1991) Research on Antarctic Coastal Ecosystem Rates (RACER): An interdisciplinary field experiment, *Deep-Sea Res.*, 38, 911-941.
- Ittekkot V.** (1991) Particle flux studies in the Indian Ocean, *Eos*, 72, 527-230.
- Ittekkot V.**, Nair R.R., Honjo S., Ramaswami V., Bartsch M., Manganini S. and Desai

B.N. (1991) Enhanced particle fluxes in the Bay of Bengal induced by injection of freshwater, *Nature*, 351, 385-387.

**Jacques G.** (1991) Is the concept of new production - regenerated production valid for the southern Ocean? *Mar. Chem.*, 35, 273-286.

**Jaffe D.A.** (2000) The nitrogen Cycle, In: *Earth System Science*, 322-340, Academic Press Limited.

**Jawed M.** (1973) Ammonia excretion by zooplankton and its significance to primary productivity during summer, *Mar. Biol.*, 23, 115-120.

**JGOFS Report No. 19.** (1996) Protocol for the Joint Global Ocean Flux Study (JGOFS) core measurements, 145-150, SCOR, Bergen, Norway.

**Jickells T.D.** (1998) Nutrient biogeochemistry of the coastal zone, *Science*, 284, 217-222.

**Jochem F.J., Pollehne, F. and Zeitschel B.** (1993) Productivity regime and phytoplankton size structure in the Arabian Sea, *Deep-Sea Res. II*, 40, 711-735.

**Joint I., Rees A. and Woodward E.M.S.** (2001) Primary production and nutrient assimilation in the Iberian upwelling in August 1998, *Progr. Oceanogr.*, 51, 303-320.

**Junk G. and Svec H.J.** (1958) The absolute abundance of the nitrogen isotopes in the atmosphere and compressed gas from various sources, *Geochim. Cosmochim. Acta*, 14, 234-243.

**Kabanova Y.G.** (1968) Primary production of the northern part of the Indian Ocean, *Oceanology*, 8, 214-225.

**Kanda J., Saino T. and Hattori A.** (1985) Nitrogen uptake by natural populations of phytoplankton and primary production in the Pacific Ocean: regional variability of uptake capacity, *Limnol. Oceanogr.*, 30, 987-999.

**Karl D.M., Tilbrook B.D. and Tien G.** (1991) Seasonal coupling of organic matter production and particle flux in the western Bransfield Strait, Antarctica, *Deep-Sea Res.*, 38, 1097-1126.

**Karl D.M., Christian J.R., Dore J.E., Hebel D.V., Letelier R.M., Tupas L.M. and Winn C.D.** (1996) Seasonal and interannual variability in primary production and particle flux at station ALOHA, *Deep-Sea Res. II*, 43, 539-568.

**Karl D.M., Letelier R., Tupas L., Dore J., Christian J. and Hebel D.** (1997) The role of nitrogen fixation in biogeochemical cycling in the subtropical North Pacific Ocean, *Nature*, 388, 533-538.

**Keeling C.D. and Bacastow R.B.** (1977) *Energy and Climate*, 72-95, National Academy of Sciences, Washington, D.C.

**Keeling C. D.** and Whorf T. P. (2000) Trends: A compendium of data on global change, Carbon dioxide information analysis center, Oak Ridge National Laboratory, Tennessee.

**Kendall C.** (1998) Tracing nitrogen sources and cycling in catchments, In :Isotope tracers in catchment hydrology (Eds) Kendall C. and McDonnell J.J., 519-576, Elsevier.

**Kirchman D.L.** (1994) The uptake of inorganic nutrients by heterotrophic bacteria, *Microb. Ecol.*, 28, 255-271.

**Kouvarakis G.**, Mihalopoulos N., Tselepides A. and Stavrakakis S. (2001) On the importance of atmospheric inputs of inorganic nitrogen species on the productivity of the eastern Mediterranean Sea, *Global Biogeochem. Cycle*, 15(4), 805-817.

**Krey J.** (1973) Primary production in the Indian Ocean, In: *The Biology of the Indian Ocean*, (Ed) Zeitschel B., 115-126, Springer, New York.

**Kumar M.D.**, Rajendran A., Somasundar K., Ittekkot V. and Desai B.N. (1992) Processes controlling carbon components in the Arabian Sea, In: *Oceanography of the Indian Ocean* (Ed) Desai B.N., 313-325, Oxford-IBH, New Delhi.

**Kumar M.D.**, Naqvi S.W.A., George M.D. and Jayakumar D.A. (1996) A sink for atmospheric carbon dioxide in the northeast Indian Ocean, *J. Geophys. Res.*, 101, 18,121-18,125.

**Kumar S.**, Ramesh R., Sardesai S. and Seshshayee S. (2004a) High new production in the Bay of Bengal: possible causes and implications, *Geophys. Res. Lett.* 31, L18304, doi: 10.1029/2004GL021005.

**LaFond E.C.** (1966) Bay of Bengal, In: *The Encyclopaedia of Oceanography*, (Ed) Fairbridge R.W., Van Nostrand Reinhold Co., New York, 110-118.

**LaViolette P.E.** (1967) Temperature, salinity and density of the world's seas, Bay of Bengal and Andaman Sea, Informal Report no. 67-57, Naval Oceanographic Office, Washington DC, 81.

**Laws E.A.**, Harrison W.G. and DiTullio G. (1985) A comparison of nitrogen assimilation rates based on <sup>15</sup>N uptake and autotrophic protein synthesis, *Deep-Sea Res.*, 32, 85-95.

**Laws E.A.**, Falkowski P.G., Smith W.O., Ducklow H. and McCarthy J.J. (2000) Temperature effects on export production in the open ocean, *Global Biogeochem. Cycles*, 14, 1231-1246.

**Lee et al.** (1998) Particulate organic carbon fluxes: compilation of results from the 1995 US JGOFS Arabian Sea Process Study, *Deep-Sea Res. II*, 45, 2489-2501.

- Lee C.M.**, Jones B.H., Brink K.H. and Fischer K.H. (2000) The upper-Ocean response to monsoonal forcing in the Arabian Sea: seasonal and spatial variability, *Deep-Sea Res. II*, 47, 1177-1226.
- L' Helguen S.**, LeCorre P., Madec C. and Morin P. (2002) New and regenerated production in the Almeria-Oran front area, eastern Alboran Sea, *Deep-Sea Res. I*, 49, 83-99.
- Liu, K.-K.** and Kaplan. I. R. (1989) The eastern tropical Pacific as a source of  $^{15}\text{N}$ -enriched nitrate in seawater off southern California, *Limnol. Oceanogr.*, 34, 820-830.
- Lohrenz S.E.**, Knauer G.A., Asper V.L., Tuel M., Michaels A.F. and Knap A.H. (1992) Seasonal variability in primary production and particle flux in the northwestern Sargasso Sea: U.S. JGOFS Bermuda Atlantic Time Series Study, *Deep-Sea Res.*, 39, 1373-1391.
- Lourey M.J.**, Trull T.W. and Sigman D.M. (2003) Sensitivity of  $\delta^{15}\text{N}$  of nitrate, surface suspended and deep sinking particulate nitrogen to seasonal nitrate depletion in the Southern Ocean, *Global Biogeochem. Cycles*, 17, 1081, doi: 10.1029/2001GB001973.
- MacIsaac J.J.** and Dugdale R.C. (1969) The kinetics of nitrate and ammonium uptake by natural populations of marine phytoplankton, *Deep-Sea Res.*, 16, 45-57.
- MacIsaac J.J.** and Dugdale R.C. (1972) Interactions of light and inorganic nitrogen in controlling nitrogen uptake in the sea, *Deep-Sea Res.*, 19, 209-232.
- Madhupratap M.**, Prasanna Kumar S., Bhattathiri P.M.A., Dileep Kumar M., Raghukumar S., Nair K.K.C. and Ramaiah N. (1996) Mechanism of the biological response to winter cooling in the northeastern Arabian Sea, *Nature*, 384, 549-552.
- Madhupratap M.**, Gauns M., Ramaiah N., Prasanna Kumar S., Muraleedharan P.M., DeSouza S.N., Sardesai S., Muraleedharan U. (2003) Biogeochemistry of the Bay of Bengal: physical, chemical and primary productivity characteristics of the central and western Bay of Bengal during summer monsoon 2001, *Deep-Sea Res. II*, 50, 881-896.
- Maier-Reimer E.**, Mikolajewicz U. and Winguth A. (1996) *Clim. Dyn.*, 12, 711.
- Malone T.C.**, Pike S.E. and Conley D.J. (1993) Transient variations in phytoplankton productivity at the JGOFS Bermuda time series station, *Deep-Sea Res.*, 40, 903-924.
- Mariotti A.**, Pierre D., Vedy J.C., Bruckert S. and Guillemot J. (1980) The abundance of natural nitrogen 15 in the organic matter of soils along an altitudinal gradient (Chablais, Haute Savoie, France) *Catena*, 7, 293-300.
- Mariotti A.**, Lancelot C. and Billen G. (1984) Natural isotopic composition of nitrogen as a tracer of origin for suspended organic matter in the Scheldt estuary, *Geochim. Cosmochim. Acta*, 48, 549-555.

- Martin J. -M.** and Whitfield M. (1983) The significance of the river input of chemical elements to the ocean, In: Trace metals in seawater, (Eds) C. S. Wong et al., 265-295, Plenum, New York.
- McCarthy J.J.** and Eppley R.W. (1972) A comparison of chemical isotopic and enzymatic methods for measuring nitrogen assimilation of marine phytoplankton, *Limnol. Oceanogr.*, 17, 371-382.
- McCarthy J.J.**, Taylor W.R. and Taft T. (1977) Nitrogenous nutrition of the plankton in the Chesapeake Bay: Nutrient availability and phytoplankton preferences, *Limnol. Oceanogr.*, 22, 996-1011.
- McCarthy J.J.** and Goldman J.C. (1979) Nitrogenous nutrition of marine phytoplankton in nutrient depleted waters, *Science*, 203, 670-672.
- McCarthy J.J.** and Carpenter E.J. (1983) Nitrogen cycling in near surface waters of the open ocean, In: Nitrogen in the Marine Environment, (Eds) Carpenter E.J. and Capone D.G., 487-512, Academic Press, New York.
- McCarthy J.J.**, Garside C. and Nevins J.L. (1992) Nitrate supply and phytoplankton uptake kinetics in the euphotic layer of a gulf stream warm core ring, *Deep-Sea Res.*, 39, S393-S403.
- McCarthy J.J.**, Garside C., Nevins J.L. and Barber R.T. (1996) New production along 140°W in the equatorial Pacific during and following the 1992 El Nino event, *Deep-Sea Res. II*, 43, 1065-1093.
- McCarthy J.J.**, Garside C. and Nevins J. (1999) Nitrogen dynamics during the Arabian Sea northeast monsoon, *Deep-Sea Res. II*, 46, 1623-1664.
- McCreary J.P.**, Kohler K.E., Hood R.R. and Olson D.B. (1996) A four component ecosystem model of biological activity in the Arabian Sea, *Progr. Oceanogr.*, 37, 193-240.
- McElroy M.B.** (1983) Marine biological controls on atmospheric CO<sub>2</sub> and climate, *Nature*, 302, 328-329.
- McGillicuddy D.J. Jr.**, McCarthy J.J. and Robinson A.R. (1995) Coupled physical and biological modelling of the spring bloom in the North Atlantic (I): model formulation and one dimensional bloom processes, *Deep-Sea Res. I*, 42, 1313-1357.
- Michaels A.F.**, Siegel D.A., Johnson R.J., Knap A.F. and Galloway J.N. (1993) Episodic inputs of atmospheric nitrogen to the Sargasso Sea: Contribution to new production and phytoplankton blooms, *Global Biogeochem. Cycles*, 7, 339-351.
- Michaels A.F.**, Bates N.R., Buesseler K.O., Carlson C.A., Knap H.H. (1994) Carbon cycle imbalances in the Sargasso Sea, *Nature*, 372, 537-540.

- Miller C.B.**, Frost B.W., Wheeler P.A., Landry M.R., Welschmeyer N. and Powell T.M. (1991) Ecological dynamics in the subarctic Pacific, a possibly iron limited ecosystem, *Limnol. Oceanogr.*, 36, 1600-1615.
- Miller C.B.** (1993) Pelagic production processes in the subarctic Pacific, *Progr. Oceanogr.*, 32, 1-15.
- Milliman J.D.** and Syvitski J.P.M. (1992) Geomorphic/tectonic control of sediment discharge to the ocean: the importance of small mountainous rivers, *The J. Geol.*, 100,525-100,544.
- Minagawa M.** and Wada E. (1986) Nitrogen isotope ratios of red tide organisms in the East China Sea: A characterization of biological nitrogen fixation, *Mar. Chem.*, 19, 245-259.
- Mino Y.**, Saino T., Suzuki K. and Maranon E. (2002) Isotopic composition of suspended particulate nitrogen ( $\delta^{15}\text{N}_{\text{sus}}$ ) in surface waters of the Atlantic Ocean from 50°N to 50°S, *Global Biogeochem. Cycles*, 16, 4, 1059.
- Miyake Y.** and Wada E. (1967) The abundance ratio of  $^{15}\text{N}/^{14}\text{N}$  in marine environments, *Rec. Oceanogr. Works Jpn.* 9, 37-53.
- Miyake Y.** and Wada E. (1971) The isotope effect on the nitrogen in biochemical, oxidation-reduction reactions, *Rec. Oceanogr. Works Jpn.* 11, 1-6.
- Montoya J.P.** and McCarthy J.J. (1995) Isotopic fractionation during nitrate uptake by phytoplankton grown in continuous culture, *J. Plankton Res.*, 17, 439-464.
- Muller L. J.** and Charles C. T (1994) Revised SeaWiFS prelaunch algorithm for the diffuse attenuation coefficient K (490); In case studies for SeaWiFS Calibration and Validation, Part 4, NASA Technical Memorandum, 104566, 28, 18-21.
- Mullin M.M.**, Perry M.J., Renger E.H. and Evans P.M. (1975) Nutrient regeneration by oceanic zooplankton: a comparison of methods, *Mar. Sci. Comm.*, 1, 1-13.
- Murray J.W.**, Downs J.N., Strom S., Wei C.L. and Jannasch H.W. (1989) Nutrient assimilation, export production and  $^{234}\text{Th}$  scavenging in the eastern equatorial Pacific, *Deep-Sea Res.*, 36, 1471-1489.
- Murray J.W.** (1991) The 1988 Black Sea Oceanography Expedition: Introduction and Summary, *Deep-Sea Res.*, 38 (Supplement 2): S655-S661.
- Murty V.S.N.**, Subrahmanyam B., Gangadhara Rao L.V. and Reddy G.V. (1998) Seasonal variation of sea surface temperature in the Bay of Bengal during 1992 as derived from NOAA-AVHRR SST data, *Int. J. Remote Sensing*, 19, 2361-2371.
- Nair P.V.R.**, Samuel S., Joseph K.J. and Balachandran V.K. (1973) Primary production and potential fishery resources in the seas around India, In: Proceedings of the symposium on Living Resources of the Seas Around India, 1968, special publication, Central Marine Fisheries Research Institute, Cochin, 184-198.

- Naqvi S.W.A.** (1987) Some aspects of the oxygen deficient conditions and denitrification in the Arabian Sea, *J. Mar. Res.*, 45, 1049-1072.
- Naqvi S.W.A.**, Noronha R.J., Somasundar K. and Sen Gupta R. (1990) Seasonal changes in the denitrification regime of the Arabian Sea, *Deep-Sea Res.*, 37, 593-611.
- Naqvi S.W. A** (1991) Geographical extent of denitrification in the Arabian Sea in relation to some physical processes, *Oceanolog. Acta*, 14, 281-290.
- Naqvi S.W.A.** and Noronha R.J. (1991) Nitrous oxide in the Arabian Sea, *Deep-Sea Res.*, 38, 871-890.
- Naqvi S.W.A.** and Shailaja M.S. (1993) Activity of the respiratory electron transport system and respiration rates within the oxygen minimum layer of the Arabian Sea, *Deep-Sea Res. II*, 40, 687-695.
- Naqvi S.W.A.** (1994) Denitrification processes in the Arabian Sea, *Proc. Indian Acad. Sci. (Earth Planet, Sci)*, 103, 2, 279-300.
- Neess J.C.**, Dugdale R.C. and Goering J.J. (1962) Nitrogen metabolism in lakes, Measurement of nitrogen fixation with  $^{15}\text{N}$ , *Limnol. Oceanogr.*, 7, 163-169.
- Olson D. B.**, Hitchcock G. L., Fine R. A. and Warren B. A. (1993) Maintenance of low-oxygen layer in the Central Arabian Sea, *Deep-Sea Res. II*, 40, 697-709.
- O'Reilly J.E.**, Maritorena S., Mitchell B.G., Siegel D.A., Carder K.L., Garver S.A., Kahru M. and McClain C. (1998) Ocean Colour chlorophyll algorithms for SeaWiFS, *J. Geophys. Res.*, 103, 24937-24953.
- Owens N.J.P.** (1987) Natural variation in  $^{15}\text{N}$  in the marine environment, *Adv. Mar. Biol.*, 24, 390-451.
- Owens N.J.P.** and Rees A.P. (1989) Determination of nitrogen-15 at sub-microgram levels of nitrogen using automated continuous-flow isotope ratio mass spectrometer, *Analyst*, 114, 1655-1657.
- Owens N.J.P.**, Priddle J. and Whitehouse M.J. (1991) Variation in phytoplanktonic nitrogen assimilation around south Georgia and in the Bransfield Strait (Southern Ocean), *Mar. Chem.*, 35, 287-304.
- Owens N.J.P.**, Burkill P.H., Mantoura R.F.C, Woodward E.M.S., Bellan I.E., Howland R.J.M. and Llewellyn C.A. (1993) Size fractionated primary production and nitrogen assimilation in the northwestern Indian Ocean, *Deep-Sea Res. II*, 40, 697-709.
- Paasche E.** and Kristjansen S. (1982) Nitrogen nutrition of the phytoplankton in the Oslofjord, *Estuarine Coastal and Shelf Science*, 14, 237-249.
- Perry M.J.** and Eppley R.W. (1981) Phosphate uptake by phytoplankton in the Central North Pacific Ocean, *Deep-Sea Res.*, 28A, 39-49.

**Peterson B.J.** and Fry B. (1987) Stable isotopes in ecosystem studies, *Ann. Rev. ecol. System.*, 18, 293-320.

**Platt T.**, Sathyendranath S., Ulloa O., Harrison W.G., Hoepffner N. and Goes J. (1992) Nutrient control of phytoplankton photosynthesis in the western North Atlantic, *Nature*, 356, 229-231.

**Platt T.** and Sathyendranath S. (1993) Estimators of primary production for interpretation of remotely sensed data on ocean color, *J. Geophys. Res.*, 98, 14561-14576.

**Pollehne F.**, Cline B. and Zeitzschel B. (1993) Low light adaptation and export production in the deep chlorophyll maximum layer in the northern Indian Ocean, *Deep-Sea Res. II*, 40, 737-752.

**Pomroy A.J.** and Joint I.R. (1999) Bacterioplankton activity in the surface mixed layer of the Arabian Sea during and after the 1994 SW monsoon, *Deep-Sea Res. II*, 46, 767-794.

**Prasanna Kumar S.**, Ramaiah N., Gauns M., Sarma V.V.S.S., Muraleedharan P.M., Raghukumar S., Dileep Kumar M. and Madhupratap M. (2001) Physical forcing of biological productivity in the Northern Arabian Sea during the Northeast Monsoon, *Deep-Sea Res.*, 48, 1115-1126.

**Prasanna Kumar S.**, Muraleedharan P.M., Prasad T.G., Gauns M., Ramaiah N., De Souza S.N., Sardesai S., and Madhupratap M. (2002) Why is the Bay of Bengal less productive during summer monsoon compared to the Arabian Sea? *Geophys. Res. Lett.*, 29 (24), 2235, doi: 10.1029/2002GL016013.

**Price N.M.**, Ahner B.A. and Morel F.M.M. (1994) The equatorial Pacific Ocean: Grazer controlled phytoplankton populations in an iron-limited ecosystem, *Limnol. Oceanogr.*, 39, 520-534.

**Qasim S.Z.** (1977) Biological productivity of the Indian Ocean, *Ind. J. Mar. Sci.*, 6, 122-137.

**Qasim S.Z.** (1982) Oceanography of the northern Arabian Sea, *Deep-Sea Res.*, 29, 1041-1068.

**Radhakrishna K.** (1978) Primary productivity of the Bay of Bengal during March-April, 1975, *Ind. J. Mar. Sci.*, 7, 58-60.

**Radhakrishna K.**, Devassy V.P., Bhargava R.M.S. and Bhattathiri P.M.A. (1978) Primary production in the northern Arabian Sea, *Ind. J. Mar. Sci.*, 7, 271-275.

**Ramage C.S.** (1971) *Monsoon Meteorology*, Academic Press, New York, 296.

**Ramaiah N.**, Raghukumar S. and Gauns M. (1996) Bacterial abundance and production in the central and eastern Arabian Sea, *Curr. Sci.*, 71(11), 878-882.

- Rau G.H.**, Sullivan C.W. and Gordon L.I. (1991)  $\delta^{13}\text{C}$  and  $\delta^{15}\text{N}$  variations in Weddell Sea particulate organic matter, *Mar. Chem.*, 35, 355-369.
- Rau G.H.**, Low C., Pennington J.T., Buck K.R. and Chavez F.P. (1998) Suspended particulate nitrogen  $\delta^{15}\text{N}$  versus nitrate utilization: Observations in Monterey Bay, CA, *Deep-Sea Res. II*, 45, 1603-1616.
- Redfield A.C.** (1934) On the proportions of organic derivatives in seawater and their relation to the composition of plankton, James Johnstone Memorial Volume, Liverpool, 176p.
- Rees A.P.**, Owens N.J.P., Heath M.R., Plummer D.H. and Bellerby R.S. (1995) Seasonal nitrogen assimilation and carbon fixation in a fjordic sea loch, *J. Plankton Res.*, 17(6), 1307-1324.
- Rees A. P.**, Woodward E.M.S., Robinson C., Cummings D. G., Tarran G. A. and Joint I. (2002) Size-fractionated nitrogen uptake and carbon fixation during a developing coccolithophore bloom in the North Sea during June 1999, *Deep-Sea Res. II*, 49, 2905-2927.
- Richards F.A.** (1965) Anoxic basins and Fjords; In: *Chemical Oceanography I* (Eds) J.P. Riley and G. Skirrow, 611-645, Academic Press, New York.
- Roman M.R.**, Dam H.G., Gauzens, A.L. and Napp J.M. (1993) Zooplankton biomass and grazing at the JGOFS Sargasso Sea time series station, *Deep-Sea Res.*, 40, 883-901.
- Ryther J.H.**, Hall J.R., Pease A.K., Bakun A. and Jones M.M. (1966) Primary production in relation to the chemistry and hydrography of the western Indian Ocean, *Limnol. Oceanogr.*, 11, 371-380.
- Saino T.** and Hattori A. (1980)  $^{15}\text{N}$  natural abundance in oceanic suspended particulate matter, *Nature*, 283, 752-754.
- Saino T.** and Hattori A. (1985) Variation of  $^{15}\text{N}$  natural abundance of suspended organic matter in shallow oceanic water, In: *Marine and Estuarine Geochemistry* (Eds) A.C. Sigleo and A. Hattori, 1-13, A.F. Lewis, New York.
- Saino T.** and Hattori A. (1987) Geographical variation of the water column distribution of suspended particulate nitrogen and its  $^{15}\text{N}$  natural abundance in the Pacific and its marginal seas, *Deep-Sea Res.*, 34, 807-827.
- Sambrotto R.N.**, Niebauer H.J., Goering J.J. and Iverson R.L. (1986) The relationship among vertical mixing, nitrate uptake, and growth during the spring phytoplankton bloom in the southeast Bering Sea middle shelf, *Cont. Shelf Res.*, 5, 161-198.
- Sambrotto R.N.** and Lorenzen C.J. (1987) Phytoplankton, phytoplankton production in the coastal, oceanic areas of the gulf of Alaska, In: Hood D.W., Zimmerman S.T. (Eds) *The Gulf of Alaska: physical environment, biological resources*. U.S. Dept. of Commerce, Washington, D.C., 249-282.

- Sambrotto R.N.**, Martin J.H., Broenkow W.W., Carlson C.A. and Fitzwater S.E. (1993) Nitrate utilization in surface waters of the Iceland Basin during spring and summer of 1989, *Deep-Sea Res. II*, 40, 441-457.
- Sambrotto R.N.** (2001) Nitrogen production in the northern Arabian Sea during the spring intermonsoon and southwest monsoon seasons, *Deep-Sea Res. II*, 48, 1173-1198.
- Sarin M.M.**, Krishnaswami S., Dilli K., Somayajulu B.L.K. and Moore W.S. (1989) Major ion chemistry of the Ganga-Brahmaputra river system: weathering processes and fluxes to the Bay of Bengal, *Geochim. Cosmochim. Acta*, 53, 997-1009.
- Sarmiento J.L.** and Siegenthaler U. (1992) New production and Global Carbon Cycle in Primary Productivity and Biogeochemical Cycles, In: *The Sea*, (Eds) Falkowski P. and Woodhead A.D., 317-332, Plenum, New York.
- Sathyendranath S.** and Platt T. (1988) The spectral irradiance field at the surface and in the interior of the ocean: A model for applications in oceanography and remote sensing, *J. Geophys. Res.*, 93, 9270-9280.
- Savidge G.** and Gilpin L. (1999) Seasonal influences on size fractionated Chlorophyll a concentrations and primary production in the north-west Indian Ocean, *Deep-Sea Res. II*, 46, 701-723.
- Sawant S.** and Madhupratap M. (1996) Seasonality and composition of phytoplankton in the Arabian Sea, *Curr. Sci.*, 71, 869-873.
- Schafer P.**, Kreilein H., Muller M. and Gravenhorst G. (1993) Cycling of inorganic nitrogen compounds between atmosphere and ocean in tropical areas off south East Asia, *Mitt. Geol.-Palaont. Inst. Univ. Hamburg*, 76, 19-36.
- Schafer P.** and Ittekkot V. (1995) Isotopic biogeochemistry of nitrogen in the northern Indian Ocean, *Mitt. Geol. -Palaont. Inst. Univ. Hamburg*, 78, 67-93.
- Schoenheimer R.** and Rittenberg D. (1939) Studies in protein metabolism: I, General consideration in the application of isotopes on the study of protein metabolism, The normal abundance of nitrogen isotopes in amino acids.
- Schott F.** and McCreary J.P. (2001) The monsoon circulation of the Indian Ocean, *Progr. Oceanogr.*, 51, 1-123.
- Schott F.**, Swallow J.C. and Fieux (1990) The Somali Current at the equator: annual cycles of currents and transport in the upper 1000m and connection with neighbouring latitudes, *Deep-Sea Res.*, 37, 1825-1848.
- Shearer G.** and Kohl D. (1986) N<sub>2</sub> fixation in field settings, estimation based on natural <sup>15</sup>N abundance, *Australian J. Plant Physiol.*, 13, 699-757.

- Shetye S.R.**, Gouveia A.D., Shenoi S.S.C., Sundar D., Michael G. S., Almeida A. M. and Santanam K. (1990) Hydrography and circulation off the west coast of India during the Southwest monsoon 1987, *J. Mar. Res.*, 48, 359-378.
- Shetye S.R.**, Shenoi S.S.C., Gouveia A.D., Michael G. S., Sundar D. and Nampoothiri G. (1991) Wind-driven coastal upwelling along the western boundary of the Bay of Bengal during the southwest monsoon, *Cont. Shelf Res.*, 11, 1397-1408.
- Shetye S.R.**, Gouveia A.D., Shenoi S.S.C., Sundar D., Michael G. S. and Nampoothiri G. (1993) The western boundary current of the seasonal subtropical gyre in the Bay of Bengal, *J. Geophys. Res.*, 98, 945-954.
- Shetye S.R.**, Gouveia A.D., Shankar D., Shenoi S.S.C., Vinaychandran P.N., Sundar D., Michael G. S. and Nampoothiri G. (1996) Hydrography and circulation in the western Bay of Bengal during northeast monsoon, *J. Geophys. Res.*, 101, 14011-14025.
- Smith R.L.** and Bottero J.S. (1977) On upwelling in the Arabian Sea, In: *A voyage of discovery* (Ed) M. Angel, 291-304, Pergamon Press.
- Smith S.L.**, Codispoti L.A., Morrison, J.M. and Barber R.T. (1998) The 1994-1996 Arabian Sea Expedition: an integrated interdisciplinary investigation of the response of the northwestern Indian Ocean to monsoonal forcing, *Deep-Sea Res. II*, 45, 1905-1915.
- Smith S. L.** (2001) Understanding the Arabian Sea: Reflections on the 1994-1996 Arabian Sea Expedition, *Deep-Sea Res. II*, 48, 1385-1402.
- Smith W.O.** and Nelson D.M. (1990) Phytoplankton growth and new production in the Weddell Sea marginal ice zone in the austral spring and autumn, *Limnol. Oceanogr.*, 35, 809-821.
- Smith W.O. Jr** (1995) Primary productivity and new production in the northeast water (Greenland) Polynya during summer 1992, *J. Geophys. Res.*, 100, 4357-4370.
- Smith W.O. Jr.**, Barber R.T., Hiscock M.R. and Marra J. (2000) The seasonal cycle of phytoplankton biomass and primary productivity in the Ross Sea, Antarctica, *Deep-Sea Res. II*, 47, 3119-3140.
- Steinberg D.K.**, Carlson C A., Bates N.R., Goldthwait S.A. Madin L.P. and Michaels A.F. (2000) Zooplankton vertical migration and the active transport of dissolved organic and inorganic carbon in the Sargasso Sea, *Deep-Sea Res. I*, 47, 137-158.
- Strickland J.D.H.** and Parson T.R. (1972) A practical handbook of seawater analysis, 127-130, Fisheries Research Board, Canada.
- Subramanian V.** (1993) Sediment load of Indian Rivers, *Curr. Sci.*, 64, 928-930.
- Sullivan C.W.**, Arrigo K.R., McClain C.R., Comiso J.C. and Firestone J. (1993) Distribution of phytoplankton blooms in the Southern Ocean, *Science*, 262, 1832-1837.

- Sweeney R.E.**, Liu K.K. and Kaplan I.R. (1978) Oceanic nitrogen isotopes and their use in determining the source of sedimentary nitrogen, in: *Stable isotopes in the earth sciences*, edited by Robinson, B.W., DSIR 220 New Zealand dept. Scientific and industrial, Wellington, 9-26.
- Takahashi, T.** (1989) The carbon dioxide puzzle, *Oceanus*, 32, 22-29.
- Takahashi, T.**, Olafsson J., Goddard J., Chipman D.W. and Sutherland S.C. (1993) Seasonal variation of CO<sub>2</sub> and nutrients in the high latitude surface oceans: A comparative study, *Global Biogeochem. Cycles*, 7, 843-878.
- Tomczak M.** and Godfrey J.S. (1994) *Regional Oceanography: an Introduction*, 422, Pergamon, Terry town, New York.
- Townsend D.W.**, Keller M.D., Sieracki M.E. and Ackleson S.G. (1992) Spring phytoplankton blooms in the absence of vertical water column stratification, *Nature*, 360, 59-62.
- Treguer P.**, Legendre L., Rivkin R.T., Ragueneau O. and Dittert N. (2003) Water column biogeochemistry below the euphotic zone, In: *Ocean Biogeochemistry* (Ed) Fasham M.J.R., 145-156, Springer, Heideberg.
- Unger D.**, Ittekkot V., Schafer P., Tiemann J. and Reschke S. (2003) Seasonality and interannual variability of particle fluxes to the deep Bay of Bengal: influence of riverine input and oceanographic processes, *Deep-Sea Res. II*, 50, 897-923.
- Urey, H.C.** (1947) The thermodynamic properties of isotopic substances, *J. Chem. Soc.*, 562-581.
- Venkateswaran S.V.** (1956) On evaporation from the Indian Ocean, *Indian Journal of meteorology and Geophysics*, 7, 265-284.
- Villareal T.A.**, Altabet M.A. and Culver-Rymsza K. (1993) Nitrogen transport by vertically migrating diatom mats in the North Pacific Ocean, *Nature*, 363, 709-712.
- Vinaychandran P.N.**, Murty V.S.N. and Ramesh Babu V. (2002) Observations of barrier layer formation in the Bay of Bengal during summer monsoon, *J. Geophys. Res.*, 107(C12), 8018, doi: 10.1029/2001JC000831.
- Vinaychandran P.N.** and Mathew S. (2003) Phytoplankton bloom in the Bay of Bengal during the northeast monsoon and its intensification by cyclones, *Geophys. Res. Lett.*, 30 (11), 1572, doi: 10.1029/2002GL016717.
- Vitousek P.M.**, Hattenschwiler S., Olander L. and Allison S. (2002) Nitrogen and nature, *Ambio*, 31, 97-101.
- Wada E.**, Miyazaki T. and Hattori A. (1971) <sup>15</sup>N abundance in nitrogenous compounds in the sea, *Proc. 1971 Fall Meet. Oceanogr. Soc. Japan*, 227.

- Wada E.** and Hattori A. (1976) Natural abundance of  $^{15}\text{N}$  in particulate organic matter in the North Pacific Ocean, *Geochim. Cosmochim. Acta*, 40, 249-251.
- Wada E.** and Hattori A. (1978) Nitrogen isotope effects in the assimilation of inorganic nitrogenous compounds by marine diatoms, *Geomicrobiol. J.*, 1, 85-101.
- Wada E.** (1980) Nitrogen Isotope fractionation and its significance in biogeochemical processes occurring in marine environments, In :*Isotope marine Chemistry*, 375-398.
- Wada E.** and Hattori A. (1991) *Nitrogen in the sea: Forms, Abundances, and rate processes*, CRC Press, Boca Raton, Fla, 208.
- Wafar M.V.M.**, Wafar S. and Devassy V.P. (1986) Nitrogenous nutrients and primary production in a tropical oceanic environment, *Bull. Mar. Sci.*, 38(2), 273-284.
- Wafar M.V.M.**, Le Corre P. and L'Helguen S. (1995) f-Ratios calculated with and without urea uptake in nitrogen uptake by phytoplankton, *Deep-Sea Res.*, 42, 1669-1774.
- Walsh J.J.**, (1981) A carbon budget for overfishing off Peru, *Nature*, 290, 300-304.
- Waser N.A.**, Yin K., Yu Z., Tada K., Harrison P.J., Turpin D.H. and Calvert S.E. (1998) Nitrogen isotope fractionation during nitrate, ammonium and urea uptake by marine diatoms and coccolithophores under various conditions of N availability, *Mar. Ecol. Prog. Ser.*, 169, 29-41.
- Watson A.J.** and Orr J.C. (2003) Carbon dioxide fluxes in the global ocean, In: *Ocean Biogeochemistry* (Ed) Fasham M.J.R., 123-143, Springer, Heideberg.
- Watts L.J.** and Owens N.J.P. (1999) Nitrogen assimilation and f-ratio in the northwestern Indian Ocean during an Intermonsoon period, *Deep-Sea Res. II*, 46, 725-743.
- Wheeler P.A.**, Glibert P.M. and McCarthy J.J. (1982) Ammonium uptake and incorporation by Chesapeake Bay phytoplankton: short term uptake kinetics, *Limnol. Oceanogr.*, 27, 1113-1128.
- Wheeler P.A.** and Kokkinakis S.A. (1990) Ammonium recycling limits nitrate use in the oceanic subarctic Pacific, *Limnol. Oceanogr.*, 35, 1267-1278.
- Wiebe P.H.**, Boyd S. and Cox J.L. (1975) Relationship between zooplankton displacement volume, wet weight, dry weight, and carbon, *Fishery Bulletin*, 73(4), 777-786.
- Wilkerson F.P.**, Dugdale R.C. and Barber R.T. (1987) Effects of El Nino on new, regenerated, and total production in eastern boundary upwelling systems, *J. Geophys. Res.*, 92, 14347-14353.

**Wong C.S.**, Whitney F.A., Matear R.J. and Iseki K. (1998) Enhancement of new production in the northeast subarctic Pacific Ocean during negative north Pacific index events, *Limnol. Oceanogr.*, 43, 1418-1426.

**Woodward E.M.S.**, Rees A.P. and Stephens J.A. (1999) The influence of south-west monsoon upon the nutrient biogeochemistry of the Arabian Sea, *Deep-Sea Res. II*, 46, 571-591.

**Wyrski K.** (1973) Physical Oceanography of the Indian Ocean, In: *The Biology of the Indian Ocean* (Eds) Zeitzschel B. and Gerlach S.A., 18-36, Chapman Hall Ltd., London.

**Zehr J.P.**, Waterbury J.B., Turner P.J., Montoya J.P., Omoregie E., Steward G.F., Hansen A. and Karl D.M. (2001) Unicellular cyanobacteria fix N<sub>2</sub> in the subtropical North Pacific Ocean, *Nature*, 412, 635-638.